Global mapping of pseudouridine in the transcriptomes of *Campylobacter jejuni* and *Helicobacter pylori* and functional characterization of pseudouridine synthases

Globale Kartierung von Pseudouridin in den Transkriptomen von *Campylobacter jejuni* und *Helicobacter pylori* und funktionelle Charakterisierung von Pseudouridin-Synthasen

Doctoral thesis for a doctoral degree at the Graduate School of Life Sciences,

Julius-Maximilians-Universität Würzburg,

Section: Infection and Immunity

submitted by

Elisabetta Fiore

from Cattolica (Italy)

Würzburg, 2022

Submitted on: ……..

Office stamp

Members of the Thesis Committee

Chairperson: Professor Thomas Dandekar

Primary Supervisor: Professor Cynthia M. Sharma

Supervisor (Second): Professor Dagmar Beier

Supervisor (Third): Professor Utz Fischer

Date of Public Defence: ……..

Date of Receipt of Certificates: ……..

Affidavit

I hereby confirm that my thesis entitled "Global mapping of pseudouridine in the transcriptomes of *Campylobacter jejuni* and *Helicobacter pylori* and functional characterization of pseudouridine synthases" is the result of my own work. I did not receive any help or support from commercial consultants. All sources and / or materials applied are listed and specified in the thesis.

Furthermore, I confirm that this thesis has not yet been submitted as part of another examination process neither in identical nor in similar form.

Würzburg, _____

Elisabetta Fiore

Eidesstattliche Erklärung

Hiermit erkläre ich an Eides statt, die Dissertation "Globale Kartierung von Pseudouridin in den Transkriptomen von *Campylobacter jejuni* und *Helicobacter pylori* und funktionelle Charakterisierung von Pseudouridin-Synthasen" eigenständig, d.h. insbesondere selbständig und ohne Hilfe eines kommerziellen Promotionsberaters, angefertigt und keine anderen als die von mir angegebenen Quellen und Hilfsmittel verwendet zu haben.

Ich erkläre außerdem, dass die Dissertation weder in gleicher noch in ähnlicher Form bereits in einem anderen Prüfungsverfahren vorgelegen hat.

Würzburg, _____

Elisabetta Fiore

This thesis is dedicated to my whole family.
But especially to my sister Eleonora and my mother Patrizia, the strongest women I know.
And to all the people that fight every day for their small or big battles.

SUMMARY

More than 150 different RNA modifications have been detected in all kingdoms of life and 60 are known to decorate bacterial RNA. Among them, pseudouridine is universally conserved and one of the most abundant modifications present in bacterial stable RNAs such as tRNAs and rRNAs. In bacteria, the nucleotide is posttranscriptionally generated by dedicated enzymes called pseudouridine synthases (PUSs). With the advent of sophisticated deep-sequencing technologies, this modification has been identified in different types of RNA classes (tRNAs, rRNAs, mRNAs, snRNAs, and lncRNAs) in diverse eukaryotic organisms. However, these techniques have never been applied to bacteria, generating a knowledge gap about the location of the modified nucleotide in prokaryotic RNAs. Mutations or deletions of specific eukaryotic PUS enzymes are linked to human diseases and therefore their absence is deleterious for the correct function of the cell. However, deletion of tRNA or rRNA PUS enzymes in the bacterial model organism *E. coli* have not revealed any such drastic phenotypes, suggesting a different role and function of the modification itself and of the enzymes in different kingdoms of life.

Since the roles of tRNA PUS enzymes in bacteria is still poorly understood, a functional characterization of these proteins is pursued in the Epsilonproteobacteria *Campylobacter jejuni* and *Helicobacter pylori.* While *C. jejuni* is the leading cause of bacterial foodborne gastroenteritis in humans, infection with *H. pylori* is associated with the development of gastric cancer. In particular, phenotypes were explored for the tRNA PUS enzymes TruA, TruB, and TruD *in C. jejuni* as well as TruA and TruD in *H. pylori*. Upon deletion of *truD*, a severe growth defect is observed for *C. jejuni* but not for *H. pylori*, highlighting a potential difference in function of the enzyme in the two related bacterial pathogens.

Moreover, a genome-wide approach called Pseudo-seq is established and applied for RNA of these two pathogens, which allows, for the first time, the global identification of pseudouridine modifications at single-nucleotide resolution in the bacterial transcriptome. Applying Pseudo-seq in RNAs of wildtype and diverse PUS enzyme deletion mutants enabled the identification of the distinct RNA substrates of tRNA PUS enyzmes in *C. jejuni* and *H. pylori*. Hereby, the tRNA-Glu was determined to be the major tRNA substrate of TruD in *C. jejuni*. Interestingly, the tRNA-Glu is expressed as a single copy in the *C. jejuni* genome. To link the growth defect observed for a *C. jejuni* Δ*truD* mutant strain to the pseudouridine modification of the tRNA-Glu, a catalytically inactive TruD complementation was generated. This strain is unable to restore the tRNA-Glu modification but surprisingly, was able to complement the growth defect. The same observation was made for a cross-complementation with a copy of *H. pylori* TruD. This indicates that there is a potential additional function of the TruD PUS

enzyme in *C. jejuni* that is independent of the pseudouridine modification. Using a combination of deep-sequencing technologies (RIP-seq, RNA-seq, Ribo-seq, and CLIP-seq), the dual function of TruD is investigated.

Overall, this study provides the first in-depth investigation into pseudouridylation of bacteria in general and the bacterial pathogens *C. jejuni* and *H. pylori* in particular. The work presented in this thesis reveals not only a global map of pseudouridine in tRNAs and rRNAs of the two bacteria but it also explores the function of the responsible tRNA PUS enzymes. In addition, this study provides evidence for a dual function of the *C. jejuni* PUS enzyme TruD that goes beyond its RNA modifying function. Future research could focus on unravelling the function of TruD and its potential interaction partners and thus reveal new mechanisms of regulation of a protein previously only described as an RNA modification enzyme.

ZUSAMMENFASSUNG

Mehr als 150 verschiedene RNA-Modifikationen sind bislang in den unterschiedlichsten Organismen nachgewiesen worden, wovon 60 dieser Modifikationen in bakterieller RNA vorkommen. In Bakterien ist Pseudouridin eine der häufigsten Modifikationen, die in stabilen RNAs wie tRNAs und rRNAs zu finden sind. Hierbei wird das modifizierte Nukleotid auf posttranskriptioneller Ebene von speziellen Enzymen, den sogenannten Pseudouridin-Synthasen (PUS), generiert. Die Entwicklung und der Einsatz fortschrittlicher Deep-Sequencing Technologien ermöglichte es, Pseudouridin in unterschiedlichen RNA Klassen (tRNAs, rRNAs, mRNAs, snRNAs und lncRNAs) in verschiedenen eukaryotischen Organismen zu identifizieren. Diese Verfahren wurden jedoch noch nie auf Bakterien angewandt. Mutationen oder Deletionen spezifischer PUS Enzyme wurden im Menschen bereits mit der Entstehung von Krankheiten in Verbindung gebracht. Diese Enzyme sind daher für die korrekte Funktionsweise einer eukaryotischen Zelle unabdinglich. Nichtsdestotrotz führte die Deletion von tRNA oder rRNA PUS Enzymen im bakteriellen Modellorganismus *Escherichia coli* zu keinen solch drastischen Phänotypen. Dies wiederum deutet auf eine unterschiedliche Rolle und Funktion der Modifikation und der verantwortlichen Enzyme in verschiedenen Organismen hin.

In der vorliegenden Arbeit werden tRNA PUS Enzyme der Epsilonproteobakterien *Campylobacter jejuni* und *Helicobacter pylori* funktionell charakterisiert. Der Lebensmittelkeim *C. jejuni* ist derzeit die häufigste Ursache für bakteriell verursachte Gastroenteritis im Menschen. Dahingegen wird eine *H. pylori* Infektion mit der Entwicklung von Magenkrebs in Verbindung gebracht. Insbesondere wurden die Funktionen der tRNA PUS Enzyme TruA, TruB und TruD in *C. jejuni* sowie TruA und TruD in *H. pylori* untersucht. Während die Deletion von TruD keine phänotypischen Auswirkungen in *H. pylori* hat, führt diese in *C. jejuni* zu einem Wachstumsdefekt. Dies weist auf eine möglicherweise unterschiedliche Funktion des Enzyms in den beiden verwandten bakteriellen Krankheitserregern hin.

Zusätzlich beschreibt diese Arbeit die Etablierung und Anwendung von Pseudo-seq in *C. jejuni* und *H. pylori*, einem genomweiten Ansatz mittels dessen zum ersten Mal die globale Identifizierung von Pseudouridin Modifikationen auf Einzel-Nukleotid-Ebene im bakteriellen Transkriptom ermöglicht wird. Durch Pseudo-seq Analysen von wildtypischer RNA und RNA isoliert aus unterschiedlichen PUS Enzym Deletionen, konnten die RNA Substrate dieser Enzyme in *C. jejuni* und *H. pylori* ermittelt werden. Für TruD stellte sich dabei die tRNA-Glu als Hauptsubstrat heraus. Interessanterweise ist diese im Genom von *C. jejuni* nur als einzelne Kopie vorhanden. Da eine TruD Deletionsmutante in *C. jejuni* einen Wachstumsdefekt

aufweist, wurde dieser Phänotyp in Zusammenhang mit dem Auftreten der Pseudouridin Modifikation an der tRNA-Glu untersucht. Zu diesem Zweck wurde ein TruD Komplementationsstamm generiert, der jedoch katalytisch inaktiv ist und somit nicht in der Lage ist die Modifikation der tRNA-Glu wiederherzustellen. Überraschenderweise komplementierte dieser Stamm dennoch den Wachstumsdefekt. Eine ähnliche Beobachtung wurde bei einer Kreuzkomplementation mit einer Kopie von *H. pylori* TruD gemacht. Dies deutet darauf hin, dass das TruD PUS Enzym in *C. jejuni* möglicherweise eine zusätzliche Funktion unabhängig von der Pseudouridin Modifikation hat. Diese potentiell duale Funktion von TruD wird in dieser Arbeit durch die Anwendung einer Kombination von Deep-Sequencing Technologien (RIP-seq, RNA-seq, Ribo-seq und CLIP-seq) untersucht.

Insgesamt stellt diese Studie die erste eingehende Untersuchung von Pseudouridin Modifikationen in Bakterien im Allgemeinen, und in den Krankheitserregern *C. jejuni* und *H. pylori* im Speziellen, dar. Die in dieser Arbeit vorgelegten Ergebnisse beschreiben nicht nur eine globale Kartierung von Pseudouridin Modifikationen in bakteriellen tRNAs und rRNAs sondern erforschen auch die Funktionen der für die Modifikation verantwortlichen tRNA PUS Enzyme. Darüber hinaus liefert diese Arbeit Hinweise auf eine duale Funktion des *C. jejuni* PUS Enzyms TruD, die über die Funktion als RNA-modifizierendes Enzym hinausgeht. Zukünftige Untersuchungen könnten sich dementsprechend darauf konzentrieren, die Funktion von TruD und seinen potenziellen Interaktionspartnern zu entschlüsseln. Dies könnte neue Erkenntnisse über Mechanismen der Regulierung eines Enzyms/Proteins liefern, das bislang nur als RNA modifizierendes Enzym beschrieben war.

Table of contents

Abbreviation index

5' OH	5' hydroxyl
5' P	5' monophosphate
5' PP	5' diphosphate
5' PPP	5' triphosphate
A	adenine
A site	aminoacyl-tRNA site
aa	amino acid
ADAT	adenosine deaminase acting on tRNA
adj. p-value	adjusted p-value
B. subtilis	*Bacillus subtilis*
BSA	bovine serum albumin
C	cytosine
C. jejuni	*Campylobacter jejuni*
C. rodentium	*Citrobacter rodentium*
CagA	cytotoxin-associated gene A
cDNA	complementary DNA
CDS	coding sequence
Cia	*Campylobacter* invasion antigens
CLAP	CMC-RT and ligation assisted PCR analysis
CMC	N-cyclohexyl-N′-(2-morpholinoethyl) carbodiimide metho-p-toluenesulfonate
CTD	cytolethal distending protein
D	dihydrouridine
DNA	deoxyribonucleic acid
E. coli	*Escherichia coli*
ELIGOS	Epitranscriptional landscape lnferring from glitches of Oxford Nanopore technology signals
ELISA	Enzyme-linked immunosorbent assay
FAD	Flavin adenine dinucleotide
G	guanine
GtRNAdb	genomic tRNA database
H. ducreyi	*Haemophilus ducreyi*
H. pylori	*Helicobacter pylori*
hESC	human embryonic stem cell lines
I	inosine

i6A	N6-isopentenyladenosine
IGB	Integrated Genome Browser
IP	immunoprecipitation
LC-ESI-MS	liquid chromatography/electrospray ionization mass spectrometry
LC-MS	liquid chromatography/mass spectrometry
M. pneumoniae	*Mycoplasma pneumoniae*
m1G	1-methylguanosine
m5C	5-methylcytosine
m6A	N6-methyladenosine
m7G	7-methylguanosine
MALDI	Matrix Assisted Laser Desorption/Ionization
MeRIP-seq	methylome-RNA immunoprecipitation coupled with RNA-seq
miRNA	microRNA
mnm5U	5-methylaminomethyluridine
mRNA	messenger RNA
ms2i6A	2-methylthio-N6-isopentenyladenosine
MVS	methyl vinyl sulfone
NAD	Nicotinamide adenine dinucleotide
NGS	Next generation sequencing
Nm	2'-O-Methylation
OD	Optical density
OMP	outer membrane protein
ORF	open reading frame
P site	peptidyl-tRNA site
PAMP	pathogen-associated molecular pattern
PUS	pseudouridine synthase
RBP	RNA-binding protein
RBS	ribosome binding site
RIP	RNA immunoprecipitation
RNA	ribonucleic acid
RNA-seq	RNA sequencing
RNases	ribonucleases
rRNA	ribosomal RNA
RT	reverse transcriptase
S. cerevisiae	*Saccharomyces cerevisiae*

S. flexneri	*Shigella flexneri*
S. marcescens	*Serratia marcescens*
S. Typhimurium	*Salmonella* Typhimurium
s2U	2-thiouridine
sRNA	small RNA
T	thymine
TLC	thin layer chromatography
tRNA	transfer RNA
TSS	transcriptional start site
U	uridine
UDP-Glc	uracil-diphosphate glucose
UDP-GlcNac	uracil-diphosphate *N*-acetylglucosamine
UMIs	Unique molecular identifiers
UTR	untranslated region
V. cholerae	*Vibrio cholera*
VacA	vacuolating cytotoxin A
W. succinogenes	*Wolinella succinogenes*
Y. pestis	*Yersinia pestis*
Ψ	Pseudouridine

Units

%	percent
° C	degree Celsius
A	Ampere
Bp	base pair(s)
Ci	Curie
Da	Dalton
g	gram
h/hrs	hour(s)
l	liter
M	molar
min	minute(s)
molar	gram molecule
nt	nucleotide(s)
pH	minus the decimal logarithm of the hydrogen concentration
rpm	rounds per minute
s/sec	second(s)
u	unit
V	Volt
W	Watt

Multiples

M	mega (10^6)
k	kilo (10^3)
c	centi (10^{-2})
m	milli (10^{-3})
µ	micro (10^{-6})
n	nano (10^{-9})
p	pico (10^{-12})

Aim of this thesis

So far, more than 150 different RNA modifications have been described to decorate abundant housekeeping RNAs such as transfer RNAs (tRNAs) and ribosomal RNAs (rRNAs) in all domains of life (Boccaletto *et al.*, 2022). Among these modified nucleotides, about 60 different types of RNA modifications have been reported in bacteria (Marbaniang & Vogel, 2016), with the majority found in tRNAs and in 16S and 23S rRNAs (Marbaniang & Vogel, 2016). However, the recent development of genome-wide approaches allowed to detect modified nucleotides also in eukaryotic and prokaryotic messenger RNAs (mRNAs) (Li *et al.*, 2016; Höfer & Jäschke, 2018a), suggesting that RNA modifications might be involved in central process in the cell such as translation or gene expression regulation. While eukaryotic mRNA pseudouridylation has been reported by various studies, its function remains elusive (Carlile *et al.*, 2014; Lovejoy *et al.*, 2014; Schwartz *et al.*, 2014; Nakamoto *et al.*, 2017). Described in 1951, pseudouridine (Ψ) is one of the first RNA modifications to be discovered (Cohn & Volkin, 1951) and represents one of the most abundantly modified nucleotides to date (Charette & Gray, 2000). Besides studies in eukaryotic systems, the knowledge about a global map of Ψ in a bacterial transcriptome and an accompanying functional characterization of PUS enzymes in bacteria is still missing.

In order to gain insights into pseudouridylation in bacteria, my PhD thesis aims to investigate the role of tRNA PUS enzymes in the two Epsilonproteobacteria *Campylobacter jejuni* and *Helicobacter pylori*. Moreover, to globally map pseudouridine modifications in the transcriptomes of the two bacterial pathogens a genome-wide approach, so-called Pseudo-seq, will be applied. In addition, to explore the function of tRNA PUS enzymes, their RNA substrates will be identified by Pseudo-seq in RNAs of wildtype and PUS mutant strains. Furthermore, this thesis aims to elucidate the roles of tRNA PUS enzymes beyond their catalytic activity.

Contribution by others

The work described here was conducted under the supervision of Professor Dr. Cynthia M. Sharma at the Institute of Molecular Infection Biology (IMIB), University of Würzburg.

Several parts of the work described here have been contributed by others and are listened below.

- The preliminary Pseudo-seq experiment of *Campylobacter jejuni* wildtype was performed by Dr. Gaurav Dugar.
- RIP-seq, RNA-seq, and CLIP-seq bioinformatic analyses were performed by Dr. Thorsten Bischler.
- Pseudo-seq analysis was performed by Dr. Thorsten Bischler and Prof. Lars Barquist.
- Ribo-seq analysis was performed by Rick Gelhausen.
- Deletion of *truA*, *truB* and *truD* and complementation of *truA* and *truB* strains of tRNA PUS enzymes in *Campylobacter jejuni* were performed by Dr. Gaurav Dugar and Dr. Patrick Tan.
- Preliminary RIP-seq experiment was conducted by Dr. Patrick Tan.
- Generation of the RIP-seq and RNA-seq cDNA libraries was performed by Vertis Biotechnologie.
- Sequencing of cDNA libraries was performed by the CORE Unit.

1. Introduction

Ribonucleic acid (RNA) is a polymeric chain consisting of four canonical ribonucleotides that is involved in a multitude of cellular processes (*The biochemistry of the nucleic acids*, 1972; Adams *et al.*, 1992). Depending on their function, RNA molecules are divided into different categories. Three classes of RNA are directly involved in protein synthesis: messenger RNA (mRNA), ribosomal RNA (rRNA), and transfer RNA (tRNA). While mRNAs convert the genetic information stored in deoxyribonucleic acid (DNA) in order to build proteins (Brenner *et al.*, 1961; Gros *et al.*, 1961), rRNAs and tRNAs are at the core of the translational machinery (Palade, 1955; Hoagland *et al.*, 1958). The coding sequence (CDS) of an mRNA represents a sequence of base triplets consisting of three nucleotides each (codon), that base pair with the anticodon sequence of a tRNA molecule. This base-pairing ensures the correct incorporation of a specific amino acid into the emerging peptide during translation. This is facilitated by the ribosome, a ribonucleoprotein complex consisting of a set of ribosomal proteins and rRNAs. In addition to those RNAs involved in translation, new types of regulatory non-coding RNA classes have been discovered (e.g., bacterial small RNAs or, for example, eukaryotic microRNAs, small interfering RNAs, and long noncoding RNAs) within the last decades. They execute their function via base-pairing with target mRNAs to regulate their expression (Lee *et al.*, 1993; Reinhart *et al.*, 2000; Storz *et al.*, 2011; O'Brien *et al.*, 2018). In the bacterial cell, these regulatory RNAs modulate central processes such as cell division, stress response, or pathogenesis (Gottesman & Storz, 2011). Together, these aspects underline the multifaceted functions of regulatory RNAs in numerous essential processes in the cell, mediated by the structure and/or the sequence of the molecules.

With the discovery of non-canonical nucleotides (or modified nucleotides), scientists hypothesized that the biological roles of RNA might be more complex than previously anticipated (Cohn & Volkin, 1951). For instance, these findings completely revolutionized the idea that RNA is merely transcribed from DNA. Instead, after its synthesis, the molecule undergoes a complex network of posttranscriptional modifications that completely changes the parental nucleotide composition, thus affecting RNA sequence, structure, and stability (Kierzek *et al.*, 2014; Liu *et al.*, 2015). For this reason, the term "RNA epigenetics" was coined to describe an emerging branch of functional genomics that studies the biological relevance of RNA modifications (He, 2010).

The following chapters are meant to provide a general overview of bacterial RNA modifications and technologies that allow their detection within the transcriptome of different organisms, with a particular focus on the pseudouridine modification.

1.1. History of RNA modifications and their distribution in the different kingdoms of life

The first RNA modification was identified in 1951 after assuming it to be an unknown compound detected after RNA hydrolysis (Cohn & Volkin, 1951). Only in 1957, the chemical structure was solved as 5-ribosyluridine (also called the fifth nucleoside or pseudouridine (Ψ)) (Davis & Allen, 1957; Cohn, 1959; Yu & Allen, 1959). In the 1970s, the methylation of adenosine at the nitrogen-6 position (m6A) was identified for the first time in mRNAs ((Desrosiers *et al.*, 1974) and reviewed in (Yue *et al.*, 2015)), but its function remained unknown for a long time. For many years, researchers were aware that RNA modifications exist, but a lack of proper methodologies did not allow their systematic detection and functional characterization. Recently, with the advent of more sophisticated high-throughput technologies, m6A has been described as one of the most abundant RNA modifications within different classes of RNA (mRNA, rRNA, tRNA, and diverse non-coding RNAs) in eukaryotes, bacteria, and archaea (Deng *et al.*, 2015).

The continuous development and optimization of high-throughput and mass-spectrometry based techniques have strongly accelerated the discovery of new RNA modifications. While DNA modifications are limited to six (Bohnsack *et al.*, 2019), more than 150 types of RNA modifications have been described in all kingdoms of life so far (Boccaletto *et al.*, 2018; Schauerte *et al.*, 2021). Ribosomal RNAs and tRNAs represent the most modified RNA species in the cell: it has been estimated that a human tRNA molecule contains on average 13 different modified nucleotides (Pan, 2018; Levi & Arava, 2021), all potentially contributing to its function.

RNA modifications are not always ubiquitous: some of them are limited to (1) a specific kingdom of life, (2) a specific class of RNA (tRNA, rRNA, mRNA, or regulatory RNA), or (3) a specific region of the molecule ((e.g., 5' untranslated region (5' UTR), 3' untranslated region (3' UTR), or coding sequence (CDS)) (McCown *et al.*, 2020). For example, m6A in bacteria has been shown to be present across the entire open reading frame (ORF) and located within a GCCAG consensus sequence. In eukaryotes however, it is mostly present in 3' UTRs or stop codons and located within an RRACU motif (Deng *et al.*, 2015). Moreover, in bacteria the ratio between m6A and unmodified adenosine seems to be stable throughout different growth phases, while in eukaryotes the ratio appears to be more dynamic (Jia *et al.*, 2011; Marbaniang & Vogel, 2016; Höfer & Jäschke, 2018b). These findings demonstrate that the same RNA modification can have a varying impact in different organisms and that the enzymes responsible for the modification have evolved to recognize different sequences/structures of the target RNAs.

1.2. RNA modifications in bacteria

In bacteria, roughly 60 RNA modifications are described so far, with the majority residing in tRNAs and rRNAs (Marbaniang & Vogel, 2016). However, besides the high number of modifications found in stable RNAs, their functions and locations in other transcripts such as mRNAs and/or regulatory RNAs are still overlooked. Based on their location within bacterial transcripts, two types of RNA modifications can be distinguished: internal and 5′ terminal modifications. While internal modifications decorate the entire transcript, 5′ terminal modifications mark the 5′ end of the RNA molecule. In addition, their location can infer different functional implications. While internal modifications, when present in mRNAs, can modulate translation, stability or recoding of the RNA, 5′–end modifications are involved in RNA processing and/or binding of processing enzymes (e.g., endo- and exonucleases). The most studied internal RNA modifications in bacteria are inosine (I), methylation of cytosine (m5C), methylation of adenosine (m6A), and methylation of the 2′-hydroxyl group of the ribose (Nm, where N stands for any nucleotide). Among these, only m6A and I have been shown to be located in prokaryotic mRNAs so far, and m5C and Nm are found in stable tRNA and rRNA. Additionally, also other 5′ terminal modifications, such as phosphorylation and cap-like structures, were detected in bacterial RNA (Schauerte *et al.*, 2021).

1.2.1. 5' terminal RNA modifications

5' triphosphorylated (PPP)/ diphosphorylated (PP)/monophosphate (P) / hydroxylated (OH) terminus. In bacteria, the phosphorylation at the 5' end of the RNA defines its origin. A triphosphate group (5' PPP) at the first transcribed nucleotide marks the RNA as a primary transcript. The triphosphate group can subsequently be processed or modified into a diphosphate (5' PP), monophosphate (5' P), or hydroxyl (5' OH) group (Bremer *et al.*, 1965; Jorgensen *et al.*, 1969; Apirion, 1973; Konrad *et al.*, 1976; Vasilyev *et al.*, 2018). These different modifications are linked to various processes in the cell. In *E. coli*, 5' P, generated by the pyrophosphohydrolase RppH, leads to RNA cleavage mediated by RNase E, thus promoting the degradation of that particular transcript (Richards & Belasco, 2016). Diphosphorylated RNAs have also recently been identified in the *E. coli* transcriptome and suggested to serve as the preferential substrate for RppH (Luciano *et al.*, 2017). 5′ OH RNAs are associated with processing of the transcripts mediated by nuclease digestion or result from degradation (Vasilyev *et al.*, 2019). Interestingly, transcription can also be initiated from short oligonucleotides (2-5 nts) called nanoRNAs derived from degradation of cellular RNAs (Goldman *et al.*, 2011). Transcription initiation based on these nanoRNAs has been described

for *Pseudomonas aeruginosa*, *E. coli*, and *Vibrio cholera*, and these new transcripts typically also carry a 5' OH group. In *E. coli* expression of these transcripts seems to be associated with specific biological functions such as biofilm formation or stress response (Nickels, 2012).

5'-capped RNAs. Similar to eukaryotic RNAs, bacterial RNAs exhibit a cap-like structure at their 5' end. While in eukaryotes, 5' ends are linked to a 7-methylguanosine triphosphate (m7G), the bacterial cap is made of cofactors like nicotinamide adenine dinucleotide (NAD) (Shatkin, 1976). A genome-wide analysis of NAD-capped RNAs in *E. coli* showed the presence of the cofactor mainly at the 5' end of sRNAs, whereas in the Gram-positive *Bacillus subtilis* the NAD cap was mostly found on mRNAs (Cahová *et al.*, 2015; Frindert *et al.*, 2018). Studies demonstrated that the NAD cap structure protects the transcripts against digestion from the 5' end by nucleases such as RNase E in *E. coli* or RNase J1 in *B. subtilis* (Cahová *et al.*, 2015; Frindert *et al.*, 2018). Besides NAD, the redox cofactor of multiple essential metabolic processes flavin adenine dinucleotide (FAD) has also been suggested to build up a non-canonical cap (Höfer & Jäschke, 2018a). Although the presence of FAD-capped RNAs in *E. coli* was demonstrated, identification of specific FAD-capped transcripts has not been reported yet. Thus, the function of this particular cap structure on bacterial RNAs is not yet clear. Other interesting examples of RNA cap structures are the precursors of UDP-glucose (UDP-Glc) and UDP-*N*-acetylglucosamine (UDP-GlcNAc). The incorporation of these precursors is mediated by the RNA polymerase on transcripts initiating with a uridine (reviewed in (Schauerte *et al.*, 2021)).
While the role of 5´-end modifications in bacterial RNA is mostly linked to stability of the molecule, the function of internal modifications is only poorly characterized.

1.2.2. Internal modifications

***Adenosine-to-Inosine (A-to-I) editing*.** A-to-I editing represents one of the most common RNA modifications described for bacterial tRNAs (ACG anticodon in the $tRNA^{Arg}$) at position 34 (Wolf *et al.*, 2002). The 34^{th} position is also called "wobble position" and refers to the first nucleotide in the tRNA anticodon that base pairs with the third nucleotide of the codon of an mRNA. The nucleotide is termed "wobble", because it can base pair with the third nucleotide of the corresponding codon in a more flexible way, thereby explaining the redundancy of the genetic code (Crick, 1966). In the case of inosine, it can base pair with A, U, or C, which allows the decoding of multiple codons, thus expanding the coding capability (Alseth *et al.*, 2014; Rafels-Ybern *et al.*, 2018). In eukaryotic RNAs, the conversion of A to I is based on the deamination of adenosine, generated by so-called tRNA adenosine deaminases (or ADATs) or

mRNA adenosine deaminases (ADARs). In *E. coli*, the enzyme that catalyzes this reaction is the tRNA adenosine deaminase A (TadA) (Auxilien *et al.*, 1996; Wolf *et al.*, 2002; Torres *et al.*, 2014; Bar-Yaacov *et al.*, 2017). Inosine-editing events can be mapped in a genome-wide manner using an RNA-sequencing (RNA-seq) approach based on the chemical property of this modification: inosine strongly and preferentially base pairs with C and when reverse transcribed into complementary DNA (cDNA) and amplified by PCR, this results in the incorporation of G instead of A (Schwartz & Motorin, 2017). High-throughput sequencing of DNA and RNA in parallel, followed by nucleotide sequence comparison in two *E. coli* strains was used to identify mRNA editing events. Interestingly, 12 sites were detected in well-known protein-coding genes and found to affect protein sequence, activity, and consequently cell physiology (Bar-Yaacov *et al.*, 2017). This study represents the first example of RNA editing reported in bacteria, where an RNA modification influences the intracellular proteome diversity. It has been additionally reported an inosine site in the gene encoding the flagellar filament protein *fliC* of *Xanthomonas oryzae* pv. *oryzicola* during exposion of the bacteria to oxidative stress (Nie *et al.*, 2020). The presence of the modification leads to the generation of a serine to proline mutation (S128P) at the protein level that affect the structure of the flagellar filaments and thus, influencing the virulence of the bacteria.

Methylation of cytosine (m5C). A well-known modification that has been shown for both DNA and RNA is the methylation of cytosine (m5C). Cytosine methylation is generated by dedicated enzymes called m5C methyltransferases (m5C-MTases). In *E. coli*, the 16S rRNA is modified at two positions (C967 and C1407) by two distinct MTases: RsmB and RsmF (Foster *et al.*, 2003; Andersen & Douthwaite, 2006). It has been suggested that both modifications might be implicated in tRNA binding (Tscherne *et al.*, 1999), however, only C1407 was shown to be involved in the ribosomal subunit association or translocation process (Andersen & Douthwaite, 2006). The identification of this particular modification in DNA was facilitated by treatment with bisulfite causing the deamination of unmodified cytosine to uracil without affecting the properties of the methylated cytosine (Frommer *et al.*, 1992). For the discovery of the m5C modification in RNA the bisulfite protocol was adapted to RNAs and high-throughput sequencing was performed (Schaefer *et al.*, 2009). In 2013, the RNA methylome of *B. subtilis* (Gram-positive), *E. coli* (Gram-negative), and *Sulfolobus solfataricus* (archaeon) was published (Edelheit *et al.*, 2013). While this study confirmed the presence of m5C in rRNAs from all three organisms, m5C modification in mRNAs was identified only in archaea and still remains elusive in bacteria.

***Methylation of adenosine (m6A)*.** Methylation of adenosine at position N6 (m6A) has been identified both in eukaryotes and prokaryotes. In *E. coli*, m6A was first described for the 23S rRNA at positions A1618 and A2030, with implications for the conformational stability of the rRNA (Sergiev *et al.*, 2008; Golovina *et al.*, 2012). Moreover, m6A was identified in mRNA isolated from seven different bacterial species by using a highly sensitive liquid chromatography method coupled with mass spectrometry (LC-MS) (Deng *et al.*, 2015). In the same study, m6A was globally identified in the transcriptomes of *E. coli* and *P. aeruginosa* using an immunoprecipitation (IP)-based approach. In *E. coli*, 265 peaks were detected and distributed among 213 protein-coding genes and 15 sRNAs. The enrichment for m6A modification was identified in well-known sRNAs, such as MicF, RybB, and GlmY. However, no biological function could be linked to the presence of the m6A modification in these regulatory RNAs. The modification was mostly identified within the ORFs of genes involved in general metabolism and species-specific traits (e.g., response to abiotic stress, cell-wall biosynthesis, and anaerobic respiration), suggesting an important role of this abundant RNA modification in bacteria. However, besides the identification of m6A in bacterial transcriptomes, the molecular function of this modification in bacteria is still unclear.

Methylation of the 2' hydroxyl group of ribose (Nm). Nm is one of the most common RNA modifications described in many species (Ayadi *et al.*, 2018; Dimitrova *et al.*, 2019). In bacteria, a relatively rare process mediated by a specific methyltransferase leads to this modification (Hori, 2017). In *E. coli*, TrmH is responsible for the methylation of different tRNAs at position 18 (Persson *et al.*, 1997), whereas TrmJ and TrmL catalyze the methylation at positions 32 and 34, respectively (Galvanin *et al.*, 2020). Methylation of guanosine at position 18 in the D-loop of tRNA-Tyr of *E. coli* was shown to help the bacteria suppress activation of the innate immune system in human cells (Karikó *et al.*, 2005; Keller *et al.*, 2018). This represents a unique example of modified RNA that reduces the activity of a pathogen-associated molecular pattern (PAMP). Due to its chemical structure, 2'-*O*-methylation promotes RNA stability against alkaline hydrolysis by altering the hydration sphere around the oxygen (Auffinger & Westhof, 1997, 1998; Helm, 2006). This property paved the way for the development of different high-throughput detection methods. One such method is called RiboMeth-Seq (Motorin & Marchand, 2018). The technique was recently applied to *E. coli* tRNAs in order to investigate changes in the 2'-*O*-methylation levels during stress conditions (mild antibiotic stress and starvation) (Galvanin *et al.*, 2020). The analysis revealed that only methylation at position 18 in different tRNAs increased under antibiotic stress, suggesting that RNA modifications contribute to a dynamic response to certain stress conditions.

Pseudouridine (Ψ). Pseudouridine (Ψ) is one of the most abundant and oldest internal RNA modifications identified in all kingdoms of life (Cohn & Volkin, 1951). The modified nucleotide is the product of the posttranscriptional isomerization of uridine mediated by enzymes called pseudouridine synthases (PUSs) (Cortese *et al.*, 1974; Arena *et al.*, 1978; Samuelsson & Olsson, 1990). Since Ψ is the focus of this PhD thesis, its properties, functional implications, and other aspects of this modification will be discussed in more detail in a separate paragraph.

1.3. Overview of methods used to identify RNA modifications

In the last decades, the discovery of RNA modifications has encountered challenges due to the limitations in methods that allow their identification, quantification, and mapping in the transcriptome. The detection of RNA modifications has often been limited to short RNA species (e.g., tRNA) and relied on biophysical methods like thin-layer chromatography (TLC), anion-exchange chromatography, or UV spectrophotometry (Marbaniang & Vogel, 2016; Höfer & Jäschke, 2018a). TLC allows for separation and identification of compounds present in a mixture. In the specific case of RNA modification detection, TLC is based on the complete digestion of an RNA molecule by nucleases, followed by the analysis of the mono- or dinucleotide products by two-dimensional thin layer chromatography (2D-TLC) (Figure 1.1 A). Each of the different nucleotides exhibit a specific migration pattern on the TLC plate, which allowed the identification of approximately 70 different RNA modifications (Grosjean *et al.*, 2004). But there are some limitations, such as the length of the RNA molecule, which cannot exceed 100-150 nt, in addition to the necessity of radioactively labeling the RNA for detection (Pomerantz & McCloskey, 1990; Grosjean *et al.*, 2004; Kellner *et al.*, 2010). This method was recently substituted by optimized liquid chromatography coupled with mass spectrometry (LC-MS), which can distinguish modified nucleotides due to different retention times and mass-to-charge ratios of their counterparts (Figure 1.1 B) (Pomerantz & McCloskey, 1990; Suzuki *et al.*, 2007).

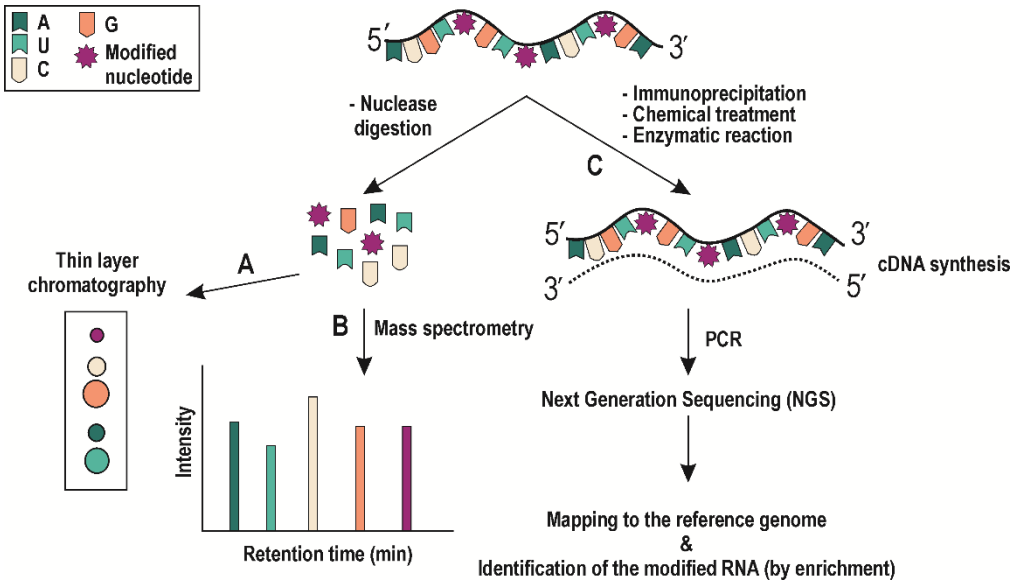

Figure 1.1: Current methods to detect RNA modifications. Identification of RNA modifications can be mediated by digestion of the RNA to single nucleotides followed by thin layer chromatography **(A)** or mass spectrometry **(B)**. **(C)** Another method to identify RNA modifications is based on immunoprecipitation, enzymatic reaction, or chemical treatment thereby isolating specific target RNAs that are subsequently identified by Next Generation Sequencing (NGS). Figure is adapted from (Höfer & Jäschke, 2018a).

However, one of the major limitations of this method is the requirement of high amounts of pure samples which might thus hide the information residing in lowly abundant mRNAs or sRNAs. Additionally, TLC and LC-MS do not provide any information about the location of the modified nucleotide in the sequence of the RNA molecule.

In an effort to overcome the shortcomings of these biophysical methods, Next Generation Sequencing (NGS) techniques have been developed, adapted, and employed to detect RNA modifications. RNA-seq based technologies rely on the generation of cDNA libraries that represent the products of a previous enrichment step of IP/chemical treatment/enzymatic reaction of the modified RNA (Figure 1.1 C). These approaches have certain advantages. For example, they need relatively low amounts of the input sample for the generation of cDNA libraries (Heinicke *et al.*, 2020). Moreover, sequencing of the entire transcriptome also provides information about the precise location of the respective modification in different RNA species. One of the limitations of these approaches is the lack of specific antibodies or chemical compounds for detection of most of the so far known RNA modifications.

The next two paragraphs focus on methods based on IP or chemical treatment followed by NGS.

1.3.1. Detection of RNA modifications by immunoprecipitation based method

RNA immunoprecipitation coupled with RNA-sequencing (RIP-seq) represents one of the most powerful methods to detect the RNA targetome of a specific RNA-binding protein (RBP). In this method, an antibody directed against the protein of interest is used to pull down the RNA-protein complexes which is then followed by RNA-seq of the bound RNA. In the specific case of RNA modifications, an antibody is generated against a modified nucleoside to selectively pull-down all modified RNAs, and subsequently cDNA libraries for NGS are produced. By comparing the reads of the immunoprecipitated (IP) libraries with the mock control (library prepared without the antibody), the presence of specifically enriched peaks in the IP libraries indicates potentially modified sites in a specific set of pulled-down RNAs (Figure 1.2).

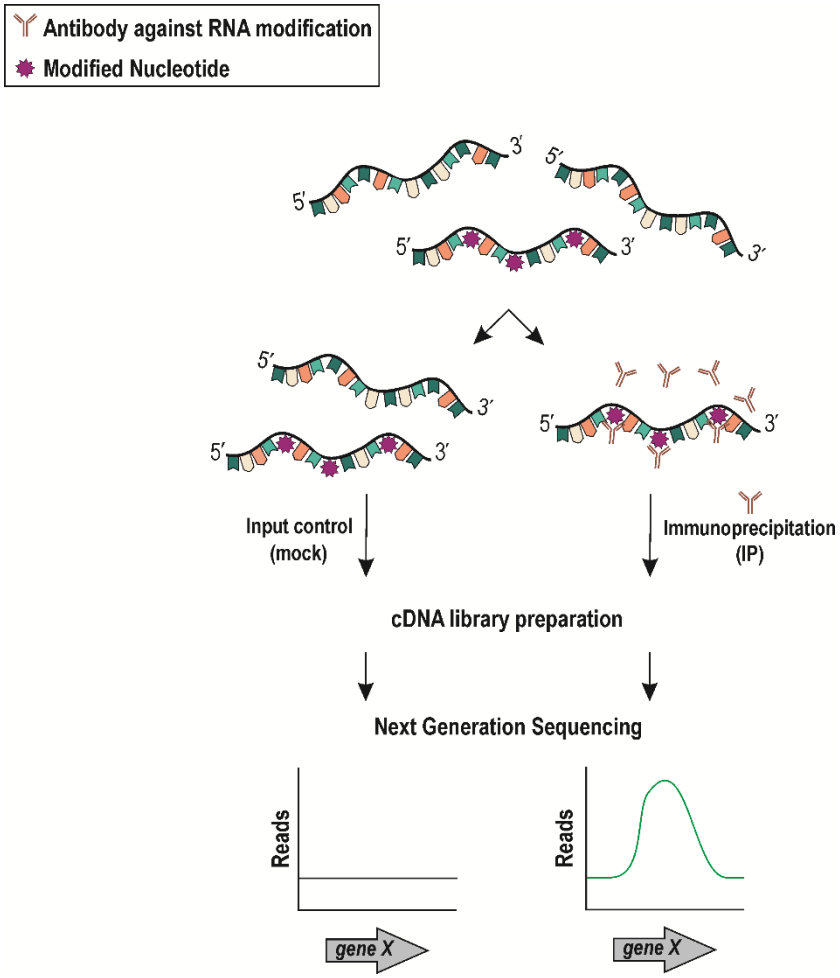

Figure legend on next page

Figure 1.2: Detection of RNA modifications by immunoprecipitation based methods. Antibodies directed against a specific RNA modification selectively pull down the modified RNAs (IP) which are consecutively used for cDNA library generation. RNA without prior antibody incubation (input control) is used as a control. After NGS, read numbers of the IP sample are compared to the mock control, thus identifying an enrichment in the modified RNA. Figure is inspired by (Höfer & Jäschke, 2018a).

Already in the 1980s, antibodies directed against m6A were used to pulldown RNAs that contained this modification, without coupling it to RNA-seq analysis (Horowitz *et al.*, 1984). This was latter adapted by two different groups for transcriptome-wide identification of m6A modification of eukaryotic RNAs using Methylome-RNA immunoprecipitation coupled with RNA sequencing (MeRIP-seq) (Dominissini *et al.*, 2012; Meyer *et al.*, 2012). However, the MeRIP-seq approach presents numerous limitations strictly dependent on the specificity and the affinity of the antibody used for the experiment. For example, antibodies for m6A can also recognize N6, 2′-O-dimethyladenosine ($m6A_m$) (Linder *et al.*, 2015).

Early trials for the experimental generation of antibodies against DNA or RNA nucleotides were largely unsuccessful due to the fact that the nucleic acids used were too short to elicit an immune response (Feederle & Schepers, 2017). Between the 1970s-1980s, scientists realised that an immune response can also be triggered by coupling the nucleotides to an immunogenic carrier protein such as bovine serum albumin (BSA). However, the oxidation reaction that allows BSA to be coupled to the nucleotides opens up the ribose ring (in position 2' and 3'), which prohibits distinguishing RNA from DNA, or nucleic acid with modified 2' and 3' positions in general (Feederle & Schepers, 2017). Recently, click chemistry offered an alternative to couple nucleotides to carrier proteins while keeping the sugar intact. Further, avoiding the oxidation reaction allowed to distinguish RNA from DNA and the presence of modified ribose groups (Feederle & Schepers, 2017).

Although the recent optimizations of antibodies against different types of RNA modifications have been of great benefit for the field (Weichmann *et al.*, 2020), most of the IP-based approaches cannot identify RNA modifications at single nucleotide resolution. Additionally, it is also possible that the antibody might bind other sequences or nucleotides (Helm *et al.*, 2019). Therefore, developing a method that takes these limitations into consideration will improve the detection of the modification at higher resolution in the RNA molecule.

1.3.2. Detection of RNA modifications by chemical reagents

To overcome the limitations associated with antibody-based approaches, different groups developed RNA-seq techniques applying chemical treatment to RNA. For example, the

detection of m5C is based on a bisulfite treatment of RNAs at alkaline pH. While the bisulfite ions generate a chemical deamination of unmodified cytosines, methylated cytosines are resistant to the treatment. The deamination will convert cytosine into uridine and comparison of the RNA-seq profiles with the reference genome will indicate which cytosines are modified (Figure 1.3) (Schaefer *et al.*, 2009). To detect pseudouridine, a similar approach was performed based on N-cyclohexyl-N′-(2-morpholinoethyl) carbodiimide metho-p-toluenesulfonate (CMC). In this case, the chemical compound will bind to pseudouridine and generate a block for the reverse transcriptase (RT) at the modified site. After cDNA library preparation and deep-sequencing the comparison between treated and untreated library will provide information about the position of the modified nucleotide within a given transcript at single-nucleotide resolution.

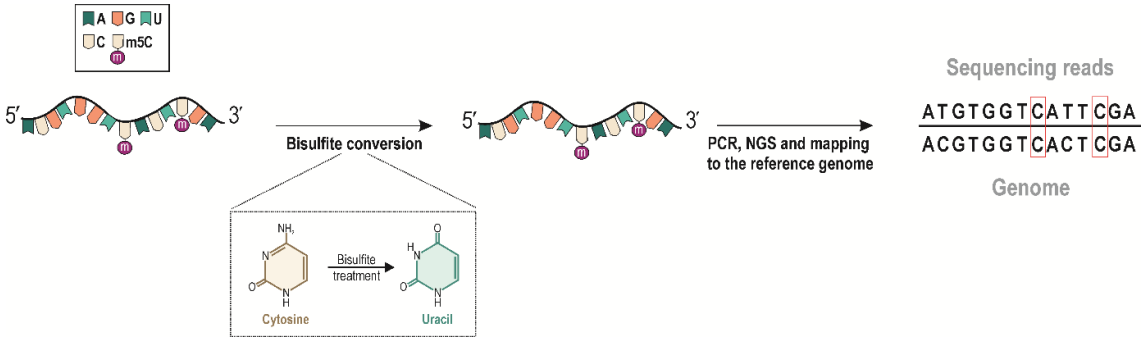

Figure 1.3: Detection of m5C modification by bisulfite treatment. The unmodified cytosines are converted to uridine after the chemical treatment with bisulfite, while the methylated cytosines are not. NGS libraries are generated after the treatment and the comparison between the mapped reads and their corresponding genomic nucleotide sequences discriminates between modified (red square) and unmodified cytosines. Figure is inspired by (Höfer & Jäschke, 2018a).

But RNA-seq based technologies also have limitations. The first limitation pertains to the differences in abundance of certain RNA classes: tRNAs and rRNAs are more abundant than mRNAs and sRNAs. As a consequence, it is conceivable that the modification will not be identified in lowly expressed genes. However, this drawback is recently overcome by the application of protocols that deplete the total RNA from rRNAs prior RNA-seq. A second limitation arises from the lack of bioinformatic tools and pipelines that allow the prediction of putatively modified sites out of a large amount of sequencing datasets.

1.3.3. Detection of RNA modifications using Nanopore sequencing technology

One of the most recent methods to identify RNA modifications is based on the Nanopore sequencing technology, which relies on real-time sequencing of native nucleic acid molecules

(DNA or RNA). Major advantages of this approach include the loss of potential bias arising from cDNA conversion and PCR amplification and the sequencing of very long reads (Xu & Seki, 2020).

The nucleic acid that enters the pore in a sequencer causes a so-called “squiggle” due to a difference in the electric current when a nucleotide passes through the synthetic polymeric membrane. In particular, the presence of a nucleotide modification causes a current blockade/errors during the sequencing reaction that can be predicted using specific tools based on machine learning and statistical tests (Xu & Seki, 2020). One of these tools is called ELIGOS (Epitranscriptional Landscape Inferring from Glitches of Oxford nanopore technologies Signals) and calculates and compares the percentage of the sequencing error in each base between the modified and unmodified ribonucleotides. The tool was used to identify ribosomal RNA modifications in different species (*Saccharomyces cerevisiae*, *E. coli*, and multiple human cell lines) (Jenjaroenpun *et al.*, 2021). Based on the properties of the Nanopore, the method has been adapted to identify m6A and m5C modifications in eukaryotic mRNAs (Garalde *et al.*, 2018; Liu *et al.*, 2019; Xu & Seki, 2020).

While the price for sequencing is not much different compared to other technologies, one disadvantage of Nanopore sequencing is that due to the long-read sequencing the error rate is higher compared to the short-read sequencing of NGS. However, this drawback is constantly improved by postsequencing correction tools and novel base-calling algorithms (Sahlin *et al.*, 2021).

1.4. Pseudouridine, the fifth nucleotide

Among the internal RNA modifications, my thesis focuses on the pseudouridine (Ψ) modification and in particular, on methods to identify this modified nucleotide in the transcriptomes of bacteria. Pseudouridine is one of the most abundant modified nucleotides, present in stable RNAs (e.g., tRNAs and rRNAs) throughout all kingdoms of life. Ψ is a universally-conserved isomer of uridine, which is posttranscriptionally generated by pseudouridine synthases (PUSs). As shown in Figure 1.4, the isomerization generates an additional hydrogen bond donor that contributes to unusual base pairing interactions between Ψ and A, C, or G (Kierzek *et al.*, 2014). In bacteria, pseudouridine is the most abundant modification detected in housekeeping RNAs such as tRNAs and rRNAs (Charette & Gray, 2000).

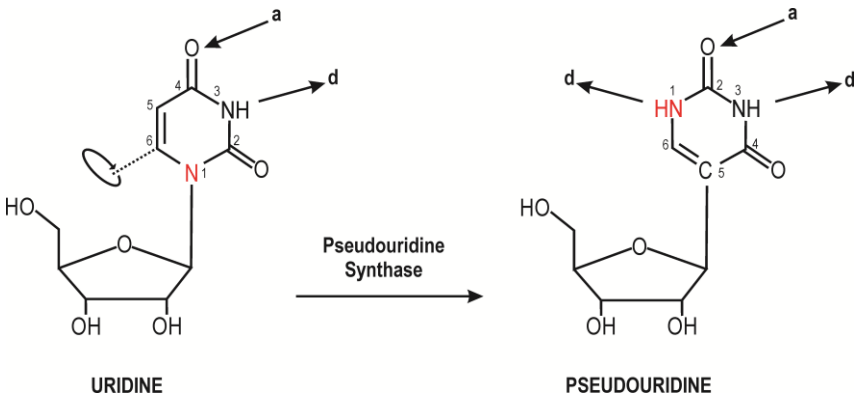

Figure 1.4: Isomerization of uridine to pseudouridine is mediated by pseudouridine synthases. Numbers indicate the different atom positions in uridine and pseudouridine pyrimidine rings. The red N and C atoms highlight the major difference in the chemical bond in uridine or pseudouridine to the ribose sugar. The "a" and "d" represent hydrogen "acceptors" and "donors".

While this modification was identified many years ago, very little is known about its function, even when present in housekeeping RNAs. In tRNAs, Ψ was suggested to modulate the structure and stability of the RNA molecule (Charette et a., 2000). Moreover, it has been shown that the presence of Ψ in the anticodon loop of tRNAs could facilitate alternative codon usage (Tomita *et al*., 1999). In rRNAs, Ψ might influence both rRNA folding and ribosome assembly (Ofengand *et al*., 1998; Cunningham *et al*., 1991). In eukaryotic mRNAs, it has been shown that the presence of this modification might affect the interaction between the RNA with a protein partner, which in turn could impact its function (Vaidyanathan *et al.*, 2017).

In the last 50 years, different aspects about pseudouridine and PUS enzymes in eukaryotes and prokaryotes were discovered by the scientific community. Figure 1.5 illustrates the timeline of some of these findings.

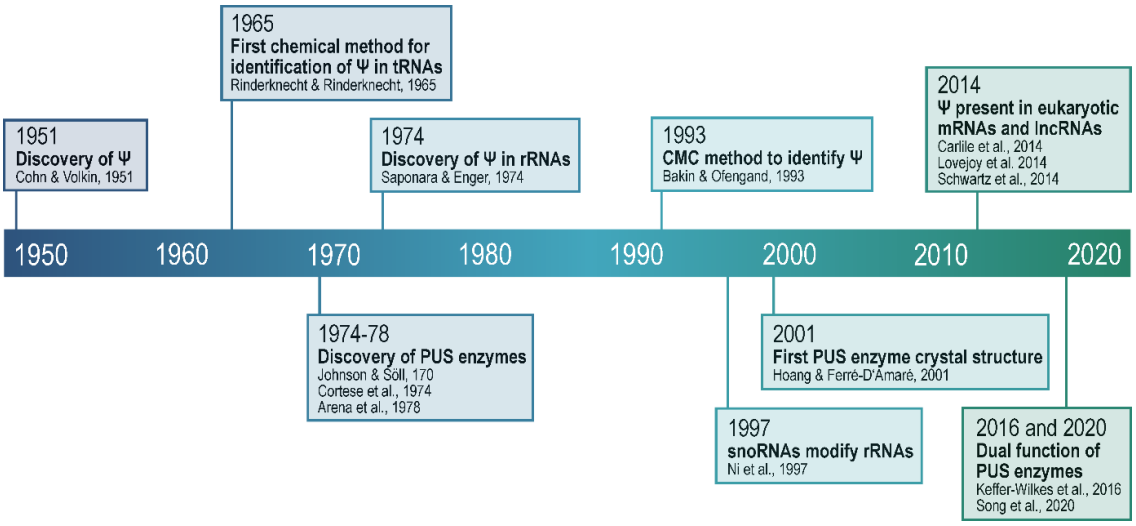

Figure 1.5: Timeline describing the major discoveries in pseudouridine and PUS enzyme biology. Historical milestones from the discovery of pseudouridine in 1951 to dual function PUS enzymes in 2020.

Starting from its discovery in 1951, pseudouridine was detected in various types of RNA in different kingdoms of life. Only in the middle of 1970, the enzymes responsible for the generation of the modification were identified. But only recently, it has been shown that specific PUS enzymes could fulfill dual functions in the cell. For example, in addition to promoting the isomerization of uridine they might also function as tRNA chaperones or enhance miRNA maturation (Keffer-Wilkes *et al.*, 2016; Kurimoto *et al.*, 2020).

1.4.1. Mechanisms of pseudouridine generation

The posttranscriptional generation of pseudouridine is based on two distinct mechanisms: an RNA-dependent and an RNA-independent mechanism (Figure 1.6) (De Zoysa & Yu, 2017).

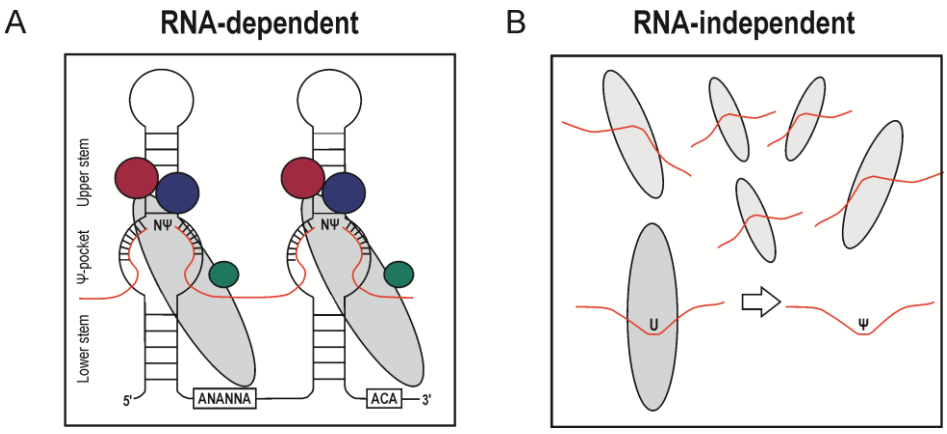

Figure legend on next page

Figure 1.6: Mechanisms for the generation of pseudouridine. (A) In the RNA-dependent mechanism, the generation of pseudouridine is mediated by a box H/ACA snoRNA, which is complementary to a specific RNA substrate (red). This snoRNA guides a protein complex (grey, purple, blue and green) leading to the isomerization of pseudouridine. **(B)** In the RNA-independent mechanism, the generation of pseudouridine is mediated by PUS enzymes (grey) that recognize a structure or sequence of the target RNA (red) and leads to the isomerization of uridine to pseudouridine.

In eukaryotes and archaea, both mechanisms exist in parallel and induce the isomerization, while in prokaryotes the modification is produced exclusively via the RNA-independent mechanism. In the RNA-dependent mechanism, four core proteins (Cbf5, Nhp2, Nop10, and Gar1 in *S. cerevisiae*) form a complex, which is guided by a box H/ACA small nucleolar RNA (snoRNA) to the target RNA and promotes its isomerization (Ni *et al.*, 1997). The box H/ACA guide RNA has a characteristic structure and in most cases consists of a hairpin-hinge-hairpin-tail conformation (Balakin *et al.*, 1996; Kiss, 2001, 2002), where the box H resides in the hinge region and the box ACA is located in the tail region (Karijolich & Yu, 2008; Huang *et al.*, 2012). The isomerization of uridine occurs in single-stranded regions located in the internal loop of each hairpin, also called pseudouridylation pockets. Moreover, the same region also contains the guide sequence that gives specificity to the target RNA by base-pairing interactions (Ganot *et al.*, 1997; Ni *et al.*, 1997). In the RNA-independent mechanism, a stand-alone enzyme recognizes either a structure or a sequence within the target RNA and promotes its isomerization (McKenney *et al.*, 2017). The RNA-independent pseudouridylation is the only mechanism described so far in bacteria and will be the focus of this thesis.

1.4.2. Pseudouridine synthases (PUS) in bacteria and their classification

Six families of PUS enzymes are described in the different domains of life: TruA, TruB, TruD, RsuA, RluA, and Pus10p (Spenkuch *et al.*, 2014), with Pus10p being identified only in archaea and some eukaryotes (Watanabe & Gray, 2000; Spenkuch *et al.*, 2014; Deogharia *et al.*, 2019; Song *et al.*, 2020). Recent studies have described crystal structures for members of each family and showed that despite the minimal similarity between the amino acid sequences, the enzymes share a common core (Hamma & Ferré-D'Amaré, 2006). This core consists of a similar fold and active-site region, even though their RNA substrates are different. The difference in substrate recognition can be explained by the presence of accessory domains discriminating between different families, which are either part of the catalytic domain or linked to it. For example, the Pus10 family contains an accessory N-terminal THUMP (named after its discovery in thiouridine synthases, methylases, and pseudouridine synthases) RNA-binding domain that is required for tRNA binding (Aravind & Koonin, 2001).

Usually, PUS enzymes distinguish their targets based on the structural or sequence context and promote isomerization without the need of any additional proteins or co-factors (Johnson & Söll, 1970; Cortese *et al.*, 1974; Arena *et al.*, 1978; Samuelsson & Olsson, 1990). While the tRNA PUS enzymes TruB and TruD recognize their targets based on specific sequences, TruA selects the substrate based on a particular structure (Hur & Stroud, 2007). TruB of *E. coli* was one of the first PUS enzymes for which the structure was solved by crystallography (Hoang & Ferré-D'Amaré, 2001; Pan *et al.*, 2003). Using biochemical approaches, the authors could show that TruB does not need the entire tRNA to modify the uridine at position 55 in the T-loop, but only requires the presence of the T-stem and the loop regions. TruB binds the uridine nucleotides and two nucleotides of the tRNA chain, promoting base flipping of the nucleotides 55, 56, and 57, thereby disrupting the tertiary structure of the tRNA (Hoang & Ferré-D'Amaré, 2001; Pan *et al.*, 2003). The crystal structure revealed that the binding is stabilized by a histidine residue which is conserved among TruB family members (Hoang & Ferré-D'Amaré, 2001). Compared to the other enzymes, TruD exhibits limited sequence homology to known PUS enzymes and has a unique domain close to the catalytic domain, which is suggested to embrace the RNA substrate. The structure of the *E. coli* TruD was solved by X-ray crystallography by two different groups in parallel and shows an overall V-shape with an RNA-binding domain positioned between the catalytic domain and an insertion domain. While the catalytic domain folds in a similar way compared to other PUS enzymes, the TruD insertion domain consists of a novel fold (Kaya *et al.*, 2004). Moreover, a recently published structure of Pus7 in *S. cerevisiae* (the TruD homolog in yeast) identified additional insertion domains that fine-tune the activity of the protein and might contribute to RNA substrate binding (Kaya *et al.*, 2004; Purchal *et al.*, 2022).

Besides the shared catalytic activity among the different PUS enzymes, their distinct structures and domains confer specificity for binding of different RNA substrates and highlight different mechanisms of action.

1.4.3. Biological functions and regulation of PUS enzymes

Pseudouridine has been identified not only in tRNAs and rRNAs in eukaryotes, but also in some mRNAs and long non-coding RNAs (Carlile *et al.*, 2014; Lovejoy *et al.*, 2014; Schwartz *et al.*, 2014; Li *et al.*, 2015; Nakamoto *et al.*, 2017; Sun *et al.*, 2019) suggesting that Ψ might have a role in regulation of gene expression. Moreover, Pus7 has been shown to induce pseudouridylation of mRNAs during heat shock, indicating that the generation of Ψ might aid the cell to respond to different environmental conditions (Schwartz *et al.*, 2014). Furthermore, PUS enzymes might affect stability, structure, or re-coding of their target

mRNAs (Rintala-Dempsey & Kothe, 2017). Additionally, it has been shown that PUS enzymes might change their cellular localization during stress conditions: Pus7 migrates from the nucleus to the cytoplasm during heat stress, where it induces pseudouridylation of certain mRNAs. In yeast, it has been shown that the transcript levels of different PUS enzymes (Pus7, Pus1, Pus3, Pus4, Pus2, and Pus9) are differentially expressed under different environmental conditions (Rintala-Dempsey & Kothe, 2017). Changing conditions can also alter the protein activity without changing its expression level (Lee *et al.*, 2014). Furthermore, it has been observed , that yeast PUS enzymes interact with other proteins (Zhao *et al.*, 2004), suggesting that the resulting protein complexes might each have a distinct role in the cell.

In the bacterial model organism *E. coli*, the tRNA PUS enzyme TruB has been investigated in more detail compared to the other tRNA or rRNA PUS enzymes. While the growth of the bacteria is not affected by the deletion of *truB* in rich or minimal medium, competition experiments show that lack of TruB confers a selective disadvantage when in competition with wild-type cells (Gutgsell *et al.*, 2000). A follow up study showed that a *truB* mutant strain showed a defect in survival at high temperature (50 °C), suggesting that the modification at position 55 in tRNAs mediated by TruB might contribute to thermal stress tolerance in the bacteria (Gutgsell *et al.*, 2000).

1.4.4 The TruD family in different domains of life

The TruD family of PUS enzymes was first discovered in *E. coli* and found to be responsible for the modification of tRNA-Glu at position 13 (Kaya & Ofengand, 2003a). However, deletion of *truD*, and consequently the absence of the Ψ in tRNA-Glu did not cause any obvious disadvantage in the mutant compared to its parental strain. Since then, homologs of TruD were identified in all domains of life, suggesting that this family potentially has ancient origins. In *S. cerevisiae*, Pus7 is the sole member of the TruD family and modifies the U2 small nuclear RNA (Rintala-Dempsey & Kothe, 2017), tRNA-Glu at position 13, and the pre-tRNA-Tyr at position 35 (Behm-Ansmant *et al.*, 2003). Pus7 was shown to participate in the pseudouridylation of mRNAs under both physiological and heat shock conditions, suggesting a potential role of this enzyme in enhancing transcript stability (Schwartz *et al.*, 2014). In *Candida albicans*, Pus7 has been suggested to impact rRNA processing, growth, and virulence of the microorganism (Pickerill *et al.*, 2019). In H9 human embryonic stem cell lines (hESC), Pus7 was identified to control stem cell differentiation and translation by inducing the modification at position 8 of tRNA-derived small RNAs, thereby adding a new layer of posttranscriptional gene regulation (Guzzi *et al.*, 2018). Overall, these recent findings highlight the potential function of TruD/Pus7 in gene expression regulation.

1.5. Challenges regarding the identification and investigation of pseudouridine

Since the biological function of pseudouridine is strictly dependent on its location in the RNA sequence, identification of its position inside an RNA molecule at single nucleotide resolution is of utmost importance. Uridine and Ψ possess similar UV spectra and molecular masses (Durairaj & Limbach, 2008). Additionally, since the isomerization does not lead to the incorporation of additional functional groups, pseudouridine cannot be uniquely radioactively labeled (e.g., 4-thiouridilation). Therefore, novel methods are required for its identification. Recently, approaches using mass spectrometry or chemical treatment followed by deep sequencing were optimized to globally identify this modification in the transcriptome of different organisms (Yamaki *et al.*, 2020).

1.5.1. Investigation of pseudouridine using mass spectrometry based approaches

A major challenge for the detection of pseudouridine using mass spectrometry approaches arises due to the inability of the method to distinguish between pseudouridine and uridine, since pseudouridylation is a mass-silent modification. Therefore, a chemical derivation with a different compound must be used to distinguish modified from canonical uridine. One of the most common approaches is liquid chromatography/electrospray ionization mass spectrometry (LC-ESI-MS) which relies on the identification of the modification in RNA hydrolysates due to a combination of chromatography retention times and mass measurements (Durairaj & Limbach, 2008). This approach, however, cannot identify the location of pseudouridine in the sequence context of the RNA.

1.5.2. Investigation of pseudouridine using a chemical treatment followed by deep sequencing

In the past, the study of Ψ was limited to abundant RNA species such as tRNAs and rRNAs. There, Ψ was identified in a single RNA using a chemical treatment specific for Ψ, followed by a primer extension assay (Bakin et al., 1993). In particular, while CMC binds pseudouridine, uridine, and guanosine at pH 8.5, alkaline treatment (pH 10.4) renders binding of CMC to uridine and guanosine unstable and only specifically stabilizes its binding to Ψ (Durairaj *et al.*, 2008). In turn, pseudouridine which was chemically modified by CMC blocks reverse transcription one nucleotide prior to the CMC-modified base and can therefore be identified at single-nucleotide resolution by primer extension (Zhao *et al.*, 2004).

However, this approach is restricted to a single RNA and a relatively limited number of nucleotides based on primer annealing for each experiment. The reported method has further limitations: 1) CMC can bind to other modified uridines such as thiouridine, leading to the wrong interpretation of the RNA modification at this site (Bakin *et al.*, 1994); 2) it cannot distinguish between pseudouridine residues that are next to each other or to other uridines (Durairaj & Limbach, 2008), and 3) for modifications residing at the 3' end of the RNA molecule, an additional tag such as a poly-A tail might be necessary for RT primer binding during reverse transcription (Ofengand *et al.*, 2001). In addition, other chemicals were less extensively used to identify pseudouridine, as for examples acrylonitrile (Mengel-Jørgensen & Kirpekar, 2002) or methyl vinyl sulfone (MVS) (Emmerechts *et al.*, 2005). However, compared to CMC and acrylonitrile, MVS cannot be classified as a selective tag since it also modifies uridine.

Recently, four different research groups independently combined the ability of CMC to mark Ψ at single-nucleotide resolution with deep sequencing to globally map Ψ in human and yeast RNAs (Pseudo-seq, Ψ-seq, PSI-seq, and CeU-seq) (Lovejoy *et al*., 2014; Carlile *et al*., 2014; Schwartz *et al*., 2014; Li *et al*., 2015). The sensitivity of deep sequencing allowed the detection of Ψ not only in tRNAs and rRNAs, but also in mRNAs and regulatory RNAs, suggesting that this type of RNA modification can potentially have a broader role in gene expression control. Moreover, they could show that Ψ formation can be induced under different stress conditions in the cell by PUS enzymes (heat shock, osmotic stress, or nutrient starvation), indicating a need for Ψ in response to stress (Carlile *et al*., 2014; Schwartz *et al*., 2014; Li *et al*., 2015). Although these sequencing-based methods allowed, for the first time, to globally identify Ψ in RNAs at single-nucleotide resolution in eukaryotes, the functional relevance of Ψ is still unclear (e.g., maintenance of RNA structure, mRNA stability, or RNA-protein interactions). However, a comprehensive analysis of these deep-sequencing approaches has revealed that only a small percentage of modified transcripts overlapped between the different experiments (Zaringhalam & Papavasiliou, 2016). Thus, optimization steps to consistently map pseudouridine will be necessary to distinguish true- from false-positive hits. While global mapping of pseudouridine in eukaryotic transcriptomes has been achieved by deep-sequencing approaches, similar methods have not been established in bacteria so far.

Only recently, the Psi-seq approach was applied to the tRNA-fraction of *B. subtilis*, thus identifying modified sites at positions 31, 32, 38, 39, and 55 in tRNAs. Contamination of the tRNA with 23S rRNA during anion exchange fractionation allowed the identification of some sites also in the *B. subtilis* rRNA mediated by RluD (de Crécy-Lagard *et al.*, 2020). Besides this recent study, global mapping of pseudouridine in the transcriptome of bacteria is still missing.

1.6. The diverse functions of pseudouridine in RNAs

A modified nucleotide in a specific RNA molecule can lead to different outcomes based on the role of that particular RNA in the cell. The presence of a modification in an mRNA, for example, can affect its translation. In tRNAs, Ψ can influence the codon-anticodon pairing or the recognition of the tRNA by the ribosome during translation. In rRNAs, Ψ can have important structural implications. The known functions of Ψ in tRNAs, rRNAs, and eukaryotic are summarized below.

Effect of Ψ in tRNAs. tRNAs represent the crucial link between the mRNA that has to be translated by the ribosome, and its protein product (Hoagland *et al.*, 1958). They present in a typical tertiary structure that is necessary for it to fit in the P (peptidyl-tRNA binding site) and A (aminoacyl-tRNA binding site) sites of the ribosome during translation (Moazed & Noller, 1989). tRNA sequence and structure are also important for the recognition by aminoacyl tRNA synthases, which are enzymes that charge the tRNAs with their respective amino acids (Hoagland *et al.*, 1958). It has been reported that a tRNA carries on average 13 modifications (Pan, 2018) with Ψ being one of them. In the bacterial model organism *E. coli*, Ψ has been detected in the TΨC (position 55), anticodon (position 32, 38-40), or D loop (position 13). Interestingly, depending on where the modification is located in the tRNA molecule, it may either affect the structure or the function of the RNA, and even influence the incorporation of additional modifications in the same tRNA (Alexandrov *et al.*, 2006). It has been reported *in vitro* that the presence of Ψ, specifically at position 55, affects the incorporation of ribothymidine at position 54 mediated by the enzyme TrmA, thus affecting the binding and therefore the catalytic function of TrmA (Schultz & Kothe, 2020). Ψ at position 32, together with Ψ at positions 39 and 55, seem to be important for stabilization of the tertiary structure of the tRNA (Nobles *et al.*, 2002; Cabello-Villegas & Nikonowicz, 2005; Denmon *et al.*, 2011).

Effect of Ψ in rRNAs. rRNA PUS enzymes modify their targets via different mechanisms. However, the number of modified sites and the positions can vary among different organisms. The *E. coli* 23S and 16S rRNAs are modified at ten positions and one position, respectively (Ofengand, 2002). While pseudouridylation of the bacterial 5S rRNA has not be reported, modification of the 5S and 5.8S rRNAs in yeast was shown (Decatur & Schnare, 2008). One of the most modified regions in the 23S rRNA of *E. coli* is the so-called helix 69 (H69). There, three modifications have been detected close to each other at positions Ψ1911, 1915, and 1917, with implications in maintenance of the structural conformation of this region. In *E. coli*, H69 is important for binding of different antibiotics (Sakakibara & Chow, 2017), therefore

representing a potential target for bacterial growth inhibition. However, the functional relevance of other Ψ modifications in the 16S and 23S rRNAs are still unclear.

Effect of Ψ in eukaryotic mRNAs. The role of pseudouridine in mRNAs is largely unknown. However, the presence of uridine at the first position of STOP codons (UAA, UAG, and UGA) led to the hypothesis that a possible isomerization of uridine to pseudouridine might promote translational read-through. To investigate this possible role, John Karijolich and Yi-Tao Yu generated an artificial box H/ACA RNA that targeted and pseudouridylated the *TRM4* gene in yeast containing an artificial nonsense codon in its CDS. They showed that pseudouridylation of the artificially introduced nonsense codon *in vivo* promoted translation of *TRM4*, suggesting a possible role of pseudouridine in translation (Karijolich & Yu, 2011; Huang *et al.*, 2012). Furthermore, it has been shown that the presence of Ψ in mRNA codons may alter tRNA selection by the ribosome, thus modulating mRNA translatability (Eyler *et al.*, 2019). However, Ψ has so far not been detected in bacterial mRNAs, thus a possible function in regulation of gene expression and translation still remains elusive.

1.7. Pseudouridine in *E. coli*

The Gram-negative bacterium *Escherichia coli* has been used as a bacterial model organism to study pseudouridylation in tRNAs and rRNAs. The first fully characterized tRNA PUS enzyme was TruA, responsible for the modification of uridine at position 38, 39, and 40 in the anticodon stem of 17 different tRNAs (Sprinzl *et al.*, 1987). The gene was first named *hisT* since it is located in the so-called *hisT* operon (Palmer *et al.*, 1983). The tRNA PUS enzyme TruB in *E. coli* has been discovered due to its high homology to a region in a *B. subtilis* gene, which generates pseudouridine at position 55 in tRNAs (Nurse *et al.*, 1995). The TruC and the TruD enzymes are responsible for the modification at positions 65 and 13 in tRNAs, and the rRNA PUS enzymes RluA and RluF for the modification at positions 32 and 35 in distinct sets of tRNAs, respectively (Figure 1.7, left). In addition to tRNAs, the 23S and 16S rRNAs are modified at various positions by a number of different PUS enzymes (Figure 1.7, right).

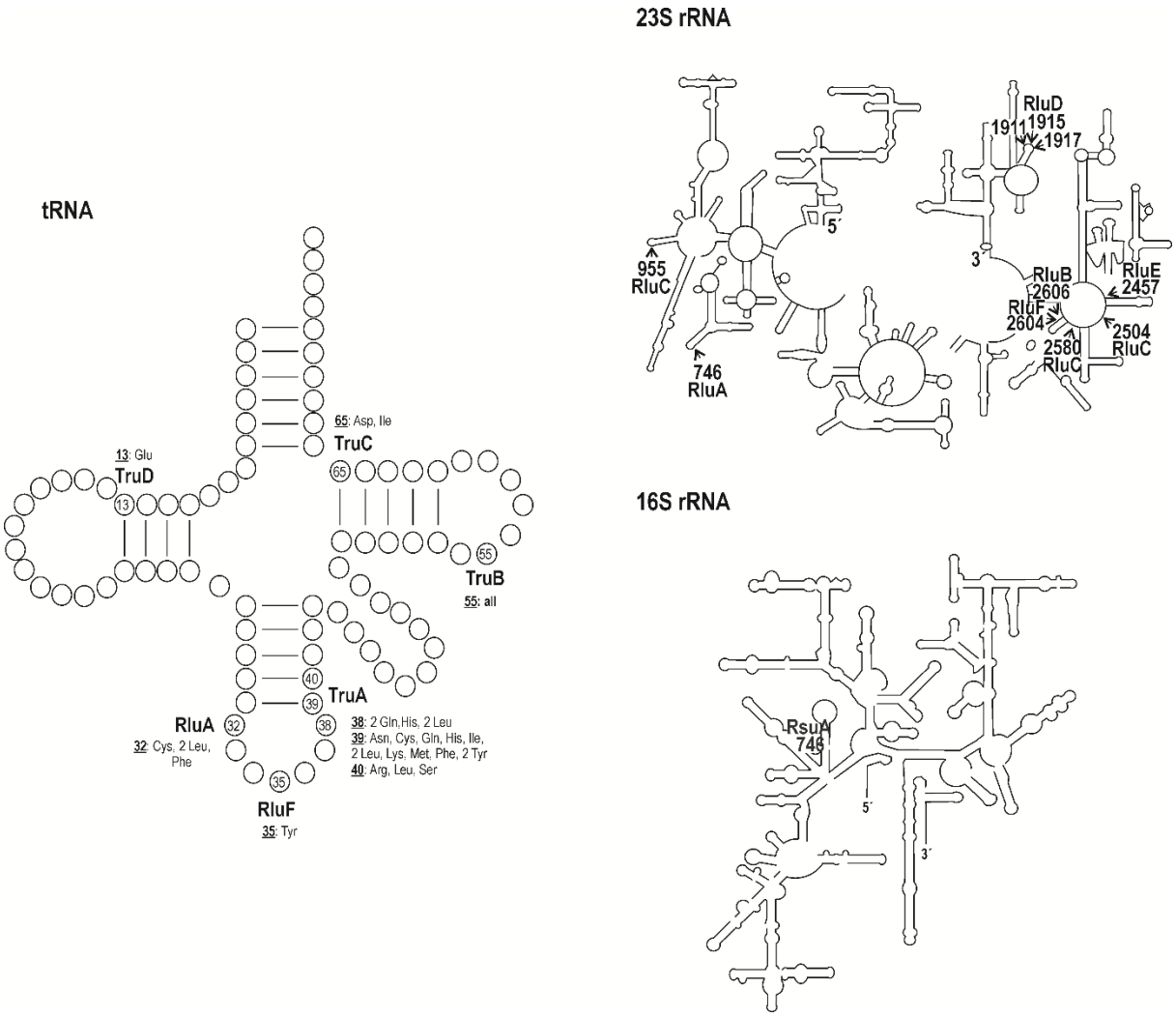

Figure 1.7: Pseudouridine in tRNAs and rRNAs of the Gram-negative bacterium *E. coli*. (*Left*) Pseudouridine sites in *E. coli* tRNAs at positions 13, 32, 35, 38-40, 55, and 65 mediated by TruD, RluA, RluF, TruA, TruB, and TruC, respectively. (*Right*) Pseudouridine sites at positions 516, 746, 955, 1911, 1915, 1917, 2457, 2507, 2580, 2604, and 2605 mediated by RsuA, RluA, RluC, RluD, RluE, RluC, RluF, and RluF, respectively. The tRNA and rRNAs structures are inspired by (Campo *et al.*, 2001).

Although it is known which tRNA and rRNA positions are modified in *E. coli* and which enzymes are responsible for this, the specific function of each modification is still poorly understood. Moreover, deletion of any of the *E. coli* PUS enzymes does not lead to a phenotype in the bacteria. Thus, mapping of pseudouridine and characterization of the enzymes responsible for its generation in bacteria other than *E. coli*, might shed light on the function of this modification in prokaryotic RNAs.

1.8. *Campylobacter jejuni* and *Helicobacter pylori* as bacterial model organisms to study RNA pseudouridylation

The study of RNA pseudouridylation using a bacterial minimal system consisting of only few PUS enzymes allows the identification of RNA substrates and functions for different PUS enzymes avoiding functional redundancy. The Epsilonproteobacteria *Campylobacter jejuni* (*C. jejuni*) and *Helicobacter pylori* (*H. pylori*) are promising alternative model organisms to study pseudouridylation in bacteria for the following reasons: 1) they have been well established as model organisms in RNA biology (Sharma *et al.*, 2010; Dugar *et al.*, 2013), 2) they harbor a small and compact genomes, and therefore encode for only a limited number of proteins/enzymes. Thus, *C. jejuni* and *H. pylori* are used in this work to study RNA pseudouridylation and functional characterization of pseudouridine synthases.

1.8.1. *Campylobacter jejuni*

C. jejuni is a Gram-negative, mostly spiral-shaped, human pathogen characterized by a small genome (1.64 mb) encoding for only few regulatory systems (Parkhill *et al.*, 2000). It is a commensal in birds and agriculture-associated animals (Burnham & Hendrixson, 2018), but causes gastroenteritis in humans and has been linked to the development of secondary autoimmune disorders such as the Guillain-Barré or Miller-Fisher syndromes (Wassenaar & Blaser, 1999). Usually, the consumption of contaminated water, unpasteurized cheese or milk, and undercooked chicken is the primary source of human infection (Costard *et al.*, 2017). Surprisingly, *C. jejuni* lacks many of the classical virulence factors used by and found in other enteric bacterial pathogens, but encodes the cytolethal distending toxin (CDT), which causes DNA damage and cell death (Lara-Tejero & Galán, 2000). Additionally, motility is considered a major virulence feature of *C. jejuni* mediated by a single flagellum localized at each cell pole of the bacterium. In certain *Campylobacter* species, the flagellum is specialized to secrete virulence factors, for example so-called Cia proteins (*Campylobacter* invasion antigens), in addition to flagellar components, which help the bacteria establish host cell colonization (Neal-McKinney & Konkel, 2012).

Recently, high-resolution transcriptome maps of multiple *C. jejuni* strains were generated using differential RNA-seq (dRNA-seq), which allowed the global annotation of transcriptional start sites (TSSs) in the *C. jejuni* transcriptome and revealed the presence of multiple sRNAs (Dugar *et al.*, 2013; Porcelli *et al.*, 2013). The role of posttranscriptional regulation mediated by sRNAs in *C. jejuni* has since been more extensively studied (Dugar *et al.*, 2013; Porcelli *et al.*, 2013; Le *et al.*, 2015; Kreuder *et al.*, 2020; Svensson & Sharma, 2021,

2022). Moreover, RNA-modifying enzymes are annotated in *C. jejuni* genome (Parkhill *et al.*, 2000), suggesting the presence of RNA modifications in the transcriptome of the pathogen.

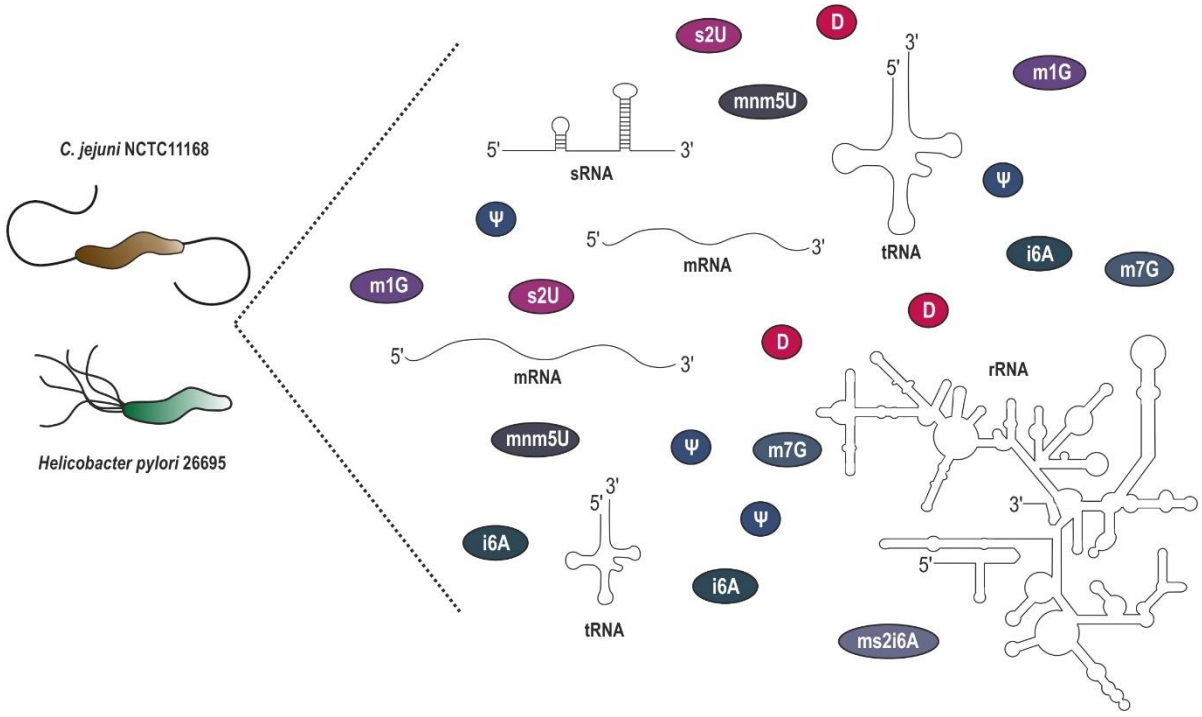

Figure 1.8: Schematic representation of potential RNA modifications present in *C. jejuni* NCTC11168 and *H. pylori* 26695. Examples of RNA modifications potentially present in *C. jejuni* and *H. pylori* mRNAs, tRNAs, rRNAs, and sRNAs. Ψ: pseudouridine; s2U: 2-thiouridine; mnm5U: 5-methylaminomethyluridine; D: dihydrouridine; m1G: 1-methylguanosine; m7G: 7-methylguanosine; i6A: N6-isopentenyladenosine; ms2i6A: 2-methylthio-N6-isopentenyladenosine.

In *C. jejuni*, the tRNA PUS enzymes TruA (Cj0827), TruB (Cj1102), and TruD (Cj1457c) are potentially involved in the posttranscriptional isomerization of uridine to pseudouridine. Another example of potential RNA modifying enzyme could be the *E. coli* MnaA homolog Cj0053c that encodes for a tRNA 2-thiouridylase. In *E. coli*, this enzyme is responsible for the biosynthesis of 2-thiouridine in different tRNAs at position 34 (Kambampati & Lauhon, 2003). Furthermore, Cj1188c encodes for the tRNA uridine 5-carboxymethylaminomethyl modification enzyme (GidA in *E. coli*) that adds the carboxymethylaminomethyl group to the wobble position (U34) in certain tRNAs. Taken together, the presence of RNA modifying enzymes and their respective RNA modifications suggests an additional level of gene regulation based on posttranscriptional control.

1.8.2. *Helicobacter pylori*

The related Epsilonproteobacterium *H. pylori* is also spiral-shaped and the first pathogen to be classified as class I carcinogen by the World Health Organization (WHO) (International Agency for Research on Cancer, 1994). Infection with *H. pylori* can lead to gastric adenocarcinoma and gastric mucosa-associated lymphoid tissue (MALT) lymphoma (Floch *et al.*, 2017). Similar to *C. jejuni*, *H. pylori* is characterized by a small genome (approximately 1.7 mb) and a limited number of transcriptional regulators. However, the bacterium uses dedicated virulence factors to promote infection. These include the vacuolating cytotoxin A (VacA) and the cytotoxin-associated gene A (CagA), which have been identified as major virulence factors manipulating host tissue during *H. pylori* infection (Salama *et al.*, 2013). In 2010, the first genome-wide map of TSSs and operons in *H. pylori* 26695 was published (Sharma *et al.*, 2010). The study revealed the presence of approximately 60 sRNAs. Two of these, NikS and RepG, have been studied in more detail (Pernitzsch *et al.*, 2014, 2021; Eisenbart *et al.*, 2020; Kinoshita-Daitoku *et al.*, 2021) and shown to play crucial roles in pathogenesis of the bacterium. Together with posttranscriptional regulation mediated by sRNAs, also genes encoding for potential RNA-modifying enzymes characterize the genome of *H. pylori.* Besides some similarities between the *C. jejuni* and *H. pylori* genomes, they encode different sets of proteins, indicating differences also in the posttranscriptional regulation mediated by RNA modifications and the specific enzymes responsible for their generation. Figure 1.8 shows potential RNA modifications that might be present in *C. jejuni* and *H. pylori* RNAs. Appendix Table 1 and Appendix Table 2 list all the potential tRNA and rRNA modification factors annotated in the genomes of *H. pylori* and *C. jejuni* identified using the KEGG database (Kanehisa & Goto, 2000; Kanehisa, 2019; Kanehisa *et al.*, 2021).

Taken together, developing a method to globally map pseudouridine in the two Epsilonproteobacteria and study the role of the enzymes that promote the modification will help to gain insights into its role in bacteria.

2. Result I: Characterization of tRNA PUS enzymes and methods to globally identify pseudouridine in bacterial transcriptomes

So far, the functional characterization of PUS enzymes was mainly investigated in eukaryotic systems. In addition, methods to globally identify Ψ at single-nucleotide resolution were almost exclusively applied and established in eukaryotes, where a large number of modified sites were detected in different types of RNAs, including mRNAs and lncRNAs. Despite the numerous advantages of bacteria as model organism to study mechanisms of gene expression regulation and several other processes in the cell, the role of RNA modifications is still poorly understood. This chapter aims to explore the presence of tRNA and rRNA PUS enzymes in bacteria, with a focus on tRNA PUS enzymes in the Epsilonproteobacteria *C. jejuni* and *H. pylori.* To globally map the position of Ψ at single nucleotide resolution in the transcriptomes of the bacterial pathogens, Pseudo-seq, is established, optimized, and applied for *C. jejuni* and *H. pylori*. In addition, a strategy to enrich for potential modified RNA targets using an anti-pseudouridine antibody is investigated.

2.1. Distribution and conservation of PUS enzymes in different bacterial species

To study pseudouridylation in *C. jejuni* and *H. pylori* the first step is to identify the enzymes responsible for this modification. Moreover, to identify the distribution of tRNA and rRNA PUS enzymes in prokaryotes, the search was extended to other bacterial species. In *E. coli* eleven PUS enzymes have been described to modify tRNAs and rRNAs at various positions (Campo *et al.*, 2001; Kaya & Ofengand, 2003b). To identify the potential homologs of PUS enzymes in other bacterial species, the amino acid sequences of the *E. coli* PUS enzymes were blasted using blastp (protein-protein blast) against 12 genomes of bacteria belonging to Gammaproteobacteria (*Salmonella* Typhimurium SL1344, *V. chloreae* 0395, *Yersinia pestis* PBM19, *Shigella flexneri* 2457T, *Citrobacter rodentium* ICC168, *Serratia marcescens* SM39, *Haemophilus ducreyi* 35000HP), Epsilonproteobacteria (*Wolinella succinogenes* DSM1740, *C. jejuni* NCTC11168, and *H. pylori* 26695), as well as Bacilli (*B. subtilis* 168) and Mollicutes (*Mycoplasma pneumoniae* M129) classes. The class of Gammaproteobacteria is constituted by ~250 genera and contains a wide variety of microorganisms that have different pathogenic traits, metabolisms, morphologies and ecological niches. *Salmonella* Typhimurium together with *E. coli*, *S. flexeri*, *S. marcenscens*, and *C. rodentium* are part of the family Enterobacteriaceae, while *V. cholerae*, *Y. pestis*, and *H. ducreyi* are part of the Vibrionaceae, Yersiniaceae, Pasteurellaceae families. Except for the model organism *E. coli*, they all are categorized as pathogens. The Epsilonproteobacteria class consists only of few genera where

the Campylobacteraceae and Helicobacteraceae families are the most represented. *B. subtilis* was included in the analysis because it is a main model organism for Gram-positive bacteria and pseudouridine has been recently identified in its tRNAs (de Crécy-Lagard *et al.*, 2020). The reason to include *M. pneumoniae* is because it possesses a very small genome and thus it would be interesting to identify the core and essential bacterial PUS enzymes that are required for modification of tRNAs and rRNAs modification.

During the computational search for *Salmonella* Typhimurium SL1344, the protein SL1344_1651 was found to be annotated as YciL, a hypothetical pseudouridine synthase that shows 98% sequence identity to the *E. coli* RluB (284/291 amino acids). In *E. coli*, RluB is responsible for the modification of the 23S rRNA at position 2605 (Del Campo *et al.*, 2001). This could potentially suggest suggesting that *Salmonella* SL1344_1651 is able to modify 23S rRNA at the same position. Additionally, the protein SL1344_1175 is annotated as RluB, but shares 83% identity with *E. coli* RluE (179/215 amino acids), the enzyme responsible for Ψ at position 2457 in the 23S rRNA (Del Campo *et al.*, 2001). A similar result was observed for *H. ducrey* 3500HP: the protein HD_0337 is annotated as RluB, but shares 58% identity (104/179 amino acids) with *E. coli* RluE and only 35% identity (56/160 amino acids) with *E. coli* RluB. In *S. marcescens* SM39, SM39_3526 is annotated as a putative pseudouridine synthase that modifies position 32 of tRNAs and 746 of 23S rRNA (Raychaudhuri *et al.*, 1999) and shares 42% identity (94/222 amino acids) with RluA of *E. coli*. However, the actual annotated RluA in the genome of *S. marcenscens* (SM39_0043) shares 77% identities (168/217 amino acids) with RluA from *E. coli*. These results could be due to either misannotation of the gene encoding the corresponding protein or there is a certain degree of amino acid similarity between proteins that belong to the same family/different families of PUS enzymes. For example, it has been shown that the RluA family (RluA, RluC, RluD, and TruC) and RsuA family (RsuA, RluB, RluE, and RluF) are the most closely related, also in terms of amino acid sequence level (Hamma & Ferré-D'Amaré, 2006). Thus, care must be taken when trying to discriminate and annotate enzymes that belong to the same family.

The overall analysis showed that the Epsilonproteobacteria encode a lower number of PUS enzymes compared to the bacteria from the other classes, with TruA and RluD being present in all the analyzed microorganisms (Figure 2.1 and Table 2.1). The difference of the number of enzymes between the different bacterial classes can be explained by a reduced genome size for the Epsilonproteobacteria compared to the Gammaproteobacteria and/or by a reduced number of RNA substrates. For instance, a correlation between bacterial genome size and total tRNA number was reported, i.e., bacteria with a smaller genome encode on average for a lower number of tRNAs (Satapathy *et al.*, 2010). Thus, the total number of tRNAs present in

the genomes of the selected bacteria was explored using GtRNAdb (http://gtrnadb.ucsc.edu/) and the analysis showed that the number of tRNAs positively correlate with the genome size of the selected organisms (Figure 2.2). Thus, it is possible that bacteria have adapted to reduce their set of enzymes based on their RNA substrates or ecological needs.

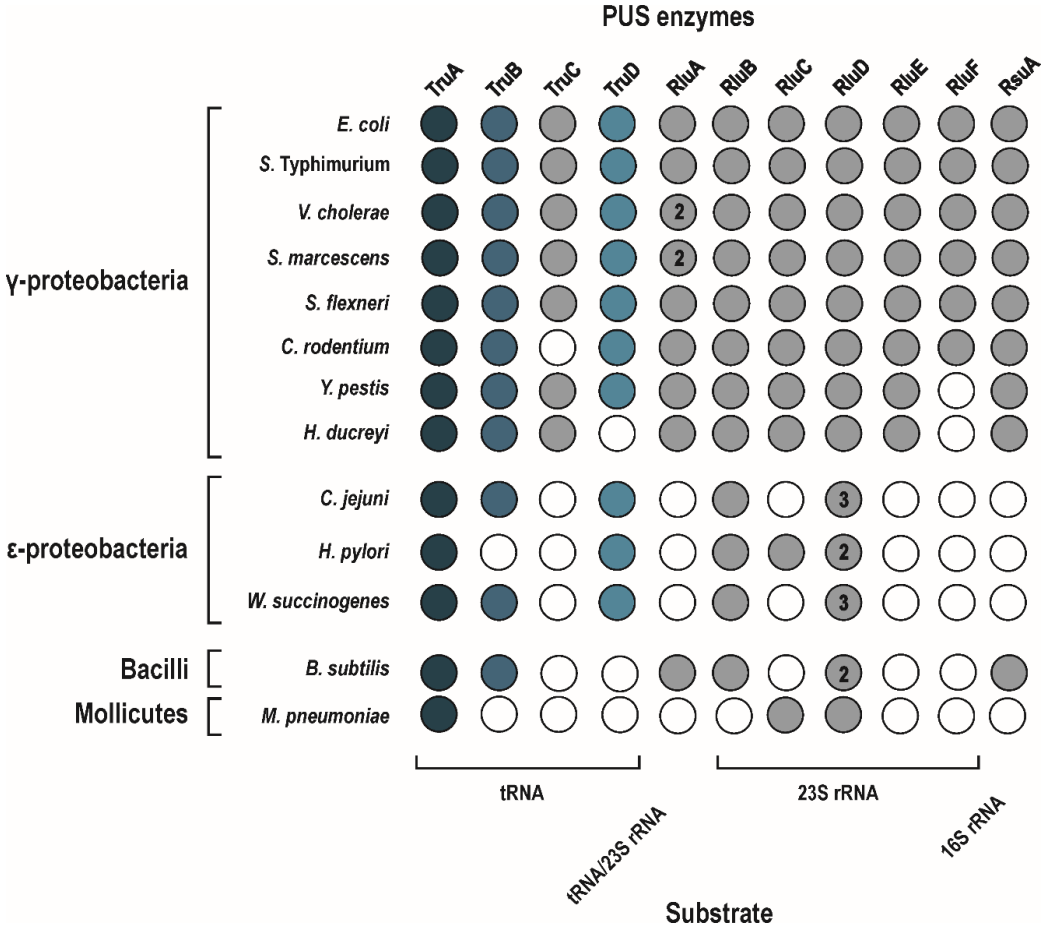

Figure 2.1: General overview of tRNA and rRNA PUS enzymes in diverse bacterial species. Schematic representation of presence or absence of tRNA and rRNA PUS enzymes and their corresponding substrates in the following strains: *Escherichia coli* K-12, *Salmonella* Typhimurium SL1344, *Vibrio cholerae* 0395, *Yersinia pestis* PBM19, *Shigella flexneri* 2457T, *Citrobacter rodentium* ICC168, *Serratia marcescens* SM39, *Haemophilus ducreyi* 35000HP, *Wolinella succinogenes* DSM1740, *Campylobacter jejuni* NCTC11168, *Helicobacter pylori* 26695, *Bacillus subtilis* 168, and *Mycoplasma pneumoniae* M129. Colored in circles representing the presence of the PUS enzyme in the respective species (dark blue: TruA, blue circles: TruB, turquoise circles: TruD). Grey circles represent the presence of the other tRNA and rRNA PUS enzymes that are not considered in this thesis. White circles represent the absence of the PUS enzyme. The known targets of each PUS enzyme in *E. coli* are listed below. For RluA and RluD enzymes, the numbers inside the circles (2 or 3) represent the multiple homologs detected for the PUS enzymes.

2.1.1 *C. jejuni* and *H. pylori* as model organisms to study RNA pseudouridylation

Our model organisms *C. jejuni* and *H. pylori* represent a so-called minimal system to study RNA pseudouridylation. Each of them encodes a specific and distinct set of tRNA and rRNA PUS enzymes: while both encode for TruA, TruD, RluB, and RluD, *H. pylori* lacks TruB and *C. jejuni* does not encode for an RluC homolog. It is worth to note that *H. pylori* is one of the few examples of bacteria that lack the TruB enzyme responsible for the generation of the well conserved pseudouridine at position 55 in tRNAs. Moreover, both the bacteria encode multiple copies of the RluD protein. Both pathogens are characterized by a small genome (1.6 and 1.7 Mbp, respectively) compared, for example, to the well-studied *Escherichia coli* K-12 (4.6 Mbp). While *C. jejuni* and *H. pylori* encode for 43 and 36 tRNAs (tRNAs decoding the standard 20 aa), respectively, *E. coli* encodes for 86 tRNAs. Both *C. jejuni* and *H. pylori* have well-characterized transcriptional landscapes (Sharma *et al.*, 2010; Dugar *et al.*, 2013; Porcelli *et al.*, 2013), but lack some of the classical RNA-binding proteins of enteric model bacteria (Holmqvist & Vogel, 2018). Moreover, despite being Gram-negative, they have ribonuclease (RNase) repertoires more similar to Gram-positive bacteria (Parkhill *et al.*, 2000). This can also be observed in the previous analysis (Figure 2.1), i.e., the Epsilonproteobacteria encode a set of tRNA and rRNA PUS enzymes more similar to *B. subtilis* compared to Gammaproteobacteria.

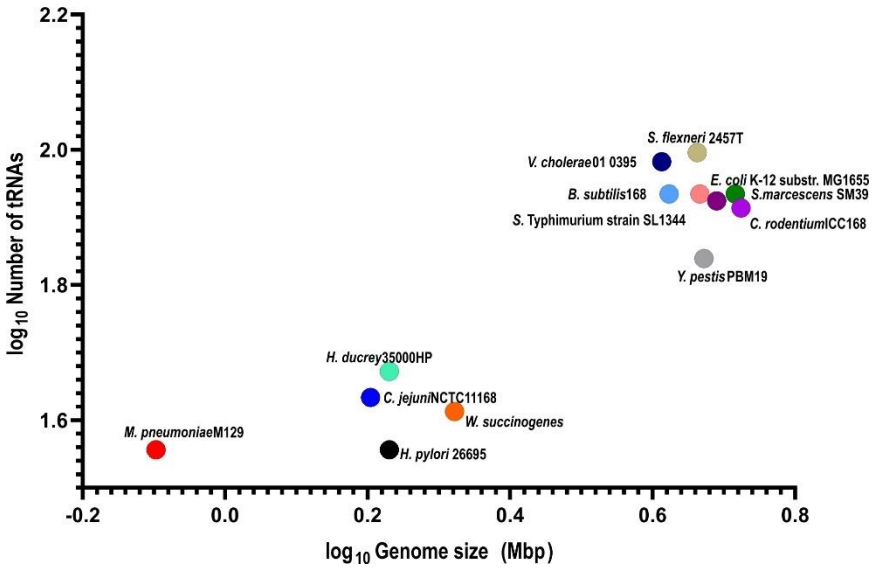

Figure 2.2: Correlation analysis of tRNA number (log10) and genome size (log10) for investigated bacterial species. The number of tRNAs identified in the genome of the different bacterial species were selected using the database GtRNAdb (http://gtrnadb.ucsc.edu/); the information regarding the genome size of the different bacterial species was investigated using NCBI

(https://www.ncbi.nlm.nih.gov/genome/?term=). The x-axis represents the genome size (log_{10} Mbp) and the y-axis represents the number of the tRNAs (log_{10}). Different bacterial species: *Escherichia coli* K-12 (pink circle), *Salmonella* Typhimurium SL1344 (dark purple), *Vibrio cholerae* 0395 (blue), *Yersinia pestis* PBM19 (grey), *Shigella flexneri* 2457T (light green), *Citrobacter rodentium* ICC168 (purple), *Serratia marcescens* SM39 (dark green), *Haemophilus ducreyi* 35000HP (turquoise), *Wolinella succinogenes* DSM1740 (orange), *Campylobacter jejuni* NCTC11168 (blue), *Helicobacter pylori* 26695 (black), *Bacillus subtilis* 168 (light blue), and *Mycoplasma pneumoniae* M129 (red).

Since in other bacterial species, phenotypes might be obscured due to a potential functional redundancy of PUS enzymes, the presence of few number of tRNA and rRNA PUS enzymes in the two bacterial pathogens confirmed that both *C. jejuni* and *H. pylori* might represent a good minimal systems to study pseudouridylation in bacteria.

Recent studies reported that human and yeast tRNA PUS enzymes Pus1 (TruA family), Pus4 (TruB family), and Pus7 (TruD family) are responsible for pseudouridine modifications not only in tRNAs, but also in mRNAs (Carlile *et al.*, 2014; Schwartz *et al.*, 2014). Since this indicates a potential broader involvement of pseudouridine in all cellular processes, I decided to focus on the characterization of only tRNA PUS enzymes in general, and on TruA, TruB and TruD proteins in particular. To demonstrate that the enzymes are not only encoded in the bacteria (Figure 2.1), but they are also functional, the enzymatic regions for their catalytic activity were investigated. To this end, a sequence logo was generated using the online tool WebLogo3 (http://weblogo.threeplusone.com/). This is helpful to identify the level of conservation of the amino acids surrounding the catalytic aspartate, which gives an indication if the proteins are functionally conserved. Based on previous studies in *E. coli*, the catalytic aspartate is at position 60 in TruA (Foster *et al.*, 2000), at position 48 in TruB (Friedt *et al.*, 2014), and at position 80 in TruD (Kaya & Ofengand, 2003). Using *E. coli* as a reference, the amino acid sequences of the TruA, TruB, and TruD, of bacterial species selected for the analysis (Figure 2.1), considering 10 residues upstream and downstream of the potential aspartate residue was investigated (Figure 2.3). This revealed that all the analyzed proteins have a highly conserved aspartate residue (D, in red) surrounded by a conserved catalytic pocket. Amino acid alignments of these regions in the *E. coli*, *C. jejuni* and *H. pylori* TruA, TruB (only *E. coli* and *C. jejuni*), and TruD proteins showed a high degree of conservation of the aspartate (Figure 2.3, bottom of each sequence logo). In addition, the amino acids surrounding the catalytic residue are also highly conserved, suggesting that not only the presence of the protein, but also a potential catalytic function of TruA, TruB, and TruD might be conserved in the two pathogens.

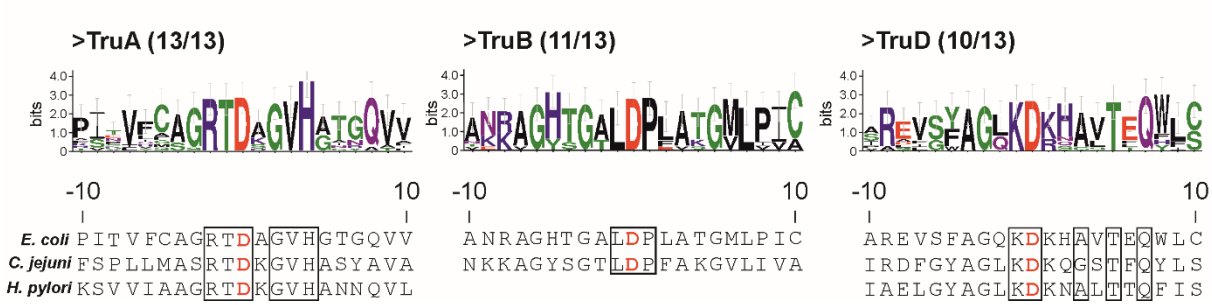

Figure 2.3: Amino acid alignment of TruA, TruB, and TruD in different bacterial species. Amino acid sequence logo of residues in the catalytic pocket of TruA, TruB, and TruD homologs from bacterial species depicted in Figure 2.1 using WebLogo3 (http://weblogo.threeplusone.com/). Green: polar amino acids, purple: neutral amino acids, blue: basic amino acids, red: acidic amino acids, and black: hydrophobic amino acids. Below the sequence logo, an amino acid sequence alignment of TruA, TruB, and TruD of *E. coli*, *C. jejuni* and *H. pylori* is shown. The conserved catalytic aspartate of TruA, TruB, and TruD is marked in red in each sequence alignment.

2.2. Investigation of targets and functions of tRNA PUS enzymes in *C. jejuni* and *H. pylori*

To study the effect of tRNA PUS enzymes on both *C. jejuni* and *H. pylori* fitness, single deletion strains of *truA*, *truB,* and *truD* in *C. jejuni* as well as *truA* and *truD* in *H. pylori* were constructed by replacement of most of the coding sequence with non-polar antibiotic resistance cassettes (Figure 2.4 A & C). Moreover, complementation strains expressing a wild-type copy of *truA*, *truB* or *truD* fused to a C-terminal *3xFLAG* under the promoter and the 5′UTR of *metk* in the non-essential *rdxA* locus were generated in *C. jejuni* (Figure 2.4 B). Complementation of *truD* fused to a C-terminal *3xFLAG* under the promoter of *tlpB* in the non-essential *rdxA* locus was generated in *H. pylori* (Figure 2.4 D).

Table 2.1: tRNA and rRNA PUS enzymes identified in various Gammaproteobacteria, Epsilonproteobacteria, Bacilli and Mollicutes using the eleven tRNA and rRNA PUS enzymes of the bacterial model organism *E. coli* as shown in Figure 2.1. The proteins were identified using the orthologs function in the Kegg database (https://www.genome.jp/kegg/) and BLASTP (https://www.genome.jp/tools/blast/). The annotation of each protein was checked using Kegg (https://www.genome.jp/kegg/) and UniProt (https://www.uniprot.org/).

Bacteria	TruA	TruB	TruC	TruD	RluA	RluB	RluC	RluD	RluE	RluF	RsuA
E. coli	eco:b2318	eco:b3166	eco:b2791	eco:b2745	eco:b0058	eco:b1269	eco:b1086	eco:b2594	eco:b1135	eco:b4022	eco:b2183
S. Typhimurium	SL1344_2337	SL1344_3257	SL1344_2945	SL1344_2907	SL1344_0096	SL1344_1651	SL1344_1123	SL1344_2622	SL1344_1175	SL1344_4128	SL1344_2199
V. cholerae	VC0395_A0520	VC0395_A0176	VC0395_A0411	VC0395_A0058	VC0395_A2087, VC0395_0035	VC0395_A0800	VC0395_A1614	VC0395_A0238	VC0395_A0710	VC0395_A1816	VC0395_A1241
S. marcenscens	SM39_2937	SM39_4775	SM39_3395	SM39_0140	SM39_0043, SM39_3526	SM39_2112	SM39_1369	SM39_0184	SM39_1505	SM39_3191	SM39_2820
S. flexneri	S2529	S3424	S2998	S2961	S0055	S1356	S1170	S2829	S1237	S3635	S2399
C. rodentium	ROD_27301	ROD_46661	/	ROD_30641	ROD_00631	ROD_17361	ROD_11481	ROD_25361	ROD_12251	ROD_37321	ROD_23141
Y. pestis	CH59_3653	CH59_2553	CH59_821	CH59_2690	CH59_1364	CH59_3908	CH59_245	CH59_2780	CH59_197	/	CH59_575
H. ducrey	HD_1104	HD_1459	HD_1138	/	HD_1762	HD_1052	HD_0645	HD_0469	HD_0337	/	HD_1057
W. succinogenes	WS0676	WS0878	/	WS1227	/	WS1979	/	WS0143, WS0417, WS2115	/	/	/
C. jejuni	Cj0827	Cj1102	/	Cj1457c	/	Cj1709c	/	Cj0022c, Cj0708, Cj1280c	/	/	/
H. pylori	HP_0361	/	/	HP_0926	/	HP_1459	HP_0956	HP_0745, HP_0347	/	/	/
B. subtilis	BSU01480	BSU16660	/	/	BSU11620	BSU23160	/	BSU09210, BSU15460	/	/	BSU30035
M. pneumoniae	MPN_196	/	/	/	/	/	MPN_548	MPN_292	/	/	/

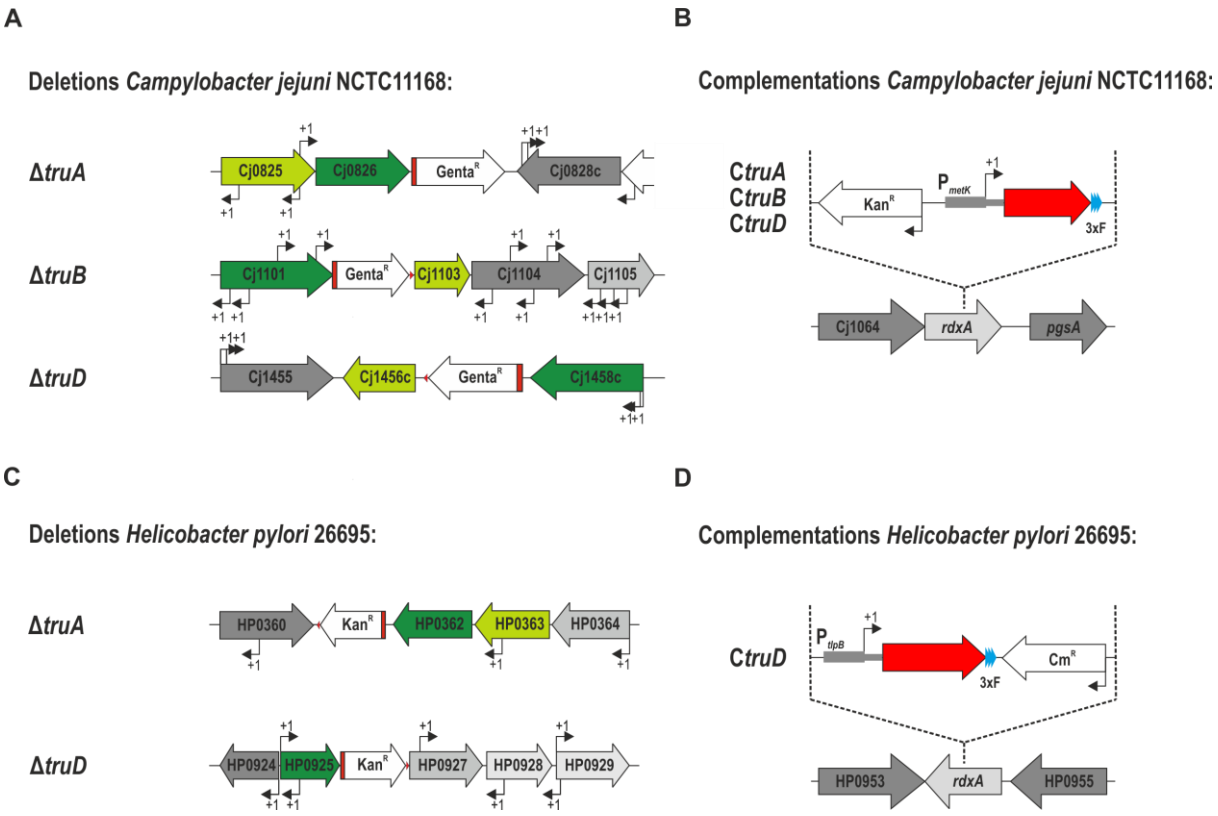

Figure 2.4: Construction of deletion and complementation strains of tRNA PUS enzymes in *C. jejuni* and *H. pylori*. (A) Schematic representation of the cloning strategy used for the construction of *C. jejuni* NCTC11168 deletions. The non-polar gentamycin cassette (Genta^R) was used to avoid potential polar effects on genes encoded downstream of the PUS enzymes. TSS are depicted with +1. Red regions surrounding the Gentamycin resistance cassette indicate the part of the deleted gene that are still present after the introduction of the resistance cassette. **(B)** *C. jejuni* deletion mutant strains were complemented in trans in the non-essential *rdxA* locus. Wild-type copies of *truA*, *truB*, and *truD* fused to a *3xFLAG* sequence at the C-terminus are expressed under the control of the *metK* promoter, while a kanamycin resistance cassette (Kan^R) was included for clone selection. **(C)** Schematic representation of the cloning strategy used for the construction of *H. pylori* 26695 deletions. The non-polar kanamycin cassette (Kan^R) was used to avoid polar effects on genes encoded downstream of the PUS enzymes. TSS are depicted with +1. Red regions surrounding the Gentamycin resistance cassette indicate the part of the deleted gene that are still present after the introduction of the resistance cassette. **(D)** Deletion of *truD* in *H. pylori* strain was complemented in trans in the non-essential *rdxA* locus. A wild-type copy of *truD* was fused to a *3xFLAG* sequence at the C-terminus and was expressed under the control of the *tlpB* promoter, while a chloramphenicol resistance cassette (Cm^R) was included for clone selection.

To study the impact of isogenic deletions of tRNA PUS enzymes on the growth of *C. jejuni* and *H. pylori*, growth curve experiments in rich media were performed in two biological replicates. The growth of the bacteria was measured every two hours after inoculation for *C. jejuni* for 24 hours in total and for *H. pylori* for 36 hours in total (Figure 2.5). Overall, the assay showed that deletion of *truA* and *truD* impacted the growth of *C. jejuni*. While Δ*truA* grew faster compared to the wild-

type strain, Δ*truD* showed a severe growth defect. Deletion of *truB* had no influence on the growth and showed a comparable growth pattern to the parental wild-type strain. Complementation strains restored the wild-type growth (Figure 2.5 A). To investigate which protein is more important for *C. jejuni* growth, double and triple deletion mutant strains were generated. The growth curve analysis showed that whenever the deletion of *truD* is coupled with the deletion of *truA* or *truB*, the strains have a similar growth defect as Δ*truD*. The same result was shown when a triple deletion strain (Δ*truABD*) strain was generated (Figure 2.5 B).

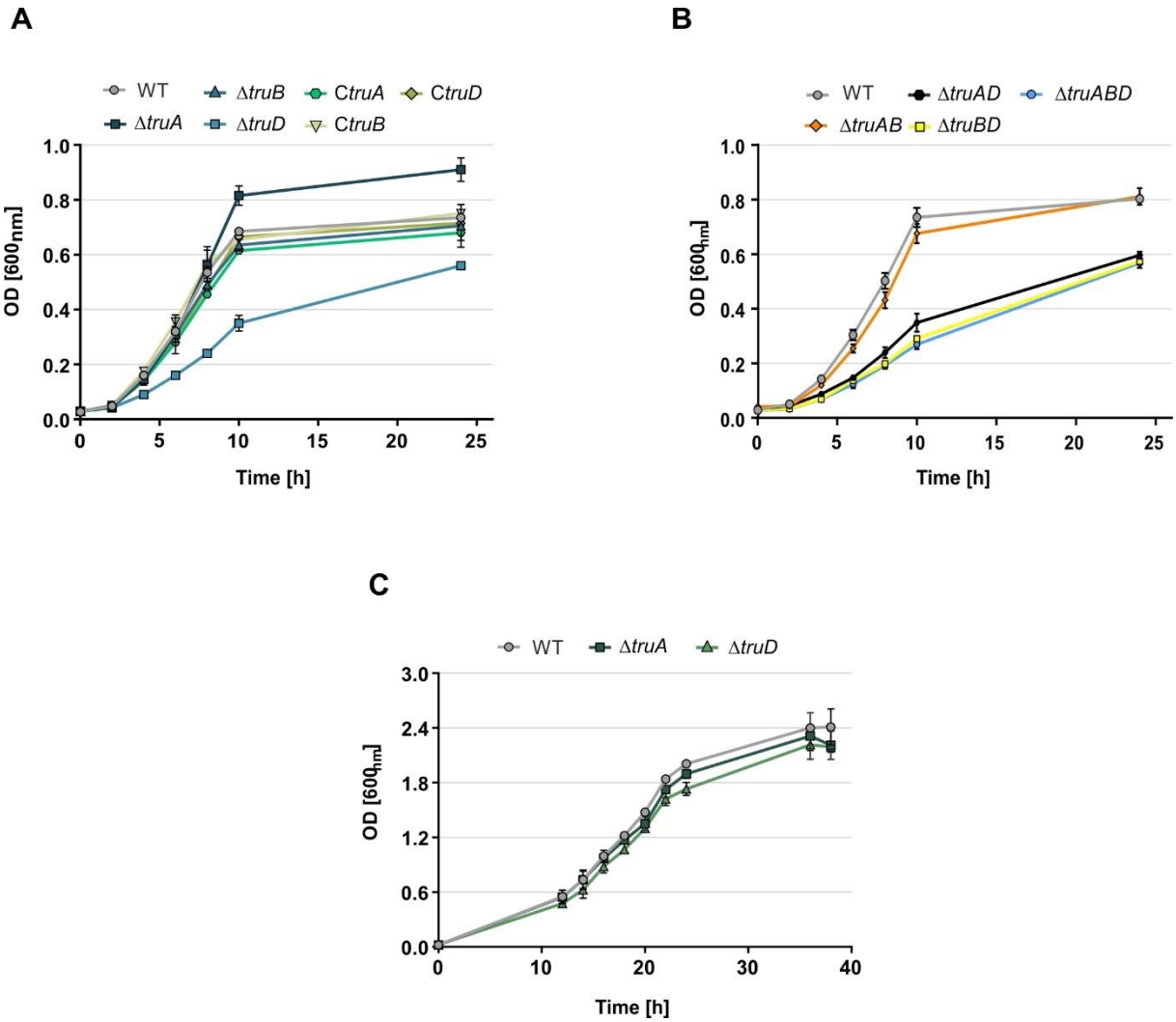

Figure 2.5: Deletion of *truA* and *truD* is affecting the growth of *C. jejuni*, whereas deletion of *truA* or *truD* in *H. pylori* does not show any growth disadvantage (A) Growth curve over 24 hours for *C. jejuni* wild-type, Δ*truA*, Δ*truB*, Δ*truD*, complementation of *truA* (C*truA*), complementation of *truB* (C*truB*), and complementation of *truD* (C*truD*) strains grown in Brucella broth in biological duplicates. **(B)** Growth curve over 24 hours for *C. jejuni* wild-type, Δ*truAB*, Δ*truBD*, Δ*truAD*, Δ*truAD*, and Δ*truABD* strains grown in Brucella broth in biological duplicates. **(C)** Growth curve over 36 hours for *H. pylori* wild-type, Δ*truA*, and Δ*truD* strains grown in brain heart infusion in biological duplicates.

This result suggests that deletion of *truD* is dominant compared to the deletions of *truA* and *truB* in *C. jejuni*. In contrast to *C. jejuni,* deletions of *truA* or *truD* did not affect *H. pylori* growth (Figure 2.5 C), suggesting a different role of these enzymes in the two related pathogens.

2.3. Transcriptome-wide detection of Ψ in *C. jejuni* WT using Pseudo-seq

In order to identify Ψ in the transcriptomes of the two bacterial pathogens, Pseudo-seq (Carlile *et al.*, 2015) was established and applied. The application of Pseudo-seq in RNAs of a wild-type strain is relevant to globally detect pseudouridine modifications in the whole transcriptome. Extending its application in RNAs of ΔPUSs strains allows in addition to identify the RNA substrates of each PUS enzymes. For this purpose, I decided to use a chemical treatment (based on the CMC molecule) as previously described by Bakin and Ofengand in 1993.

As a first step, the capacity of CMC to label Ψ in bacterial RNAs and promote the block of the reverse transcriptase (RT) in a low-throughput manner by a primer extension assay was first tested. Upon CMC treatment (CMC +), the RT will generate a shorter cDNA product compared to a longer one without the treatment (CMC -) (Figure 2.6 A). This was tested on RNAs of *C. jejuni* where, so far, Ψ has never been detected in any tRNAs or rRNAs, but the presence of TruB (Figure 2.1) suggests that Ψ55 in tRNAs might be present. Thus, as potential positive control, I checked Ψ at position 55 on the abundant tRNA-Leu (Cjp16). By comparing the primer extension products of CMC +/CMC - cDNAs of the tRNA-Leu, I confirmed the capability of the method to map Ψ at the 3′ end (C56) of the modified residue at position 55 (Figure 2.6 B, lanes 1 and 2).

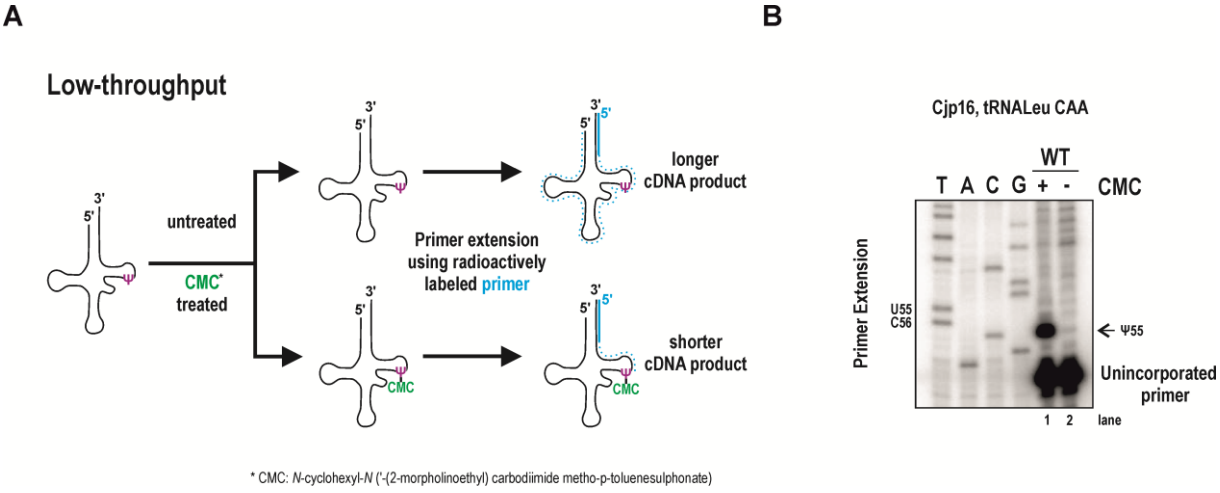

Figure legend on next page

Figure 2.6: Low-throughput detection of pseudouridine. (A) Schematic representation of CMC treatment followed by primer extension assay for low-throughput identification of Ψ in tRNAs. CMC treated tRNA that contains a Ψ in the TΨC loop will be labeled by CMC, while untreated tRNA will not be labeled at that position. Since the presence of CMC will block the incorporation of nucleotides during reverse transcription by a reverse transcriptase at the 3' end of the modification, primer extension using radioactively labeled primer, will generate short cDNA products in the treated sample and long cDNA products in the untreated sample. **(B)** Total RNA was isolated from *C. jejuni* wildtype that was grown to exponential phase (OD_{600nm} of ~0.4/0.5). Total RNA was used in primer extension assays with ^{32}P-end labeled oligo CSO-5145 for reverse transcription of Cjp16 in the presence (lane 1) or absence (lane 2) of the CMC compound. A sequencing ladder corresponding to the Cjp16 region was used as reference (lanes T, A, C, G). cDNA products were analyzed on a 10% PAA gel under denaturing conditions. Primer extension showed a band in lane 1 that is absent in lane 2 that corresponds to the block of the reverse transcriptase at the 3' end of the Ψ-CMC (C56).

Global identification of Ψ *in vivo* at single nucleotide resolution was next performed using Pseudo-seq. This first Pseudo-seq experiment was performed by Dr. Gaurav Dugar in our lab. Briefly, total RNA was treated with CMC or left untreated, fragmented and size-selected. cDNA libraries were then generated using the protocol for ribosome profiling (Ribo-seq) (Lovejoy *et al.*, 2014) (Figure 2.7). The size-selected RNAs were ligated at their 3′ end to an adenylated DNA linker that was used as a binding site for a modified primer (RT primer) in a reverse transcription (RT) reaction. The RT primer contains two modifications that facilitate the intramolecular circularization of the single-stranded cDNA (sscDNA) that was afterwards used as a template for the amplification of the region for Illumina sequencing. Figure 2.7 depicts the different step of the cDNA library protocol used for Pseudo-seq of RNA of *C. jejuni* WT.

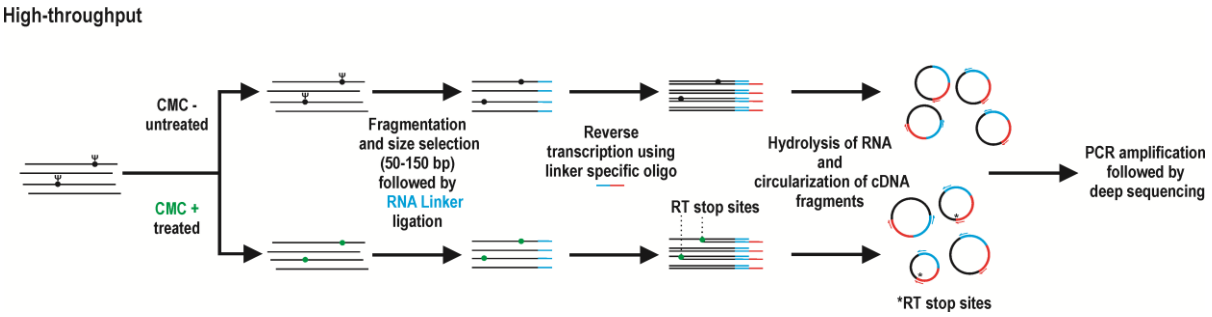

Figure 2.7: High-throughput detection of pseudouridine. cDNA library construction for identification of Ψ using high-throughput Pseudo-seq method. Total RNA was treated with CMC or left untreated, fragmented, and size-selected. The RNA was then ligated at the 3' end to an adapter/linker sequence that contains the binding site for the reverse transcription (RT) primer. After the reverse transcription, single-stranded cDNA (sscDNA) was circularized and amplified. cDNA libraries were sequenced using an Illumina platform.

Since the RNA sample was not depleted from rRNAs, the reads were mapped to the reference genome on different types of RNA including mRNAs, tRNAs, rRNAs, sRNAs and transcripts. To investigate whether the method worked, known modified transcripts (tRNAs and rRNAs) were first checked to demonstrate the presence of Ψ. By comparing the reads from CMC + with those from CMC - libraries Ψ was identified at position 55 on different tRNAs located in the same operon (Figure 2.8).

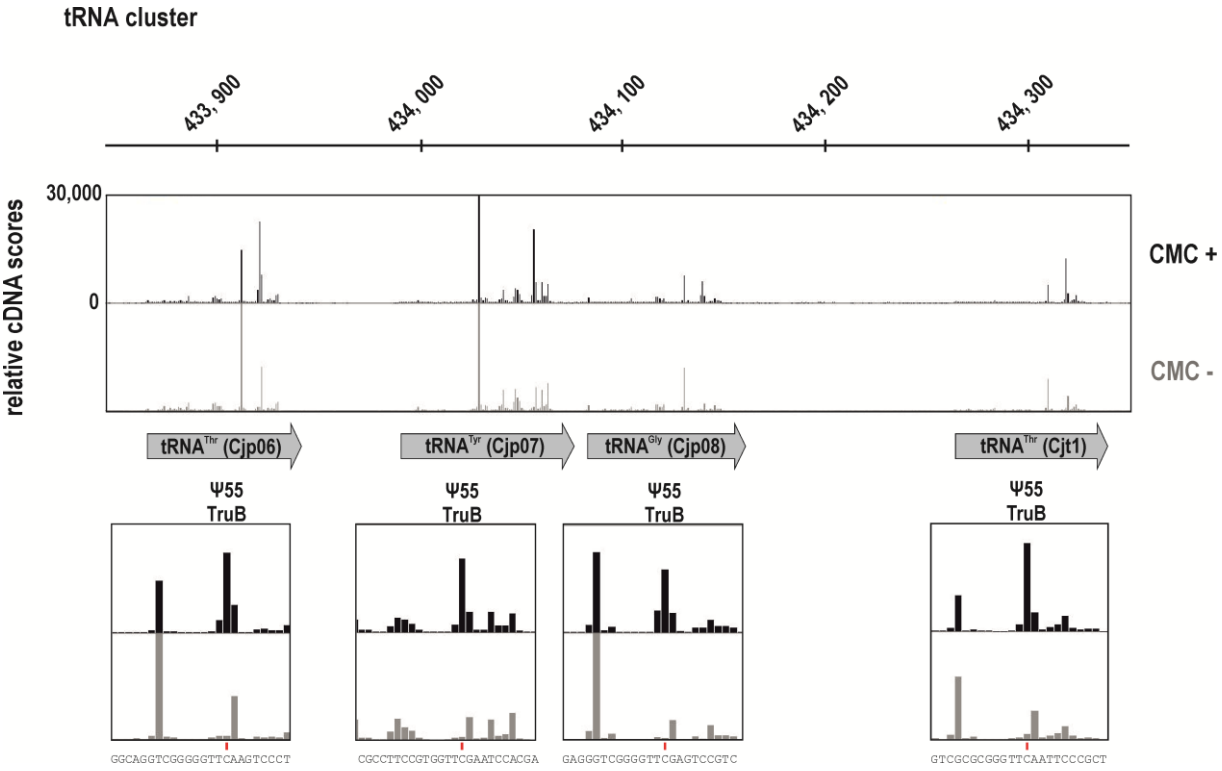

Figure 2.8: Pseudo-seq in RNA of *C. jejuni* WT identifies modified tRNAs. Pseudo-seq reads of *C. jejuni* wild-type CMC + (black) and CMC - (grey) libraries were aligned to the genome of C. jejuni strain NCTC11168 and are visualized as coverage plots in the Integrated Genome Browser (IGB). A representative screen shot of the tRNA locus containing the tRNAs Cjp06, Cjp07, Cjp08 and Cjt1 is shown. Genomic coordinates are indicated in the upper part of the figure and the number of reads is shown on the left (0 – 30,000) outside the black box.

Regarding the rRNAs, based on known sites that are pseudouridylated in the 23S rRNA of *E. coli*, the nucleotide sequences of the 23S rRNA of *C. jejuni* and *E. coli* were aligned and the positions that are known to be modified by the *E. coli* rRNA PUS enzymes were checked in the genome browser. The *C. jejuni* 23S rRNA (Cjr08) is modified in at positions 1927, 1933, 2520, and 2621 (Figure 2.9). The RT stops at 3′ ends of tRNAs and rRNAs in known positions, suggesting that Pseudo-seq can be applied to identify Ψ sites in bacteria.

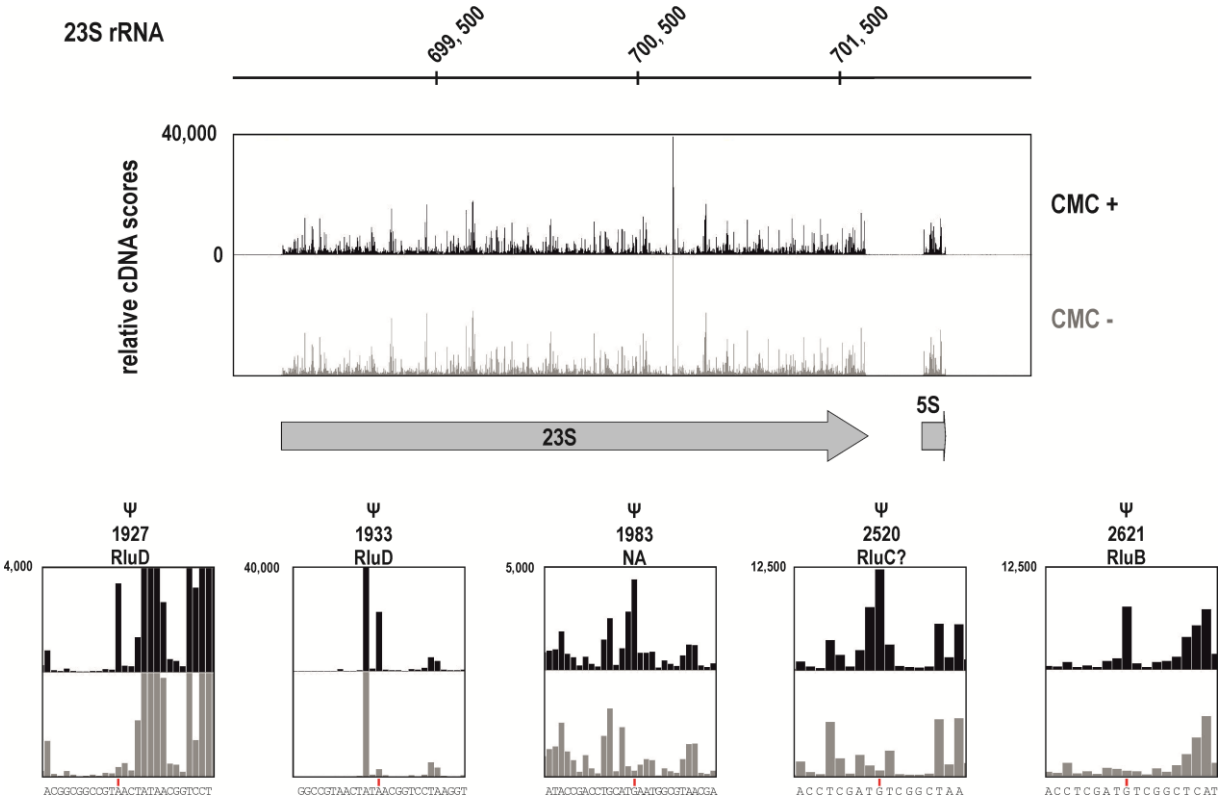

Figure 2.9: Pseudo-seq in RNA of *C. jejuni* WT identifies pseudouridine modification sites in 23S rRNA. (*Upper panel*) A representative screen shot of the rRNA locus containing the Cjr08 and Cjr09 (23S rRNA and 5S rRNA) on the leading strand is shown. Genomic coordinates are indicated in the upper part of the figure and the number of reads is shown on the left (0-40,000) outside the black box. (*Lower panel*) Enlarged view of screenshots of Cjr08 regions where different Ψ sites have been identified and corresponding rRNA PUS enzymes (positions 1927-RluD, 1933-RluD, 1983-NA (Enzyme Not Available), 2520-RluC?, and 2621-RluB) are labeled on top of each box. Different number of reads are indicated on the left side of each black box. The red rectangles show the nucleotide at the 3′ end of the modification.

2.4. Pseudo-seq allows the re-annotation of the rRNA PUS enzyme RluC in *C. jejuni*

Pseudo-seq performed on RNA of *C. jejuni* WT identifies Ψ at position 2520 in the *C. jejuni* 23S rRNA that corresponds to 2504 in the *E. coli* 23S rRNA, a site modified by RluC in *E. coli* (Figure 2.9). The presence of RluC in *C. jejuni* (CjRluC) is still unclear, as Cj0022c, Cj0708, and Cj1280c are annotated as RluD orthologs (CjRluDs) (Figure 2.1 and Table 2.1). In contrast, the related *H. pylori* codes for RluC (HpRluC), annotated as HP0956. To determine whether one of the CjRluD orthologs might represent CjRluC, the genomic context of CjRluDs and HpRluC in the two related Epsilonproteobacteria was investigated. In *H. pylori* the *rluC* gene is located downstream of the HP0957, which is coding for KdtA together with an uncharacterized protein (HP0958). A similar

conservation and organization in the operon structure was identified for Cj0708 in *C. jejuni* (Figure 2.10 A). Moreover, when comparing the protein similarity of Cj0708 or CjRluC with EcRluC, EcRluD, HpRluC, HpRluD (two copies), a higher amino acid similarity was observed for CjRluC and HpRluc. In particular, CjRluC shares 30.5-33.3% sequence identity with the *E. coli* or *H. pylori* RluD whereas the same protein shares 46.3% amino acid identity with HpRluC (Figure 2.10 B). This suggests that Cj0708 can be re-annotated as CjRluC. This level of conservation is additionally reflected when comparing the amino acid sequences between the two proteins (Figure 2.10 C).

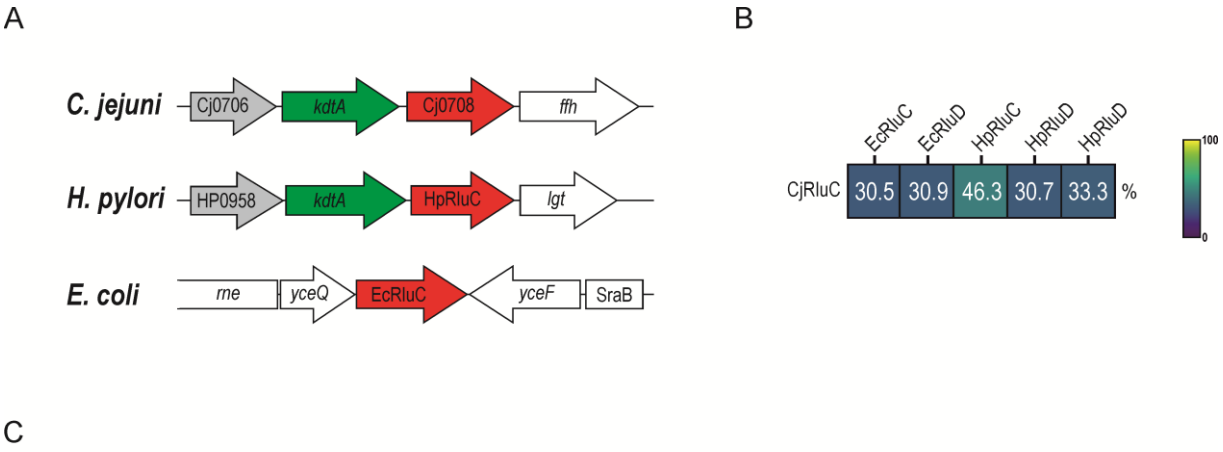

Figure 2.10: Cj0708 can be re-annotated as CjRluC. (A) Genomic context of *C. jejuni* Cj0708, *H. pylori* HpRluC, and *E. coli* RluC. The genes are represented with red arrows, while the *kdtA* with green arrows. The genes encoding for the uncharacterized, but homologus proteins Cj0706 and HP0958 are shown in grey arrows. The genes *ffh* (*C. jejuni*), *lgt* (*H. pylori*), *rne*, *yceQ*, *yceF*, and the small RNA SraB (*E. coli*) are shown in white **(B)** Amino acid identity shown as a percentage between CjRluC and EcRluC, EcRluD, HpRluC, and the two copies of HpRluD. **(C)** Amino acid sequence alignment between Cj0708 (CjRluC) and HP0956 (HpRluC).

Taken together, Pseudo-seq is a powerful method to 1) identify pseudouridine in the transcriptome of bacteria and 2) re-annotate genes encoding tRNA and rRNA PUS enzymes.

2.5. Optimization of cDNA libraries for Pseudo-seq

Recently, different groups have developed deep-sequencing approaches to identify pseudouridine at single-nucleotide resolution in eukaryotic RNAs (Lovejoy A. et al., 2017; Carlile T. M. et al., 2014; Schwartz S. et al., 2014; Li X. et al., 2015). These techniques derive from the primer extension method for pseudouridine detection described by Bakin and Ofengand in 1993, but they differ from each other regarding the generation of cDNA libraries. The preliminary Pseudo-seq data-set for *C. jejuni* WT described in paragraph 2.3. was generated by Dr. Gaurav Dugar and it is based on a cDNA library protocol used previously for Ribosome profiling (Ribo-seq) experiments (Ingolia *et al.*, 2012; Lovejoy *et al.*, 2014). This protocol is optimized for large amounts of RNA corresponding to ribosome footprints in which an adenylated DNA linker is first ligated to the fragmented RNAs, followed by reverse transcription and circularization of the cDNA. Unfortunately, the approach presented limitations regarding the reproducibility of library generation, probably due to several gel extraction steps that might generate variations between the samples. In 2017, McGlincy and Ingolia published an optimized protocol based on the circularization of cDNA that has less gel extraction steps and includes the use of 5´ adenylated DNA linkers containing sample barcodes and unique molecular identifiers (UMIs). Less extraction steps lead to a reduced loss of RNA and, consequently lower amounts of RNA are needed as input. This is particularly useful when the input material is derived from an mRNA enrichment step where the rRNAs are depleted from the cellular RNAs. For this reason, the gel extraction step that was used in the preliminary Pseudo-seq experiment to extract the ligated RNA before the reverse transcription reaction in order to avoid contamination of the linker (Figure 2.11 A) was substituted with incubation of the RNA with a 5´ deadenylase and the exonuclease RecJ enzymes (Figure 2.11 B). The two enzymes cooperate to promote the deadenylation followed by degradation of the single stranded linker. Figure 2.11 A & B shows the differences between the two approaches used for Pseudo-seq cDNA library preparation.

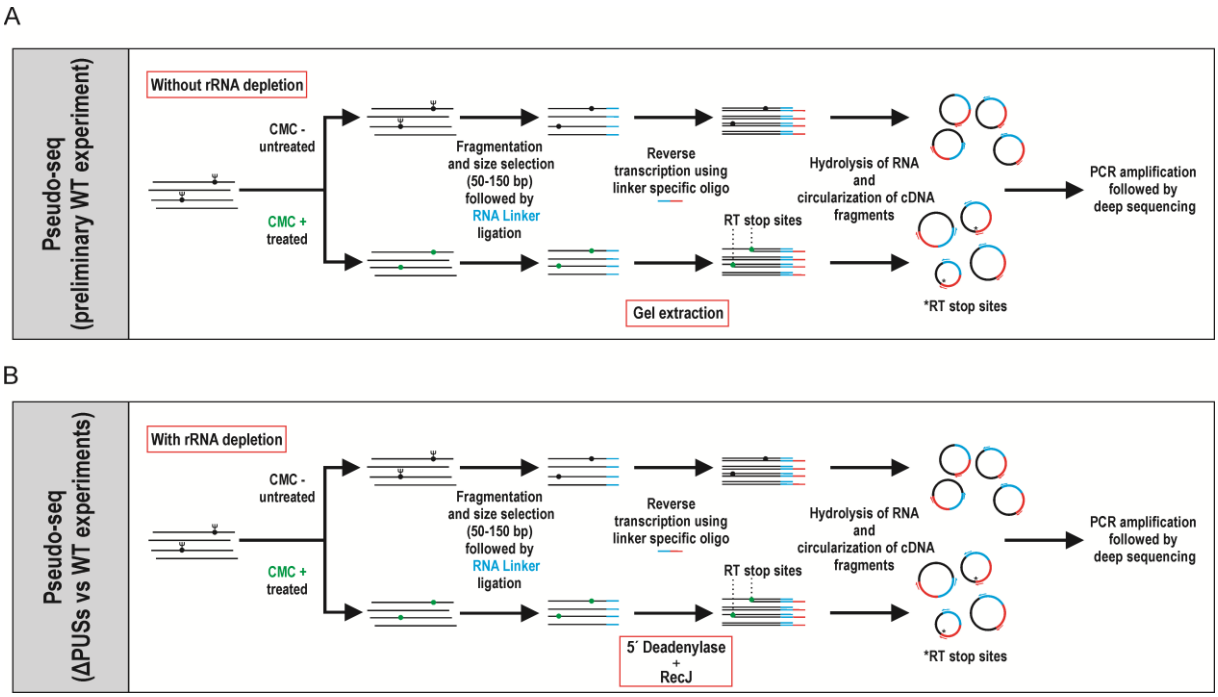

Figure 2.11: Differences between the cDNA library protocols used for Pseudo-seq experiments. (A, B) The workflows describe the different steps during cDNA library preparation for Pseudo-seq. **(A)** Preliminary Pseudo-seq experiment in *C. jejuni* WT strain was performed without the step of rRNA depletion and a gel extraction was performed after linker ligation. **(B)** Pseudo-seq experiments in *C. jejuni* and *H. pylori* WT and ΔPUSs were performed using the protocol of McGlincy and Ingolia where a deadenylase and RecJ treatment was performed after linker ligation. Moreover, an rRNA depletion step was performed on the input RNA. The red rectangles represent the major changes in the two protocols.

To generate libraries for both bacteria using Pseudo-seq, I established the optimized protocol in our lab, without using the DNA-barcoded linkers. Internal modifications in tRNAs (e.g., positions 13 and 38-39-40) were detectable using the optimized protocol (data not shown). Thus, this protocol was used for the following Pseudo-seq experiments where libraries generated from ΔPUSs enzymes compared to those generated from wild-type samples.

2.6. Identification of pseudouridine in *C. jejuni* WT and ΔPUS strains.

To globally identify the sites modified by PUS enzymes in *C. jejuni*, Pseudo-seq on total RNA (rRNA depleted) isolated from *C. jejuni* wild-type and Δ*truA*, Δ*truB*, Δ*truD*, Δ*truABD* strains grown to exponential phase was performed. In total 20 cDNA libraries for *C. jejuni* were generated in two biological replicates (CMC treated/CMC +, CMC untreated/CMC -) and sequenced. For the identification of the modified site, each strain was analyzed separately and for each nucleotide the

significant enrichment of CMC + over the CMC - value was calculated. Moreover, a minimum number of 5 reads per nucleotide was set as a threshold for the analyses. A site was considered significantly modified when the log_2 fold change (log_2FC) was > 1.0 and the adjusted p-value (adj.p-value) corrected for multiple testing was < 0.1. Moreover, only potential sites that mapped to the 3´ end of a thymine (uridine) residue were considered. As a first step, the sites in the wildtype strain were determined, where all the modifications should be present, and then the log_2FC of the wildtype strain to the log_2FC of each mutant strain was compared to define the PUS enzyme responsible for generating the respective modification. For mutant analysis, a PUS was defined as responsible for the modification at a specific position if the log_2FC of the peak corresponding to a potential Ψ is reduced (log_2FC < 1.0 and additional manual inspection in the genome browser) in the deletion of a particular PUS compared to all other strains. In *C. jejuni* wildtype strain a total of 72 Ψ sites were identified. These include 44 sites in tRNAs, 25 in mRNAs, one site in the 3′ UTR and two sites in the 5′ UTRs. Only six sites were identified with a log_2FC > 1.0 in mRNA/5′ UTR also in Pseudo-seq of ΔPUS strains. However, except for one site in the 5′ UTR of *purD* which seems to be potentially modified by TruD, all the other sites were detected with a log_2FC > 1.0 only in the wildtype strain. In addition, in the wildtype *C. jejuni* known Ψ sites at position 13, 39, 40, and 55 in tRNAs were identified. Some potential sites did not pass the cut-off of adj.p-value<0.1 in the mutant strain libraries. However, they showed logFC>1.0 and therefore they were considered in the analysis. For example, the presence of the modification at position 55 in *C. jejuni* wildtype suggested to be modified by TruB, as this was missing in the Δ*truB* library. Moreover, loading the Pseudo-seq experiment using the Integrated Genome Browser (IGB; http://genoviz.sourceforge.net/) allows to directly visualize the results in a genome-wide manner. Figure 2.12 shows examples of screenshots of potentially modified sites in wild-type, Δ*truA*, Δ*truB*, Δ*truD,* and Δ*truABD* strains. Normalized reads of different cDNA libraries were loaded in IGB and the presence or absence of the peak at the coordinates identified by Pseudo-seq is observed. While clear peaks are visible for more internal modifications mediated by TruA and TruD, modification at position 55 is more variable. This variability can be explained by the fact that modification at position 55 is located more at the 3´ end and thereby, during library preparation, the sequencing of this position might be compromised.

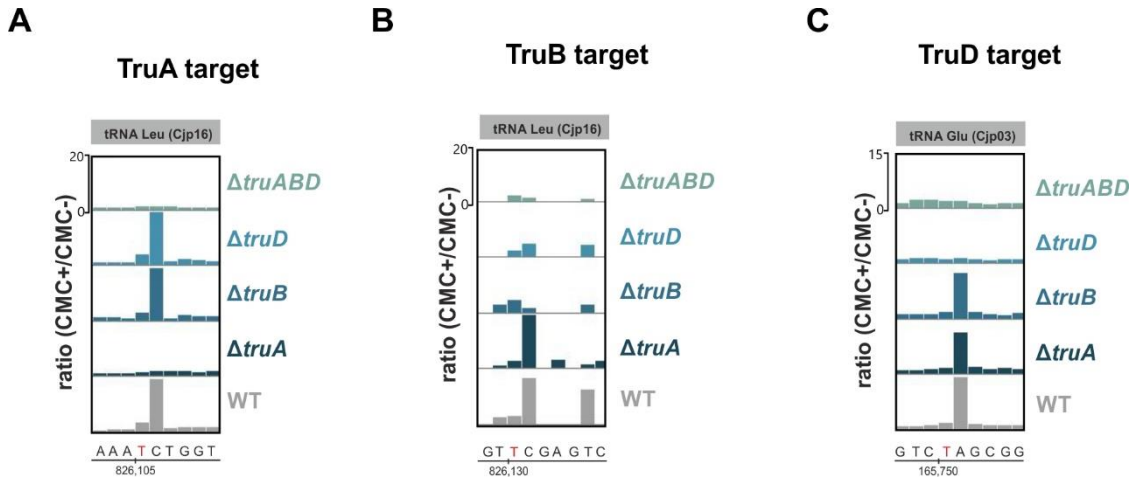

Figure 2.12: Examples of tRNA targets of tRNA PUS enzymes in *C. jejuni* identified by Pseudo-seq. Pseudo-seq reads of *C. jejuni* wild-type (grey), Δ*truA* (dark blue), Δ*truB* (blue), Δ*truD* (light blue), and Δ*truABD* (turquoise) ratios of normalized CMC +/CMC - libraries were mapped to the genome of *C. jejuni* strain NCTC 11168 and are visualized as coverage plots in the Integrated Genome Browser (IGB). Each Pseudo-seq dataset represents the normalization of the two replicates/strain. A representative screen shot of the tRNA targets of TruA (Cjp16, position 40), TruB (Cjp16, position 55) and TruD (Cjp03, position 13) is visualized. Genomic coordinates are indicated in the lower part of the figure and the number of reads is shown on the left outside of the black box. The red T shows the potential pseudouridine identified by Pseudo-seq.

In detail, in *C. jejuni* tRNAs, three sites modified by TruA (CjTruA) were mapped at position 40 of Cjp26 (tRNA-Sec), Cjp28 (tRNA-Leu), and position 41 of Cjt05 (tRNA-Leu). In addition, I found Ψ at position 39 of Cjt05 (tRNA-Leu) and at position 39 of Cjp16 (tRNA-Leu) by manual inspection of the genome browser. These two sites could be missed since the threshold for the identification of the RNA substrates is log2FC ≤ 1.0 for the ΔPUS compared to the wild-type strain It is possible that the modification at position 41 in the tRNA-Leu (log2FC in WT: + 2.2) is the product of a "stuttering"/STOP of the RT probably due to the adjacent Ψ39 site (log2FC in WT: +6.9). Twenty sites are modified by TruB (CjTruB) at position 55 of diverse tRNAs and four sites at position 54. However, since it is known that bacterial tRNAs do not have Ψ modification at position 54 that is rather converted to a version of ribothymidine, it is possible that these sites derive from a "stuttering" effect of the RT termination in the modified CMC treated site as previously reported (Bakin & Ofengand, 1998; Schwartz *et al.*, 2014). Additionally, TruB-dependent sites are identified at unusual positions 60 and 43 in Cjp28 (tRNA-Leu). One site is modified by TruD (CjTruD) at position 13 of a single tRNA (Cjp03, tRNA-Glu). This analysis suggested that another site might be modified by TruD at position 31 of Cjt1 (tRNA-Thr), but contrary to the modification at position 13, it was not possible to define a clear and sharp peak in the different strains. The modified sites are listed in Table 2.2.

Table 2.2: Potentially modified nucleotides which show a log$_2$FC>1.0 change in the *C. jejuni* Pseudo-seq including WT, Δ*truA*, Δ*truB*, Δ*truD,* and Δ*truABD* data-sets. The columns represent the position at 3′ of Ψ, the locus tag, the type of RNA, the RNA, the position of Ψ in the RNA, the log$_2$FC of WT, Δ*truA*, Δ*truB*, Δ*truD*, and Δ*truABD* and the sequence (5′→3′) of the tRNA/mRNA/5′UTR/3′UTR and the potential Ψ site is highlighted in red. Values in bracket indicate sites with adj.p-value>0.1.

Position at 3′ of Ψ/Strand	Locus tag	Type of RNA	RNA	Position	log2 FC WT	log2 FC Δ*truA*	log2 FC Δ*truB*	log2 FC Δ*truD*	log2 FC Δ*truABD*	Sequence 5 → 3 (in red the pseudouridine site)
878243:-	Cjp19	tRNA	tRNA Val anticodon TAC	55	3,4	(4,7)	(0,7)	(3,9)	/	GGTCGCTTAGCTCAGTTGGTAGAGCGCCACCCTTACAAGGTGGATGTCATAAGTTCGAGTCTTATAGTGACCACCA
434032:+	Cjp07	tRNA	tRNA Tyr anticodon GTA	40	2,0	(1,1)	(2,0)	(1,1)	(-0,1)	GGTGAGTTACTCAAGTGGCCAACGAGGGCAGACTGTAAATCTGCTGGCTTTCGCCTTCCGTGGTTCGAATCCACGACTC ACCACCA
435870:+	Cjp09	tRNA	tRNA Trp anticodon CCA	39	5,4	(2,3)	(3,7)	(5,9)	(0,0)	AGACAGGTGTCCGAGCGGTTGAAGGAGCACGCCTGGAACGCGTGTAAAGTGCAAGCTTTCGAGGGTTCGAATCCCTTCC TGTCTGCCA
435863:+	Cjp09	tRNA	tRNA Trp anticodon CCA	32	4,3	(2,5)	4,9	4,4	(4,2)	GCGGATGTGGTGAAATTGGCAGACACGCCAGACTTAGGATCTGGTGCAGCAATGCGTGAAGGTTCAAGTCCTTTCATCC GCACCA
433922:+	Cjp06	tRNA	tRNA Thr anticodon TGT	55	4,2	(4,3)	(0,9)	(3,5)	(-0,2)	GCCCGGGTGGTGGAATTGGTAGACACAAGGGACTTAAAATCCCTCGGAATTTTTCTTCCGTGCCGGTTCAAGTCCGGCC TCGGGCACCA
434037:+	Cjp07	tRNA	tRNA Thr anticodon GTA	45	2,4	(0,5)	(2,0)	(-0,2)	(0,8)	GGTGAGTTACTCAAGTGGCCAACGAGGGCAGACTGTAAATCTGCTGGCTTTCGCCTTCCGTGGTTCGAATCCACGACTC ACCACCA
434296:+	Cjt1	tRNA	tRNA Thr anticodon GGT	31	1,5	(1,6)	(1,7)	(0,7)	(0,8)	GCGGGAATAGCTCAGGGGTAGAGCACAACCTTGCCAAGGTTGGGGTCGCGAGTTCGAATCTCGTTTCCCGCTCCA
1550010:+	Cjp30	tRNA	tRNA Ser anticodon TGA	55	4,1	(4,4)	/	(3,4)	(1,2)	CGGGAGATGGCTGAGTGGTCGAAAGCGGCGGTCTTGAAAACCGTTGAGGGTCACACCTCCAGGGGTTCGAATCCCTTTC TCCCGGCCA
1287757:-	Cjp25	tRNA	tRNA Ser anticodon GTC	55	3,4	(5,2)	(-0,3)	(3,2)	(-0,8)	GGACAGATGGGTGAGTGGCTGAAACCACACCCCTGCTAAGGGTGCAGATCTTAACGGGTCTCGAGGGTTCAAATCCCTC TCTGTCCGCCA
1626558:+	Cjt06	tRNA	tRNA Ser anticodonGGA	55	4,3	(6,2)	/	(4,6)	/	GGTTGGATAGCTCAGTCGGTAGAGCAGCAGACTGAAAATCTGCGTGTCGGCAGTTCGATTCTGCCTCTAACCACCA
1432427:-	Cjp26	tRNA	tRNA SeC anticodon TCA	40	5,2	(0,6)	4,7	5,3	(0,2)	GGAAGATTAGCGTATCTGGTGATCGCCACTGACTTCAAATCAGATGAAAGGATAGTTGACTATTCTTTGGGGAGTTCG ATTCTCTCATCTTCTCGCCA
1432414:-	Cjp26	tRNA	tRNA SeC anticodon TCA	52	1,9	(1,3)	(1,3)	(1,1)	(0,8)	GGAAGATTAGCGTATCTGGTGATCGCCACTGACTTCAAATCAGATGAAAGGATAGTTGACTATTCTTTGGGGAGTTCG ATTCTCTCATCTTCTCGCCA
1215277:-	Cjp24	tRNA	tRNA Phe anticodonGAA	39	4,6	3,3	(3,5)	(5,3)	(-0,2)	GCCCGAGTGGTGAAACTGGTAGACGCGCCAGACTCAAAATCTGGTAAGGGCAACCTTGTGTCGGTTCGAGTCCGACCTC GGGCACCA

533136:-	Cjp12	tRNA	tRNA Met anticodon CAT	36	2,9	(1,3)	(1,4)	(1,0)	(1,6)	CGCGAAGTAGAGCAGTGGTTAGCTCGTCGGGCTCA**T**AACCCGAAGGTCGGGAGTTCAAATCTCCCCTTCGCAACCA
533117:-	Cjp12	tRNA	tRNA Met anticodon CAT	55	3,6	(4,9)	(1,1)	(3,1)	(1,3)	CGCGAAGTAGAGCAGTGGTTAGCTCGTCGGGCTCATAACCCGAAGGTCGGGAGT**T**CAAATCTCCCCTTCGCAACCA
1590313:-	Cjt05	tRNA	tRNA Leu anticodon TAG	41	2,2	(0,4)	2,0	(1,8)	(-0,3)	GCGGATGTGGTGAAATTGGCAGACACGCCAGACTTAGGA**T**CTGGTGCAGCAATGCGTGAAGGTTCAAGTCCTTTCATCC GCACCA
1590291:-	Cjt05	tRNA	tRNA Leu anticodon TAG	55	4,1	(4,0)	(0,5)	(3,8)	(-0,2)	GCGGATGTGGTGAAATTGGCAGACACGCCAGACTTAGGATCTGGTGCAGCAATGCGTGAAGGT**T**CAAGTCCTTTCATCC GCACCA
1590315:-	Cjt05	tRNA	tRNA Leu anticodon TAG	39	6,9	(1,4)	5,8	5,6	(-0,2)	GCGGATGTGGTGAAATTGGCAGACACGCCAGACTTAGGATCTGGTGCAGCAATGCGTGAAGGTTCAAGTCCTTTCATCC GCACCA
1549785:+	Cjp28	tRNA	tRNA Leu anticodon TAA	43	1,3	(1,5)	(1,0)	(1,2)	(0,5)	GCCCGGGTGGTGGAATTGGTAGACACAAGGGACTTAAAATCCC**T**CGGAATTTTTCTTCCGTGCCGGTTCAAGTCCGGCC TCGGGCACCA
1549814:+	Cjp28	tRNA	tRNA Leu anticodon TAA	60	2,7	(1,8)	(0,7)	(2,3)	(-0,9)	GCCCGGGTGGTGGAATTGGTAGACACAAGGGACTTAAAATCCCTCGGAATTTTTCTTCCGTGCCGGTTCAAG**T**CCGGCC TCGGGCACCA
1549808:+	Cjp28	tRNA	tRNA Leu anticodon TAA	54	2,3	(2,1)	(1,2)	2,8	(-1,2)	GCCCGGGTGGTGGAATTGGTAGACACAAGGGACTTAAAATCCCTCGGAATTTTTCTTCCGTGCCGGT**T**CAAGTCCGGCC TCGGGCACCA
1549781:+	Cjp28	tRNA	tRNA Leu anticodon TAA	40	5,3	(0,6)	5,2	5,4	(0,1)	GCCCGGGTGGTGGAATTGGTAGACACAAGGGACTTAAAA**T**CCCTCGGAATTTTTCTTCCGTGCCGGTTCAAGTCCGGCC TCGGGCACCA
826132:+	Cjp16	tRNA	tRNA Leu anticodon CAA	55	3,9	(4,9)	(0,7)	(2,6)	(1,0)	ATGAAAATTTCATATGAAGATGCAGGCGTAAGTATAGATAATGGAAATACCTTTGTAGAGGCTATAAAACCTTTGGTT AAAGAAACTT**T**TAATGATAATGTTGTAGGTGGAATTGGTT
826106:+	Cjp16	tRNA	tRNA Leu anticodon CAA	39	4,4	(1,2)	4,6	5,1	(0,1)	ATGGCAGATATTACTGATATAAAGACTATACTTTACACAGAAAAAAGTT**T**GAATTTGCAAGAGCAAGGTGTCGTAGTT ATTCAAACTTCGCCAAAAATGACTAAAACAGGCTTAAAAGCGGTTTTAAAAGAGTATTTTGGTGTAACTCC
395887:+	Cjp05	tRNA	tRNA Ile anticodon GAT	55	3,3	(3,3)	(0,3)	(2,7)	(-0,6)	GGGCCTATAGCTCAGCTGGTTAGAGTGCACCCCTGATAAGGGTGAGGTCACAAGT**T**CAAGTCTTGTTAGGCCCACCA
698181:+	Cjp15	tRNA	tRNA Ile anticodon GAT	55	3,3	(3,3)	(0,3)	(2,7)	(-0,6)	GGGCCTATAGCTCAGCTGGTTAGAGTGCACCCCTGATAAGGGTGAGGTCACAAGT**T**CAAGTCTTGTTAGGCCCACCA
41006:+	Cjp02	tRNA	tRNA Ile anticodon GAT	55	3,3	(3,3)	(0,3)	(2,7)	(-0,6)	GGCCTATAGCTCAGCTGGTTAGAGTGCACCCCTGATAAGGGTGAGGTCACAAGT**T**CAAGTCTTGTTAGGCCCACCA
826217:+	Cjp17	tRNA	tRNA Gly anticodon GCC	55	3,9	(3,3)	/	(3,0)	/	GCGGGAATAGCTCAGGGGTAGAGCACAACCTTGCCAAGGTTGGGGTCGCGAGT**T**CGAATCTCGTTTCCCGCTCCA
1549722:+	Cjp27	tRNA	tRNA Gly anticodon GCC	65	1,7	(1,1)	(0,3)	(0,7)	(-0,8)	GCGGGAATAGCTCAGGGGTAGAGCACAACCTTGCCAAGGTTGGGGTCGCGAGTTCGAATCTCGT**T**TCCCGCTCCA
1549711:+	Cjp27	tRNA	tRNA Gly anticodon GCC	55	5,8	(4,7)	(0,3)	(5,2)	(-0,3)	GCGGGAATAGCTCAGGGGTAGAGCACAACCTTGCCAAGGTTGGGGTCGCGAGT**T**CGAATCTCGTTTCCCGCTCCA
1549710:+	Cjp27	tRNA	tRNA Gly anticodon GCC	54	2,8	(1,9)	(1,0)	3,3	(1,1)	GCGGGAATAGCTCAGGGGTAGAGCACAACCTTGCCAAGGTTGGGGTCGCGAG**T**TCGAATCTCGTTTCCCGCTCCA

165782:+	Cjp03	tRNA	tRNA Glu anticodon TCC	55	5,6	(4,9)	(1,1)	(2,5)	(0,4)	GGCCCATTCGTCTAGCGGTTAGGACATCGCCCTTTCACGGCGGTAACACGAGTTCGAGTCTCGTATGGGTCACCA
165741:+	Cjp03	tRNA	tRNA Glu anticodon TCC	13	3,3	2,8	3,0	(-0,4)	(-0,1)	GGCCCATTCGTCTAGCGGTTAGGACATCGCCCTTTCACGGCGGTAACACGAGTTCGAGTCTCGTATGGGTCACCA
1549901:+	Cjp29	tRNA	tRNA Cys anticodon GCA	55	3,7	(4,3)	(0,7)	(3,1)	(0,6)	GGCGACATAGCCAAGCGGTAAGGCATGGGCCTGCAAAGCCTTGATCTCCGGTTCGAATCCGGATGTCGCCTCCA
943575:+	Cjp21	tRNA	tRNA Arg anticodonGCG	40	5,7	(2,7)	(5,4)	(6,2)	(0,0)	GCGCTCATAGCTCAGCTGGATAGAGCATTTGATTGCGGTTCAAAAGGCCAGAGGTTCGAATCCTCTTGAGCGCACCA
460303:+	Cjp10	tRNA	tRNA Arg anticodon CCT	33	3,9	(4,7)	4,8	3,9	(3,9)	GTCCTCGTAGCTCAGCAGGATAGAGCGCAAAATTCCTAATTTTGAGGCCGTGAGTTCGAATCTCGCCGTGGACACCA
698096:+	Cjp14	tRNA	tRNA Ala anticodon TGC	55	3,4	(4,0)	(-0,1)	(3,6)	/	GGGGAATTAGCTCAGCTGGGAGAGCGCCTGCTTTGCACGCAGGAGGTCAGCGGTTCGATCCCGCTATTCTCCACCA
698095:+	Cjp14	tRNA	tRNA Ala anticodon TGC	54	1,6	(2,0)	(0,7)	(1,3)	(-0,1)	GGGGAATTAGCTCAGCTGGGAGAGCGCCTGCTTTGCACGCAGGAGGTCAGCGGTTCGATCCCGCTATTCTCCACCA
40921:+	Cjp01	tRNA	tRNA Ala anticodon TGC	55	3,4	(4,0)	(-0,1)	(3,6)	/	GGGGAATTAGCTCAGCTGGGAGAGCGCCTGCTTTGCACGCAGGAGGTCAGCGGTTCGATCCCGCTATTCTCCACCA
40920:+	Cjp01	tRNA	tRNA Ala anticodon TGC	54	1,6	(2,0)	(0,7)	(1,3)	(-0,1)	GGGGAATTAGCTCAGCTGGGAGAGCGCCTGCTTTGCACGCAGGAGGTCAGCGGTTCGATCCCGCTATTCTCCACCA
395802:+	Cjp04	tRNA	tRNA Ala anticodon TGC	55	3,4	(4,0)	(-0,1)	(3,6)	/	GGGGAATTAGCTCAGCTGGGAGAGCGCCTGCTTTGCACGCAGGAGGTCAGCGGTTCGATCCCGCTATTCTCCACCA
395801:+	Cjp04	tRNA	tRNA Ala anticodon TGC	54	1,6	(2,0)	(0,7)	(1,3)	(-0,1)	GGGGAATTAGCTCAGCTGGGAGAGCGCCTGCTTTGCACGCAGGAGGTCAGCGGTTCGATCCCGCTATTCTCCACCA
1626680:+	Cjp35	tRNA	tRNA Ala anticodonGGC	55	3,7	(5,0)	(2,0)	(3,3)	/	GGGGCATTAGCTCAGCTGGGAGAGCACAACGCTGGCAGCGTTGGGGTCAGCGGTTCGAACCCGCTATGCTCCACCA
878325:-	?	tRNA	Potential tRNA	55	4,1	(1,6)	(0,7)	(2,2)	/	Potential sequence: GTTATGACCCTTTCGTCTAGTGGCCCAGGACAACACTCTCTCTGTGTGGAAACAGAGGTTCAAATCCTCTAGGGGTCGCCA
1107868:-	Cj1181	mRNA	*tsf*	924	4,1	(0,9)	(-0,2)	/	/	GGGTCAGTTTTATGTAATGGAT
1212627:-	Cj1279c	mRNA	*trmB*	285	3,7	/	/	/	/	AAACTTGTAGGCACTATTAAAGATAAGTTTCAAACT
407082:+	Cj0437	mRNA	*sdhA*	1749	4,3	/	/	/	/	ATTATCCAAAGCGAGATGATAAAAATTTCTTAAAACATAGCATT
339267:+	Cj0370	mRNA	*rpsU*	196	3,1	(0,9)	(1,5)	(0,5)	(0,5)	TGCTTAAAAGACTTTATATGCTTAGACGCT
339259:+	Cj0370	mRNA	*rpsU*	189	2,4	(2,0)	(2,0)	(1,4)	(1,1)	AAAAAATGCTTAAAAGACTTTATATGCTT
931477:+	Cj1001	mRNA	*rpoD*	286	3,8	(-0,4)	/	/	/	AGCCTTGAGAACGAATTTGATTTAGCCAATGAAAACGATT
1619140:-	Cj1705c	mRNA	*rplW*	50	4,4	(-0,7)	(0,6)	(-0,3)	/	GACTATACTTTACACAGAAAAAAGTTT
1620130:-	Cj1707c	mRNA	*rplC*	249	3,8	(-0,1)	(-0,3)	(-0,2)	/	CTTTAGAAGTAGCAAATACTGAAGCAGGAGATTTAGAT

1618468:-	Cj1704c	mRNA	*rplB*	439	1,4	(0,0)	(0,4)	(-0,5)	(-2,0)	CTTAAAAACATTCCTGTGGGTACTATTGTTCATAATGTTGAG**T**
868257:-	Cj0933c	mRNA	*pycB*	1307	3,8	(-3,5)	/	(-0,4)	/	TAAAGATGAGAGTAAAAGTATAGCTTATACCAAAACCTTGCTTGAAAAAGAGGGTA**T**
1462404:-	Cj1529c	mRNA	*purM*	89	4,5	/	/	(-0,8)	/	CTTTGTAGAGGCTATAAAACCTTTGGTTAAAGAAACTT**T**
1453018:+	Cj1516	mRNA	oxidoreductase	1418	3,8	/	(-0,5)	/	/	TTAGAGCCTTCAGAGATACTATAAATG**T**
222192:-	Cj0239c	mRNA	NifU-like protein	695	4,2	(-1,1)	(-0,8)	(0,5)	/	AAACTAGAGCTGAAATAGATAGAGAAAAACTCAAAAATACAA**T**
1045299:-	Cj1112c	mRNA	methionine sulfoxide reductase B	294	4,0	/	/	/	/	TTTAGGTCATGTTTTTGAAGGAGAAGGATT**T**
648768:+	Cj0691	mRNA	membrane protein	239	3,8	(0,0)	(1,4)	/	(-0,9)	ATTTTTTAACAAAGCTTGACT**T**
1442647:-	Cj1506c	mRNA	MCP-type signal transduction protein	339	4,2	(-0,4)	/	(-0,2)	/	GATAATAGTGCTTATTCTAATTTTACTTATTTATATC**T**
342725:+	Cj0375	mRNA	lipoprotein	110	3,8	/	/	/	/	CTTGATGGTTTTGATTGCTTCCCCTATGA**T**
1430996:-	Cj1497c	mRNA	hypothetical protein	99	4,2	/	/	/	/	TTAATCAAGCCAAACAAAGACAGCTTGAACA**T**
688488:-	Cj0734c	mRNA	hisJ	192	3,9	/	/	/	/	AAAACTTACAGGTTTTGATACTGATTTGGTTGAAGAGAT**T**
382663:+	Cj0415	mRNA	GMC oxidoreductase subunit	995	3,9	/	/	/	/	TAAAGGAACTTTAGGTAGAAATTA**T**
788346:-	Cj0840c	mRNA	*fbp*	701	3,9	/	/	/	/	CTTTCCTCTAGCCTTTATCA**T**
1085680:+	Cj1153	mRNA	cytochrome c	301	3,9	(0,6)	(1,1)	(0,4)	(0,2)	CTATCGAAGCTCATATTGAAACTTTAAAA**T**
914869:-	Cj0981c	mRNA	*cjaB*	659	4,3	/	/	/	/	GTTCAAAATGAAAAGAAAATTTTAAGTT**T**
471654:+	Cj0506	mRNA	*alaS*	2027	4,2	/	/	/	/	TTTACATAGTTAAAGAAAGTGGTGTGAGTGCTGGAG**T**
1222872:-	Cj1290c	mRNA	*accC*	762	4,2	(0,0)	/	/	/	CTGCGATTTTGCTTGATGAAAAAACACGCAC**T**
1179731:+	Cj1250	5′UTR	5′UTR *purD*	Minus 56 START codon	3,6	(2,6)	(1,6)	(0,2)	(0,2)	TTTTCTT**T**GACTTTTTGGGGTCAATCTTTGTTAAACGGCTGTTTGGGTTTAAAAGGAGATATAA**ATG**
1179609:+	Cj1250	5′UTR	5′UTR *purD*	Minus 179 START codon	1,9	(1,2)	(1,4)	(-0,1)	(-0,4)	**T**AAAGTGATCCAACACATTTTTATTAACTGCGATTGTGTGATTTACCGTGTTCTGTGGCATCGTTTGAGCTTTGAAAAAAGCGAGAAGTTGCAGCCTTTAAAAATTACCTAGCGGTTTTCTTTGACTTTTTGGGGTCAATCTTTGTTAAACGGCTGTTTGGGTTTAAAAGGAGATATAA**ATG**
1269230:-	Cj1339	3′UTR	3′UTR of *flaA*	Plus 1 STOP codon	1,4	(0,4)	(0,2)	(0,5)	(0,6)	AAGATTACTACAG**TAG**TTACAAAAGCTGC

2.7 Validation of pseudouridine in *C. jejuni* wild-type and tRNA PUS mutant strains using a chemical treatment followed by primer extension

To confirm the modifications identified in the Pseudo-seq analysis, independent CMC treatment followed by primer extension assays were performed with RNA of *C. jejuni* wildtype and PUS mutant strains. Total RNA was extracted from the different bacterial strains and treated with CMC or left untreated. Primer extension reactions were performed using radioactively-labeled reverse transcription primer that annealed to the different tRNAs identified in the Pseudo-seq analysis. Cjp16 was identified as a potential target of TruA at position 39, Cjp16 of TruB at position 55, and Cjp03 of TruD at position 13. Figures 2.13 A, B, and C show the result of the primer extension assays. A band corresponding to the pseudouridine identified in the Pseudo-seq analyses was detected at the 3´ end of each modified nucleotide, confirming the targets of TruA, TruB, and TruD.

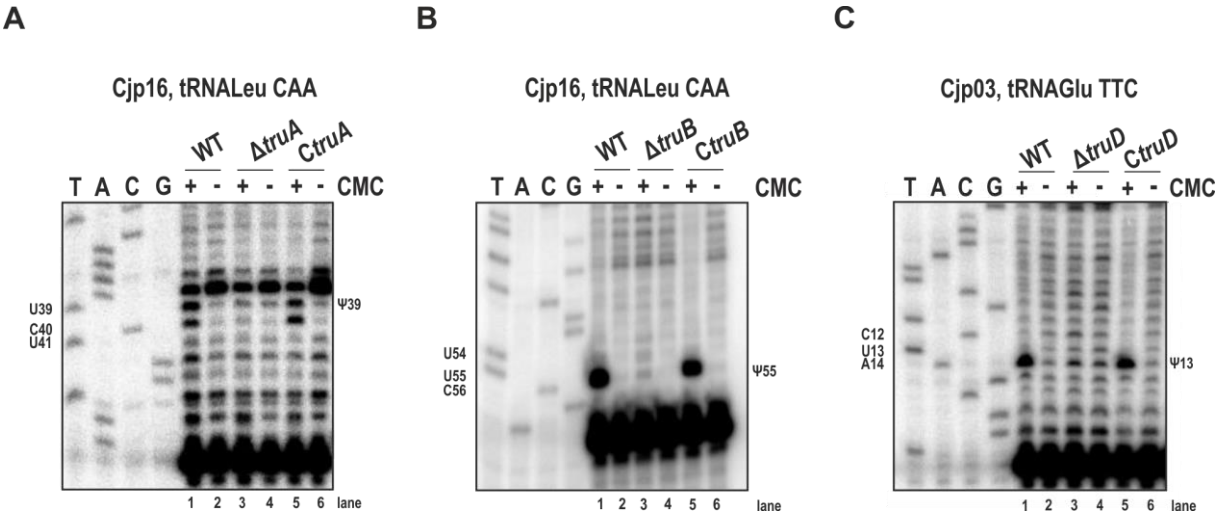

Figure 2.13: Targets of tRNA PUS enzymes in *C. jejuni* identified by Pseudo-seq. (A) Total RNA was isolated from *C. jejuni* wild-type, Δ*truA*, complementation of *truA* (C*truA*) **(B)** wild-type, Δ*truB*, complementation of *truB* (C*truB*)**(C)** wild-type, Δ*truD*, complementation of *truD* (C*truD*) and primer extension was performed to check modification in **(A)** Cjp16 **(B)** Cjp16, and **(C)** Cjp03.

2.8. Validation of pseudouridine in *C. jejuni* wild-type and tRNA PUS mutant strains using an *in-vitro* approach

As an alternative method to validate whether pseudouridine formation is mediated by TruA, TruB, and TruD, as observed in the Pseudo-seq experiment, an *in-vitro* pseudouridylation experiment using recombinant TruA and TruD, purified from *E. coli* by affinity purification, together with *in-vitro* transcribed tRNA transcripts corresponding to specific tRNA targets was performed. In *E. coli*, the *truA*, *truB,* and *truD* ORFs of *C. jejuni* were cloned on a plasmid under the control of an arabinose-inducible P_{BAD} promoter, using the ribosome binding site (RBS) of the *Helicobacter pylori* ArsR protein. This protein was already purified in our lab and used as a positive control to check whether the induction mediated by L-arabinose worked out. Additionally, *E. coli* TOP10 cells that do not contain any plasmid were used as a negative control. To specifically purify the protein of interest, the C-terminus of TruA, TruB, and TruD was fused to a Streptavidin epitope tag of eight amino acids and a two amino acid spacer was added between the protein and the tag to guarantee the accessibility of the TAG during the purification step. As shown in Figure 2.14 A, bands of the corresponding sizes of tagged ArsR (~26 kDa), TruA (~28 kDa), TruB (~31 kDa) and TruD (~ 42 kDa) can be observed in the arabinose-induced *E. coli* TOP10 cells (lane 4, 6, 8, and 10). However, while the induction of TruB can be promoted in the presence of 0.02% of L-arabinose (Figure 2.14 A), its purification turned out to be unsuccessful due to the insolubility of the protein and its potential incorporation into inclusion bodies (data not shown). In contrast, purification of TruA and TruD was successful (Elution 1-5) (Figure 2.14 B and 2.14 C). Based on this, *in-vitro* pseudouridylation experiments were conducted using only purified TruA and TruD.

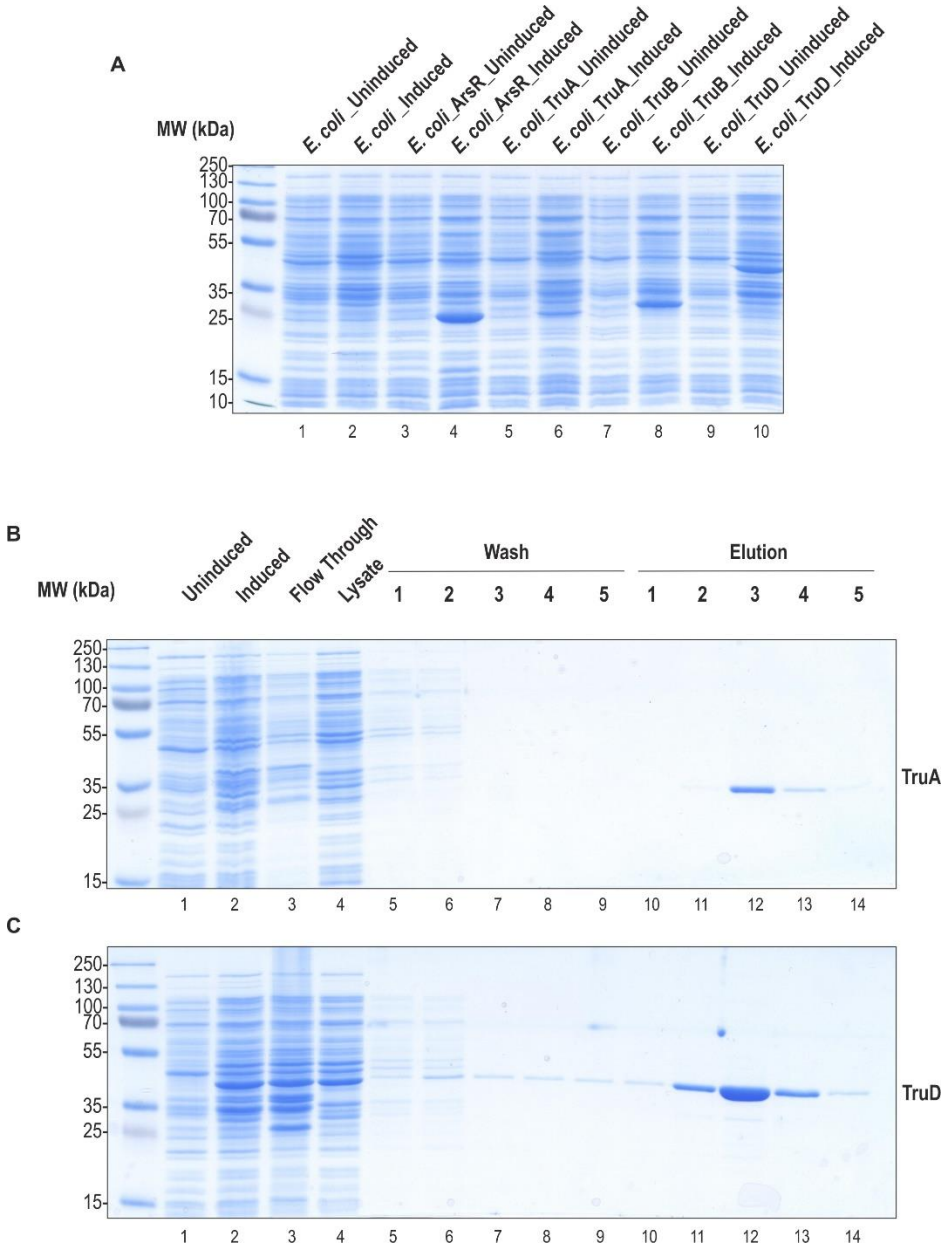

Figure 2.14: Purification of tRNA PUS enzymes TruA and TruD for in-vitro pseudouridylation assay. **(A)** L-arabinose induction of *E. coli* TOP10 cells carrying a plasmid that express either ArsR, TruA, TruB and TruD. Whole cell lysate of uninduced (lanes 1, 3, 5, 7 and 9) and induced (lanes 2, 4, 6, 8 and 10) *E. coli* TOP10 cells were analyzed on a 12%PAA gel. **(B)** Purification of TruA or **(C)** TruD. All the detail about expression and purification of TruA and TruD are described in the material and method part.

In-vitro pseudouridylation experiments consisted in the incubation of T7 *in-vitro* transcribed tRNA (Cjp16 or Cjp03) with increasing concentrations of the protein of interest and, as a control, the tRNA was incubated only with the buffer, without any enzyme. This is followed by a CMC treatment followed by primer extension. As shown in Figure 2.15, specific reverse transcription stops were identified at positions corresponding to Pseudo-seq data.

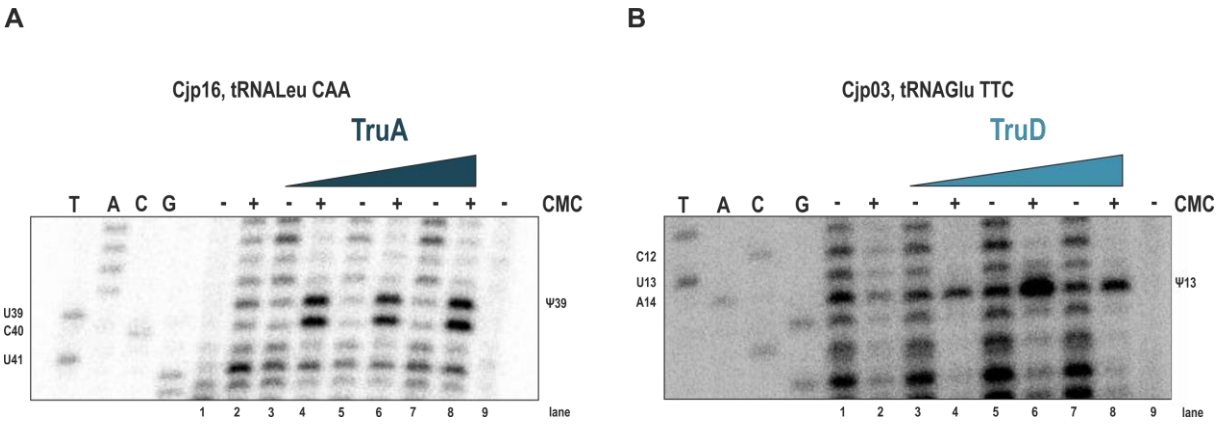

Figure 2.15: In-vitro pseudouridylation assay confirms TruA and TruD targets. (A) *In-vitro* pseudouridylation assay using *in vitro*-transcribed Cjp16 and increasing concentrations of TruA **(B)** *In-vitro* pseudouridylation assay using *in vitro*-transcribed Cjp03 and increasing concentrations of TruD. For each experiment 20 pmol of *in vitro* transcribed tRNA was incubated with increasing concentration of TruA or TruD (20, 100, and 200 pmol).

Therefore, *in-vitro* pseudouridylation assays validated the targets of TruA and TruD resulting from the previous global Pseudo-seq analysis.

2.9. Identification of pseudouridine in *H.pylori* WT and ΔPUS strains

Next, a Pseudo-seq analysis was performed for *H. pylori*. Pseudo-seq was performed with total RNA (rRNA depleted) isolated from *H. pylori* wildtype, Δ*truA,* and Δ*truD* grown to exponential phase. In total, 12 cDNA libraries for *H. pylori* were generated in biological replicates (CMC treated/CMC +, CMC untreated/CMC -) and sequenced. In *H. pylori*, we identified two tRNAs modified by TruA (HpTruA) at position 39 (Hpt13, tRNA-Leu; Hpt23, tRNA-Leu). Moreover, we identified two potential tRNA-Glu targets of TruD (HpTruD) at position 13 (Hpt01 and Hpt04). Furthermore, the Pseudo-seq analysis revealed that TruD of *H. pylori* potentially generates Ψ at one site in 23S rRNA (Hpr01/Hpr06). Moreover, probably due to an incomplete depletion of the 23 and 16 rRNAs in the *H. pylori* Pseudo-seq samples, we were able to identify Ψ sites in the 23S rRNA. By comparing with the known Ψ sites in rRNA of *E. coli* and *C. jejuni*, we were able to identify sites dependent on the rRNA PUS RluB (2693), RluC (2592), and RluD (1999 and 2005). A newly identified site in the 23S rRNA of *H. pylori* (2055) corresponds to the site that was identified in *C. jejuni* at position 1983, highlighting potential differences between the Epsilonproteobacteria and

the Gammaproteobacteria. Additionally, an RluF-dependent site at position 2692 was identified. The modified sites are listed in Table 2.3.

Figure 2.16 shows examples of screenshots of potentially modified sites in wildtype, Δ*truA,* and Δ*truD* strains. Normalized reads of the different cDNA libraries were loaded in the Integrated Genome Browser (IGB) and the presence or absence of the peak in the coordinates identified by Pseudo-seq was observed. A clear peak is observed in the WT and Δ*truD* libraries for position 39 of Hpt23, while it is absent in the Δ*truA* library, suggesting that TruA modifies this tRNA at this position. For Hpt04, a clear peak is observed in the WT and Δ*truA* libraries, while it is absent in the Δ*truD* library, suggesting that this tRNA is a target of TruD.

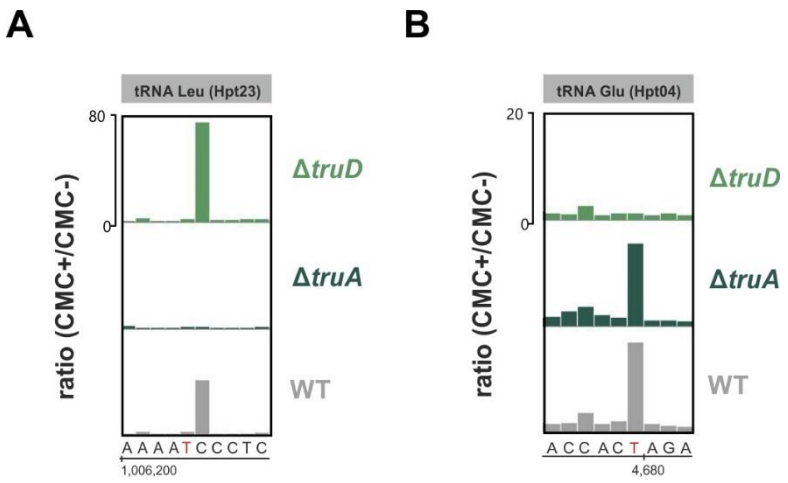

Figure 2.16: Targets of tRNA PUS enzymes in *H. pylori* identified by Pseudo-seq. Pseudo-seq reads of *H. pylori* wild-type (grey), Δ*truA* (dark green) and Δ*truD* (light green) ratios of normalized CMC +/CMC - libraries were mapped to the genome of *H. pylori* strain 26695 and are visualized as coverage plots in the Integrated Genome Browser (IGB). Each Pseudo-seq reads/strain represents the normalization of the two replicates per strain. A representative screen shot of the tRNA targets of TruA (Hpt23) and TruD (Hpt04) are visualized. Genomic coordinates are indicated in the lower part of the figure and the number of reads is shown on the left part outside the black box. The red T shows the potential pseudouridine identified by Pseudo-seq.

Table 2.3: Potentially modified nucleotides, which show a log$_2$FC>1.0 change in the *H. pylori* Pseudo-seq including WT, Δ*truA*, Δ*truD* data-sets. The columns represent the position at 3′ of Ψ, the locus tag, the type of RNA, the RNA, the position of Ψ in the RNA, the log$_2$FC of WT, Δ*truA*, Δ*truD* and the sequence (5′→3′) of the tRNA/mRNA/5′ UTR/3′UTR and the potential Ψ site is highlighted in red. Values in bracket indicate sites with adj.p-value>0.1

Position at 3 of the peak/ Strand	Locus tag	Type of RNA	RNA	Position	log2FC WT	log2FC Δ*truA*	log2FC Δ*truD*	Sequence 5-->3 (in red the pseudouridine site)
1006206:+	Hpt23	tRNA Leu anticodon TAA	tRNA Leu	39	5,2	(0,7)	6,0	GCCCAGGTGGTGGAATTGGTAGACACAAGGGACTTAAAATCCCTCGGTAGCAATACCGTGCCGGTTCAAGTCCGGCTTTGGGCA
1249321:-	Hpt28	tRNA Met anticodon CAT	tRNA Met	31	4,8	4,5	(5,6)	GTCAAGGTAGCTCAGCTGGTTTAGAGCGCTGGTCTCATAAGCCGGAGGTCGGGGGTTCAAGTCCCCCTCTTGACA
1474199:-	Hpr06	23S rRNA	23S rRNA	2693>>2621 in Cj RluB dependent	5,7	6,0	5,9	CGCCATTTAAAGCGGTACGCGAGCTGGGTTCAGAACGTCGTGAGACAGTT
1474200:-	Hpr06	23S rRNA	23S rRNA	2692>> Cj RluF dependent	3,2	(2,8)	2,9	TCGCCATTTAAAGCGGTACGCGAGCTGGGTTCAGAACGTCGTGAGACAGT
1474300:-	Hpr06	23S rRNA	23S rRNA	2592>> RluC dependent	4,6	5,2	5,0	AAGAGCTCACATCGACGGGGAGGTTTGGCACCTCGAT
1474838:-	Hpr06	23S rRNA	23S rRNA	2055>>1983 in CJ	3,1	3,3	(-0,5)	AGCGAAATTCCTTGTCGGTTAAATACCGACCTGCAT
1474888:-	Hpr06	23S rRNA	23S rRNA	2005>>1917 RluD dependent	3,9	(3,7)	4,0	TGAATTGAAGCCCGAGTAAACGGCGGCCGTAACTAT
1474894:-	Hpr06	23S rRNA	23S rRNA	1999>>1911 RluD dependent	3,9	(3,8)	3,8	CAGTCGCAAGATGAAGCGTTGAATTGAAGCCCGAGTAAACGGCGGCCGT
374869:+	Hpt13	tRNA Leu anticodon TAG	tRNA Leu	39	6,8	(1,1)	(7,3)	GCGGAAGTGGCGAAATTGGTAGACGCACTAGACTTAGGATCTAGCGCCGCAAGGCATGAAGGTTCGATTCCTTTCTTCCGCACCATTCTTAATGATTAA
4309:-	Hpt01	tRNA Glu anticodon TTC	tRNA Glu	13	3,5	3,6	(0,0)	GACCCTTTCATCTAGTGGCCAAGGATACCACCCTTTCACGGTGGAAACGGAAGTTCAAATCTTTCAAGGGTCG
447248:+	Hpr01	23S rRNA	23S rRNA	1999>>1911 RluD dependent	3,9	(3,8)	3,8	GGTGGGGTAAGAGCCCACCARAGCT
447254:+	Hpr01	23S rRNA	23S rRNA	2005>>1917 RluD dependent	3,9	(3,8)	4,0	CCCGAGTAAACGGCGGCCGTAACTAT
447304:+	Hpr01	23S rRNA	23S rRNA	2055>>1983 in CJ	4,9	5,3	(-0,2)	TTGTCGGTTAAATACCGACCTGCAT
447841:+	Hpr01	23S rRNA	23S rRNA	2592>> RluC dependent	4,7	5,2	5,0	CGACGGGGAGGTTTGGCACCTCGAT
447941:+	Hpr01	23S rRNA	23S rRNA	2692	3,1	(2,7)	2,9	TGGGTTCAGAACGTCGTGAGACAGT
447942:+	Hpr01	23S rRNA	23S rRNA	2693>>2621 in Cj RluB dependent	5,5	5,8	5,6	GTTCAGAACGTCGTGAGACAGTT
4680:-	Hpt04	tRNA Glu anticodon TTC	tRNA Glu	13	3,8	3,7	(-0,1)	GGCTCCTTCATCTAGTGGTTAGGATACCACCCTTTCACGGTGGTTACAGGGGTTCAAATCCCCTAGGAGTCA

2.10. Validation of pseudouridine in *H. pylori* wild-type and tRNA PUS mutant strains using using a chemical treatment followed by primer extension

To confirm the modifications identified in the Pseudo-seq analysis, independent CMC treatment followed by primer extension assays were performed with total RNA of *H. pylori* wildtype and PUS mutant strains. Total RNA was extracted from the different bacterial strains and treated with CMC or left untreated. Primer extension reactions were performed using radioactive labeled reverse transcription primer that annealed to the different tRNAs identified in the Pseudo-seq analysis. Hpt23 was identified as potential target of TruA in the Pseudo-seq experiment at position 39, and Hpt04 as target of TruD at position 13. Figures 2.17 A and B show the results of the primer extension assays. A band corresponding to the pseudouridine identified in the Pseudo-seq analyses was detected at the 3´ ends of each modified nucleotide, confirming the targets of TruA and TruD.

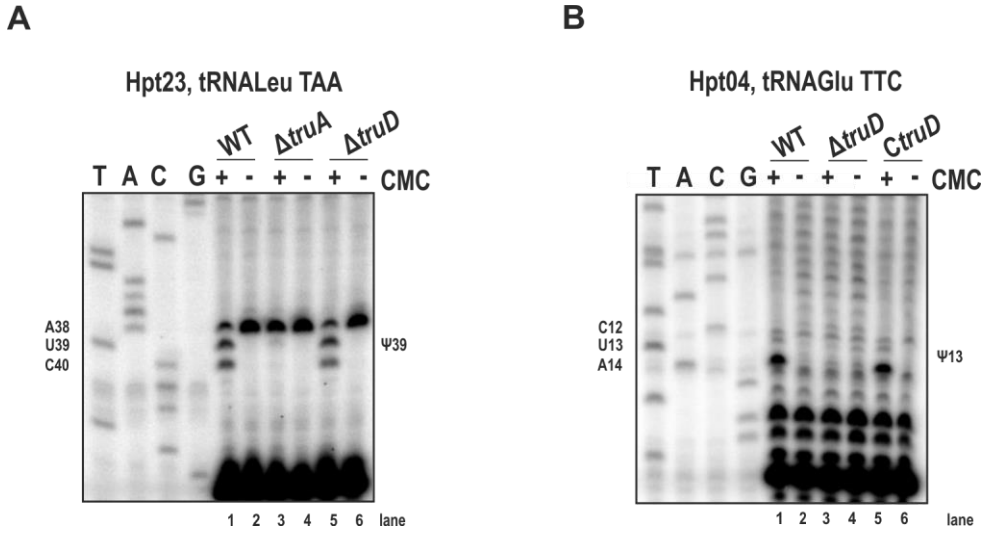

Figure 2.17: Targets of tRNA PUS enzymes in *H. pylori* identified by Pseudo-seq. (A) Total RNA was isolated from *H. pylori* wildtype, Δ*truA*, Δ*truD* **(B)** wild-type, Δ*truD*, C*truD* and primer extension was performed to check for modifications in **(A)** Hpt23 and **(B)** Hpt04.

Moreover, the Pseudo-seq experiment in *H. pylori* showed no modification in tRNAs at position 55. To confirm the absence of pseudouridine at position 55 in tRNAs, the CMC treatment followed by primer extension assay was performed in parallel with RNA isolated from *C. jejuni* wildtype

and *H. pylori* wildtype. CMC-treated and untreated RNAs was probed using an oligonucleotide complementary to the tRNALeu of *C. jejuni* (Cjp16) and of *H. pylori* (Hpt34) (Figure 2.18). The primer extension showed that while modification at position 55 was detected in *C. jejuni* (lane 1), the tRNA modification was absent in *H. pylori* (lane 3).

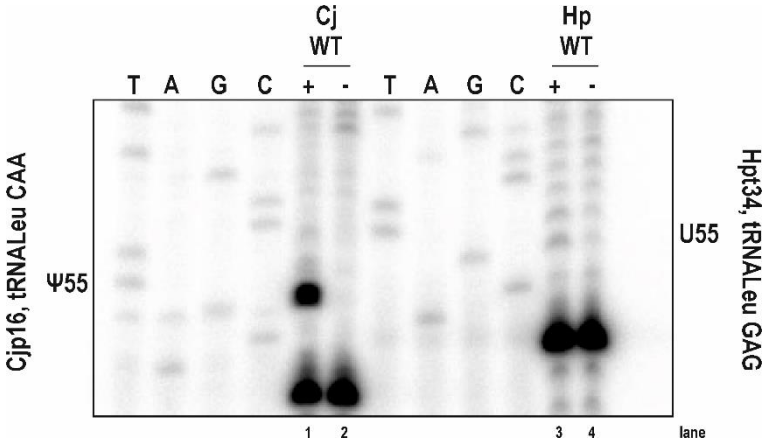

Figure 2.18: Validation of the lack of modification at position 55 in *H. pylori* tRNA Hpt34. Total RNA was isolated from *C. jejuni* and *H. pylori* wildtype that was grown to exponential phase (OD_{600nm} of ~0.4/0.5 for *C. jejuni* and OD_{600nm} of ~0.6/0.8 for *H. pylori*). 1.0 µg of total RNA was used in primer extension assays with ^{32}P-end labeled oligo CSO-5145 (for *C. jejuni* Cjp16) and CSO-3521 (for *H. pylori* Hpt34) for reverse transcription of Cjp16 and Hpt34 in the presence (lanes 1 and 3) or absence (lanes 2 and 4) of the CMC compound. A sequencing ladder corresponding to Cjp16 or Hpt34 region was used as reference (lanes T, A, C, G). cDNA products were analyzed on a 10% PAA gel under denaturing conditions. Primer extension showed a band in lane 1 that is absent in lane 2, 3, and 4, which corresponds to the block of the reverse transcriptase at the 3' end of the Ψ-CMC (C56).

Taken together, this result showed that the lack of TruB in *H. pylori* led to the absence of pseudouridine at position 55.

Moreover, Pseudo-seq experiments in *H. pylori* wild-type and PUS mutant strains showed that TruD might be responsible for the modification of the 23S rRNA (Table 2.3; coordinates: 1474838 and 447304). To verify the Pseudo-seq result, CMC treatment followed by primer extension was performed in RNAs of *H. pylori* wild-type, Δ*truD,* and *truD* complementation strain (HpTruD). Figure 2.19 showed that besides a slight decrease in the potentially modified nucleotide in the Δ*truD* strain (lane 3 vs lane 1 and 5), the band did not disappear in this strain, suggesting that TruD is not responsible for the modification of rRNA.

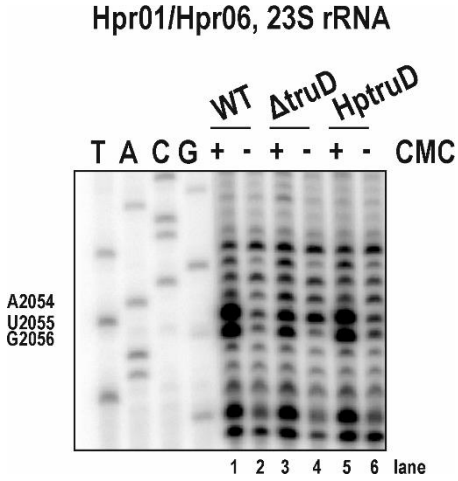

Figure 2.19: TruD does not modify 23S rRNA (Hpr01/Hpr06). Total RNA was isolated from *H. pylori* wildtype, Δ*truD*, Hp*truD* grown to exponential phase (OD_{600nm} of ~0.7-0.8). DNase I digested CMC treated/untreated total RNA was used in primer extension assays with ^{32}P-end labeled oligo CSO-5179 for reverse transcription of 23SrRNA (Hpr01/Hpr06) in the presence (lane 1, 3, 5) or absence (lane 2, 4, 6) of the CMC compound. A sequencing ladder corresponding to Hpr01/Hpr06 region was used as reference (lanes T, A, C, G). cDNA products were analyzed on a 10% PAA gel under denaturing conditions.

2.11. RNA immunoprecipitation (RIP) experiment using an antibody against Ψ does not pull down modified tRNAs.

A different strategy to identify pseudouridine in RNAs is based on the enrichment of the potentially modified RNAs using an antibody against the modification of interested. Antibodies against the pseudouridine modification are commercially available (https://www.mblbio.com/bio/g/dtl/A/?pcd=D347-3). APU-6 anti-pseudouridine mouse monoclonal antibody has already been used for immunohistochemistry, immunocytochemistry, ELISA, and immuno-northern blot analysis (Itoh *et al.*, 1989, 1992; Masuda *et al.*, 1993; Mishima & Abe, 2019). But so far, it has not been reported that this antibody can be used to immunoprecipitate modified RNAs in a RIP-seq experiment. In parallel to the Pseudo-seq experiments, I tested the ability of this antibody to pull down targeted RNAs in a RIP-seq experiment using a protocol that has been described before in the Sharma lab (Dugar *et al.*, 2016). The experiment was performed with mid-exponential-phase lysates of *C. jejuni* wildtype and, as a control, a Δ*truABD* strain. RNA and protein samples corresponding to the different steps of the RIP-seq experiment (culture, lysate, IP, supernatant, wash and eluate) were taken and analysed by northern and western blot experiments (Figure 2.20).

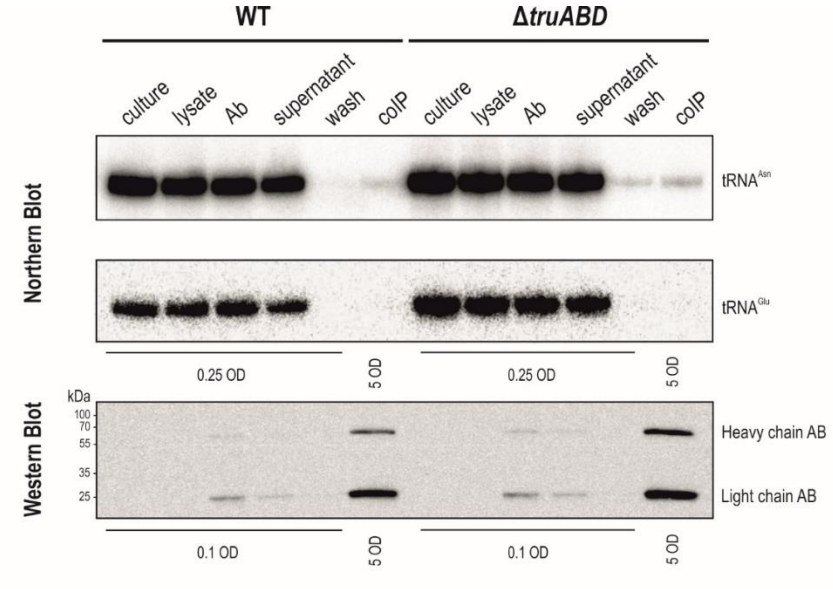

Figure 2.20: Immunoprecipitation of potentially modified RNAs using an antibody against pseudouridine. (*Upper panel*) Northern blot analysis of coIP-RNA samples of *C. jejuni* WT and Δ*truABD* strains using an anti-pseudouridine antibody. (*Lower panel*) Western blot analysis of coIP-protein samples of *C. jejuni* WT and Δ*truABD* strains using anti-pseudouridine antibody.

Northern blot analysis of RNA samples using probes specific for different tRNAs (Cjp22 and Cjp03) showed that there was no specific enrichment for pseudouridinylated tRNAs in the wildtype-coIP compared to Δ*truABD*-coIP. As a control, to verify the pulldown of the antibodies during the different steps, protein samples were separated on a polyacrylamide SDS-gel and the membrane was probed using anti-mouse antibody. The presence of the heavy and light chains of the IgG antibody in the eluate sample confirmed the correct pulldown of the antibodies in the RIP-seq experiment. Taken together, this result suggests that Pseudo-seq remains the more promising experiment to detect pseudouridine in the bacterial transcriptome.

3. Result II. Functional characterization of TruD in *Campylobacter jejuni* using microbial genetics, molecular biology, and biochemistry.

For many years, the functions of eukaryotic pseudouridine synthases were simply reduced to enzymes that modify stable RNAs (rRNAs and tRNAs), thus limiting the further characterization of these proteins (Rintala-Dempsey & Kothe, 2017). However, it has been recently reported that eukaryotic tRNA PUS enzymes modify mRNAs and other non-coding RNAs. This greatly expanded the study of the biological functions of tRNA PUS. While the broader role of these PUS proteins is better studied in eukaryotes, the function of these enzymes in bacteria is still unknown. Deletion of specific tRNA PUS enzymes in *C. jejuni* affects bacterial growth in a different manner compared to the wildtype strain, suggesting that they might play a role in bacterial physiology (Chapter 2 of this thesis). In particular, the deletion of *truD* in *C. jejuni* resulted in impaired growth, whereas in *H. pylori* deletion of *truD* did not affect the growth of the pathogen. Therefore, this chapter aims to characterize the *C. jejuni* TruA, TruB, and TruD, with a particular focus on TruD.

3.1. TruA, TruB and TruD are constitutively expressed during different growth phase of *C. jejuni*

In *S. cerevisiae*, mRNAs modified by Pus1 show increased modification during post-diauxic growth (Carlile *et al.*, 2014). The transcript level of different PUS enzymes are also downregulated under different stresses or environmental conditions (e.g., fermentation, osmotic or heat stress) in yeast (Wanichthanarak *et al.*, 2014). To determine whether the expression of TruA, TruB, and TruD varies during growth of *C. jejuni*, the protein levels were analyzed in different growth phases. For this, *truA*, *truB,* and *truD* genes were chromosomally fused with a *3xFLAG* epitope tag at their C-terminus and expressed from their native locus. Since the construction of the complementation strains described in the previous chapter is based on the same principle and the strains do not show any growth defect and are able to rescue the pseudouridine modification in their corresponding targets, I assume that the generation of FLAG-tagged strains should not compromise their catalytic activity. The *C. jejuni* wild-type, TruA-3xFLAG, TruB-3xFLAG, and TruD-3xFLAG strains were grown in Müller-Hinton broth and protein samples were taken at different phases (early exponential phase, late exponential phase, and overnight). Protein levels were collected and subsequently analyzed by western blot using an anti-FLAG antibody (Figure 3.1). The expression of TruA, TruB, and TruD does not change during the investigated growth

phases, showing that the expression of these proteins is constitutive throughout *Campylobacter* growth in rich media and does not depend on growth phase.

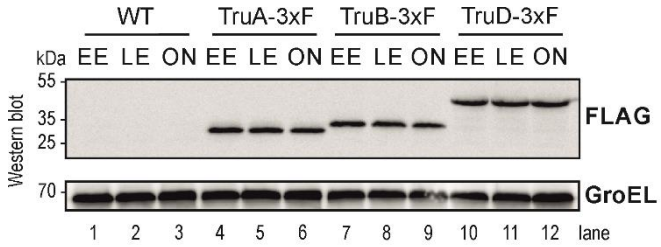

Figure 3.1: TruA, TruB, and TruD are constitutively expressed in the different growth phases in *C. jejuni*. Western blot analysis of *C. jejuni* wild-type, TruA-3xFLAG, TruB-3xFLAG, and TruD-3xFLAG strains grown to different growth phases (EE=early exponential; LE=late exponential, ON=overnight). Protein samples corresponding to an OD_{600nm} of 0.1 were loaded on a 12% SDS-PAGE gel and transferred to a nitrocellulose membrane. The FLAG tagged proteins were detected using anti-FLAG antibodies (1:1000). GroEL served as loading control.

3.2. Potential physiological roles of tRNA PUS enzymes in *C. jejuni*

In human and yeast, pseudouridylation can be induced when the cells are subjected to different types of stress such as heat shock, nutrient deprivation, or hydrogen peroxide treatment (van der Feltz *et al.*, 2018). For example, it has been shown that putative 265 putative Ψ sites are induced in yeast in response to the heat shock treatment (Schwartz *et al.*, 2014). Moreover, the authors showed that the enzyme Pus7p is required for pseudouridylation during this stress condition. To investigate potential stress-induced pseudouridylation in *C. jejuni*, the expression of TruA, TruB and TruD was checked using TruA-3xFLAG, TruB-3xFLAG, and TruD-3xFLAG strains during the exposure of the cells to heat shock. *C. jejuni* strains were grown at 37 °C until mid-log phase, then exposed to heat shock treatment for 30 minutes at 48 °C. The heat shock response in *C. jejuni* is transcriptionally regulated by the HrcA and HspR (Holmes *et al.*, 2010), leading to the expression of so-called heat shock genes, like those encoding for the chaperones GroEL, DnaK, and ClpB (Duqué *et al.*, 2021). To verify if the heat shock response was induced in *C. jejuni*, the expression of *groEL* mRNA was investigated by northern blot analysis. Indeed, *groEL* induction was observed after incubation of the bacteria at 48°C (data not shown). Protein samples were collected before and after heat shock and expression of PUS enzymes were assayed by western blot using an anti-FLAG antibody. Comparison of protein expression in the two conditions (37 °C and 48 °C) showed that neither TruA, TruB, nor TruD protein levels were affected by heat shock (Figure 3.2 A).

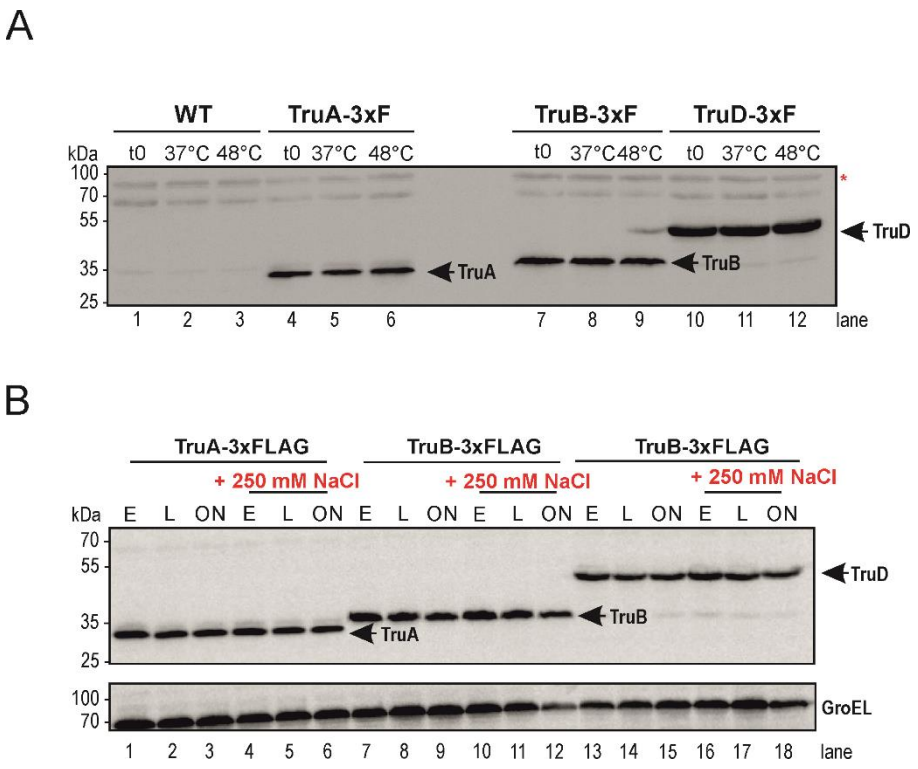

Figure 3.2: TruA, TruB, and TruD expression is not induced during heat shock or osmotic stress. (A) Western blot analysis of *C. jejuni* wild-type, TruA-3xFLAG, TruB-3xFLAG, and TruD-3xFLAG strains were grown to exponential growth phase and proteins samples were collected before the treatment (t0), after treatment for 30 minutes at 37°C (37°C) and after treatment for 30 minutes in the water bath at 48°C (48°C). Protein samples corresponding to an OD_{600nm} of 0.1 were loaded on a 12% (vol/vol) SDS-PAA gel, blotted to nitrocellulose membrane and FLAG tagged proteins were detected with an anti-FLAG antibody (1:1,000). The nonspecific bands after incubation with an anti-FLAG antibody, indicated with a red asterisk, served as loading control. **(B)** Western blot analysis of *C. jejuni* TruA-3xFLAG, TruB-3xFLAG and TruD-3xFLAG strains grown to exponential growth phase (E=early exponential; L=late exponential, ON=overnight) either without or with 250 mM NaCl. Protein samples corresponding to an OD_{600nm} of 0.1 were loaded on a 12% SDS-PAA gel, blotted to nitrocellulose membrane and FLAG-tagged proteins were detected with an anti-FLAG antibody (1:1,000). GroEL served as loading control.

Furthermore, *C. jejuni* and other gastrointestinal bacteria encounter constant changes in osmolarity in their host environment through exposure to food processing (Cameron *et al.*, 2012). NaCl is one of the most important agents in food preservation and *C. jejuni* uses specific mechanisms to maintain its osmotic homeostasis. Based on this, potential involvement of TruA, TruB, and TruD in the *Campylobacter* response to increased concentrations of salt (250 mM NaCl) was determined by measuring their protein expression levels. The expression of PUS proteins was analyzed by Western blot using an anti-FLAG antibody. No difference in PUS protein levels was observed between the two conditions, indicating that the response of the bacteria to hyperosmotic stress might not involve an induction of pseudouridylation (Figure 3.2 B).

The microaerophilic *C. jejuni* possesses specific regulatory mechanisms involved in oxidative stress resistance (Kim *et al.*, 2015). It has been reported that pseudouridine formation in human mRNA is dependent on hydrogen peroxide treatment (Li *et al.*, 2015). To test the involvement of pseudouridylation in *C. jejuni* oxidative stress response, the sensitivity of *C. jejuni* WT, PUS deletion and complementation strains was checked in the presence of hydrogen peroxide (H_2O_2) by a disk diffusion assay. Under these experimental conditions, PUS deletion strains did not show differences in the sensitivity to hydrogen peroxide compared to the wild-type strain, suggesting that pseudouridylation might not be involved in oxidative stress tolerance (Figure 3.3).

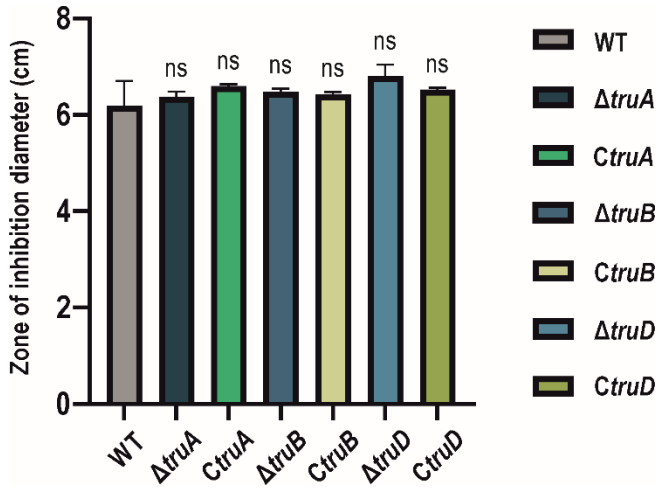

Figure 3.3: PUS mutant strains are not sensitive to hydrogen peroxide treatment. Hydrogen peroxide sensitivity testing of *C. jejuni* wildtype, Δ*truA*, Δ*truB*, Δ*truD* and the corresponding complementation strains grown to exponential growth phase using disk diffusion assay. *C. jejuni* strains were spread on an MH agar plate supplemented with vancomycin and the disk with 10 µl of 30% H_2O_2 was located in the center of the plate. The plates were incubated overnight at 37°C in microaerobic conditions and the inhibition zone was measured. Columns indicate the mean of two replicates and bars indicate standard deviations. ns: not significant. The Student´s *t*-test was employed for statistical analysis

C. jejuni flagella and flagellar motility are vital to many aspects of *C. jejuni* biology and pathogenesis. Since growth curve experiments suggested a potential role for TruA and TruD in *C. jejuni* physiology (Figure 2.6), a motility assay using soft agar plates was performed to determine the involvement of PUS enzymes in regulating flagella. For this analysis, *C. jejuni* wildtype, Δ*truA*, Δ*truB*, Δ*truD* and their corresponding complementation strains were used. As a positive control, a Δ*flaA* strain was used. The *flaA* gene encodes for the major flagellin A of *C. jejuni* and its deletion lead to an almost complete loss of motility (Guerry *et al.*, 1991). The assay showed that while *truB* deletion does not affect *C. jejuni* motility (Figure 3.4 B), *truA* and *truD* deletions result in a motility defect that can be rescued by complementation with C*truD* and partially rescued by C*truA*, respectively (Figure 3.4 A and C).

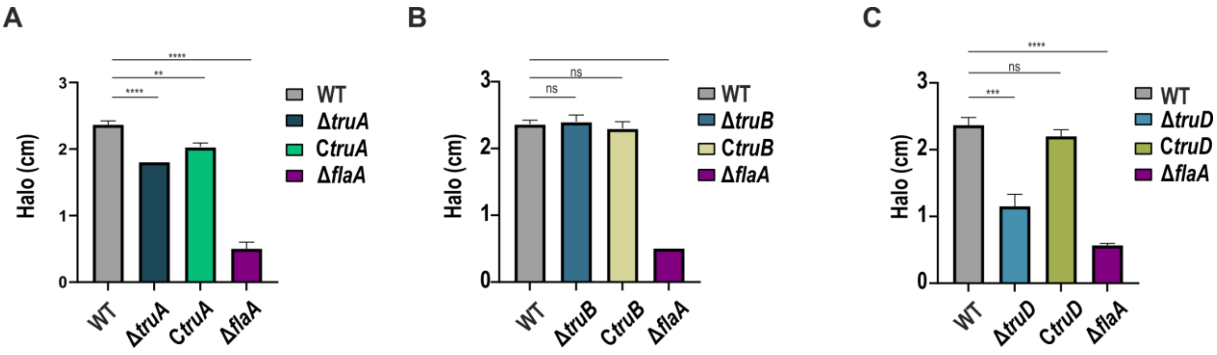

Figure 3.4: Motility assay of *C. jejuni* deletion strains. (A) Motility assay of *C. jejuni* wild-type (WT), Δ*truA*, C. *truA* and Δ*flaA*. Strains were grown in Brucella Broth overnight to exponential phase and stabbed in 0.4% soft agar Brucella Broth (BB) plates supplemented with 5% fetal bovine serum (FBS). The OD_{600nm} of the different strains was adjusted to OD_{600nm} of 1.0 and 1.0µl was stabbed in the motility plates. After incubation at 37°C overnight in a microaerobic conditions, the swimming halo diameter was measured. **(B)** Motility assay of *C. jejuni* wild-type (WT), Δ*truB*, C. *truB* and Δ*flaA*. Strains were grown in Brucella Broth overnight to exponential phase and stabbed in 0.4% soft agar Brucella Broth (BB) plates supplemented with 5% fetal bovine serum (FBS). The OD_{600nm} of the different strains was adjusted to OD_{600nm} of 1.0 and 1.0µl was stabbed in the motility plates. After incubation at 37°C overnight in microaerobic conditions, the swimming halo diameter was measured. **(C)** Motility assay of *C. jejuni* wild-type (WT), Δ*truA*, C. *truA* and Δ*flaA*. Strains were grown in Brucella Broth overnight to exponential phase and stabbed in 0.4% soft agar Brucella Broth (BB) plates supplemented with 5% fetal bovine serum (FBS). The OD_{600nm} of the different strains was adjusted to OD_{600nm} of 1.0 and 1.0µl was stabbed in the motility plates. After incubation at 37°C overnight in microaerobic conditions, the swimming halo diameter was measured. Bars indicate standard deviations of three biological replicates ****: $p < 0.0001$, **: $p < 0.01$. ns: not significant. The Student´s *t*-test was employed for statistical analysis.

Flagella are necessary for initiating the formation of *C. jejuni* surface-associated biofilm (Svensson *et al.*, 2014). Since TruA and TruD seem to be involved in *C. jejuni* motility, the role of PUS enzymes in biofilm formation was investigated. Using crystal violet staining, formation of biofilms was measured for the wild-type strain, PUS deletion mutants and their respective complementation strains. Δ*flaA* strain and Brucella Broth (BB) without any bacteria were used as negative control. Impaired biofilm formation was observed for *truA* and *truD* deletion strains compared to the parental strain.

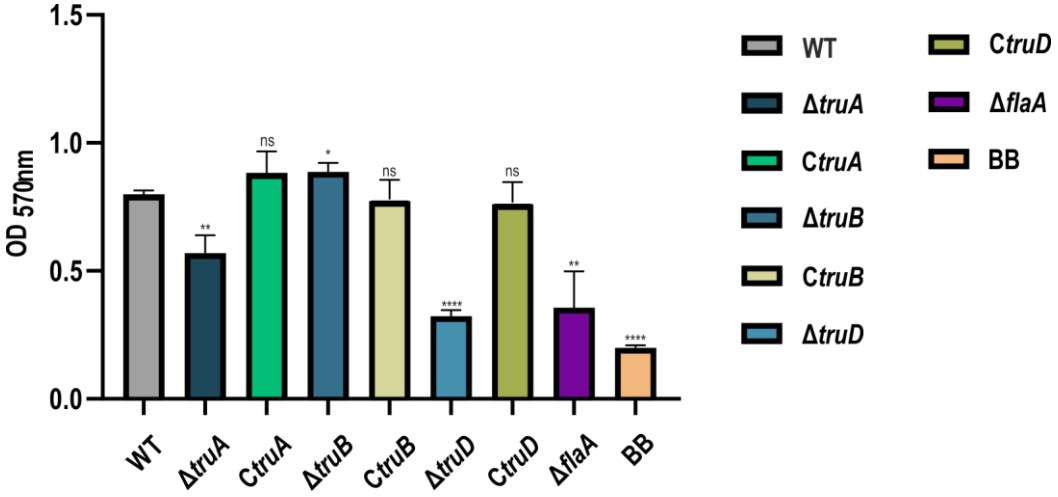

Figure 3.5: Biofilm formation assay reveals impaired biofilm formation in *truA* and *truD* deletion strains. *C. jejuni* wildtype, Δ*flaA*, Δ*truA*, Δ*truB*, Δ*truD* and the corresponding complementation strains were grown overnight in liquid culture. The following day the strains were diluted in 2 ml of Brucella Broth to an OD_{600nm} of 0.002 into glass tubes. The strains were grown at 37°C in microaerobic conditions without shaking for 3 days. 500 µL of 1 % crystal violet were added in each tubes. For quantification (OD_{570nm} measurements), 3 ml of biofilm destaining solution (40 % ethanol, 10 % acetic acid) was added in each tube and the tube was vortexed until the stain is completely dissolved. Δ*flaA* strain and Brucella Broth (BB) without any bacteria are used as negative control. Bars indicate standard deviations of three biological replicates. ****: $p < 0.0001$, **: $p < 0.01$, *: $p < 0.05$, ns: not significant. The Student's t-test was employed for statistical analysis.

Taken together, these data suggest that TruA and TruD might contribute to *C. jejuni* pathogenesis-associated phenotypes, although the details of this role and potential target genes remain to be clarified. In Chapter II, a dominant growth defect of *truD* compared to *truA* and *truB* deletions was observed (Figure 2.6 B). For this reason, the remaining part of this thesis will focus on the characterization of TruD in *C. jejuni*.

3.3. The *truD* gene in *C. jejuni* is encoded next to an essential gene in *C. jejuni*

When investigating for a potential additional function of TruD in *C. jejuni*, I first focused on the analysis of the genomic context of TruD in *C. jejuni*, *H. pylori*, and *E. coli* bacterial species. Looking at the genomic context can reveal unexplored aspects in genomes that can be used to predict novel functions (Korbel *et al.*, 2004). Thus, observation of *truD* neighbouring genes would allow to hypothesize about a role of the enzyme other than its modifying activity and subsequently test these hyphotheses.

Based on differential RNA-seq (dRNA-seq) applied to different *C. jejuni* species, the 1,119 nt *truD* ORF of *C. jejuni* NCTC11168 seems to be transcribed from a primary transcription start site (pTSS, Figure 3.7 A) located upstream of the *thiL* (Cj1458c), encoding a thiamine monophosphate kinase protein. *C. jejuni thiL* was identified as an essential gene by a global genetic screen using high density transposon mutant library (Tn-seq) (Svensson, Alzheimer and Sharma, unpublished).

In *C. jejuni* strains (except for strain 81116), *truD* is encoded in an operon together with *thiL* and Cj1456c (encoding a periplasmic protein) (Dugar *et al.*, 2013). In addition, amino acid analysis of TruD from different *C. jejuni* isolates, *Campylobacter coli* (*C. coli*) and *Campylobacter lari* (*C. lari*) showed almost 100% conservation among these bacteria (Figure 3.6 B), thereby suggesting that the protein might have a similar function among the *Campylobacteraceae* family.

For most *Campylobacter* species, the *truD* operon is located in a conserved genomic context (Figure 3.6 C) surrounded by *pfrB* and the hypothetical gene Cj1459. In *Helicobacter pylori* species, *truD* is encoded together with the gene encoding the response regulator *recR* and the heat shock protein *hptX*. For instance, dRNA-seq analysis of *H. pylori* shows that *truD* is the second gene of an operon consisting of eleven genes (Sharma *et al.*, 2010). Additionally in *E. coli*, the *truD* gene has its own promoter and seems to represent a single transcription unit between *umpG* (5'(3')-nucleotidase and polyphosphatase) and *ispf* (2-C-methyl-D-erythritol 2,4-cyclodiphosphate synthase) (http://regulondb.ccg.unam.mx/).

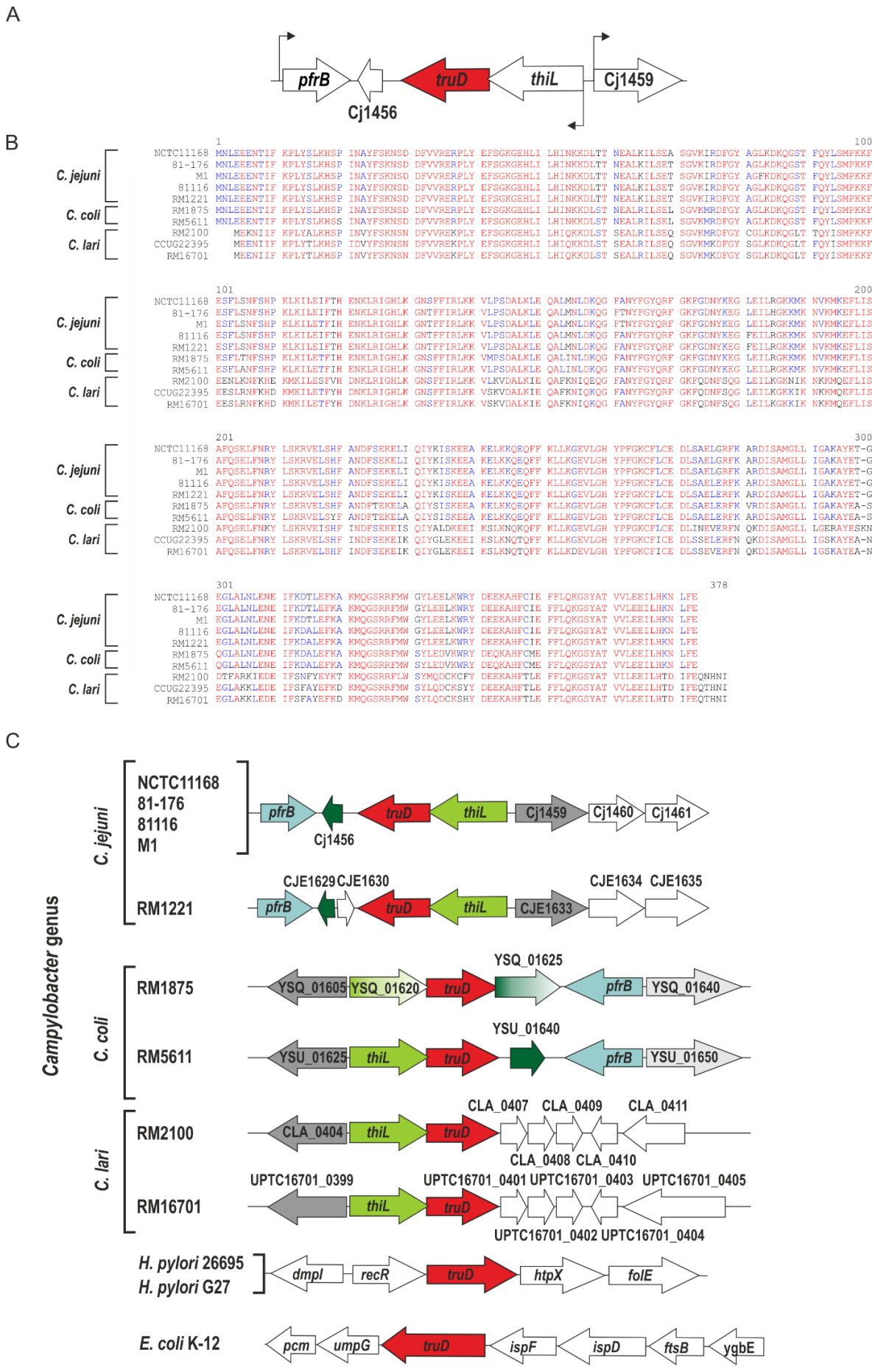

Figure legend on next page

Figure 3.6: Genomic context and sequence alignment of *truD* orthologous in different *Campylobacter* species, *H. pylori*, and *E. coli* strains. (A) The 1,119-nt *truD* (Cj1457c in red) gene is encoded between the 822 nt thiamine monophosphate kinase *thiL* (Cj1458c) and a gene of 104 nt encoding for a periplasmic protein (Cj1456). Transcriptional start sites (TSS, +1; Dugar et al., 2013) are indicated by black arrows. **(B)** Amino acid sequence alignment of TruD in different *Campylobacter* species. Highly conserved residues are marked in red and low consensus residues are marked in blue. **(C)** Orthologs of *truD* in different *Campylobacter*, *Helicobacter pylori* and *Escherichia coli* strains are illustrated using the same colors, while unrelated genes are depicted white.

The diversity in operon composition identified in the cross-species comparison, showed that in the different genomes *truD* is located in unrelated operons, thus suggesting that it might be implicated in a different function in the different bacteria.

3.4. Stability of tRNA-Glu in wildtype and Δ*truD* strains in *C. jejuni*

Pseudo-seq has identified the tRNA-Glu as one of the targets of TruD. Although bacterial tRNA genes are usually organized in clusters, the *C. jejuni* tRNA-Glu location in the genome is different. Based on *C. jejuni* dRNA-seq data, tRNA-Glu is not encoded in a tRNA cluster, but it is expressed with its own promoter between the Cj0167c and Cj0168c genes, both expressed from the opposite strand of the tRNA-Glu (Dugar *et al.*, 2013).

It has been suggested that in tRNAs, pseudouridine might regulate the structure and stability of the RNA molecule (Lorenz *et al.*, 2017). To test if the lack of modification at position 13 in the tRNA-Glu mediated by TruD can affect its stability, a rifampicin RNA stability experiment was performed in the WT and Δ*truD* strains. Rifampicin is an antibiotic that inhibits the bacterial RNA polymerase, thus promoting inhibition of RNA synthesis (Fukuda & Nagasawa-Fujimori, 1983; Laguerre *et al.*, 2018).

For RNA half-life determinations, rifampicin was added to the culture at OD_{600nm} of 0.5-0.6 and cells were harvested after 0, 30, 60, 120, 240, and 480 minutes of incubation with the drug. The rifampicin assay revealed that the level of tRNA-Glu is very stable and similar in the wild-type and Δ*truD* mutant even after 480 minutes, indicating that the stability of the tRNA-Glu is not affected by the lack of pseudouridylation mediated by TruD (Figure 3.7 A & B). As a control, the stability of the small RNA CJnc190 was determined. The experiment revealed that while the tRNA-Glu is stable during the different time points, the small RNA CJnc190 showed a decrease in its stability after the treatment (Figure 3.7 A & B).

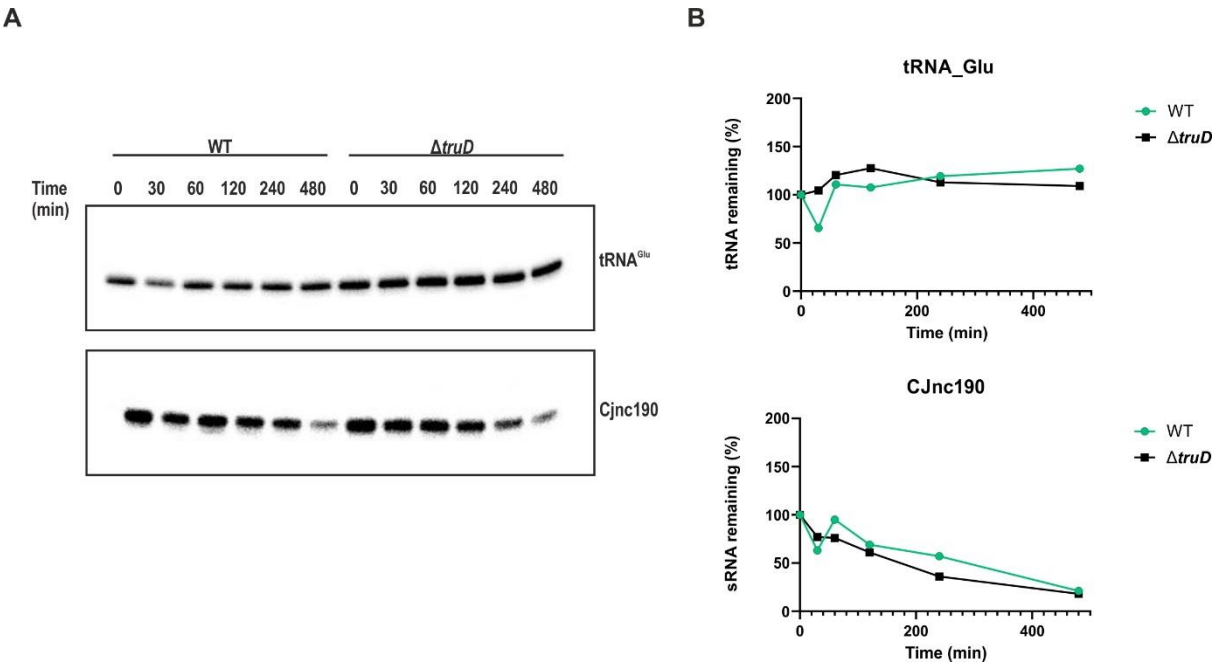

Figure 3.7: The stability of tRNA-Glu is not affected by deletion of *truD*. (A) tRNA-Glu half-life was monitored by northern blot analysis of equal amounts of total RNA extracted from wildtype and Δ*truD* cells at different times point (30, 60, 120, and 480 minutes) after the addition of rifampicin to exponential phase cultures. **(B)** Quantification of the northern blot in panel A.

3.5. TruD from *H. pylori* can complement the growth defect of Δ*truD* in *C. jejuni* but not its enzymatic activity

I next sought to understand why *C. jejuni* Δ*truD* has a growth phenotype, while *H. pylori* Δ*truD* does not. Based on our Pseudo-seq analyses and consistent with TruD function in *E. coli* (Kaya & Ofengand, 2003), both Epsilonproteobacteria enzymes modify tRNA-Glu at a conserved uridine at position 13 (Figure 3.9 A). tRNA-Glu (Cjp03) is present in only one copy in *C. jejuni*, while two tRNA-Glu (Hpt01 and Hpt04) and four tRNA-Glu (gltW, V, T, and U) are expressed in *H. pylori* and *E. coli*, respectively.

As shown in Figure 2.3 of chapter 2 of this thesis, PUS enzymes are highly conserved in the different kingdoms of life in their catalytic domains. For this reason, the amino acid sequence from TruD of *C. jejuni* with *E. coli* and *H. pylori* TruD was compared. The analysis showed that the *E. coli* and *H. pylori* proteins share 34.4 % and 44.5 % identity, respectively, with the *C. jejuni* protein (Figure 3.8).

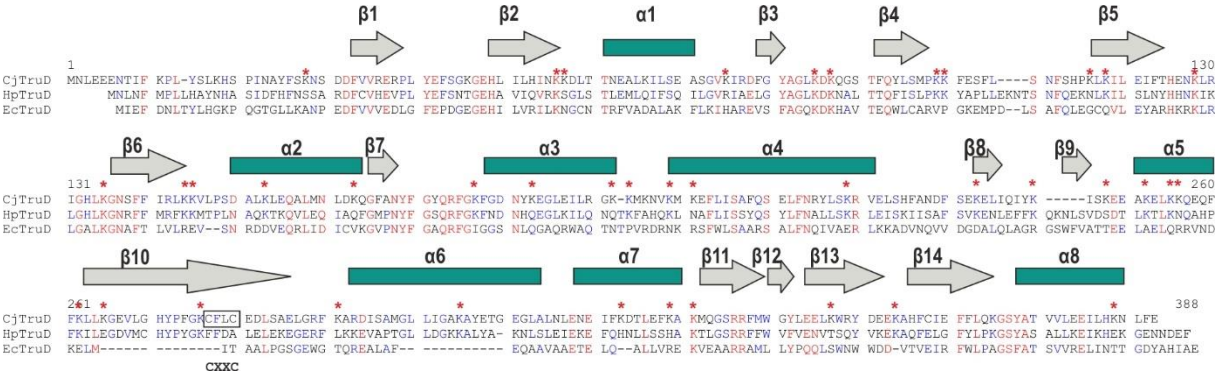

Figure 3.8. Amino acid sequence alignment of EcTruD, HpTruD and CjTruD. Red and blue represents conserved and similar aa residues, respectively. The alpha and beta helix of EcTruD are marked by green bars and grey arrows, respectively.

Based on these data, I hypothesized that *E. coli truD* (Ec*truD*) and *H. pylori* (Hp*truD*) could rescue the growth defects of the *C. jejuni* Δ*truD* strain, and functionally replace it. To test this, the Ec*truD* or the Hp*truD* gene was first introduced in the *rdxA* locus of *C. jejuni* Δ*truD* fused at the C-terminus to a 3xFLAG epitope. To investigate if the proteins can rescue the growth defects and the function of *C. jejuni truD* (Cj*truD*) the growth of these strains was analyzed. This revealed that, while the introduction of Ec*truD* does not complement the growth of Δ*truD*, Hp*truD* is able to complement the phenotype (Figure 3.9 B). To verify if EcTruD and HpTruD proteins are expressed in *C. jejuni*, total protein extracts of the different strains was analyzed by western blot. This confirmed that the proteins are expressed in *C. jejuni* (Figure 3.9 C). Moreover, to investigate if the proteins are functional, we performed CMC treatment followed by primer extension and checked the modification of one of the known targets of CjTruD, Cjp03 (tRNA-Glu). While EcTruD is not able to rescue the growth phenotype, it is able to modify the tRNA-Glu. In contrast, HpTruD rescues the growth defect, but it does not modify the tRNA-Glu (Figure 3.9 D).

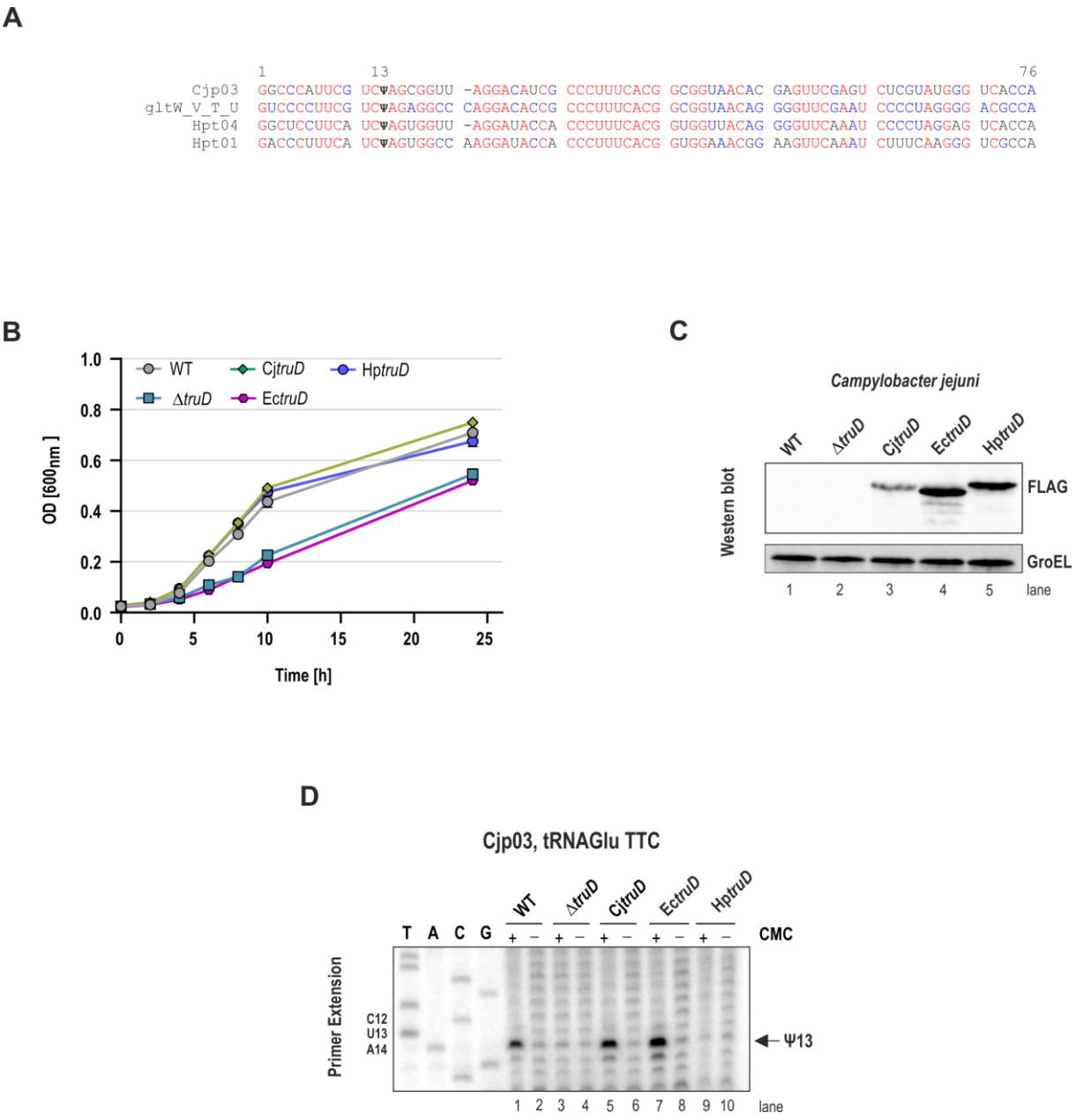

Figure 3.9: Complementation of Δ*truD* in *C. jejuni* with Ec*truD* and Hp*truD*. (A) Sequence alignment of tRNA-Glu of *C. jejuni* (Cjp03), *E. coli* (gltW, gltV, gltT and gltU), and *H. pylori* (Hpt01 and Hpt04). The numbers indicate positions with respect to the first nucleotides of the processed tRNAs. The modified uridine identified by Pseudo-seq at position 13 in tRNAs in Cjp03, gltW, gltV, gltT, gltU, Hpt01, and Hpt04 is represented by a "Ψ". Nucleotides in red are perfectly conserved, nucleotides in blue have a conservation value > 50%, nucleotides in black have a conservation value < 50%. **(B)** Growth curve over 24 hours for *C. jejuni* wild-type, Δ*truD*, Cj*truD*, Ec*truD* and Hp*truD* strains grown in Brucella broth in biological duplicates. **(C)** Western blot analysis of *C. jejuni* wild-type, Δ*truD*, Cj*truD*, Ec*truD* and Hp*truD* strains grown to exponential growth phase. Cj*truD*, Hp*truD* and Ec*truD* strains express TruD with a 3xFLAG epitope tag at the C-terminus. Protein samples corresponding to an OD_{600nm} of 0.1 were loaded on a 12% (vol/vol) SDS-PAA gel, blotted to a nitrocellulose membrane and TruD proteins were detected with anti-FLAG antibodies (1:1000). GroEL served as loading control. **(D)** Total RNA was isolated from *C. jejuni* wild-type, Δ*truD*, Cj*truD*, Ec*truD* and Hp*truD* grown to exponential phase (OD_{600nm} of ~0.4/0.5). DNase I digested CMC treated/untreated total RNA was used in primer extension assays with ^{32}P-end labeled oligo CSO-3108 for

reverse transcription of Cj03 in the presence (lane 1, 3, 5, 7, 9) or absence (lane 2, 4, 6, 8, 10) of the CMC compound. A sequencing ladder corresponding to Cjp03 region was used as reference (lanes T, A, C, G). cDNA products were analyzed on 10% PAA gel under denaturing conditions. Primer extension showed a band in lane 1, 5, and 7 that is absent in lane 2, 3, 4, 6, 8, 9, and 10 that corresponds to the block of the reverse transcriptase at the 3' end of the Ψ-CMC (A14).

These results could be explained by the fact that a tagged version HpTruD is not catalytically active and therefore cannot modify the tRNA-Glu. Even though HpTruD complemented the Δ*truD* growth defect, without showing modification activity towards tRNA-Glu, I wanted to confirm that the tagged version of the protein was functional to understand why it did not modify *C. jejuni* tRNA-Glu. Complementation of *H. pylori* Δ*truD* with CjTruD or HpTruD at the *rdxA* locus was generated. As above, the genes were fused to a 3×FLAG sequence and introduced in the *H. pylori rdxA* locus. The genes were fused to a 3xFLAG sequence. Introduction of Ec*truD* (data not shown) was not successful as no positive clones could be generated. In contrast, H*ptruD* and Cj*truD* could be successfully introduced into in *H. pylori* Δ*truD.* Western blot analysis of total protein extracts showed that HpTruD and CjTruD are expressed from the recombined locus in *H. pylori* (Figure 3.10 A). Primer extension assays of CMC treated RNA showed that both H*ptruD* and Cj*truD* can modify both tRNA-Glu of *H. pylori* (Hpt01 and Hpt04) (Figure 3.10 B & C), indicating that CjTruD is catalytically active when expressed in *H. pylori*.

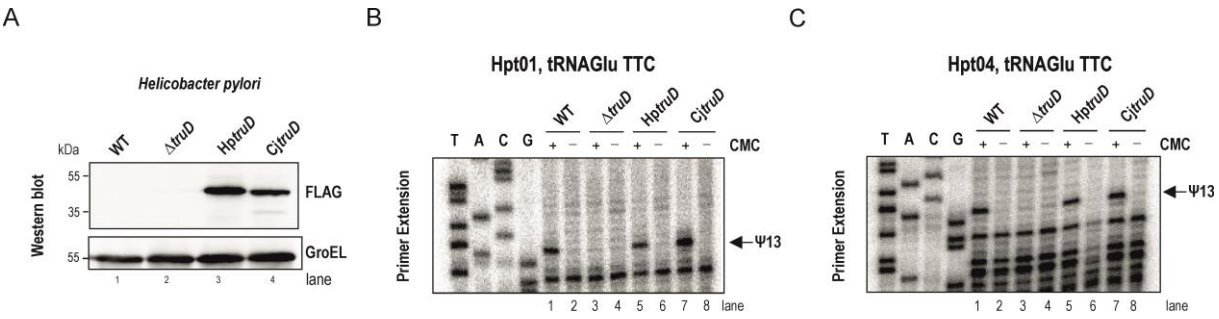

Figure 3.10: Complementation of Δ*truD* in *H. pylori* with Cj*truD*. (A) Western blot analysis of TruD expression in *H. pylori* wild-type, Δ*truD*, Hp*truD*, Cj*truD* strains grown to exponential growth phase. Protein sample corresponding to an OD600 of 0.1 were loaded on a 12% SDS-PAGE gel, blotted to PVDF membrane and TruD proteins were detected with anti-FLAG antibodies (1:1,000). GroEL served as loading control. **(B and C)** Total RNA was isolated from *H. pylori* wild-type, Δ*truD*, Hp*truD*, and Cj*truD* strains that were grown to exponential growth phase (OD_{600nm} of ~0.7). DNase I digested CMC treated/untreated total RNA was used in primer extension assays with ^{32}P-end labeled oligo CSO-4286 for reverse transcription of Hpt01 **(B)** or CSO-4285 for reverse transcription of Hpt04 **(C)** in the presence (lane 1, 3, 5, 7) or absence (lane 2, 4, 6, 8) of the CMC compound. A sequencing ladder corresponding to Hpt01 region was used as reference (lanes T, A, C, G). cDNA products were analyzed on 10% PAA gel under denaturing conditions. Primer extension

showed a band in lane 1, 5 and 7 that is absent in lane 2, 3, 4, 6, 8, 9 that corresponds to the block of the reverse transcriptase at the 3' end of the Ψ-CMC (14).

Since HpTruD can complement the growth defect of *C. jejuni ΔtruD* without promoting the generation of the modification in the tRNA-Glu (Figure 3.9), it strongly indicates that the modification at position 13 of the tRNA-Glu is not essential for the growth of the bacteria. Thus, these results suggest that in *C. jejuni* the phenotype that is associated with the deletion of *truD* seems to be due to an additional function of the enzyme, independent from the generation of Ψ.

3.6. *In-vitro* pseudouridylation assays confirms that HptruD expressed in *C. jejuni* fails to modify the *C. jejuni* tRNA-Glu

In section 3.5 of this chapter, I showed that expression of HpTruD in *C. jejuni* rescues the growth phenotype of deletion of *truD*; however, the enzyme is not able to modify the tRNA-Glu of *C. jejuni*. The lack of activity of HpTruD in *C. jejuni* might be due to difference in folding of HpTruD protein in *C. jejuni* or the absence of accessory factors that are indispensable for its function. To explore whether the expression of TruD and potential auxiliary factors might contribute to the function of the enzyme, the ability of *H. pylori* cell extracts to modify *C. jejuni* tRNA-Glu was determined using an *in-vitro* pseudouridylation assay with T7-transcribed Cjp03 (tRNA-Glu). Based on the result of the primer extension reported in Figure 3.9 D, where *Ec*TruD is able to modify the tRNA-Glu of *C. jejuni*, indicating that the enzyme is able to promote the isomerization of this target. As a positive control, the *E. coli* cell extract was used to check the modification at position 13 of Cjp03.

An assay using *H. pylori* and *E. coli* extracts showed that the incubation with both cell extracts led to the generation of the modification at position 13 in the tRNA-Glu (Figure 3.11 A, lane 3 & 5). This suggests that *H. pylori* extract is functional and is able to promote the isomerization. In addition, the presence of the modification in the tRNA-Glu at position 55 in the *in-vitro* assay with *E. coli* extract and the absence of the modification when the tRNA-Glu is incubated with *H. pylori* cell extract further confirms absence of TruB, or any similar activity, in this Epsilonproteobacterium.

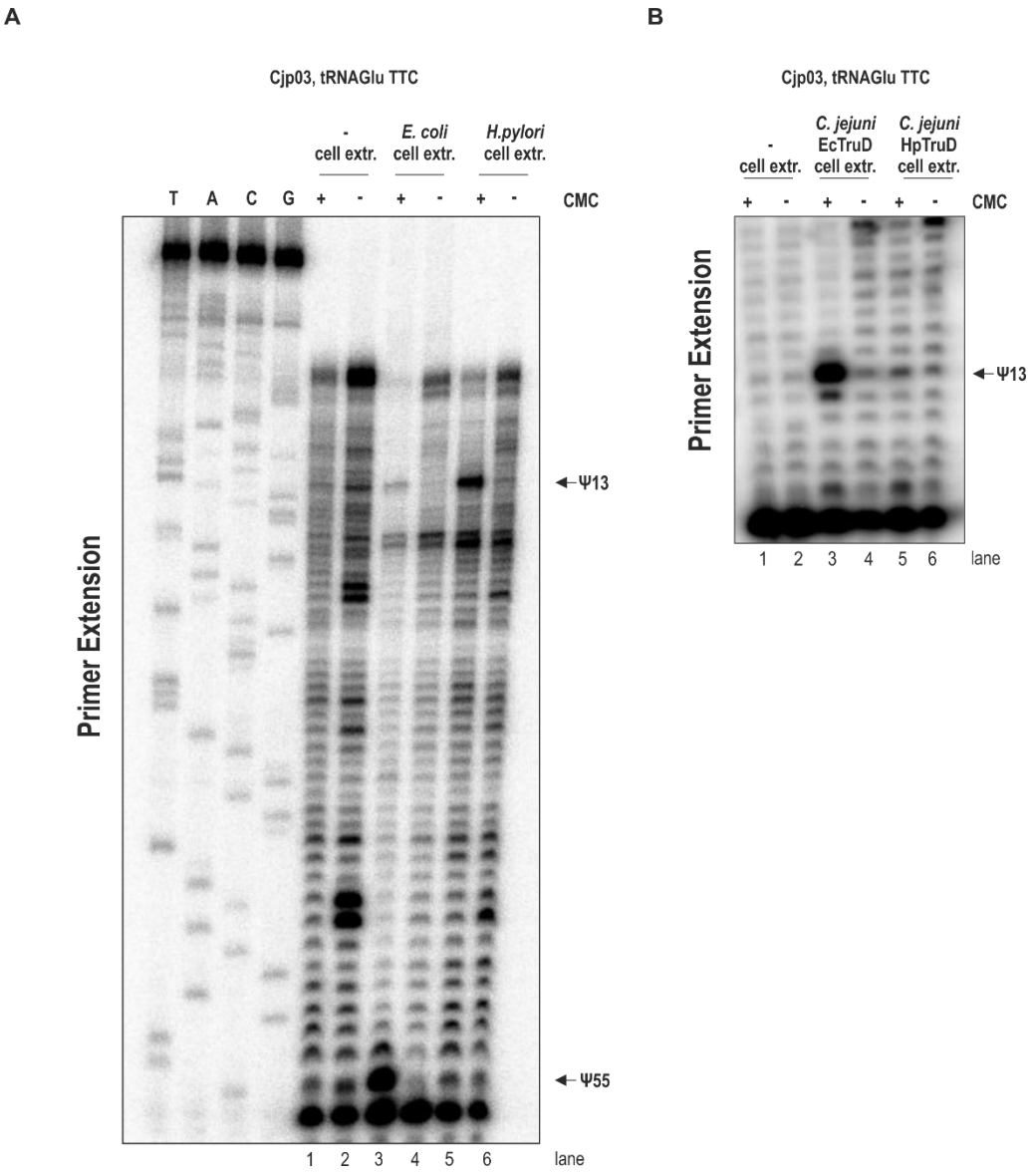

Figure 3.11. *In-vitro* pseudouridylation assay reveals that *E. coli* and *H. pylori* extracts promote the Ψ formation at position 13 in the Cjp03 tRNA-Glu. (A) Primer extension of tRNA-Glu (Cjp03) treated without (-) cell extract (lanes 1 & 2), or with the *E. coli* (lane 3 & 4) or *H. pylori* extract (lane 5 & 6). **(B)** Primer extension of *in-vitro* modified tRNA-Glu (Cjp03) without cell extract (-) (lanes 1 & 2), with *C. jejuni* expressing EcTruD (lanes 3 & 4), and with *C. jejuni* expressing HpTruD (lanes 5 & 6) extracts.

Additionally, a second *in-vitro* assay using *C. jejuni* extracts either expressing CjTruD or HpTruD was performed. The assay showed that cell extract from *C. jejuni* expressing HpTruD failed to modify Cjp03 *in vitro*, consistent with the *in-vivo* observations (Figure 3.11 B). To discern if *H. pylori*, HpTruD is responsible for the modification in the tRNA-Glu, an *in-vitro* assay using wildtype, Δ*truD*, Hp*truD* and Cj*truD* was performed. While extract from *H. pylori* expressing

CjTruD efficiently generated Ψ (Figure 3.12 lanes 5 & 6), expression of HpTruD did not lead to a strong isomerization (Figure 3.12 lanes 7 & 8), supporting the *in-vivo* observations.

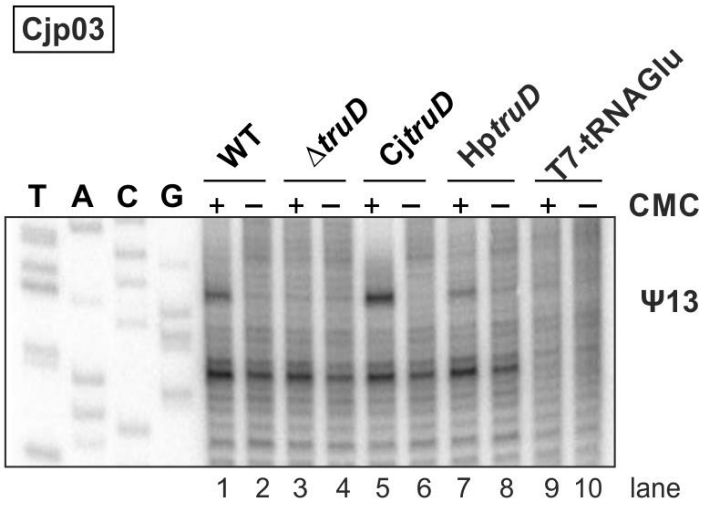

Figure 3.12. *In-vitro* pseudouridylation assay with different *H. pylori* cell extracts shows that HpTruD is able to modify Cjp03 with low efficiency. Primer extension of in-vitro modified Cjp03 with *H. pylori* WT cell extract (lanes 1 & 2), with *H. pylori* Δ*truD* (lane 3 & 4), *H. pylori* extract expressing CjTruD (lane 5 & 6), *H. pylori* extract expressing HpTruD (lane 5 & 6) and (T7/Cjp03) without (-) cell extract

3.7. Mutational studies on CjTruD support the hypothesis that TruD could have a moonlighting function in *C. jejuni*.

It has been shown that the aspartate at position 80 of *E. coli* TruD is important for the nucleophilic attack of the uridine, the initial step in the formation of Ψ (Kaya & Ofengand, 2003a). To test whether TruD might have an additional function other than its catalytic activity, the 3xFLAG-tagged TruD of *C. jejuni* was mutated in its catalytic residue. Specifically, the aspartate (D) at position 85 in the amino acid sequence of TruD was mutated in alanine (N), resulting in the strain D85N. This construct was used to complement Δ*truD* of *C. jejuni*. Western Blot analysis showed that the level of D85N was comparable to the level of wild-type CjTruD, suggesting that the introduction of the mutation in the catalytic aspartate does not lead to a decrease in the protein stability (Figure 3.13 A). CMC treatment followed by primer extension confirmed that the enzyme is not able to modify the tRNA-Glu at position 13 confirming the role of the aspartate at position 85 in catalysis (Figure 3.13 B). Interestingly, the growth phenotype of Δ*truD* was complemented

by the expression of the catalytically inactive TruD (D85N) (Figure 3.13 C). Taken together, these observations support the hypothesis that TruD might have an additional function in *C. jejuni*.

Since the C*truD* and D85N strains have a comparable growth rate, similar to the wild-type strain (Figure 3.13 C), the rifampicin assay was repeated using these strains. The assay was performed to test the stability of the tRNA-Glu in *C. jejuni* wild-type, C*truD* and D85N strains (Figure 3.14). The bacterial cells were collected after 4, 8, 16, 32, and 128 minutes after rifampicin addition. While small RNA CJnc180 showed a decrease in its stability in the different strains at the selected time points, the tRNA-Glu was stable under the same conditions and in the different strains. This indicates that the stability of the tRNA-Glu is not affected by the catalytic inactivity of the *C. jejuni* TruD.

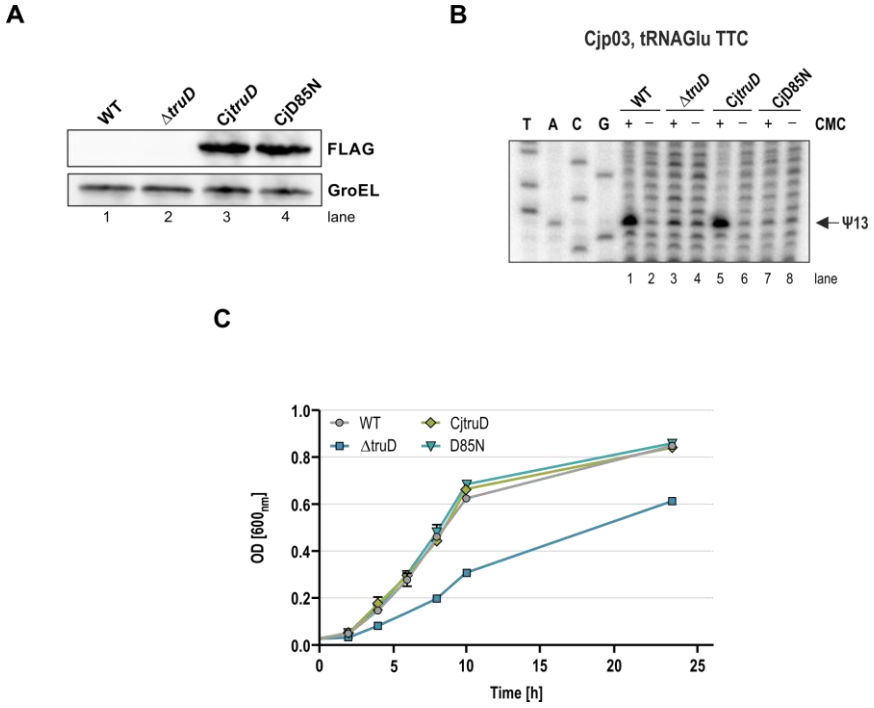

Figure 3.13: A catalytically inactive TruD rescues the growth defects of Δ*truD* in *C. jejuni*, which might indicate an additional function of TruD in *C. jejuni*. (A) Western blot analysis of *C. jejuni* wild-type, Δ*truD*, Cj*truD* and D85N strains grown to exponential growth phase. Protein sample corresponding to an OD600 of 0.1 were loaded on a 12 % SDS-PAA gel, blotted to PVDF membrane and TruD proteins were detected with an anti-FLAG antibodies (1:1,000). GroEL served as loading control. **(B)** Total RNA was isolated from *C. jejuni* wild-type, Δ*truD*, Cj*truD* and D85N strains that were grown to exponential growth phase (OD_{600nm} of ~0.4/0.5). DNase I digested CMC treated/untreated total RNA was used in primer extension assays with ^{32}P-end labeled oligo CSO-3108 for reverse transcription of Cj03 in the presence (lane 1, 3, 5, 7) or absence (lane 2, 4, 6, 8) of the CMC compound. A sequencing ladder corresponding to Cjp03 region was used as reference (lanes T, A, C, G). cDNA products were analyzed on 10% PAA gel under denaturing conditions. Primer extension showed a band in lane 1, 5 and is absent in lane 2, 3, 4, 6, 7, and 8 that corresponds to the block of the reverse transcriptase at the 3' end of the Ψ-CMC (A14). **(C)** Growth curve over 24 hours for *C. jejuni* wild-type, Δ*truD*, Cj*truD* and D85N strains grown in Brucella broth in duplicates.

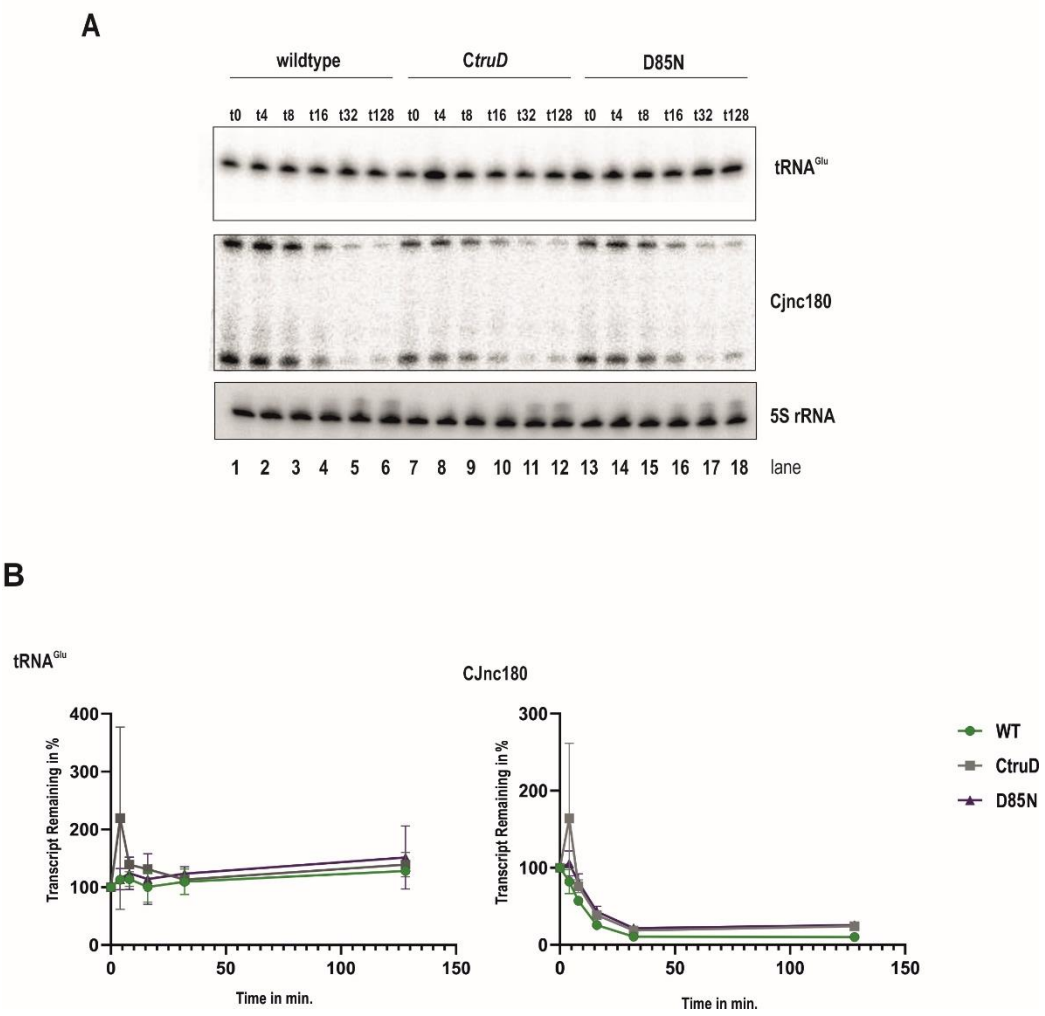

Figure 3.14: The stability of tRNA-Glu is not affected by the catalytically inactive mutant. (A) tRNA-Glu half-life was monitored by northern blot analysis of equal amounts of total RNA extracted from wildtype and Δ*truD* cells at different times point (4, 8, 16, 32 and 128 minutes) after the addition of rifampicin to exponential phase cultures. As a positive control small RNA CJnc180 and the housekeeping 5S rRNA **(B)** Quantification of northern blot of figure 3.14 A for the tRNA-Glu and CJnc180.

To further probe that CjTruD has an additional function, a strain with a point mutation in the uridine at position 13 (tRNA-Glu T13C strain) in the tRNA-Glu was generated (Figure 3.15 A). Since the introduction of the *aac(3)-IV* gene (that confers gentamicin resistance to the bacteria) and a transcriptional terminator next to the tRNA-Glu could potentially destabilize the tRNA locus, as a control, a strain that carries a wildtype copy of the tRNA-Glu (tRNA-Glu T13C strain) was generated. While CMC treatment followed by primer extension showed that the tRNA-Glu is not modified in the tRNA-Glu T13C strain (Figure 3.15 B), the strain does not show growth defects (Figure 3.15 C), supporting the hypothesis that loss of modification of tRNA-Glu at position 13 is not responsible for the growth defects that we observed when deleting *truD*. Moreover, to check

the level of charging of the tRNA-Glu in the different strain, an acidic northern blot was performed. The assay shows no difference in the level of charging of the tRNA-Glu in the different strains, suggesting that the lack of the modification at position 13 in the tRNA-Glu does not affect the aminoacylation of the tRNA (Appendix Figure 1). However, in the strains where the modification is lacking (Δ*truD*, D85N, and, tRNA-GluT13C), it looks like that all the tRNA-Glu that is expressed in the cell is charged, with no detectable uncharged tRNA-Glu in this experimental condition.

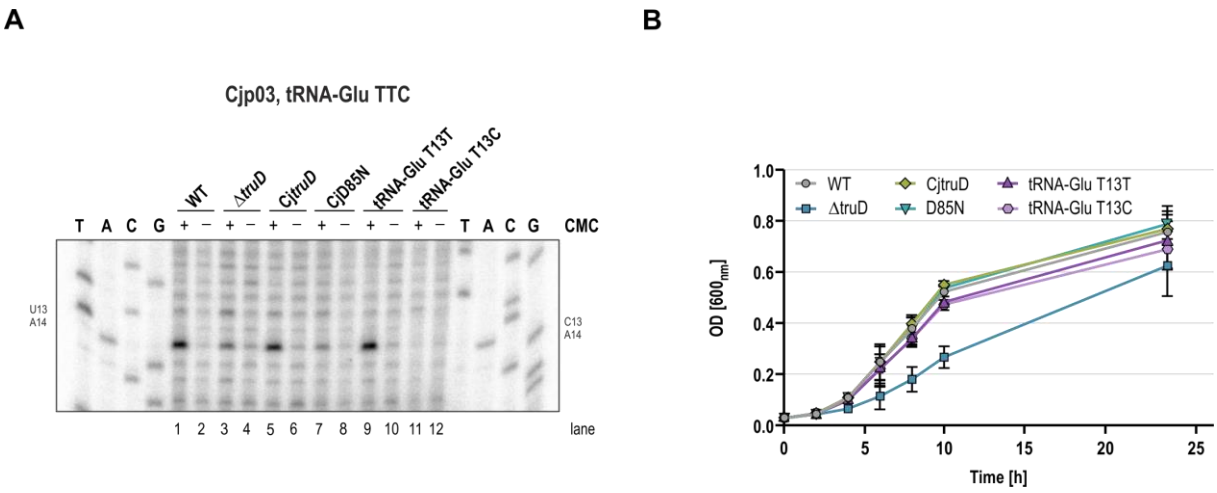

Figure 3.15: Mutation of tRNA-Glu of *C. jejuni* at position 13 does not affect the growth of the bacteria. (A) Total RNA was isolated from *C. jejuni* wild-type, Δ*truD*, Cj*truD*, D85N, tRNA-GluT13T, and tRNA-GluT13C that were grown to exponential growth phase (OD_{600nm} of ~0.4/0.5). DNase I digested CMC treated/untreated total RNA was used in primer extension assays with ^{32}P-end labeled oligo CSO-3108 for reverse transcription of Cj03 in the presence (lane 1, 3, 5, 7, 9, 11) or absence (lane 2, 4, 6, 8, 10, 12) of the CMC compound. A sequencing ladder corresponding to Cjp03 region was used as reference (lanes T, A, C, G). cDNA products were analyzed on 10% PAA gel under denaturing conditions. Primer extension showed a band in lane 1, 5 and 9 and is absent in lane 2, 3, 4, 6, 7, 8, 10, 11 and 12 that corresponds to the block of the reverse transcriptase at the 3' end of the Ψ-CMC (A14). **(B)** Growth curve over 24 hours for *C. jejuni* wild-type, Δ*truD*, Cj*truD*, D85N, TT and TC strains grown in Brucella broth in duplicates. Error bars represent standard deviation of the two biological replicates.

3.8. TruD might co-sediment with the 30S ribosomal subunit in *C. jejuni* cells.

Enzymes from the RsuA and RluA families have an N-terminal S4-like domain that is necessary for the binding to rRNA (Jayalath *et al.*, 2020) Moreover, it has been recently shown that rRNA modifying enzyme RsuA might be important for ribosome biogenesis (Jayalath *et al.*, 2020). Sedimentation profile using glycerol gradient is a powerful technique to separate the cellular components based on their size and shape (Erickson, 2009). After ultracentrifugation, the cellular

particles will migrate from the low molecular (upper part of the gradient) to the high molecular size (lower part of the gradient).

To investigate the sedimentation of CjTruD in different fractions in the cell and identify potential co-sedimentation partners, glycerol gradients using different *C. jejuni* strains were performed. The strain expressing the TruD-3xFLAG was used to detect TruD in the different cellular fractions and the wildtype untagged *C. jejuni* strain was used as control. Additionally, the L1-3xFLAG and S1-3xFLAG strains expressing the large ribosomal protein L1 and the small ribosomal protein S1 were used as controls to verify the correct assembly of the ribosomal subunit in the gradient. The protocol was adapted from Grad-seq (Smirnov *et al.*, 2016; Hör *et al.*, 2020b). *C. jejuni* wildtype, TruD-3xFLAG, S1-3xFLAG, and L1-3xFLAG were grown to OD_{600nm} of 0.5 and cell pellets were lysed and loaded in the glycerol gradients. After ultracentrifugation, 20 fractions and the pellet fraction were collected and measured in order to calculate the absorbance at 260nm and to check the correct assembly of the ribosome. Glycerol fractions were mixed with protein loading dye and analyzed by western blot. Figure 3.16 shows the A260 of the 20 fractions isolated during density fractionation and the corresponding western blot. Western blot analysis of the L1-3xFLAG and S1-3xFLAG profiles, validate the intact complexes of the L1 protein with the 50S fractions and S1 with the 30S fractions. TruD-3xFLAG co-sediments with the low molecular fraction of the gradients (fractions 1-8), in agreement with Grad-seq of tRNA PUS enzymes in *S.* Typhimurium (Smirnov *et al.*, 2016). Moreover, low levels of TruD protein were detected around the 30S fraction (fractions 9 and 10) and the pellet fraction (containing the 70S ribosome). This indicates a possible interaction of TruD with rRNA and/or proteins that co-migrate with the 30S subunit.

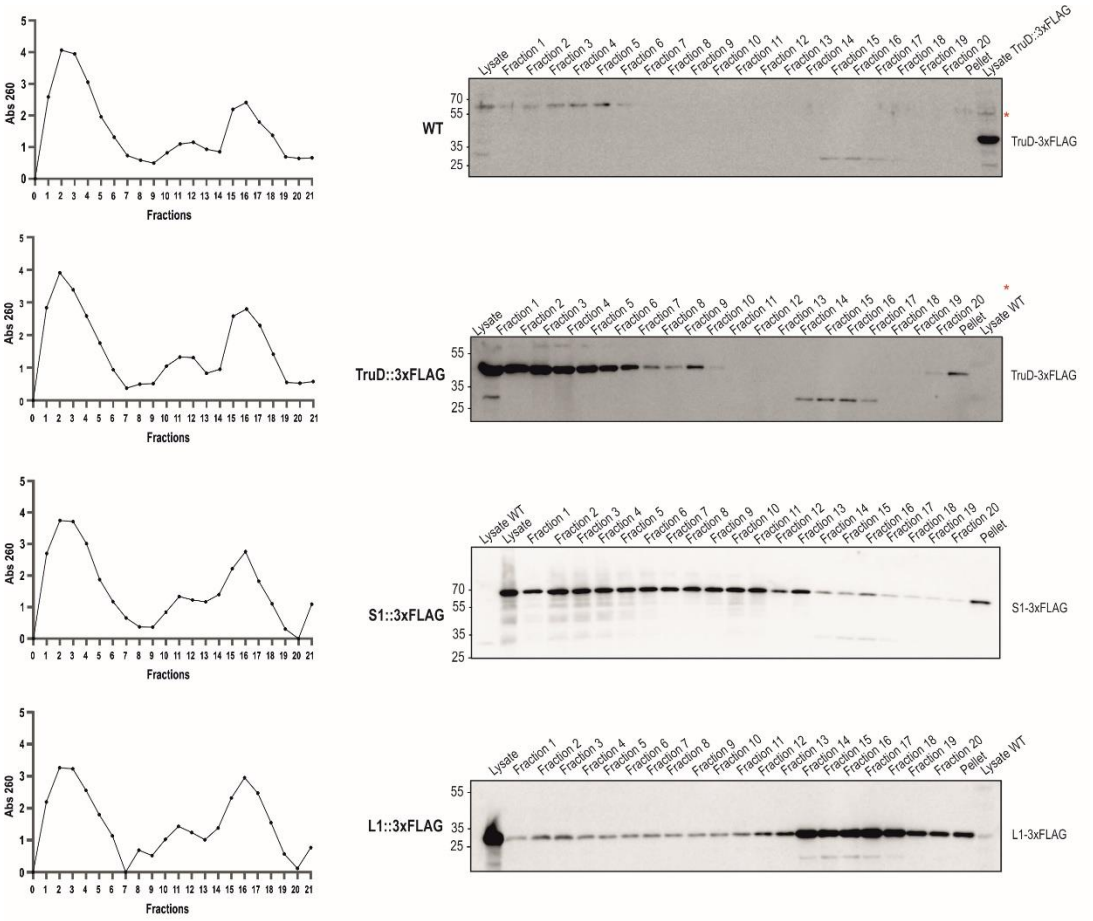

Figure 3.16. Glycerol gradient profiles and associated western blot of *C. jejuni* WT, TruD-3xFLAG, S1-3xFLAG and L1-3xFLAG strains. (*left*) Glycerol gradient profiles monitored by UV measurements (Abs 260) of RNA in the different fractions of *C. jejuni* WT, TruD-3xFLAG, S1-3xFLAG and L1-3xFLAG strains. The peaks correspond to free RNA (1-9 fractions), 30S (10-13 fractions), 50S (14-20 fractions), and 70S complexes (fraction 21 or pellet fraction). **(*right*)** Western blots of lysates and 1-21 fractions of the corresponding strains probed for anti-FLAG antibody.

3.9. Deletion of *truD* affects the growth of *C. jejuni* 81-176 and *C. coli* NCTC12668

To investigate whether the absence of *truD* could affect the growth of other *C. jejuni* strains, the *truD* gene was deleted in the virulent *C. jejuni* 81-176 strain The genomic location and operon organization of *truD* in *C. jejuni* 81-176 is comparable with the one of *C. jejuni* NCTC11168 (Figure 3.17, *Upper panel*). Moreover, the alignment of the amino acid sequence of TruD proteins of the two strains showed almost 100% of identity (368/372 amino acid) (Figure 3.17, *lower panel*). To investigate a possible conserved function for *C. jejuni* TruD, a *truD* deletion was generated in the *C. jejuni* 81-176 strain. Deletion of the *truD* gene abolished the modification in the tRNA-Glu at position 13 (Figure 3.18 A) and a similar growth defect was observed for Δ*truD* in *C. jejuni* 81-176 (Figure 3.18 B).

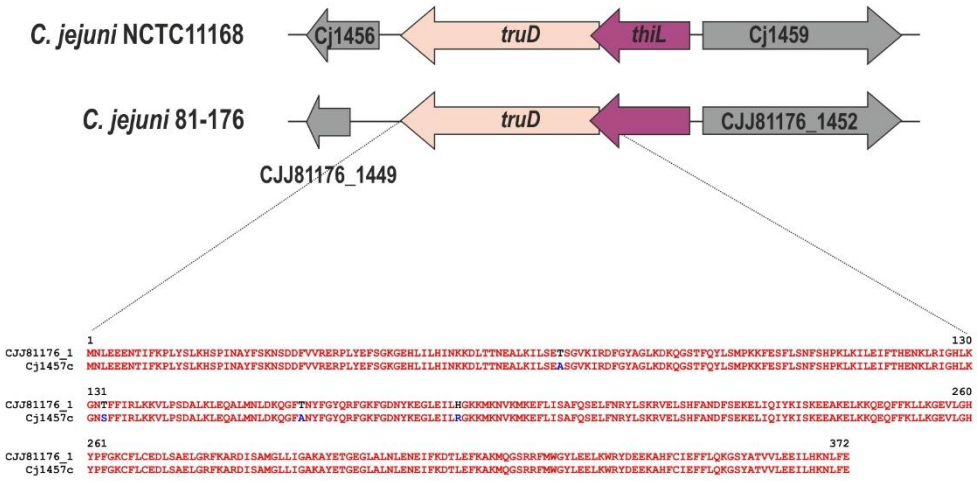

Figure 3.17. Genomic location of the *truD* gene in *C. jejuni* NCTC11168 and 81-176 strains. *(Upper panel)* The *truD* gene is represented as a pink arrow located in the lagging strand. Together with the *thiL* gene (purple) and Cj1456, *truD*, *thiL* and Cj1456 are part of the same operon. *(Lower panel)* Amino acid sequence alignment of TruD protein of the *C. jejuni* NCTC11168 (Cj1457c) and 81-176 (CJJ81176_1450) strains.

Expression of the catalytically inactive TruD (D85N) of *C. jejuni* NCTC11168 in Δ*truD* of *C. jejuni* 81-176 strain is able to complement the catalytic activity of the enzyme (Figure 3.18 C), but rescues the growth defect of *C. jejuni* 81-176, indicating that the function of TruD is conserved between the NCTC11168 and 81-176. To further confirm that the function of TruD is conserved in other *Campylobacter* species, *truD* was deleted in the *C. coli* strain NCTC12668. Growth analyses of *C. coli* wildtype and Δ*truD* showed that deletion of *truD* affects the growth of this strain as well (Figure 3.18 D), suggesting an important physiological role for the enzyme in the *Campylobacter* genus.

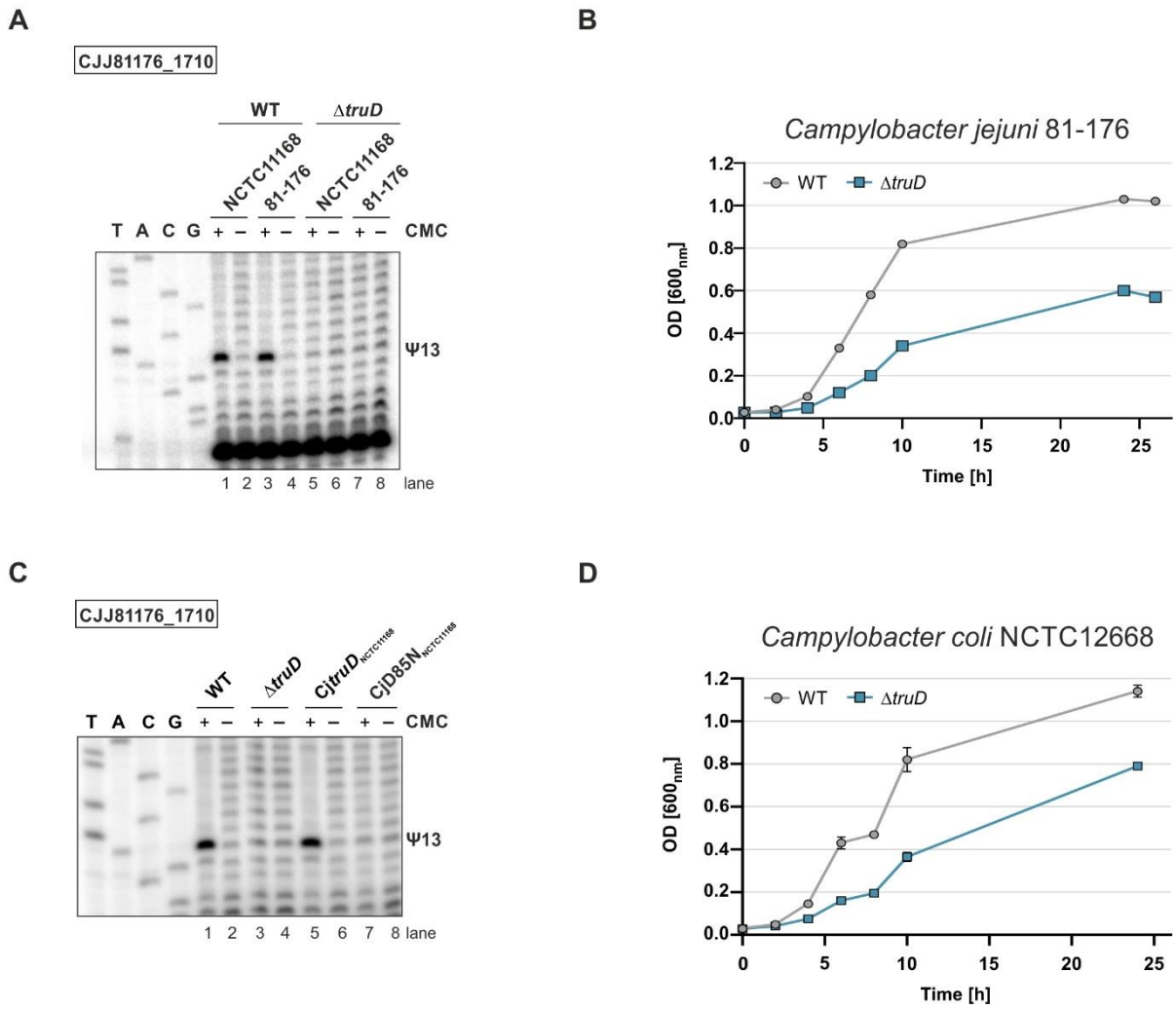

Figure 3.18: Deletion of *truD* in *C. jejuni* 81-176 and *C. coli* NCTC12668 impacts the growth of the bacteria. (A) Total RNA was isolated from *C. jejuni* NCTC11168 and 81-176 wild-type and Δ*truD* strains that were grown to exponential growth phase (OD_{600nm} of ~0.4/0.6). DNase I digested CMC treated/untreated total RNA was used in primer extension assays with ^{32}P-end labeled oligo CSO-3108 for reverse transcription of Cj03 in strain NCTC11168 and CJJ81176_1710 in *C. jejuni* 81-176 in the presence (lane 1, 3, 5, 7) or absence (lane 2, 4, 6, 8) of the CMC compound. A sequencing ladder corresponding to Cjp03/ CJJ81176_1710 region was used as reference (lanes T, A, C, G). cDNA products were analyzed on 10% PAA gel under denaturing conditions. Primer extension showed a band in lane 1 and 3 and it is absent in lane 2, 4, 6, 7, 8 that corresponds to the block of the reverse transcriptase at the 3' end of the Ψ-CMC (A14). **(B)** Growth curve over 24 hours for *C. jejuni* 81-176 wild-type and ΔtruD strains grown in Brucella broth in duplicate. **(C)** Total RNA was isolated from *C. jejuni* 81-176 wild-type, Δ*truD*, C*truD* and D85N strains that were grown to exponential growth phase (OD_{600nm} of ~0.4/0.6). DNase I digested CMC treated/untreated total RNA was used in primer extension assays with ^{32}P-end labeled oligo CSO-3108 for reverse transcription of CJJ81176_1710 in the presence (lane 1, 3, 5, 7) or absence (lane 2, 4, 6, 8) of the CMC compound. A sequencing ladder corresponding to Cjp03/ CJJ81176_1710 region was used as reference (lanes T, A, C, G). cDNA products were analyzed on 10% PAA gel under denaturing conditions. Primer extension showed a band in lane 1 and 5 and it is absent in lanes 2, 3, 4, 6, 7, 8 that corresponds to the block of the reverse transcriptase at the 3' end of the Ψ-CMC (A14). **(D)** Growth curve over 24 hours for *C. coli* NCTC12668 wild-type and Δ*truD* strains grown in Brucella broth in duplicate.

4. Result III: Exploring the potential regulon of TruD in *Campylobacter jejuni* using deep-sequencing approaches

Pseudo-seq identified tRNA-Glu as one of the major targets of TruD in *C. jejuni* (Chapter 2). Moreover, the growth defect that was observed upon deletion of *truD* seems to be independent of its catalytic activity (Chapter 3). TruB has been shown to act as a tRNA chaperone in *E. coli* (Keffer-Wilkes *et al.*, 2016) and a potential role of eukaryotic PUS enzymes as regulator of gene expression has also been recently uncovered (Rintala-Dempsey & Kothe, 2017). To investigate whether TruD binds to RNAs and thereby acts as an RNA-chaperone, I aimed to identify direct TruD targets by RNA immunoprecipitation followed by deep-sequencing (RIP-seq) and by cross-linking immunoprecipitation (CLIP-seq) experiments. Moreover, to explore the hypothesis that TruD potentially contributes to regulation of gene expression, I investigated changes in the transcriptome and translatome of the *truD* deletion mutant compared to the parental wild-type strain by RNA sequencing (RNA-seq) and ribosome profiling (Ribo-seq), respectively.

4.1. RIP-seq revealed direct RNA targets of TruD in *C. jejuni*

To investigate direct RNA-binding partners of *C. jejuni* TruD on a global scale, a RIP-seq experiment was performed by Dr. Hock Siew Tan from our lab using a previously described protocol (Dugar *et al.*, 2016) The experiment was performed using a *C. jejuni* untagged wildtype strain as control and a tagged strain, where the 3xFLAG epitope tag was fused to the C-terminus of TruD. The coIP experiment was carried out on lysates of *C. jejuni* untagged wildtype and TruD-3xFLAG tagged strains using anti-FLAG antibody. After coIP, the purified RNA was converted into cDNA libraries and sequenced. 96-97.2% of aligned reads (compared to the number of input reads, Appendix Table 6) aligned to the reference genome and a GFOLD analysis was performed to identify enriched RNAs in the TruD-3xFLAG coIP compared to the wildtype (Feng *et al.*, 2012). An overview of the different RNA classes (sRNAs, 5' UTRs, ORFs, rRNAs, tRNAs, housekeeping RNAs, and pseudogenes) showed a slight increase in the co-purified RNAs belonging to 5' UTRs, ORFs, tRNAs, and housekeeping RNAs (Figure 4.1).

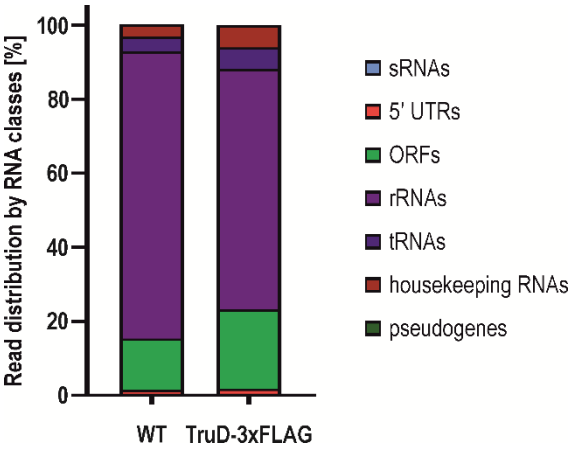

	WT/control	TruD-3xFLAG
sRNAs	0%	0%
5' UTRs	1%	1%
ORFs	14%	22%
rRNAs	78%	65%
tRNAs	4%	6%
housekeeping RNAs	3%	6%
pseudogenes	0%	0%

Figure 4.1: Read distribution for WT/control and TruD-3xFLAG coIPs. (*left panel*) Bars showing the read distributions (in %) of each RNA class (pseudogenes, housekeeping RNAs, tRNAs, rRNAs), ORFs, 5' UTRs, and sRNAs) in the WT and TruD-3xFLAG libraries. (*right panel*) Percentage of each RNA class for the respective WT/control and TruD-3xFLAG RIP-seq experiment.

Forty-three potential binding partners were enriched in the TruD-3xFLAG RIP-seq with a GFOLD ≥ 1.0. Specifically, four 5´ UTRs, 36 coding regions (CDS), two tRNAs, and one transfer-messenger RNA (tmRNA) were found to be enriched (Appendix Table 7). Cjp03 (tRNA-Glu), the known tRNA target of TruD identified using Pseudo-seq, was enriched (GFOLD of +1.4), confirming the viability of the coIP. Cjp28 (tRNA-Leu) was additionally found to be enriched (GFOLD of +1.0) as the second tRNA. This tRNA however was not identified as modified by TruD in the Pseudo-seq analysis and no nucleotide sequence homology was observed between the tRNA-Glu and the tRNA-Leu (data not shown). Among the enriched regions identified inside the CDS, the NADH dehydrogenase subunits A (*nuoA*, Cj1579c; GFOLD of +1.1), H (*nuoH*, Cj1572c; GFOLD of +1.0) and L (*nuoL*, Cj1568c; GFOLD of +1.0) were enriched. Additionally, RNAs from Cj1006c (GFOLD of +1.9), encoding a MiaB like tRNA-modifying enzyme, and Cj0245 (GFOLD of +1.2) encoding the 50S ribosomal protein *rplT*, were found to be bound by TruD. In parallel, the reads of each coIP were visualized using the Integrated Genome Browser (IGB). The presence of peaks corresponding to the regions bound by TruD in the mentioned co-purified RNAs in the TruD-3xFLAG library versus the untagged WT control confirms the GFOLD result (Figure 4.2 A-D).

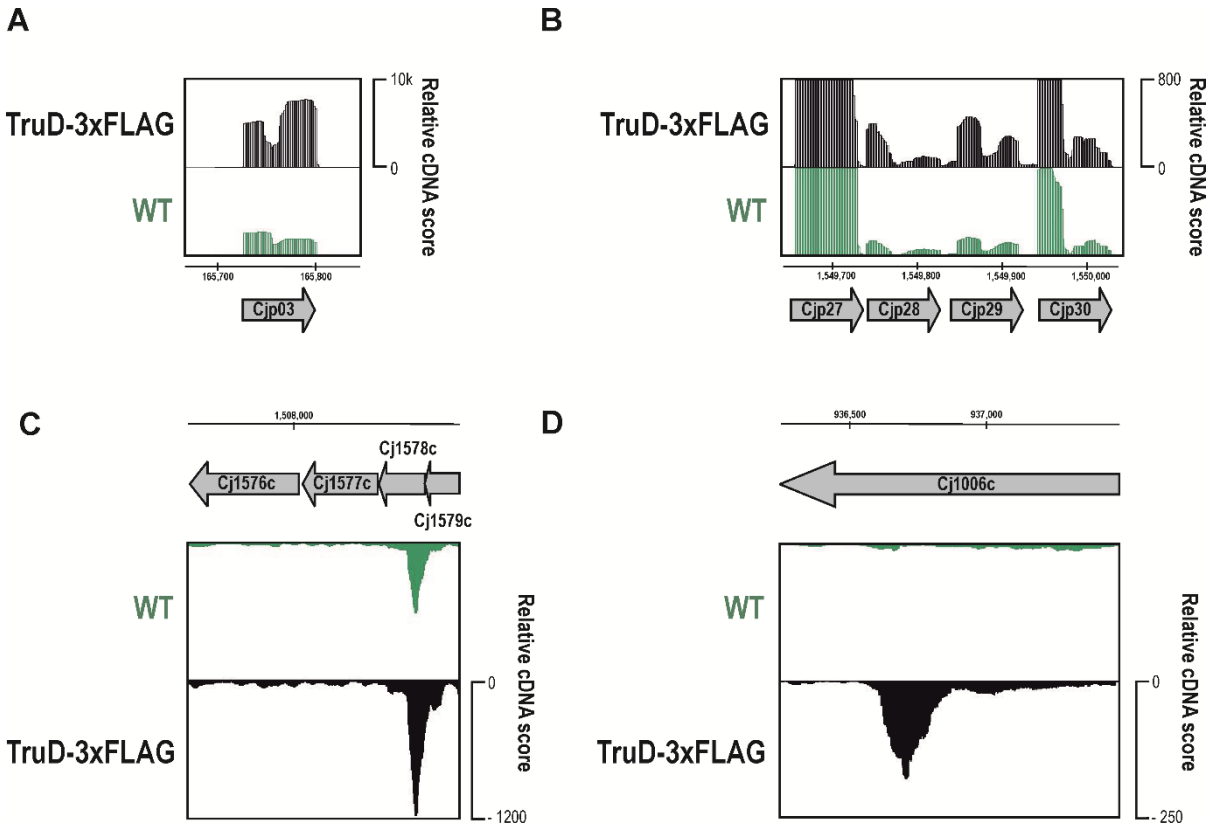

Figure 4.2: Potential RNA targets of TruD based on RIP-seq. (A-D) cDNA reads from the RIP-seq analysis of the TruD-3xFLAG and WT (wildtype) untagged strains were mapped to the **(A)** tRNA-Glu(Cjp03), **(B)** $tRNA^{Gly}$- $tRNA^{Leu}$- $tRNA^{Cys}$- $tRNA^{Ser}$ (Cjp27-Cjp28-Cjp29-Cjp30), **(C)** Cj1576c-Cj1577c- Cj1578c- Cj1579c, and **(D)** Cj1006c regions in the *C. jejuni* NCTC11168 genome. Grey arrows represent annotated tRNAs/CDSs. Numbers represents the genomic coordinates of the tRNAs/CDSs (below/above the IGB screenshots) as well as the relative cDNA scores (to the right of the boxes).

4.2. Transcriptome analysis of *C. jejuni* wildtype, Δ*truD*, C*truD* and D85N strains by RNA-seq

As TruD binds a small number of RNAs in *C. jejuni*, it is intriguing to determine the role of TruD in regulation of gene expression. To investigate potential changes in gene expression that might be dependent on the enzymatic activity of TruD, RNA-seq of *C. jejuni* wildtype, Δ*truD*, C*truD* strains and a catalytic inactive D85N strain was performed. Bacterial strains were grown in two replicates to OD_{600nm} of 0.5/0.6 for wildtype, C*truD*, and D85N strains and to OD_{600nm} of 0.4 for Δ*truD*. While the bacterial cells were collected at different OD_{600nm}, they belong to the same growth phase due to the growth defect of Δ*truD*. Afterwards, total RNA was extracted and the 23S and 16S rRNAs were depleted using the Ribo-zero kit (for bacteria, Illumina). cDNA libraries were generated by Vertis Biotechnologie and were mapped to the reference genome after sequencing. An overview

of the different RNA classes (transcripts, tRNAs, rRNAs, CDS, 5' UTRs, and sRNAs) in the sequenced strains is shown in Figure 4.3. While the reduction in the rRNAs classes in the Δ*truD* strain can probably be due to a different efficiency of the rRNA depletion step, the Δ*truD* strain, compared to the WT, C*truD*, and D85N show an increase in the sRNAs and transcripts categories.

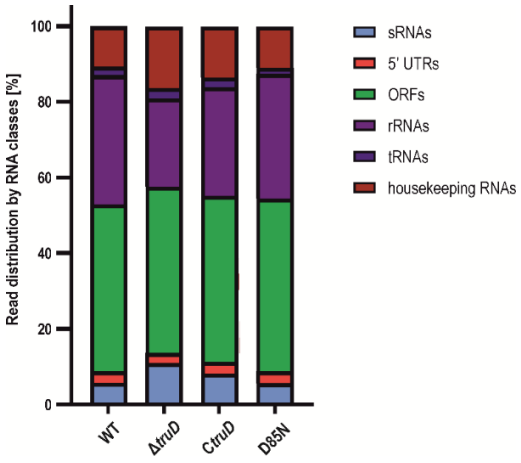

	WT	**Δ*truD***	**C*truD***	**D85N**
sRNAs	6%	11%	5%	6%
5' UTRs	3%	3%	3%	3%
ORFs	44%	44%	45%	46%
rRNAs	34%	23%	34%	33%
tRNAs	2%	3%	2%	2%
housekeeping RNAs	11%	16%	11%	11%

Figure 4.3: Read distribution for WT, Δ*truD*, C*truD*, and D85N RNA-seq. (*Upper panel*) Bars showing the read distribution of each RNA class (transcripts, tRNAs, rRNAs, CDS, 5' UTRs, and sRNAs) in the WT, Δ*truD*, C*truD*, and D85N libraries. *(Lower panel*) percentage of each RNA class for each WT, Δ*truD*, C*truD*, and D85N libraries.

Further, DeSeq2-analysis was performed to quantify differentially expressed genes between the strains. An RNA is considered upregulated (for example WT vs Δ*truD*) when the log2FC is greater or equal to 1.0 and with a p-value lower or equal to 0.05, and downregulated when the log2FC is lower or equal to -1.0 and with a p-value lower or equal to 0.05. Figures 4.4 A and B show Venn diagrams for upregulated and downregulated 5' UTRs and CDS in Δ*truD* versus WT (wildtype), C*truD*, and D85N strains. In particular, seventeen 5' UTRs and eight CDS are downregulated and eight 5' UTRs and one CDS are upregulated in Δ*truD* compared to WT, C*truD*, and D85N. In addition, the small RNA CJnc20 is downregulated and 6S RNA is upregulated in Δ*truD* compared to the other strains. Overall, the Δ*truD* strain showed differences in gene expression compared to the wildtype strain that were restored in both C*truD* and D85N suggesting that, for the majority

of the 5' UTRs and CDS, the effects were independent from the tRNA-modifying activity of TruD (Figure 4.4 A & B).

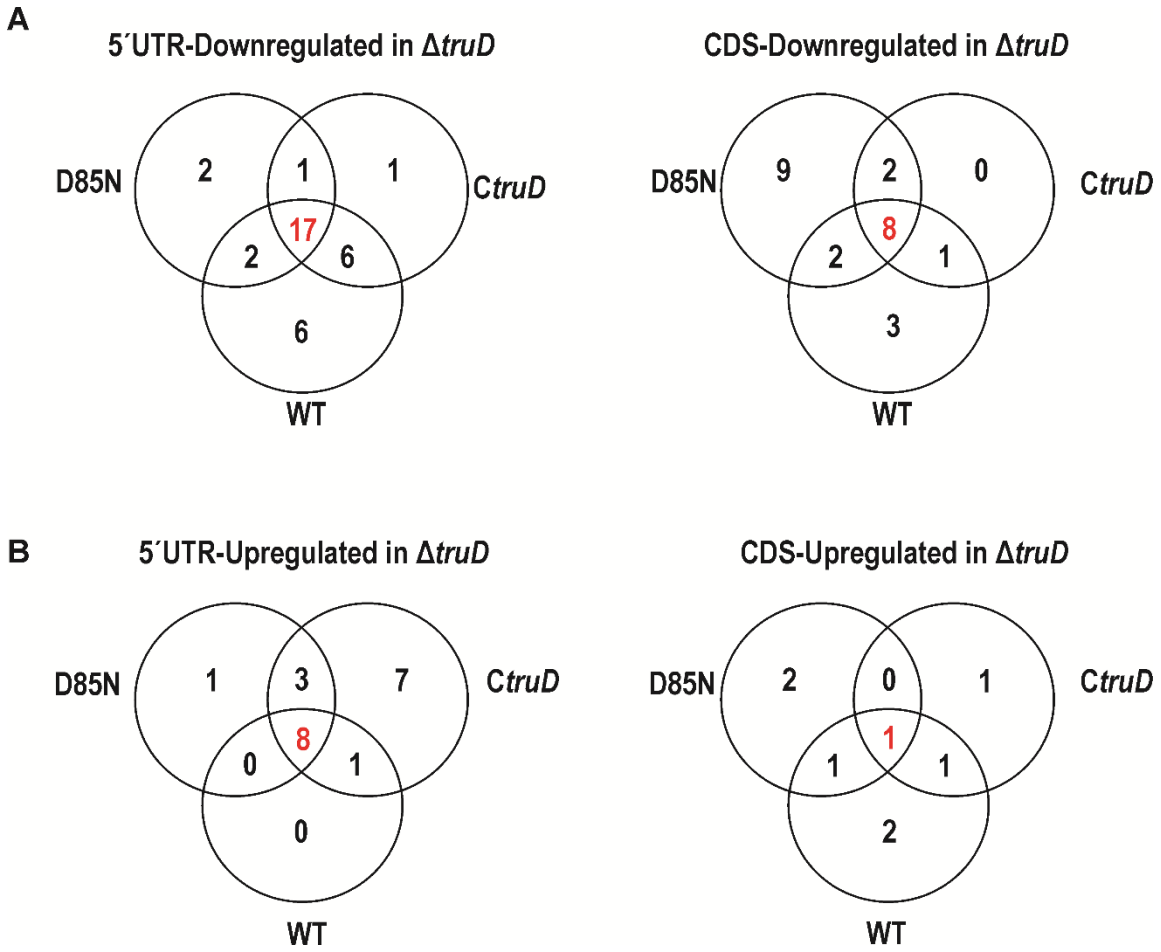

Figure 4.4: RNA-seq revealed changes in gene expression in Δ*truD* that were restored in C*truD* and D85N. (A) Venn diagram showing the overlap of 5'UTRs (left) and CDS (right) that are downregulated (log2FC≤1.0, p-value≤0.05) in different RNA-seq experiments. The number of 5'UTRs and CDS differentially expressed in *C. jejuni* wildtype, C*truD*, and D85N compared to the expression of Δ*truD* are shown. **(B)** Venn diagram showing the overlap of 5' UTRs (left) and CDS (right) that are upregulated (log2FC≥1.0, p-value≤0.05) in different RNA-seq experiments. The number of 5' UTRs and CDS differentially expressed in *C. jejuni* wildtype, C*truD*, and D85N compared to the expression of Δ*truD* are shown. The Venn diagrams were generated with VENNY 2.1 (https://bioinfogp.cnb.csic.es/tools/venny/).

Focusing on CDS, the eight genes that showed downregulation in Δ*truD* are: Cj0735, Cj1457c, Cj0449c, Cj0414, Cj0415, Cj0988c, Cj1500, and Cj1628. As expected, the Cj1457c gene that encodes TruD was downregulated in Δ*truD* compared to WT, C*truD*, and D85N strains. Furthermore, the 5' UTRs and the CDS of Cj0414 and the CDS of Cj0415 showed downregulation in Δ*truD* (Appendix Table 9, 11, and 14) Cj0735 showed downregulation in the Δ*truD* strain and encodes for a periplasmic protein of 239 amino acid and has been identified as a phase variable gene that contains homopolymeric simple sequence repeats (Saunders *et al.*, 1998; Salaün *et al.*,

2004). The CDS of *metE* (Cj1201) was found as the only gene to be upregulated in Δ*truD* compared to the other strains. *metE* encodes a N5-methyl-H4-folate:homocysteine methyltransferase that is involved in amino acid biosynthesis and has been suggested to be essential in *C. jejuni* (Stahl & Stintzi, 2011) (Figure 4.5). Furthermore, the RNA-seq analysis revealed that the tRNA fraction was not deregulated in Δ*truD* compared to the other strains. Interestingly, the tRNA-Glu, target of TruD, is not affected in its expression by the absence of TruD (Appendix Table 9, 11, and 14) indicating that *truD* is not involved in the regulation of transcription or stability of this tRNA.

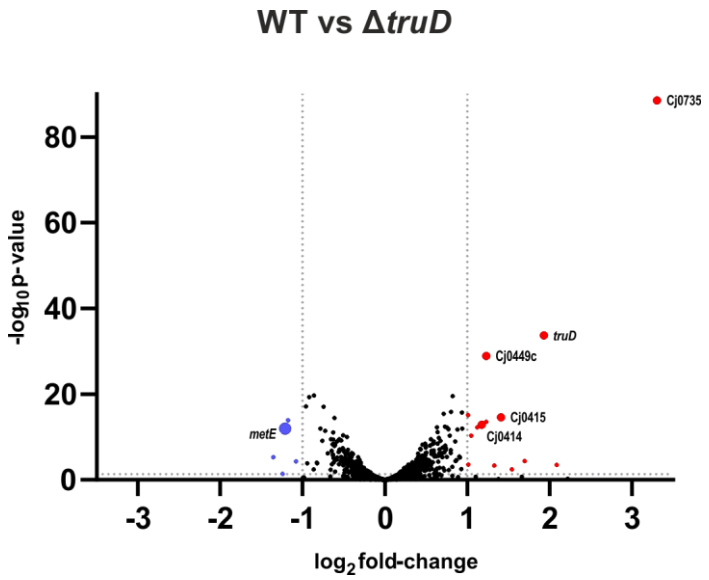

Figure 4.5: Differentially regulated targets in wildtype versus Δ*truD* RNA-seq dataset. A Volcano plot representation of the differentially regulated genes in *C. jejuni* wildtype vs. Δ*truD* (RNA-seq). The y axis shows the negative $\log_{10}$ of p-values and the x-axis shows the difference in expression (log2 fold changes). Red dots represent the genes with significantly different expression (p-value≤0.05) and $\log_2$ fold-changes ≥+1. Blue dots represent the genes with significantly different expression (p-value≤0.05) and $\log_2$ fold-changes ≤-1. Dashed grey lines represent the chosen cut-off for downregulated and upregulated genes, respectively. Big dots for *metE*, Cj0735, Cj0449c, *truD*, Cj0414, and Cj0415 are examples of downregulated and upregulated genes discussed in the text.

Overall, RNA-seq suggests that TruD might affect the steady-state of Cj0414 and Cj0415. Sequencing coverage reads of the RNA-seq experiments showed that the transcript levels of both Cj0414 and Cj0415 are less abundant in the Δ*truD* compared to wildtype, C*truD*, and D85N, supporting the DESeq2 analysis (Figure 4.6).

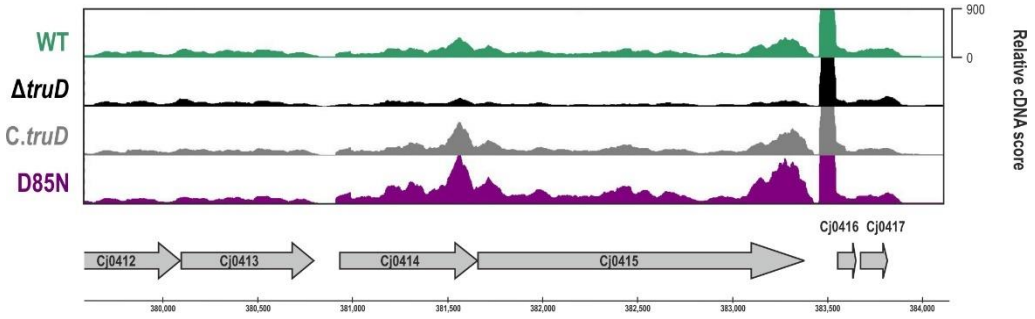

Figure 4.6: Potential RNA targets of TruD based on RNA-seq. cDNA reads from the RNA-seq analysis of the WT (wildtype; green), Δ*truD* (black), C*truD* (grey), and D85N (purple) libraries were mapped to the Cj0412-Cj0413-Cj0414-Cj0415-Cj0416-Cj0417 regions in the *C. jejuni* NCTC11168 genome. Grey arrows represent annotated ORFs. Numbers represents the genomic coordinates of the ORFs.

4.3. Validation of RNA-seq results using qRT-PCR

Among the genes that showed downregulation in Δ*truD* compared to wildtype, C*truD*, and D85N strains, expression of Cj0414 and Cj0415 in the different strains was validated by quantitative RT-PCR (qRT-PCR). The choice to validate only these two genes was based on the following criteria: 1) Cj0735 is a phase variable gene whose expression can stochastically change in the different strains (Pernitzsch *et al.*, 2014); 2) Cj0449c is annotated as a hypothetical protein, whose function and relevance in *C. jejuni* is still unknown; 3) based on the DESeq2 analysis, transcript levels of Cj0988c, Cj1500, and Cj1628 were identified to be not abundant in this experimental condition (based on the reads number, Appendix Table 9, 11, and 14).

Cj0414 and Cj0415 are already characterized in the related *C. jejuni* 81-176 strain, where they encode for orthologs of gluconate dehydrogenase enzyme (GADH) of *Pectobacterium cypripedii* (Pajaniappan *et al.*, 2008), suggesting that these genes are involved in the general metabolism of *C. jejuni*. In addition, strains with deletion of Cj0415 were shown to be defective in establishing colonization in chicks (Pajaniappan *et al.*, 2008). Taken together, analysis of the regulation of Cj0414 and Cj0415 operon could also link TruD with pathogenesis of *C. jejuni*.

To validate the RNA-seq results, qRT-PCR was performed on total RNA isolated from *C. jejuni* wildtype, Δ*truD*, C*truD*, and D85N using primers specific for Cj0414 and Cj0415 CDS; *gyrA* (that did not show deregulation in Δ*truD* in the RNA-seq experiment) was used as an internal negative control (Figure 4.7).

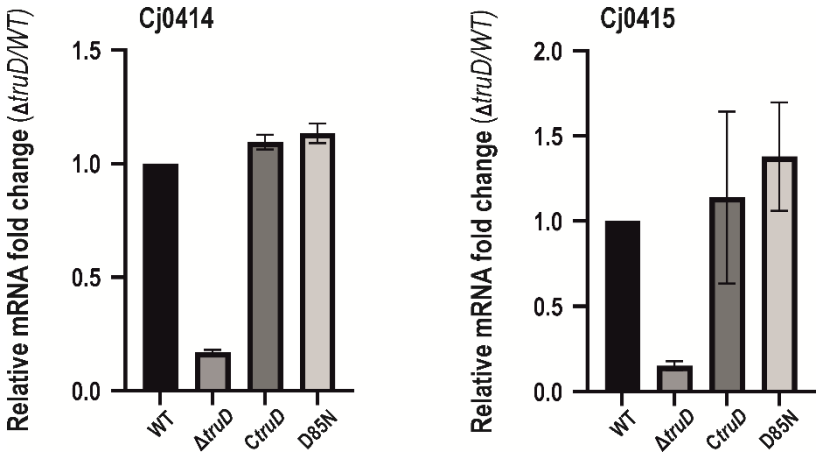

Figure 4.7: qRT-PCR result confirms downregulation of Cj0414 and Cj0415 in Δ*truD* vs. WT, C*truD*, and D85N. DNase *I* treated RNA samples isolated from WT, Δ*truD*, C*truD*, and D85N were used in one-step qRT-PCR reactions. WT mRNA levels were set to 1.0, and relative mRNA fold-changes in mutant strains compared to the WT are shown as bar graphs. Values are shown as mean ± standard deviation from two biological replicates.

The qRT-PCR experiment confirmed the RNA-seq analysis and validated the downregulation of both Cj0414 and Cj0415 in Δ*truD* compared to WT. Additionally, the mRNA expression level of both genes was restored in C*truD* and D85N, confirming that deletion of *truD* is involved in the regulation of the genes (Figure 4.7).

4.4. Deletion of the entire Cj0414_Cj0415 operon affects the growth of *C. jejuni* NCTC11168

Deletion of *truD* shows a severe growth defect in *C. jejuni*. To address whether this growth defect is directly linked to the deletion of one of its targets, independent deletions of Cj0414 and Cj0415 were generated and the growth of these deletion mutants was analysed over time. Neither Cj0414 nor Cj0415 deletions led to a growth defect of *C. jejuni* compared to the parental wild-type strain (Figure 4.8 A). Since in the Δ*truD* strain the entire Cj0414 and Cj0415 operon shows downregulation in the RNA-seq experiment, a deletion of the entire operon was generated. Growth curve analysis of the deletion of the entire operon (ΔΔCj0414/5) was analysed for two clones (ΔΔCj0414/5 1 and 2). Both clones showed a similar growth compared to the wildtype strain in the lag phase, but did exhibit a growth defect in the late exponential and stationary phase (Figure 4.8 B), suggesting an important role of the two proteins during the late growth phase of *C. jejuni*.

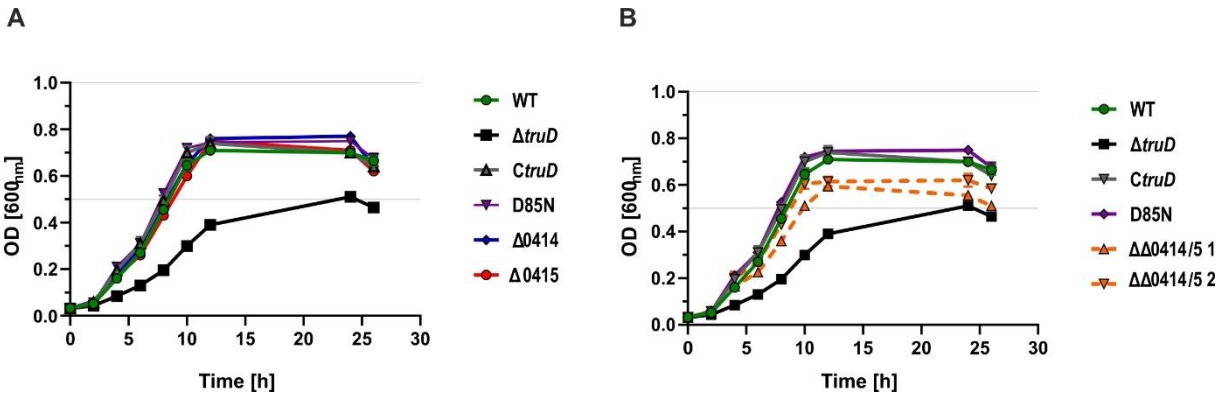

Figure 4.8: Deletion of Cj0414 or Cj0415 does not affect the growth of *C. jejuni*, whereas deletion of the entire operon affects the growth of the bacteria in late exponential/stationary phase. (A) Growth curve over 26 hours for *C. jejuni* wildtype, Δ*truD*, C*truD*, D85N, ΔCj0414, and ΔCj0415 grown in Brucella broth in biological duplicates. **(B)** Growth curve over 26 hours for *C. jejuni* wildtype, Δ*truD*, C*truD*, D85N, and two clones of ΔΔCj0414/5 (1&2) grown in Brucella broth in biological duplicates.

Furthermore, a deletion of *truD* in *C. jejuni* ΔΔCj0414/5 was generated and a growth curve analysis on the different strains was conducted. The assay showed that Δ*truD* in ΔΔCj0414/5 strain affected the growth of the bacteria behaving like a Δ*truD* strain for most of the growth of the strains, with a decrease in the growth for late stationary phase (Figure 4.9).

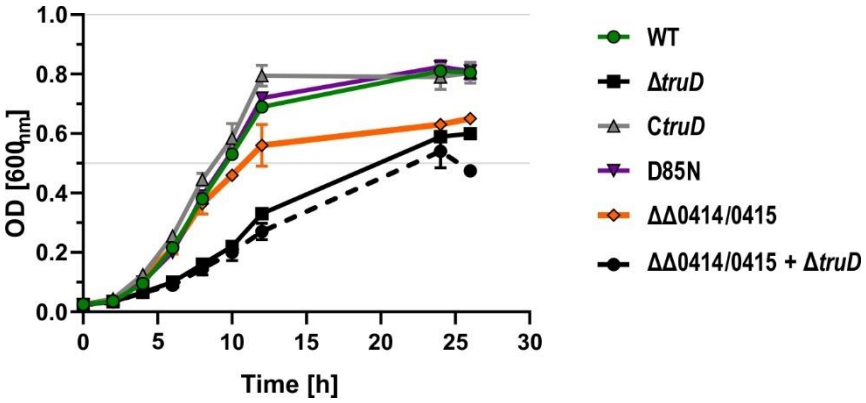

Figure 4.9: Deletion of *truD* in ΔΔCj0414/5 shows a slight decrease in the growth compared to Δ*truD*. Growth curve over 26 hours for *C. jejuni* wild-type, Δ*truD*, C*truD*, D85N, ΔΔCj0414/5, and ΔΔCj0414/5 + Δ*truD* grown in Brucella broth in biological duplicates.

Overall, the phenotype associated with the deletion of the entire ΔΔCj0414/5 operon could explain the growth defect of Δ*truD*. However, the "intermediate" growth defect (between wildtype and Δ*truD* levels) observed for ΔΔCj0414/5, suggested that additional factors might contribute to the observed growth defect of Δ*truD* (e.g. deregulation of other genes identified in the RNA-seq experiment).

4.5 TruD might regulate the Cj0414/Cj0415 operon at the post-transcriptional level.

To uncouple transcriptional and post-transcriptional regulation of Cj0414 and Cj0415 mediated by TruD, transcriptional reporter fusions were generated and introduced in the non-essential *rdxA* locus of *C. jejuni*. Based on published differential RNA-seq (dRNA-seq) of *C. jejuni* NCTC11168 (Dugar *et al.*, 2013), the promoter of Cj0414/Cj0415 (150 nt upstream and 6 nt downstream of the predicted primary TSS, excluding the RBS and depicted as purple rectangle in Figure 4.10 A) was fused to the 5´ UTR and the CDS of the DNA-binding gene *hupB* (Cj0913c) fused to super-folder GFP (sfGFP) (Figure 4.10 C). Unpublished RNA-seq data from our lab revealed that the transcript levels of Cj0414 and Cj0415 are induced and Cj1358c levels are repressed upon deletion of the transcriptional regulator Cj0883c (Alzheimer, Svensson, and Sharma unpublished). To investigate whether the promoter region used for the generation of the transcriptional fusion contained all the functional elements necessary for the expression of sfGFP, Cj0883c was deleted in strains expressing the reporter under the control of the promoter of Cj0414/5 or Cj1358c. Analysis of total protein extracts of the different strains showed that the deletion of Cj0883c (clones 1-4) led to an increase in the sfGFP level when the expression is driven by the promoter of Cj0414/5, supporting the role of Cj0883c in the post-transcriptional regulation of the Cj0414/5 operon (Figure 4.10 D, clones 1-4). Similar to the RNA-seq dataset, fusion of the promoter region of Cj1358c with *hupB-sfGFP* showed a decrease in the sfGFP level upon deletion of Cj0883c (Figure 4.10 D, clones 5 & 7). Next, *truD* was deleted in the strains that express the transcriptional reporter fusions and western blot analysis of whole protein lysates from Δ*truD* and their respective wild-type background was performed (Figure 4.10 E).

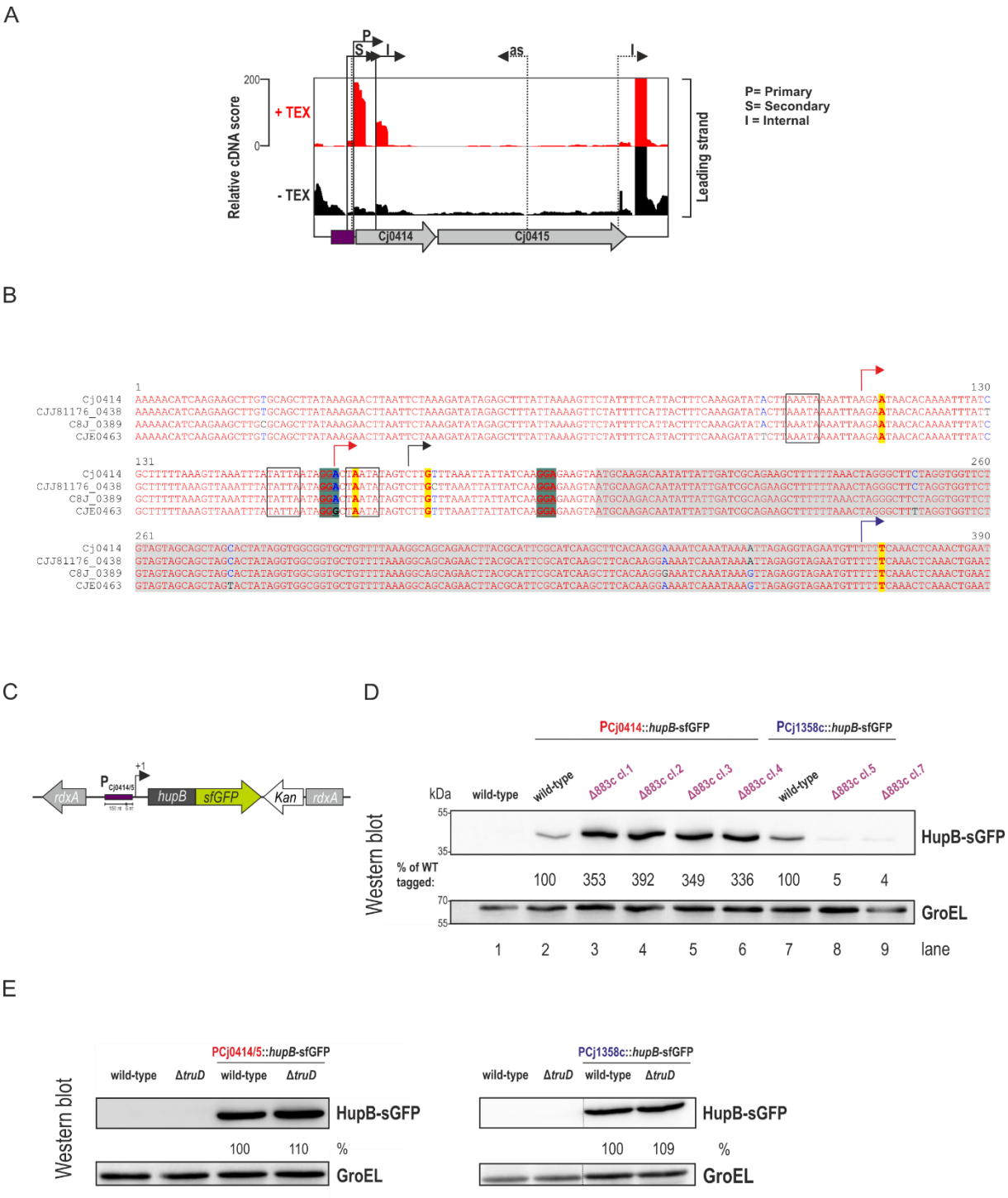

Figure 4.10: TruD might regulate the Cj0414/Cj0415 operon at the post-transcriptional level. (A) Screenshot of differential RNA-seq (dRNA-seq, +/− TEX treatment) reads mapped to the *C. jejuni* NCTC11168 genome in the Cj0414-Cj0415 region located in the leading strand. Black arrows indicate different types of promoter identified in the analysis (P=primary, S=secondary, as=antisense, I=internal). **(B)** nucleotide sequence alignment of promoter region of Cj0414 and Cj0415 in different *C. jejuni* strains. **(C)** Schematic representation of the transcriptional reporter fusion. Grey arrow represents the direction of the *rdxA* locus, white arrow represents the direction of the kanamycin resistance cassette, green arrow represents the direction of the sfGFP protein fused to the *hupB* 5´ UTR (purple) and the white rectangle is the promoter region of Cj0414 and Cj0415 (excluding the ribosome binding site) used for the transcriptional fusion. 150 nt and 6 nt represent the region upstream and downstream of the transcriptional

start site (TSS) used for this fusion. **(D)** Western blot analysis of P_{Cj0414} or $P_{Cj1358c}$::*hupB-sfGFP* transcriptional fusion analysed in the wildtype or ΔCj0883c background. The percentage is relative to the untagged wild-type control. The membrane is probed against the anti-GFP antibody and anti-GroEL is used as a loading control. **(E,** *left***)** Western blot analysis of P_{Cj0414} or **(E,** *right***)** PCj1358c::*hupB-sfGFP* transcriptional fusion in the wild-type or Δ*truD* background. The percentage is relative to the untagged wild-type control. The membrane is probed against the anti-GFP antibody and anti-GroEL is used as a loading control.

Western blot analysis showed that the level of sfGFP was not affected by the deletion of *truD* (Figure 4.10 E), indicating that TruD might regulate the expression of Cj0414 and Cj0415 on the post-transcriptional level.

4.6. TruD might stabilize Cj0414 and Cj0415 expression at the transcript level, but not significantly at the protein level.

To test whether Cj0414 and Cj0415 are downregulated at the protein level, a 3xFLAG epitope tag was fused to the C-terminal of the coding sequence of Cj0414 and Cj0415 and tagged proteins were analysed in the wildtype and in the Δ*truD* background (Figure 4.11) by western blot. While the expression of Cj0414 and Cj0415 was downregulated at the transcript level (Figure 4.7), the protein levels of Cj0414-3xFLAG and Cj0415-3xFLAG were only mildly affected by the deletion of *truD*. In particular, a different trend of regulation was observed when comparing the transcript and the protein levels: a slight upregulation can be observed when comparing the Cj0414-3xFLAG and Cj0415-3xFLAG in the Δ*truD* background compared to the parental strain. A polar effect due to the presence of the 3xFLAG at the C-terminus of Cj0415 can be excluded, since a qRT-PCR was performed to check the transcript of Cj0415-3xFLAG in the wildtype and Δ*truD* cells and confirmed downregulation of Cj0415-3xFLAG in Δ*truD* strain (data not shown).

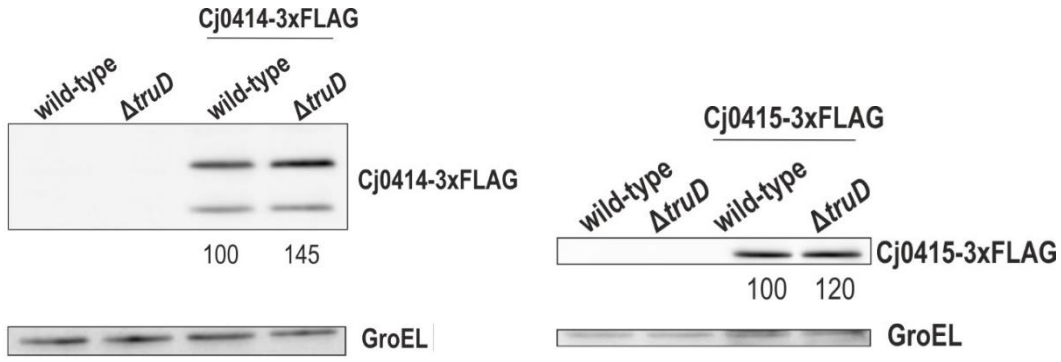

Figure 4.11: TruD might stabilize Cj0414 and Cj0415 expression at the transcript level, but not significantly at the protein level. *(left)* Western blot analysis of *C. jejuni* wildtype, Δ*truD*, wildtype + Cj0414-3xFLAG and Δ*truD* + Cj0414-3xFLAG or *(right) C. jejuni* wildtype, Δ*truD*, wild-type + Cj0415-3xFLAG and Δ*truD* + Cj0415-3xFLAG strains grown to exponential growth phase. Protein samples corresponding to

an OD600 of 0.1 were loaded on a 12 % SDS-PAA gel, blotted to PVDF membrane and FLAG- tagged proteins were detected with an anti-FLAG antibody (1:1,000). GroEL served as a loading control.

Overall, these results showed that the regulation at the RNA level of Cj0414 and Cj0415 is indirectly mediated by TruD. However, differences in regulation of Cj0414 and Cj0415 at the RNA and protein level still remain unclear.

4.7. Ribo-seq reveals translational changes in Δ*truD* compared to wildtype and complementation strains

To identify a potential correlation between the RNA targetome of TruD, analysed by RIP-seq, and changes in gene expression due to the lack of TruD in the cell, a comparison of the RNAs that showed an enrichment in the TruD-3xFLAG versus WT coIPs (Appendix Table 7) and RNAs that showed deregulation in the RNA-seq of Δ*truD* versus WT, C*truD*, and D85N strains was performed. The comparison showed that none of the TruD targets reported in the RIP-seq dataset overlapped with the RNA-seq experiment (data not shown), suggesting that the deregulation observed in the RNA-seq experiment in the *truD* deletion strain is indirect due to the absence of the protein. However, TruD could act as a translational regulator. To investigate changes in the translational efficiency of *C. jejuni* genes, directly or indirectly affected by the deletion of TruD, a global translatome analysis using Ribo-seq was performed in *C. jejuni* wildtype, Δ*truD*, and complemented *truD* strains. Figure 4.12 shows the major steps of the protocol. Briefly, the strains were grown to exponential phase and cells were treated with chloramphenicol to arrest translation. Bacterial cells were lysed and the RNA was digested with micrococcal nuclease (MNase) to obtain monosomes. In addition, as a control, undigested lysate was loaded in parallel onto a 10-55% sucrose gradient followed by ultracentrifugation. The ultracentrifugation step allows to separate the cellular complexes among the different fractions of the sucrose gradient based on their density from the low molecular fractions to the heavy molecular fractions. Polysome profiles of *C. jejuni* wildtype, Δ*truD*, and complemented *truD* strains are shown in Figure 4.13.

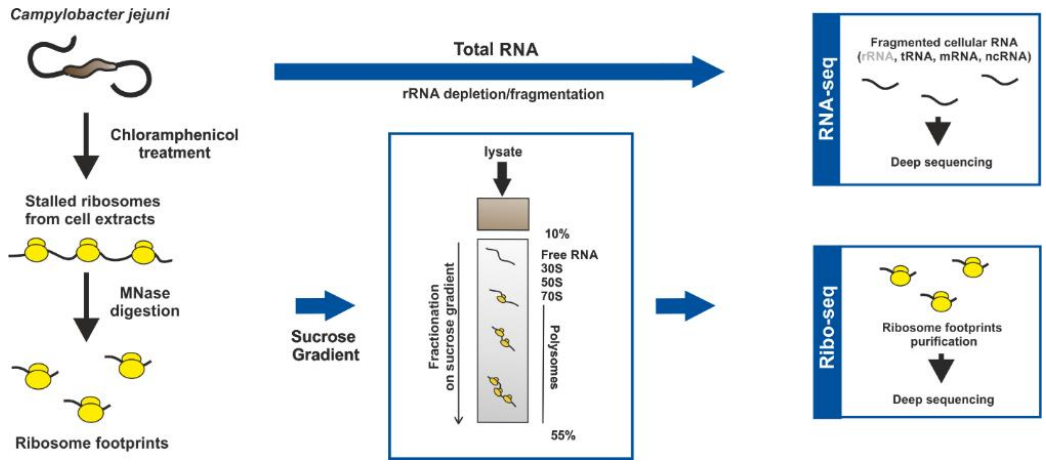

Figure 4.12: Schematic of the ribosome profiling protocol in *C. jejuni*. The scheme depicts the different steps during the Ribo-seq experiment in *C. jejuni*: after lysis, the polysome fraction is digested by MNase and the lysate is loaded onto a 10-55% sucrose gradient, the monosome fraction is extracted and ribosome footprints are used to generate cDNA libraries together with total RNA.

When comparing polysome profiles of Δ*truD* to wildtype and C*truD* strains, a reduction in the 50S peak and a lower number of polysomes were observed, suggestive of lower level of global translation

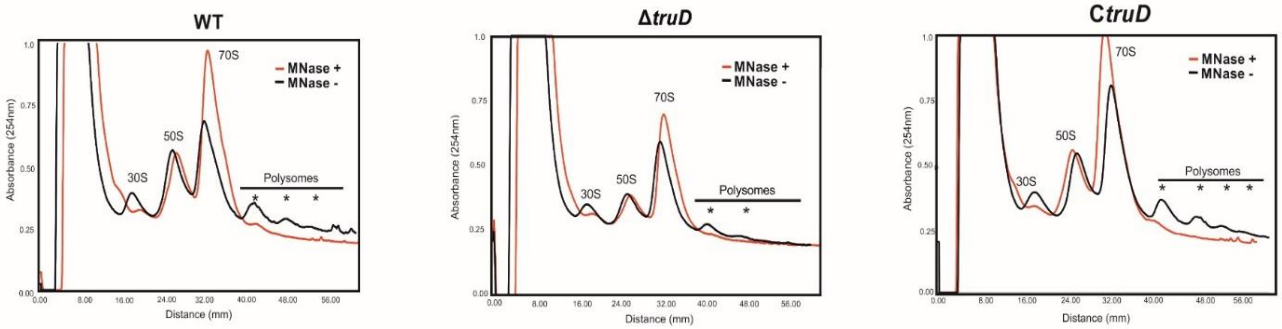

Figure 4.13: Polysome profile of *C. jejuni* WT, Δ*truD*, and C*truD*. Polysome profile plot for *C. jejuni* WT (left), Δ*truD* (middle), and C*truD* (right) strains based on absorbance (Abs 254nm) profile of sucrose gradient over the sedimentation (mm). Black graphs indicate absence of MNase treatment (MNase-) and red graphs indicate the treatment with MNase prior to sequencing (MNase-).

To investigate which mRNAs are differentially translated in the Δ*truD* versus wildtype and C*truD* strains, 70S ribosome footprints and total RNA samples were purified and converted to cDNA libraries and sequenced. The translational efficiency (TE) was calculated using HRIBO (Gelhausen *et al.*, 2021). A mRNA is considered less translated in one condition/strain when the TE is ≤-1.0 or more translated when the TE is ≥+1.0.

The analysis revealed that deletion of *truD* leads to a decrease in the TE of eight genes: Cj0011c, Cj0168c, Cj0170, Cj0266c, Cj0370, Cj0492, Cj0616, and Cj0648. Interestingly, two out of the eight

genes encode for ribosomal proteins, specifically Cj0370 encodes for the 70 amino acid 30S ribosomal subunit S21 (or RpsU) and Cj0492 encodes the 156 amino acid 30S ribosomal subunit S7 or (RpsG). In *E. coli*, RpsU has been shown to be one of the last ribosomal proteins to associate with the ribosome during its assembly. Thus, the polysome defect observed in Δ*truD* compared to wildtype and C*truD* (Figure 4.13) might be linked to the decrease in the TE of the two ribosomal proteins RpsU and RpsG.

4.8. CLIP-seq identifies the 5´ UTR of *rpsU* as a potential target of TruD

It has been suggested that the binding of tRNAs by PUS enzymes might be a transient process in the cell (Rintala-Dempsey & Kothe, 2017). For this reason, a CLIP-seq approach that covalently stabilizes the interactions between the TruD protein and RNA targets by UV crosslinking (254nm) was performed. The CLIP-seq technique was established in *S.* Typhimurium to identify the targets of the RNA binding proteins (RBPs) Hfq, CsrA, and ProQ and lately applied to other RBPs of Gram-negative and positive bacteria (Holmqvist *et al.*, 2016, 2018; Hör *et al.*, 2020a; Basu & Altuvia, 2021). However, this method was never applied to RBPs of *C. jejuni* (e.g., CsrA or Cas9) (Dugar *et al.*, 2016, 2018). To identify the RNA targetome of TruD in *C. jejuni* using CLIP-seq, strains expressing *truD-3xFLAG* (TruD-3xFLAG) in its native locus, C*truD3xFLAG* (C*truD*), and *D85N3xFLAG* (D85N) were used. As a control, the non-crosslinked culture was used to identify unspecific peaks. Thus, *C. jejuni* strains were cultured in rich media to an OD_{600nm} 0.5-0.6. For each strain, 50 ml of culture were irradiated with UV light (crosslinked sample), while 50 ml of culture were left untreated (non-crosslinked culture). After mechanical lysis, the lysate was incubated with anti-FLAG magnetic beads, followed by on-bead benzonase treatment, dephosphorylation, and radioactive labeling of the 5´ end of bound RNAs. The TruD-RNA complexes were eluted, separated by SDS-PAGE and transferred to nitrocellulose membrane. Figure 4.14 shows that the radioactive signal was detected only in the crosslinked samples compared to the non-crosslinked controls, highlighting the ability of the protein to bind RNA (Figure 4.14, lanes 2, 4, and 6 vs. lanes 1, 3, and 5). Moreover, a stronger intensity was detected in C*truD* and D85N crosslinked sample compared to $TruD^{3F}$ crosslinked sample (lanes 4 and 6 vs. lane 2). Differences in the intensity could reflect a different expression of the TruD protein in the *rdxA* locus versus its native locus (data not shown). TruD-RNA complexes from crosslinked and untreated samples were extracted from the membrane by proteinase K treatment. The purified RNA was used to generate cDNA libraries using the NEB small RNA kit for further analysis by Illumina sequencing.

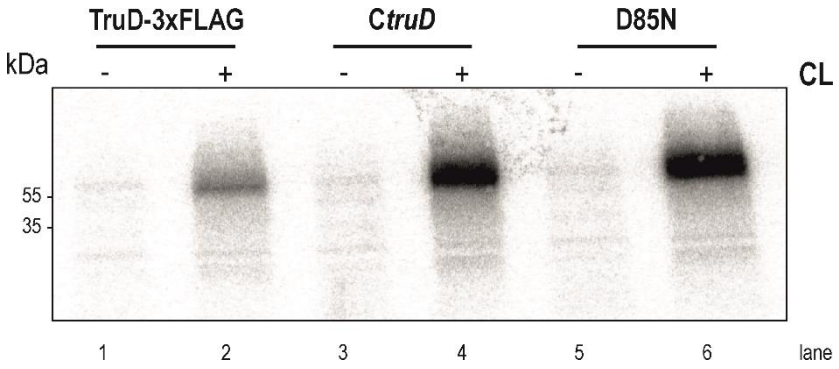

Figure 4.14: Autoradiograph of crosslinked RNAs bound by TruD. TruD-RNA complexes were run on an SDS-page gel and radioactive signal derived from the labeled RNAs is observed in the crosslink (+) samples (lanes 2, 4, and 6) compared to the non-crosslinked (-) samples (1, 3, and 5).

After mapping the reads to the reference genome, enriched reads in the crosslinked versus the non-crosslinked libraries were investigated. Firstly, Cjp03, the known TruD target, was checked in the different libraries. Figure 4.15 A shows an IGB screenshot of Cjp03 region in the different libraries. While for TruD-3xFLAG and C*truD* a slight enrichment was identified in the crosslinked versus the non-crosslinked libraries, in the D85N strain a stronger enrichment in the crosslinked library was observed, suggesting that the catalytically inactive enzyme can still bind its target, but since it is not able to modify it, it might not be able to release it within the cell. Surprisingly, among the RNAs that have been shown to be crosslinked to TruD, the 5´ UTR of the *rpsU* transcript was observed to be enriched in the crosslinked libraries from all strains.

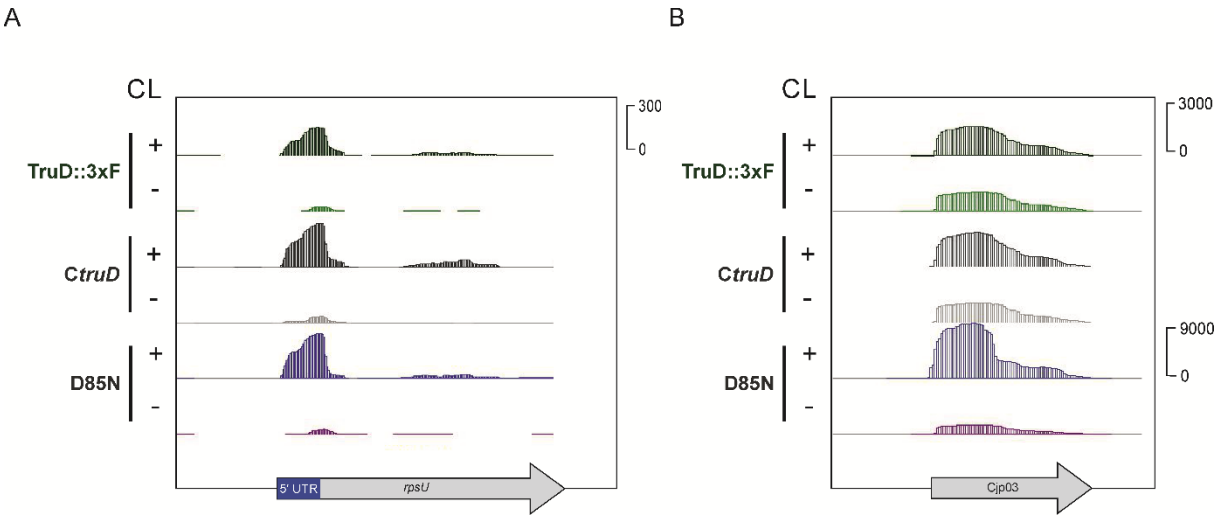

Figure 4.15. Screenshot of examples of RNAs bound by TruD-3xFLAG, C*truD*, and D85N. cDNA reads from the CLIP-seq analysis of the TruD-3xFLAG, CtruD, and D85N strains were mapped to the tRNA-Glu (Cjp03, B) and Cj0370 (*rpsU*, A) in the *C. jejuni* NCTC11168 genome. Grey arrows represent the annotated tRNAs and ORF, respectively.

4.9. Deletion of *truD* is not the cause of a lower translational rate of *rpsU*

Based on the Ribo-seq experiment, *rpsU* was found to be less translated in the Δ*truD* versus WT and C*truD* strains. Moreover, preliminary CLIP-seq results showed a potential interaction between TruD and the 5´ UTR of *rpsU* (Figure 4.15 A). In order to confirm the lower translational rate of *rpsU* in the Δ*truD* strain, FLAG- or HA-tagged versions of RpsU were generated. However, mutations in both HA or FLAG tag indicated that manipulation of the C-terminus of RpsU might affect the function of the ribosomal protein and thereby be lethal for the cell. For this reason, a translational fusion was generated. The construct is introduced into the *rdxA* locus of *C. jejuni* and includes the 5´ UTR and the first ten codons of *rpsU* driven by the promoter of the *metK* gene and fused to the nucleotide sequence of sfGFP. Investigation of the sfGFP level by western blot in the wildtype and in the Δ*truD* strains showed that deletion of *truD* does not affect the reporter levels (Figure 4.16, lanes 3 and 4), indicating that deletion of *truD* is not responsible for the decrease in the translational level of *rpsU*.

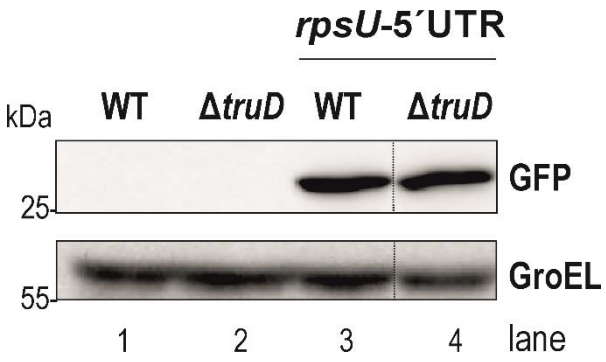

Figure 4.16: Deletion of truD is not responsible for decreased translation of *rpsU*. Western blot analysis of *C. jejuni* wildtype, Δ*truD*, P_{metK}-5´ UTR *rpsU*-sfGFP in the wildtype and in the Δ*truD* background (lanes 3 and 4) grown to exponential phase. Protein samples corresponding to an OD_{600nm} of 0.1 were loaded on a 12 % SDS-PAA gel, blotted to a nitrocellulose membrane and sfGFP level detected with an anti-GFP antibody (1:1,000). GroEL served as a loading control.

5. Discussion

Methods to globally identify pseudouridine in a bacterial transcriptome

Among the different types of RNA modification, pseudouridine is widely distributed in the different classes of RNA, including eukaryotic mRNAs and long non-coding RNAs (lncRNAs). Identification of this modification in low abundant RNA species (e.g., mRNAs and lncRNAs) is possible due to the depletion of abundant RNA species (e.g., rRNAs) from the total RNA pool before cDNA library preparation. It is not surprising that most of the methods used for the identification of RNA modifications are established in eukaryotes. Polyadenylation of the 3´ end of the RNA (poly-(A) tail) is a particular characteristic of eukaryotic mRNAs and long non-coding RNAs and a poly-(A) enrichment step is typically applied during cDNA library preparation for RNA-seq based approaches. Thus, modifications can also be identified in RNAs that are usually underrepresented in the cell. So far, the identification of pseudouridine on a global scale was never performed in a bacterial transcriptome. Only recently, depletion of rRNAs was introduced as a separate step prior to library preparation and sequencing in certain protocols. One of the first examples of bacterial rRNA depletion before deep-sequencing is the dual RNA-seq protocol for simultaneous identification of gene expression changes of pathogen and eukaryotic host cells during infection (Westermann *et al.*, 2016). This allowed the discovery of lowly abundant bacterial RNA species such as small non-coding RNAs during the infection of human host cells by *Salmonella* Typhimurium. To assess coverage of translated mRNAs in Ribosome profiling (Ribo-seq) experiments, an mRNA enrichment step is usually applied to bacterial RNA-seq libraries. Therefore, an rRNA depletion step is also necessary for the investigation of pseudouridine beyond stable and abundant RNAs (e.g., rRNAs and tRNAs).

Besides the identification of the modified nucleotide in RNAs, another important point is the identification of specific pseudouridine synthases responsible for the modification. It has been observed that mutations in the pseudouridine synthases are associated with the development of human diseases. This is the case of missense mutations in the pseudouridine proteins Pus1 and DKC1 responsible for mitochondrial myopathy/sideroblastic anaemia and X-linked dyskeratosis congenita, respectively (Heiss *et al.*, 1998; Bykhovskaya *et al.*, 2004). Due to the importance of pseudouridine and PUS enzymes in human pathology, the scientific community started to focus on the functional roles of these proteins. In the bacterial model organism *E. coli*, tRNA PUS enzymes are not essential for the growth of the bacteria in standard conditions. However, it has been shown that the TruB, a tRNA-modifying PUS enzymes, has an additional function in the cell. In an *in vitro* study, the author showed that TruB is able to fold the tRNA-Phe independently of its enzymatic activity, thus acting as a tRNA chaperone (Keffer-Wilkes *et al.*, 2016). This reveals a new role of the enzyme in bacterial physiology.

Taken together, the optimization of the protocol for the identification of the pseudouridine in bacteria and the identification of a proper bacterial model organism aimed to address two understudied questions: (1) Can pseudouridine be detected and mapped in a genome-wide manner in bacteria? (2) Do bacterial PUS enzymes take on moonlighting functions in the cell beyond their RNA-modifying activity?

The first part of this thesis describes a first global mapping of pseudouridine in bacterial transcriptomes using a Pseudo-seq approach that was already applied to diverse eukaryotes (Carlile *et al.*, 2014; Schwartz *et al.*, 2014; Rajan *et al.*, 2019). A lower number of tRNAs can be beneficial for the Pseudo-seq approach that is based on a deep sequencing technology. For instance, tRNAs that are present in the genome as multi-copy genes have similar/identical sequences and can be discarded during the mapping of the reads to the reference genome, thus, generating missing information about the modification in that specific tRNAs. Moreover, the selection of a bacterial model organism with low numbers of PUSs is helpful in case of genetic and functional redundancy of these enzymes. So far, in the literature, there are no examples of different PUS enzymes that modify the same site, but it is still possible that enzymes with the same function might compensate the absence of others.

A first global Pseudo-seq approach was applied on total RNA of the foodborne pathogen *Campylobacter jejuni*. This analysis revealed the presence of pseudouridine in stable tRNAs and rRNAs providing a first global snapshot of this RNA modification in bacteria. The analysis revealed the presence of modifications in predicted positions of tRNAs and rRNAs, suggesting that CMC treatment of rRNAs and tRNAs was effective and therefore the protocol can be used for identification of pseudouridine with high confidence.

Pseudo-seq of wildtype and PUS deletion mutant strains allowed to identify pseudouridylated rRNAs and tRNAs in *H. pylori* and *C. jejuni* and linked them to specific tRNA PUS enzymes. In the presented study, Pseudo-seq confirms pseudouridine modification at position 55 in tRNAs of *C. jejuni*, but no modification at this position in *H. pylori*. This result was additionally validated by independent CMC treatment followed by primer extension analysis. Overall, this result is quite intriguing since most of the organisms carry such a modification at position 55 in tRNAs and modification at this position is universally conserved and described so far in all domains of life. The enzymes responsible for the generation of this modification in bacteria and eukaryotes are members of the TruB/Pus4/Cfb5 family, and recently also Pus10 was identified to be responsible for the modification at this position in tRNAs in archaea (Nurse *et al.*, 1995; Becker *et al.*, 1997a, 1997b; Tatusov *et al.*, 2003). In the thermophile archaeon *Thermus thermophilus*, disruption of *truB* causes a severe growth defect at 50 °C. Thus, it seems to be necessary for low temperature adaptation (Ishida *et al.*, 2011). To the best of my knowledge, *H. pylori* and *M. genitalium*, and *M. pneumonia*e are the only bacteria known so far that lack this modification (Gutgsell *et al.*, 2000).

It is possible that specific growth conditions of those bacteria do not require the modification at position 55 in tRNAs. This result is also in line with the absence of the corresponding TruB enzyme in their bacterial genome. Future experiments will be necessary to explore the reason for the lack of the modification at this almost universally conserved position.

Additionally, this study showed that TruA of *C. jejuni* and *H. pylori* share common tRNA targets: for example, they both show that TruA modifies position 39/40 of tRNA-Leu. Moreover, in both bacteria, TruD modifies tRNA-Glu at position 13. While *C. jejuni* encodes only one copy of the tRNA-Glu (Cjp03), *H. pylori* codes for two copies (Hpt01 and Hpt04). Modification of tRNA-Glu at position 13 mediated by TruD was already detected in *E. coli*, but no function for this particular nucleotide in that specific position was addressed.

It is worth to note that Ψ sites were identified in noncanonical position, e.g. positions 33, 36, 52 in the Pseudo-seq analysis of *C. jejuni*. There are possible explanations for this result: either these sites are false positive since their enrichment in the CMC + over the CMC - libraries are not as strong for canonical tRNAs sites (positions 13, 38-40, 55), or it is still possible that in other conditions (e.g. stress response) these sites are generated in *C. jejuni* tRNAs. Sites at position 31 have been detected in cytoplasmic tRNAs in *S. cerevisiae*, where Pus6p has been identified as the enzyme responsible for the modification (Ansmant et al. 2001). However, neither *C. jejuni* or *H. pylori* encode for the orthologs of this protein. It remains unclear whether other proteins might be involved in this modification (e.g., rRNA PUS or uncharacterized protein).

Additionally, Pseudo-seq revealed modification in various mRNAs in *C. jejuni*. While these sites could not be assigned to any of the tRNA PUS enzymes involved in the Pseudo-seq analysis (exept the 5' UTR of *purD*), it is possible that they are modified by other pseudouridine synthases or might be redundantly targeted by multiple PUS enzymes forming a protein-complex. A similar result was also observed in a global Pseudo-seq analysis performed in yeast and human cells (Carlile *et al.*, 2014; Schwartz *et al.*, 2014).

Similar to the majority of deep-sequencing technologies, Pseudo-seq has limitations related to the generation of cDNA libraries. The strategy for cDNA library preparation is important for the successful outcome of the experiment. Because of the stop of the reverse transcriptase during reverse transcription in the presence of Ψ-CMC, a simultaneous ligation of adaptors to 5′ and 3′ end of the RNA is not recommended. This will automatically exclude the synthesis of the adaptor at the 5′ in the cDNA and compromise the sequencing run. In addition, in the case of Pseudo-seq, both low- and high-throughput methods rely on the CMC chemical treatment. It has already been observed that the treatment has some limitations: the CMC treatment and the CMC reversion are performed at 37°C for 40 minutes and 4 hours, respectively. The temperature might promote the degradation of unstable mRNAs and sRNAs in particular in bacteria, since it is well known that prokaryotic transcripts are less stable compared to eukaryotic RNAs (Richards *et al.*, 2008). Thus,

many modified mRNAs and sRNAs could have been degraded during CMC treatment and would thereby not be detected during the analysis. For these reasons, alternative methods for the identification of pseudouridine have been recently developed and optimized.

One method that has recently been used to identify pseudouridine in human transcripts is based on an enrichment step of modified targets before sequencing: the CMC molecule is additionally modified by CLICK chemistry and carries a biotin molecule (Li *et al.*, 2015). The CMC will then bind to pseudouridine and the biotinylated RNAs will be pulled down using streptavidin beads. This method allowed to identify a higher number of modifications compared to Pseudo-seq/Ψ-seq in eukaryotic mRNAs and non-coding RNA. Unfortunately, the method was never performed in bacteria. Another approach that could be used to enrich for potentially modified RNA targets, could make use of the anti-pseudouridine-antibody. As shown in figure 2.20, a preliminary experiment to pull-down RNAs containing pseudouridine was performed using commercially available antibody against pseudouridine While the western blot analysis showed the effective pull-down of antibody across the different steps of the experiment, northern blot analysis of purified RNAs did not show differences in the band corresponding to modified tRNAs in the Δ*truABD* deletion background compared to the wild-type coIP samples. There are different explanations about the lack of enrichment of modified tRNAs in the wildtype coIP samples: a) The antibody against pseudouridine might not work for a coIP experiment, but only for other biochemical assays (e.g., ELISA, immunocytochemistry, and immunohistochemistry); b) It is possible that the antibody against pseudouridine is not specific only for this modification and by cross-reacting with other modifications it pulls down other modified RNAs. Similar observations have been made previously where antibodies binding modified nucleotides showed low specificity (Weichmann *et al.*, 2020) and could cross-react with other modifications (Mishima *et al.*, 2015); c) Buffers and conditions used in our coIP experiment need to be optimized to efficiently pull down modified RNAs. In a recent paper for example, the authors incubated the purified RNAs directly with the antibodies and UV-crosslinked them (Weichmann *et al.*, 2020). Newly optimized pseudouridine antibodies for RNA-coIP experiments are only recently available (Weichmann *et al.*, 2020), therefore it will be possible to compare the Pseudo-seq results with coIP experiments.

As an additional alternative, a method called HydraPsiSeq was recently developed to identify the modification in yeast and human rRNAs and yeast mRNAs (Marchand *et al.*, 2020). The technique relies on the protection of pseudouridine from hydrazine/aniline cleavage followed by deep-sequencing (Peattie, 1979) and offers a precise quantitative information about pseudouridine localization compared to previous methods. Moreover, since this method does not rely on the identification of pseudouridine localization after CMC binding, it will avoid all the “harsh” treatment (e.g., long incubation at 37°C) of CMC labeling and reversion.

Recently, the first tRNA map of pseudouridine modifications in the Gram-positive *Bacillus subtilis* was performed (de Crécy-Lagard *et al.*, 2020). In this paper, the authors identified the modification in the tRNA-enriched fraction of *B. subtilis* RNAs without a global overview of pseudouridine in other RNAs (e.g, mRNAs and sRNAs), thus the presence of modified mRNAs in other bacterial species remains still unknown.

Another important step after Pseudo-seq is the validation of the RNA targets. CMC treatment followed by primer extension using RNA extracted from wildtype and PUS deletion strains is the typical method to validate the pseudouridine position and the enzyme responsible for the modification. *In-vitro* validation using recombinant purified protein and *in-vitro* transcribed RNAs can be additionally performed. However, this is also based on CMC treatment followed by primer extension. One of the disadvantages of the RT-based method is that it can be used only for abundant RNA species such as tRNAs and rRNAs, but it cannot consistently validate modifications in mRNAs (Zhang *et al.*, 2019).

Recently, several groups developed different assays to validate pseudouridine identified in sequencing data. One of them is CLAP (CMC-RT and ligation assisted PCR analysis), a RT-PCR method that allows to quantitatively identify pseudouridine in eukaryotic mRNAs and lncRNAs. The assay relies on CMC labeling followed by site-specific ligation and PCR that generates two distinct product populations corresponding to the modified and unmodified substrates, respectively (Zhang *et al.*, 2019). Another method is based on CMC labeling of RNAs that generate deletion or mutation of the corresponding site in the cDNAs and, therefore leading to different melting temperatures during qPCR (Lei & Yi, 2017). While these assays are applied to eukaryotic rRNAs, mRNAs, and lncRNAs species, validation of modification in bacterial mRNAs using those methods is still lacking.

Exploring the function of tRNA PUS enzymes in C. jejuni.

Besides their role as RNA modifying enzymes, tRNA pseudouridine synthases function is overall unexplored, especially in bacteria. Moreover, this study aimed to identify the RNA substrates of different tRNA PUS enzymes in both *C. jejuni* and *H. pylori*. The first step to characterize tRNA PUS enzymes is the generation of deletion of strains for each PUS enzyme. Interestingly, growth curve analysis of PUS deletion strains in *C. jejuni* showed that while deletion of *truA* led to faster growth of the bacteria, *truD* deletion caused a strong defect in the growth. It is worth to note that in *E. coli* the deletion of the tRNA PUS enzymes does not affect the growth of the bacteria in standard laboratory conditions (Gutgsell *et al.*, 2000). This aspect highlights the potentially different functions of the enzymes in the different bacterial species with respect to their physiological niches. Due to the differences in bacterial genomes size, it is possible that some enzymes in bacteria with smaller genomes such as *C. jejuni* or *H. pylori* have to take on moonlighting functions

in addition to their primary activity. Only recently, it has been shown that deletion of *truA* in *Pseudomonas putida* and *Pseudomonas aeruginosa* leads to an increase in the mutation frequency potentially affecting translational fidelity (Tagel *et al.*, 2020). While deletion of *truA* in this study did not impact the growth of the bacteria, it opens up the possibility of additional functions of this particular PUS enzyme beyond its RNA-modifying activity.

Contrary to *H. pylori*, deletion of *truD* in *C. jejuni* causes a severe growth defect. So far, this phenotype has never been observed in bacteria for the deletion of the enzyme responsible for the modification of tRNA-Glu. In *E. coli,* TruD is also responsible for this modification and it has been shown that deletion of the gene does not cause any growth defect in rich or minimal media (Kaya & Ofengand, 2003a). Interestingly, other bacteria like *B. subtilis* and *M. pneumoniae* do not encode a TruD homolog. Sequence analysis of the tRNA-Glu in both organisms at position 13 shows that the U13 is replced by a C13 or G13 that base-paired with a G24 in *B. subtilis* and a C26 in *M. pneumoniae*, respectively. Bacteria that have lost TruD also often do not conserve the U13 in their tRNA-Glu, suggesting that this modification might not be essential during standard growth conditions. In contrast to previous examples, *Chlamydia avium* or *Bacteroides thetaiotaomicron* do not encode a homolog of TruD, but nevertheless conserve a uridine at position 13 of their tRNA-Glu. It is worth to note that in eukaryotes, TruD might have a broader function than in prokaryotes, potentially evolved to be involved in different functions or have different substrates. In eukaryotes, in particular in *Saccharomyces cerevisiae,* Pseudo-seq revealed that Pus7, the eukaryotic TruD homolog, modifies different RNA species: snoRNAs, tRNAs, rRNAs, and mRNAs (Behm-Ansmant *et al.*, 2003; Ma *et al.*, 2003; Decatur & Schnare, 2008; Schwartz *et al.*, 2014). In addition, deletion of the gene leads to a modest growth defect. *Candida albicans* Pus7 is important for rRNA biogenesis and its deletion resulted in changes in growth, virulence, and fitness (Pickerill *et al.*, 2019). In humans, where two Pus7 homologs are expressed, Pus7 mediates the modification of a class of tRNA-derived small RNAs that are important for controlling protein synthesis and stem cell determination (Guzzi *et al.*, 2018). Moreover, mutation of human Pus7 is associated with developmental defects (Han *et al.*, 2022). Collectively, these studies suggest a broader function for Pus7 than is associated with its catalytic activity.

Generation of *C. jejuni* mutants of TruA, TruB, and TruD with a C-terminal 3xFLAG epitope tag allowed to investigate their expression using commercially available anti FLAG antibodies. Western blot analysis of protein samples of bacteria over different growth phases showed a constitute expression of the FLAG-tagged TruA, TruB and TruD (Figure 3.1). To the best of my knowledge, there are no other studies demonstrating changes in protein expression of tRNA PUS enzymes over growth. However, it has been shown in eukaryotes that PUS7 shows higher expression in cancer tissue compared to normal tissue, suggesting a potentially specified role for this protein under certain cell growth conditions (Cui *et al.*, 2021). Moreover, in eukaryotes,

expression of tRNA PUS enzymes is induced during different stress responses, indicating a dynamic role for pseudouridylation during specific and immediate responses of the cells under non-standard conditions (Schwartz *et al.*, 2014). Analysis of the *C. jejuni* tagged proteins under heat shock response or osmotic stress did not show changes in expression level (Figure 3.2). Overall, it is interesting to speculate that while protein levels did not change, protein activity, functionality, and/or localization could still be regulated during stress or growth. Future experiments, especially based on transcriptome-wide mapping of pseudouridines using the Pseudo-seq approach during different stress conditions, might provide evidence and insights into specific cellular responses involving differential pseudouridylation. In *E. coli*, it has been shown that a *truB* deletion mutant strain is more sensitive to high temperatures compared to its parental strain, suggesting a possible role of this tRNA PUS enzyme during temperature stress response (Kinghorn *et al.*, 2002).

Since *C. jejuni* is a microaerophilic bacterium that survives under low oxygen (O_2) conditions, the generation of products derived from the O_2 metabolism (such as hydrogen peroxide or H_2O_2) represents one of the major sources of stress for the pathogen (Kim *et al.*, 2015). However, *truA*, *truB*, or *truD* deletion mutants do not shown any difference in the H_2O_2 sensitivity compared to its parental strain (Figure 3.3), suggesting that tRNA PUS enzymes in *C. jejuni* are less likely to be involved in survival of the bacteria under oxidative stress.

Motility and biofilm formation represent major virulence factors for *C. jejuni* pathogenesis. While motility is necessary for the bacteria to penetrate the intestinal mucus layer (Szymanski *et al.*, 1995), biofilm formation seems to be fundamental for the environmental survival of the pathogen during transmission (Tram *et al.*, 2020). Motility and biofilm formation are affected by deletion of *truA* and *truD*. Since a growth defect can be observed for the *truD* deletion strain (Figure 3.4 and 3.5) it is possible that impaired biofilm formation and the motility defects can be attributed to the slow growth of the bacteria. Thus, the role of TruD in pathogenesis remains still unclear. Additionally, *truA* deletion confers a growth advantage for *C. jejuni* (Figure 2.6) and it is known that non-motile *C. jejuni* mutants grow faster than the motile strains (Wösten *et al.*, 2004; Radomska *et al.*, 2016). It is possible that TruA is involved in the motility of *C. jejuni*. In *Pseudomonas aeruginosa* TruA is involved in the expression of type III secretion genes (Ahn *et al.*, 2004). The authors speculated that TruA might indirectly control the expression of type III secretion genes at the posttranscriptional level by modification of a tRNA that is essential for the translation of a transcriptional regulator necessary for expression of these specific genes. In summary, besides the role of TruA in *P. aeruginosa*, the role of tRNA PUS enzymes in bacterial pathogenesis is still poorly understood.

Since deletion of *truD* in *C. jejuni* leads to a severe growth phenotype, the role of this tRNA synthases was further investigated. As a first hint to investigate the importance of TruD in *C. jejuni*

physiology, I explored its genomic context in different *C. jejuni* strains and bacterial species. Here, the *truD* gene is located together with the thiamine monophosphate kinase *thiL* and Cj1456, encoding for a periplasmic protein, generating a polycistronic operon consisting of three genes with a conserved organization across *Campylobacter* species. While a genetic screen in our lab (Svensson and Sharma, unpublished) identified *thiL* as an essential gene in *C. jejuni* NCTC11168 strain, *truD* was not described as essential for *C. jejuni* survival. However, as bacterial genes are usually grouped into clusters of functionally related genes (Sáenz-Lahoya *et al.*, 2019) the conservation of the operon structure across multiple *C. jejuni* species, might indicate that *truD* is, together with *thiL*, important for the physiology of *C. jejuni*. In the related pathogen *H. pylori*, *truD* is the second gene of a eleven-gene operon (Sharma *et al.*, 2010; Pernitzsch & Sharma, 2012) together with genes encoding the recombination protein *recR,* the heat shock protein *htpX,* the GTP cyclohydrolase 1 *folE*, *ispA,* 5'-nucleotidase *surE,* HP0931, HP0932, *queD*, *queE*, and HP0935. In *E. coli, truD* is located between *umpG* and *ispD*. Taken together, the *truD* genes in *E. coli* and *H. pylori* are located in different operons, suggesting a potential different role of TruD in *C. jejuni*.

An amino acid alignment between CjTruD, HpTruD, and EcTruD showed high conservation between the proteins and also in their catalytic pocket (Figure 2.3). It is interesting to note that while EcTruD has 16 lysines, both CjTruD and HpTruD show a considerably higher lysine content (Figure 3.8). Due to the presence of a large number of lysines CjTruD and HpTruD have a higher positive charge surface compared to EcTruD and therefore might interact more efficiently with nucleic acids. Moreover, the amino acid lysine is often subjected to post translation modification (PTM) (Azevedo & Saiardi, 2016). While in eukaryotes PTM is a well-known mechanism of regulation to quickly respond to environmental conditions, in bacteria it is poorly understood. Among the different kinds of PTM, acetylation is one of the major post translational modifications that is conserved in all domains of life (Drazic *et al.*, 2016), where the complexity of an organism is positively correlated with increasing levels of acetylated proteins (Soppa, 2010). A recent study in *E. coli* demonstrated that thirty-one proteins are acetylated under different growth conditions (Schmidt *et al.*, 2016). Only recently, the acetylation of proteins in *C. jejuni* started to be investigated (Jeter & Escalante-Semerena, 2021). It would be interesting to investigate whether proteins with similar structure and amino acid identity, have a different function based on their PTM status.

In our system, cross-complementation of *C. jejuni truD* with homologs from *E. coli* and *H. pylori* showed that while HpTruD is able to restore the growth phenotype, EcTruD is not. It has already been shown that even proteins with high amino acid sequence similarity cannot fully substitute another in a different bacterial organism. For example, the proteins FlhC and FlhD are flagellar master regulators in the two closely related species *E. coli* and *S. enterica* that exhibit high sequence similarity (Albanna *et al.*, 2018). However, by independently replacing the *flhD* and *flhC*

coding sequence in *S. enterica* (*flhD$_{SE}$ and flhC$_{SE}$*) with the *E. coli* genes (*flhD$_{EC}$ and flhC$_{EC}$*), the authors showed that the flagellar gene expression is lower when *flhC$_{EC}$* is expressed instead of the other. These differences are due to a different DNA binding of the FlhC$_{EC}$ compared to the FlhC$_{SE}$ on the promoter region of the flagellins A and B when in a complex with FlhD$_{SE}$, suggesting that heterologous expression of proteins in bacteria with a significant level of genetic synteny can lead to different outcomes. In the case of HpTruD, differences in the activity of the proteins on the Cjp03 modification *in vivo* and *in vitro*, could be due to a different structure/folding/sequence of the Cjp03 compared to Hpt04 and Hpt01. Appendix Figure 2 shows a representation of the secondary structure and nucleotide composition of Cjp03, Hpt01, and Hpt04. Compared to Cjp03, Hpt01 and Hpt04 show differences in the nucleotide composition (marked in red), with Hpt04 presenting major differences in the D-loop closed to the Ψ13. Moreover, the lack of TruB, and consequently the pseudouridine at position 55 in tRNAs in *H. pylori* could impact the folding of Hpt01 and Hpt04 compared to the related Cjp03. Additional modifications might be present in the *C. jejuni* tRNA-Glu that can impact the structure of the tRNA and thus the recognition of HpTruD. Methylation of adenosine (m6A) or inosine (I) modifications, both present in the two pathogens, can affect the folding of the modified tRNA (Tanzer *et al.*, 2018).

The generation of a catalytically inactive CjTruD (D85N) capable of restoring the growth defects resulting from *truD* deletion led to the hypothesis that CjTruD has an additional function in *C. jejuni* beyond its catalytic activity. In *E. coli*, RluD is an rRNA PUS enzyme that modifies 23S rRNA at positions 1911, 1915, and 1917 (Raychaudhuri *et al.*, 1998). While deletion of *rluD* showed a severe growth defect compared to the wild-type strain (Raychaudhuri *et al.*, 1998), catalytically inactive RluD was able to restore the phenotype (Gutgsell *et al.*, 2001). A similar result was described for the *E. coli* TruB, although the growth defect of the *truB* deletion strain was detected only by competition experiments (Gutgsell *et al.*, 2000). Interestingly, TruB has recently been shown to have a dual function: it modifies tRNAs at position 55 and is necessary to fold the tRNA (Keffer-Wilkes *et al.*, 2016). The human Pus10p is important for the modification of tRNAs at position 55. It has also been described to bind unprocessed primary miRNAs and be important for their biogenesis with a mechanism that is independent of its catalytic activity (Song *et al.*, 2020). More likely, PUS enzymes in the different kingdoms of life have distinct roles in the cell. Additionally, deletion of *truD* in *C. jejuni* 81-176 and *C. coli* NCTC12668 led to a similar phenotype of deletion of *truD* in *C. jejuni* NCTC11168, suggesting that TruD might be involved in similar biological functions in *Campylobacter* species and/or isolates. Overall, proteins with a dual function is a relatively recent concept (Wakasugi & Schimmel, 1999) and it is likely to be widespread throughout all different kingdoms of life.

Elucidate the role of TruD using deep-sequencing approaches.

The study of pseudouridine synthases in various organisms in the last years suggested an emerging role of these proteins as regulators of gene expression. However, little is known about how these proteins achieve this function. Besides Pseudo-seq, which allows to identify direct targets of PUS enzymes, other genome-wide approaches have also been used to identify direct or indirect targets of the proteins. In eukaryotes, it was recently shown using a high-throughput sequencing crosslinking immunoprecipitation method (HITS-CLIP-seq) that TruB1 is responsible for modification in tRNAs and mRNAs (Becker *et al.*, 1997c; Carlile *et al.*, 2014; Schwartz *et al.*, 2014; Li *et al.*, 2015; Safra *et al.*, 2017), binds to let-7 miRNA and regulates the maturation of the miRNA in an enzyme-independent manner (Kurimoto *et al.*, 2020).

A similar function was observed for PUS10 in human, the pseudouridine synthase responsible for the modification of tRNAs at position 54 and 55 (Deogharia *et al.*, 2019). RNA-seq of the small RNA fraction revealed that depletion of the PUS10 protein resulted in the decrease of the mature miRNAs and a parallel increase in the unprocessed primary miRNAs. Moreover, by photoactivatable-ribonucleoside-enhanced crosslinking and immunoprecipitation (PAR-CLIP), the authors showed that independently of its enzymatic activity, Pus10 binds to specific pri-miRNAs and promotes their processing by recruiting the microprocessor DROSHA and DGCR8.
A different function was recently identified for Pus7 in human cells. The study demonstrated that Pus7, the homolog of TruD, regulates the generation of a new class of RNAs, called tRNA-derived fragments (tRFs), specifically 5´ derived tRFs (Guzzi *et al.*, 2018). In fact, the regulation of the pseudouridylation status of 5´ tRFs has an impact on translation initiation. Based on these studies, pseudouridine synthases might be involved in different layers of gene expression regulation.
In this chapter, different high-throughput sequencing methods were used to explore the function of TruD in the foodborne pathogen *C. jejuni*. A first RIP-seq experiment was performed to identify the direct targets of TruD. Among the enriched targets, Cjp03 was identified, confirming that the experiment could successfully pulldown TruD together with its tRNA-target. Moreover, many other transcripts were also enriched in the TruD-3xFLAG RIP-seq compared to the WT. Among them were three CDS coding for NADH dehydrogenase subunits (NuoA, H and L), which act as electron acceptors and use flavodoxin as a respiratory substrate in *C. jejuni* (Weerakoon & Olson, 2008). It is possible that TruD binds to metabolically relevant transcripts, either as a mechanism to protect or to localize them in specific areas of the cell, thus contributing to maintaining the proper amount of RNAs that encode for proteins necessary to preserve the bacterial respiratory chain. However, RNA-seq experiments did not show any changes in the expression of these transcripts. RNA-seq showed that Cj0414 and Cj0415 genes were downregulated upon deletion of *truD* in comparison to the wild-type, complemented and catalytically inactive strains. These genes encode for gluconate dehydrogenase subunits that use gluconate as an electron donor

(Pajaniappan *et al.*, 2008). Transcriptional fusion of the primary promoter of Cj0414/Cj0415 showed that TruD might not affect the RNA level transcriptionally, but post-transcriptionally. However, FLAG tag proteins abundance did not show differences in the *truD* deletion strains compared to the wildtype. Moreover, a comparison between RIP-seq and RNA-seq candidates showed no overlap between the two datasets, suggesting that changes in gene expressions are more likely to be indirect. RNA-binding proteins (RBPs) can exert their functions in many different ways in a bacterial cell. For example, they can be involved in 1) transcription terminator like the Rho or Nus proteins, or 2) antitermination like cold shock proteins (CSPs), 3) regulation of translation like Hfq and ProQ, 4) RNA decay like RhlB, or 5) RNA stabilization and processing like CsrA and CSPs (Holmqvist & Vogel, 2018). RBPs that modify tRNAs and rRNAs are part of the category of r-proteins, the largest functional class of RBPs involved in protein synthesis (Holmqvist & Vogel, 2018). In bacteria, one of the most characterized r-proteins is the 30S ribosomal protein S1. S1 is described as an "unusual" ribosomal protein since it is weakly associated with the small ribosomal subunit, but it is involved in the regulation of transcription, translation, and RNA stability (Delvillani *et al.*, 2011). In *E. coli*, S1 is involved in the activation of protein synthesis by binding and unfolding structured mRNAs and therefore facilitating the access and the correct position of the 30S subunit on the start codon (Sørensen *et al.*, 1998; Duval *et al.*, 2013). However, a global transcriptomic analysis of S1-RNA targets has not been performed yet. Regarding the role of TruD in *C. jejuni*, it is possible that TruD binds directly to metabolic genes and mediates translational activation or repression without affecting mRNA levels. The carbon storage regulator A (CsrA) in *C. jejuni* and *Borrelia burgdorferi* mediates translational repression without affecting the level of their target mRNAs (Sze *et al.*, 2011; Dugar *et al.*, 2016). Thus, it is possible that the effect of TruD binding to RNAs can occur at the translational level. For this reason, a global translatome analysis (Ribo-seq) was performed as a next step. By comparing the reads of RNA and 70S footprints, Ribo-seq experiments allow to identify differential translational efficiency of actively translated gene in different strains/conditions. In literature, not many examples of Ribo-seq experiments were performed to investigate the effect of deletion of a particular RBP in bacteria. In this work, a Ribo-seq experiment was performed in *C. jejuni* wildtype, *truD* deletion and complementation strains. The analysis of differentially translated mRNAs revealed that eight genes showed less translation efficiency in the deletion of *truD* compared to wildtype and complementation. *C. jejuni* strain NCTC11168 encodes approximately 1,600 protein-coding genes. Thus, deletion of *truD* does not lead to major changes in the translatome of *C. jejuni*. This result is also supported by the analysis of total protein extract from *C. jejuni* wildtype, Δ*truD*, and complementation strain by two-dimensional gel electrophoresis (2D-PAGE), where no differences were observed between the strains (data not shown). Loss in translation of *rpsU* could have explained the defect in the polysome profile and in the growth phenotype of the *truD* deletion strain compared to wildtype and complementation strain. It has

been shown in *B. subtilits* that deletion of *rpsU* leads to motility and growth defect. Moreover, polysome profile analysis showed high levels of the 30S subunit and lower levels of the 70S ribosome in the Δ*rpsU* compared to the parental strains (Akanuma *et al.*, 2012). Additionally, the preliminary CLIP-seq analysis showed enrichment in the *rpsU* 5' UTR in the crosslink samples compared to the non-crosslinked libraries, suggesting that TruD might activate the translation of *rpsU* by recruiting proteins involved in translation. However, investigation of the sfGFP level in the translational fusion of the 5' UTR of *rpsU* with sfGFP showed that Δ*truD* does not affect the level of the reporter fusion, suggesting that TruD is not directly binding the 5' UTR of *rpsU.* Thus, the function of TruD is still under investigation.

6. Conclusion and outlook

Since 2014, different groups applied high-throughput sequencing technologies to map and identify pseudouridine in eukaryotic RNAs. However, the function of pseudouridine in bacteria is still largely unknown. The application of Pseudo-seq in RNAs of the pathogens *C. jejuni* and *H. pylori* revealed for the first time the position of pseudouridine modifications at single nucleotide resolution in rRNAs and tRNAs, providing a global map of this modification in a genome-wide manner. Comparison of the modification in rRNAs and tRNAs between the two bacteria highlights the differences in the PUS repertoire and on the function that the modified nucleotides exert in the different RNA species. Pseudo-seq can be applied in RNAs of other bacteria where a different composition of rRNA and tRNA PUS enzymes is expressed and therefore a different map of pseudouridine is present. It would be interestingly to explore if pseudouridine is located in bacterial mRNAs and sRNAs. Additionally, Pseudo-seq can be used under different conditions (e.g., heat shock), where a sudden and dynamic pseudouridylation response might be needed for the survival of the bacteria or for different growth phases. In this thesis, Pseudo-seq was performed under standard laboratory conditions. However, it would be interesting to apply the technique in infected-host cells. It has been already shown that To this end, a human three-dimensional (3D) infection model was developed in our lab (Alzheimer *et al.*, 2020) could be infected with *C. jejuni* and subsequently, the RNAs from host and pathogen could be simultaneously isolated and subjected to CMC treatment and deep sequencing. This would allow the detection and mapping of pseudouridine modifications during an infection for the first time in parallel. Moreover, it is possible to improve the Pseudo-seq method. For example, an optimized pseudouridine antibody could be used instead of CMC and crosslinked to the modified RNA that will be reverse transcribed and subjected to deep sequencing. Using antibodies specific to pseudouridine will avoid unspecific binding of CMC to other RNA modifications. Moreover, this would circumvent harsh treatment (CMC treatment and reversion), thus preserving the transcriptome of the bacteria.

The second and the third parts of the result session were focused on the function of TruD in *C. jejuni.* It is interesting to note that conserved proteins with homologous function in different domains of life, could have evolved and acquired different functions.

Since no clear function could be attributed to TruD with the methods applied in this study, it is worth to note that it could be an enzyme that only transiently interacts with RNAs. It is possible that the RIP-seq method is not able to catch all the possible interactions of TruD with RNAs. Preliminary results from a pilot CLIP-seq experiment indicate that TruD could potentially binds to 43 transcripts. Thus, it is possible that it does not act as a global RNA chaperone like Hfq in *E. coli* and *S*. Typhimurium or CsrA in *C. jejuni*. However, except the pulldown of the tRNA-Glu, target of TruD, validation of the other RNA targets is required to attribute a specific function to TruD.

Some open questions still need to be clarified by future work. For example, it is possible that TruD might directly interact with other proteins. To investigate putative protein partners, TruD will be purified together with other proteins which identity will be identified by mass spectrometry.
Overall, this thesis shines light to an emerging field of epitranscriptomic modifications in bacteria in an attempt to identify and describe the role of a potential RNA chaperone in the foodborne pathogen *C. jejuni*.

7. Material and methods

7.1. Material

7.1.1. Instruments

Table 7.1: Instruments and devices.

Instrument/device	Manufacturer
Cell culture hood, HERAsafe	Thermo Scientific
Cell culture hood, Safe 2020	Thermo Scientific
Centrifuge, 5415C	Eppendorf
Centrifuge, 5418R	Eppendorf
Centrifuge, 5424R	Eppendorf
Centrifuge, Heraeus Fresco 17	Thermo Scientific
Centrifuge, Heraeus X3R	Thermo Scientific
Centrifuge, Sorvall RC 5B Plus	Thieme Labortechnik
Eraser for imaging plates	GE Healthcare
Fume hood	Renggli Laboratory System
Gel Dryer Model 583	Bio-Rad
Heating Oven	Memmert
Horizontal electrophoresis system Perfect Blue Mini S, M, L	PeqLab
Hybridization Oven HB-1000	UVP
Imaging system Image Quant LAS 4000	GE Healthcare
Incubator for agar plates Hera cell 240i CO_2	Thermo Scientific
Incubator for liquid cultures Hera cell 150i CO_2	Thermo Scientific
Led transilluminator	Nippon Genetics
Lysis system Fast Prep-24	MP
Magnetic Stirrer MS-20A	WITEG Labortechnik
Mini-centrifuge, I R	ROTH
Mixer, Rotamax 120	Heidolph
PhosphoImager Typhoon FLA7000	GE Healthcare
Power supplies PeqPower300	PeqLab
Retsch MM400	Retsch
Scale Kern ADB and EW2200-2NM	Kern and Sohn
Semi-dry electroblotter PerfectBlue, Sedec M for Western Blot	PeqLab
Shaker *Escherichia coli* SM-30	Edmund Bühler
Spectrophotometer Genesys 10S UV-Vis	Thermo Scientific
Spectrophotometer, Nanodrop 2000	Thermo Scientific
Tank electroblotter PerfectBlue Web M for Northern Blot	PeqLab
Thermal Cycler, MJ Mini	Bio-Rad
Thermo Cycler, T3	Biometra
Thermo Mixing Block, MB-102	BIOER
Ultracentrifuge, Optima L-80 XP (Rotor SW40Ti)	Beckman Coulter
UV Crosslinker	Vilber
UV Transilluminator	Intas
Vacuum pump	KnF LAB
Vertical sequencing gel system CBS SG-400-200	C.B.S. Scientific Co

Vortex-Genie 2	Scientific Industries
Waterbath	GFL

7.1.2. Labware and consumables

Table 7.2: glass/plastic ware and consumables

Labware	Manufacturer
1.5 ml, 2.0 ml Microtube	Sarsted
250 ml buckets for centrifuge	Thieme Labortechnik
Hybond™-XL membrane for nucleic acid transfer	GE Healthcare
Protran™ 0.45 µM nitrocellulose membrane for protein transfer	GE Healthcare
Cell culture flasks 25 cm^3	Corning
Cell culture flasks 75 cm^3	Corning
Centrifuge tubes 15 ml and 50 ml	Sarstedt
G-25, G-50 MicroSpin columns	GE Healthcare
Glass bottles	Simax
Glass beads (0.1 mm)	Roth
Imaging plates BAS-IP MS 2325, 2340 Fujifilm	Fujifilm
Imaging plates cassettes BAS 2325, 2340	Fujifilm
Low binding tubes 0.5 ml, 1.5 ml, 2.0 ml	Eppendorf
Box (metal), 10 x 21 cm	Hartenstein
Boxes (plastic), 20.5 x 20.5 cm or 9.5 x 20.5 cm	Hartenstein
PCR tubes (8 x 0.5 cm)/PCR lids	Brand
Petri Dishes	Nerbe plus
Phase Lock Gel (PLG)-tubes, 2 ml	5 Prime
Pipetboy Accu-jet ® Pro	BRAND
Pipettes 2.5 µl, 10 µl, 20 µl, 200 µl, 1000 µl	BRAND
Pipette tips 10 µl, 200 µl, 1000 µl	Sarstedt
Racks for centrifuge tubes	Hartenstein
Safe-lock tube 1.5 ml	Eppendorf
Serological pipet (plastic) 10 ml	Sarstedt
Spectrophotometer cuvettes	Rationlab
Sterile cotton swab	Delta lab
Sterile filters (0.20 µm pore size)	PALL life science
Syringe	Brawn
Whatman paper	Hahnemühle FineArt

7.1.3. Chemicals, media, and reagents

Table 7.3: Chemicals, media, reagents, and dyes.

Chemical/reagents	Manufacturer
10x DNA loading buffer	Self made
2x Gel loading buffer (RNA, GLII)	Self made
6x DNA gel loading dye	Thermo Scientific
Acetic acid (100 %)	Roth
Acetone	Roth
Agarose NEEO ultra quality	Roth
Albumin Fraktion V	Roth
Ammonium persulfate (APS)	Applichem
Ampicillin sodium salt	Roth
Bacto Brain Heart Infusion (BHI)	Roth
BBL™ Brucella Broth	Becton, Dickinson and Company
Bicine	Sigma
Boric Acid	Roth
Chloramphenicol	Roth
CMC	Sigma/Chemcruz
DEPC H_2O	Roth
Difco Agar	BD
Dimethyl sulfoxide (DMSO)	Sigma
Dithiothreitol (DTT)	Roth
Donor horse serum (DHS)	Biochrom AG
D-saccharose	Roth
Ethanol	Roth
Ethanol (absolute for analysis)	Merck
Ethylenediaminetetraacetic acid disodium salt dehydrate (EDTA)	Roth
Fetal calf/bovine serum (FCS/FBS)	Biochrom AG
Formaldeyde (37 %)	Roth
Formamide (99.5 %)	Roth
GC-agar base	Oxoid
Gene Ruler 1 kb plus	Thermo Scientific
Gentamicin sulfate salt	Sigma
Glycerol (99 %)	Roth
GlycoBlue™	Ambion
Hydrochloric acid (HCl, 32 %)	Roth
Hydrogen peroxide (H_2O_2, 30 %)	AppliChem
Hygromycin B	Sigma
Isopropanol	Roth
Kanamycin sulfate	Roth
Magnesium chloride	Roth
Methanol	Roth
Midori Green	Nippon Genetics Europe
Milk powder	Roth
Mueller Hinton	Becton, Dickinson and Company
NaOH	Roth
Nystatin	Sigma
Page Blue Protein Staining Solution	Thermo Scientific
Page Ruler™ Plus Prestained Protein Ladder	Thermo Scientific

PBS	Gibco
Phenol	Roth
pUC Marker Mix, 8	Thermo Scientific
Rifampicin	Roth
RNA ladder High Range	Thermo Scientific
RNA ladder Low Range	Thermo Scientific
Roti Aqua-P/C/I	Roth
Roti Hybri-Quick	Roth
Rotiphorese gel 40 (19:1)	Roth
Rotiphorese gel 40 (37.5:1)	Roth
SDS	Roth
Sodium carbonate	Roth
SYBR green	Invitrogen
Trimethoprim	Sigma
Triton-X100	Roth
TRIzol Reagent	Ambion/Life Technologies
Tween^{20}	Apllichem
Vancomycin sulfate	Roth
Vitamin B12	Roth
Yeast RNA	Ambion
γ-^{32}P-ATP	Hartmann Analytic

7.1.4. Commercial kits

Table 7.4: Commercial kits.

Commercial kits	Manufacturer	Ref. number
5′ DNA adenylation KIT	NEB	#E2610L
CircLigase™ II ssDNA ligase (5,000 units)	Epicentre	CL9021K
DNA cycle sequencing KIT	Jena Bioscience	PCR-401S
Megascript T7 *in vitro* transcription kit	Ambion	AMB13345
NucleoSpin Gel and PCR clean-Up	Macherey-Nagel	11992242
NucleoSpin plasmid	Macherey-Nagel	2502823
Protoscript II	NEB	M0368S
Set #1 and #2 Illumina primers	NEB	#E7335S, #E7500S
Strep-tag® protein purification system	IBA GmbH	Streptactin Sepharose #2-1202-001, Strep-tag Buffer W #2-1003-100, Strep-tag Buffer E #2-1000-025

7.1.5. Enzymes

Table 7.5: Enzymes.

Enzymes	Manufacturer
5′ deadenylase (500 u/ µl)	NEB
Antarctic Phosphatase (5 u/ µl)	NEB
Benzonase (250 u/ µl)	Sigma
Calf Intestinal Phosphates (CIP, 10 u/µl)	NEB
Deoxyribonuclease I (DNaseI, 1 u/µl)	Thermo Scientific
*Dpn*I (20 u /µl)	NEB
Lysozyme	Roth
Maxima RT (200 u/ µl)	Thermo Scientific
Micrococcal nuclease (MNase 2,000 u/ µl)	NEB
Proteinase K (20 mg/ ml)	Roth
Protoscript II (200 u/µl)	NEB
RecJ exonuclease (10 u/ µl)	Epicentre
Restriction enzymes (*Dpn*I, *Cla*I, *Kpn*I)	NEB
Ribonuclease Inhibitor (20 u/µl)	MOLOX
S7 Phusion Polymerase (2 u/ µl)	Thermo Fisher
SUPERaseIN RNase Inhibitor	Ambion
SUPERscriptII Reverse Transcriptase	Invitrogen
T4 DNA Ligase (5 u/µl)	Thermo Scientific
T4 Polynucleotide Kinase (PNK, 10 u/µl)	Thermo Scientific
Taq DNA Polymerase (5 u/µl)	NEB

7.1.6. Antibodies

Table 7.6: Antibodies

Antibody	Origin	Dilution	Manufacturer	Ref. number
ECL anti-mouse IgG, HRP-conjugate	Goat	1:10,000	GE Healthcare	#RPN4201
ECL anti-rabbit IgG, HRP-conjugate	Donkey	1:10,000	GE Healthcare	#RPN4301
Monoclonal anti-FLAG M2	Mouse	1:1,000	Sigma-Aldrich	#F1804-1MG
Monoclonal anti-GFP	Mouse	1:1,000	Roche	#11814460001
Monoclonal anti-pseudouridine (APU-6)	Mouse	For RIP-seq	Medical and Biological Laboratories Company	#D347-3
Polyclonal anti-GroEL antiserum	Rabbit	1:10,000	Sigma-Aldrich	#G6532-5ML
Monoclonal anti-FLAG® M2 magnetic beads	Mouse	For CLIP-seq	Sigma-Aldrich	#M8823

7.1.7. Oligonucleotides

Table 7.7: Synthetic oligonucleotides.

Sequences are given in 5'→3' direction; P~ denotes a 5' monophosphate.

Name	Sequence 5'→3'	Description
CSO-0017	gtttttTCTAGAGATCAGCCTGCCTTTAGG	Sense oligonucleotide for amplification of *rdxA* (500 bp) complementation in *H. pylori* 26695
CSO-0018	gtttttCTCGAGCTTAGCGCTTAATGAAACGC	Antisense oligonucleotide for amplification of *rdxA* (500 bp) for complementation in *H. pylori* 26695
CSO-0023	CCACCAGCTTATATACCTTAGCA	Antisense oligonucleotide for verification of integration of *aphA3*
CSO-0065	GACTACAAAGACCATGACGGT	Sense oligonucleotide that binds at start of FLAG tag
CSO-0205	AATTACAACAGTACTGCGATGAGT	Sequencing oligonucleotide, binds sense in 3'part of chloramphenicol cassette
CSO-0207	AGTTCTGATTTCATGCCCTT	Oligonucleotide for complementation in *rdxA* locus in *H. pylori*
CSO-0347	gtttttATCGATCTCTAGCTAGCATACTTTACAGTGC	Sense oligonucleotide for complementation in *rdxA* locus in *C. jejuni*
CSO-0349	CTGCAAAAGAAGCATTGACA	Antisense oligonucleotide for verification of complementation in *C. jejuni*
CSO-0483	gtttttGGATCCTTTTATGGATAATTTTTAAAATCATTTG	Sense oligonucleotide, binds in the kanamycin resistance cassette
CSO-0576	gtttttCATATGAAACACCCCCATAAGTGCAATTATGGGGAT AAATCATCTCGTTCTCCGCTC	Antisense oligonucleotide, binds in the gentamycin resistance cassette
CSO-0759	gttttttCCCGGGAGTTGATTTTAACTAACTTTTGCTTAA	Sense oligonucleotide for amplification of *metK* promoter
CSO-0760	gttttttATGCATAAAAAGTCCTTTCATTTAAAATG	Antisense oligonucleotide for amplification of *metK* promoter
CSO-0873	gttttttCTAGAGGCATCAAATAAAACGAAA	Oligonucleotide for the amplification of pJV572.1
CSO-0874	gtttttCTCGAGGTGAAGACGAAAGG	Oligonucleotide for the amplification of pJV572.1
CSO-1056	agcgcgTGGAGCCACCCGCAGTT	Sense oligonucleotide for introduction of Ser-Ala liner region for Strep tagging
CSO-1100	GAGATGAAAGAATCAGAAATCTTG	Deletion of *truB* in *C. jejuni*
CSO-1101	TCCTAGTTAGTCACCCGGGTACTGCAAAGATCTTGTTCAT ACTG	Deletion of *truB* in *C. jejuni*
CSO-1102	AGAAGATCTACTTAGTGAAATTTC	Deletion of *truB* in *C. jejuni*
CSO-1209	TGTGTTTTAGTACCTGGAGGGAATAGTCGAAGAATTAGAA TTTCATGA	Deletion of *truB* in *C. jejuni*
CSO-1210	TAAAAAACTCGCACAATCGCTA	Deletion of *truB* in *C. jejuni*
CSO-1956	AACCACAATTGTATCCAAATAAACTTAT	Antisense oligonucleotide for amplification of *metK* promoter
CSO-2213	TCCTAGTTAGTCACCCGGGTAAGAAAATATAATTTTTATT TTCATCAATAT	Deletion of *truA* in *C. jejuni*
CSO-2214	CGCCCTAAACATAAAGCAG	Deletion of *truA* in *C. jejuni*
CSO-2215	TGTTTTAGTACCTGGAGGGAATAAAGCAATACAATCACTT TTTAGC	Deletion of *truA* in *C. jejuni*
CSO-2216	TCCAAGTTGATGATGAAGAAATA	Deletion of *truA* in *C. jejuni*
CSO-2217	CTACAAAACAGGAGAATTTGG	Deletion of *truA* in *C. jejuni*
CSO-2218	TCCTAGTTAGTCACCCGGGTAGCTATTTTTACTAAAATAC GCATT	Deletion of *truD* in *C. jejuni*
CSO-2219	TAGTCTTACTATCATTTCAAAGATT	Deletion of *truD* in *C. jejuni*
CSO-2220	TGTTTTAGTACCTGGAGGGAATACATAAAAATTTGTTTGA ATGAAATAATTA	Deletion of *truD* in *C. jejuni*
CSO-2221	TCACAGAATAATAAACTCTTTTCTT	Deletion of *truD* in *C. jejuni*
CSO-2222	TCATAGGCGGTGATACTATAA	Deletion of *truD* in *C. jejuni*
CSO-2270	GAAGATGAAATTATAATCAAACAAAG	DNA template Cjp03 for primer extension

CSO-2271	ATATCAAAAGCTATTCGTATTCTAC	DNA template Cjp03 for primer extension
CSO-2276	CTTAATTTAACTTATCCTTTTGAAAC	Oligonucleotide for amplification of *rdxA* in *C. jejuni*
CSO-2277	CAAGCATTTTATCGGCTAATGG	Oligonucleotide for amplification of *rdxA* in *C. jejuni*
CSO-2596	GTATAATTTTAGCTTTAAATCTTAAAAAT	DNA template Cjp16 for primer extension
CSO-2597	CGCAAAAAATAAGTGGTGCC	DNA template Cjp16 for primer extension
CSO-2598	ACCGACACAAGGTTGCCC	Oligonucleotide to detect Ψ40 in Cjp16 by primer extension
CSO-2627	gtttttATGCATATGAAAATAAAAATTATATTTTCTTATGATG	Sense oligonucleotide for translational fusion of *truA* to *metK* promoter in *rdxA*
CSO-2628	gtttttATGCATAACAAGATCTTTGCAGCCTTTAA	Sense oligonucleotide for translational fusion of *truB* to *metK* promoter in *rdxA*
CSO-2629	gtttttATGCATAATTTAGAGGAAGAGAACACCAT	Sense oligonucleotide for translational fusion of *truD* to *metK* promoter in *rdxA*
CSO-2651	GCGAACCTGATGCCAAAGG	Deletion of Cj0883c in *C. jejuni*
CSO-2652	GCAAAAGCCCCGTAAAAAGG	Deletion of Cj0883c in *C. jejuni*
CSO-2653	CTCACAGCTTCAGGGCCG	Deletion of Cj0883c in *C. jejuni*
CSO-2959	gtttttATGCATACTTCAATTAACTCCTTCAATGATTTCTGC	Antisense oligonucleotide for amplification of the Shine Dalgarno of *arsR*
CSO-3108	GTGAAAGGGCGATGTCCTA	Oligonucleotide to detect Ψ13 in Cjp03 by primer extension
CSO-3159	TGGTGACCCATACGAGACTC	Antisense oligonucleotide for generation of T7-Cjp03 transcript
CSO-3226	GCTTAGTGGGTAAAATTTCTATT	Antisense oligonucleotide for amplification of downstream region of Cjp03
CSO-3279	*P*-AGCAAAGGAGAAGAACTTTTCACT	Sense oligonucleotide for amplification of sfGFP, 5' phosphorylated
CSO-3491	GGTTTAGAAAACCCCTATCTG	Deletion of *truD* in *H. pylori*
CSO-3492	TCCTAGTTAGTCACCCGGGTATCAATGCTCGCATGGTTATAAG	Deletion of *truD* in *H. pylori*
CSO-3493	ATTGTTTTAGTACCTGGAGGGAATAGCGCAATTTGAATTGGGATTTTA	Deletion of *truD* in *H. pylori*
CSO-3494	CGATGAGGGAATTGGATTCAT	Deletion of *truD* in *H. pylori*
CSO-3495	CTTATAAAAACAGCTTGAATCACT	Deletion of *truD* in *H. pylori*
CSO-3496	CCTCTCTCAAGAAAGCTTCA	Deletion of *truA* in *H. pylori*
CSO-3497	TCCTAGTTAGTCACCCGGGTAGGCTGTTTGGCATAGCCTA	Deletion of *truA* in *H. pylori*
CSO-3498	ATTGTTTTAGTACCTGGAGGGAATATCCATAACCTCAAAGCCACT	Deletion of *truA* in *H. pylori*
CSO-3499	CTAAAATAGCGGATTTTAAATGCG	Deletion of *truA* in *H. pylori*
CSO-3500	AGAGCGGGTGAATTTGGGCA	Deletion of *truA* in *H. pylori*
CSO-3521	TGGTGCCGAAGGTCGGAC	Oligonucleotide to detect Ψ55 in Hpt34 by primer extension
CSO-3545	CTCGTGCGAGTTCGAGTCT	DNA template HPt34 for primer extension
CSO-3546	ACTCACTAGTCTATCATTTATTCG	DNA template HPt34 for primer extension
CSO-3657	GCTTAAAGCCTGAATTGCCC	DNA template HPt23 for primer extension
CSO-3658	CCATGTTTAATTTGGTTTAATTTGC	DNA template HPt23 for primer extension
CSO-3659	CCGGCACGGTATTGCTAC	Oligonucleotide to detect Ψ39 HPt23 by primer extension
CSO-3690	GCAAAAGCTGTTATGCCGT	DNA template HPt04 for primer extension
CSO-3691	AGAGTGGTGACTCCTAGG	DNA template HPt04 for primer extension
CSO-3779	CGCCACCAAGTGCTTTTTAAAT	DNA template HPt01 for primer extension
CSO-3780	GTAGTTTGGAATTTTTGTGGCG	DNA template HPt01 for primer extension
CSO-3839	CAGGGCTTAAAAACAAGCAAGGATCAACCTTTC	Sense oligonucleotide for site directed mutagenesis of *truD* D85N
CSO-3840	TCCTTGCTTGTTTTTAAGCCCTGCATAACCAAAAT	Antisense oligonucleotide for site directed mutagenesis of *truD* D85N
CSO-3939	gtttttggtaccGTTTCAATTAAAACAAAGGAGCTTTTAT	Sense oligonucleotide to amplify *hupB* for transcriptional fusion
CSO-3959	gtttttCTCGAGAGTGCATCGATACTCGTAGC	Sense oligonucleotide for amplification of 500 nt upstream of Cjp03 tRNA
CSO-3960	gtttttTCTAGAGGAGGAAAATATGAAAAAAGTTGT	Antisense oligonucleotide for amplification of 313 nt downstream of Cjp03 tRNA

CSO-3961	gtttttGGATCCTGAAGATGAAATTATAATCAAACAAAG	Sense oligonucleotide for amplification of Cjp03 locus 40 nt upstream of the native promoter
CSO-3962	gtttttCATATGATTTTTTATAAAATTTTAGGATTTGTTATG	Antisense oligonucleotide for amplification of Cjp03 locus 40 nt upstream the native promoter
CSO-3996	GGCCCATTCGTCCAGCGGTTAGGACATCGCC	Sense oligonucleotide for point mutation T→13C in tRNA-Glu (Cjp03)
CSO-3997	TGTCCTAACCGCTGGACGAATGGGCCACTTTTAAG	Antisense oligonucleotide for point mutation T→13C in tRNA-Glu (Cjp03)
CSO-4004	CTTTGCCTGACGCAAGAGATGGTT	Sense oligonucleotide for *gyrA* amplification in *C. jejuni* for qRT-PCR
CSO-4005	AGCACCCACTATACGGGCTGATTT	Antisense oligonucleotide for *gyrA* amplification in *C. jejuni* for qRT-PCR
CSO-4046	ACAATCAGCCCCACTTCCAG	Sense oligonucleotide for Cj0415 amplification in *C. jejuni* for qRT-PCR
CSO-4047	ACCTTGCCCTCCTACGGTAA	Antisense oligonucleotide for Cj0415 amplification in *C. jejuni* for qRT-PCR
CSO-4048	GGGCTTCTAGGTGGTTCTGT	Sense oligonucleotide for Cj0414 amplification in *C. jejuni* for qRT-PCR
CSO-4049	GAAGCTTGATGCGAATGCGT	Antisense oligonucleotide for Cj0414 amplification in *C. jejuni* for qRT-PCR
CSO-4096	gtttttATGCATATTGAGTTTGATAATCTCACTTAC	Sense oligonucleotide for amplification of *truD* in *E. coli* MGM1655 K12 strain
CSO-4097	CTCAGCAATATGCGCATAATC	Sense oligonucleotide for amplification of *truD* in *E. coli* MGM1655 K12 strain
CSO-4098	gtttttATGCATAATTTAAATTTTATGCCCCTATTGCA	Sense oligonucleotide for amplification of *truD* in *H. pylori* 26695
CSO-4099	AAATTCGTCATTATTTTCTCCTTTC	Antisense oligonucleotide for amplification of *truD* in *H. pylori* 26695
CSO-4213	gtttttATGCATTTATCTCCTATAAATCATTTTTAAGTC	Antisense oligonucleotide binding on 5´UTR of *tlpB* for translational fusion
CSO-4215	TGATCTTTATAATCACCGTCATGGTCTTTGTAGTCAAATT CGTCATTATTTTCTCCTTTC	Antisense oligonucleotide for amplification of *truD* in *H. pylori* 26695
CSO-4216	TGATCTTTATAATCACCGTCATGGTCTTTGTAGTCTTCAA ACAAATTTTTATGCAAAATTTCT	Antisense oligonucleotide for amplification of *truD* in *C. jejuni*
CSO-4285	GAACCCCTGTAACCACCG	Oligonucleotide to detect Ψ13 HPt04 by primer extension
CSO-4286	TGAACTTCCGTTTCCACCG	Oligonucleotide to detect Ψ13 HPt01 by primer extension
CSO-4287	*P*-TGATATCGACTACAAAGATGACGACGATAAATAGTAATAA ATGTCCAGACCTGCAGTT	Sense oligonucleotide translational fusion, 5' phosphorylated
CSO-5006	GGGTGTGAGTAAGGATTTAAAT	Deletion of Cj0414
CSO-5007	GATGGACAAATGGCCTCAAG	Deletion of Cj0414
CSO-5008	TCCTAGTTAGTCACCCGGGTATGTCTTGCATTACTTCTCCT TG	Deletion of Cj0414
CSO-5009	ATTGTTTTAGTACCTGGAGGGAATAAATTTTTTAACATTG AACCTATGGG	Deletion of Cj0414
CSO-5010	TCCGCTAAAGGATTTGGTTC	Deletion of Cj0414
CSO-5011	CAAACTCAAACTGAATTTGATACC	Deletion of Cj0415
CSO-5012	TCGATAATCAGCTAGCTAGTG	Deletion of Cj0415
CSO-5013	TCCTAGTTAGTCACCCGGGTAGCTCCAACTGTTACTACAT CTA	Deletion of Cj0415
CSO-5014	ATTGTTTTAGTACCTGGAGGGAATATAGCTTGATAATAAC TTGAGAGTT	Deletion of Cj0415
CSO-5015	ATCTTGTCACTAGAACTTATCAAC	Deletion of Cj0415
CSO-5145	GTGCCCGAGGTCGGAC	Oligonucleotide to detect Ψ55 in Cjp16 by primer extension
CSO-5179	AGCTCCCATCTCGTTACGC	DNA template Hpr01/Hpr06 for primer extension
CSO-5180	ACCTCCACTACAATTTCACTG	DNA template Hpr01/Hpr06 for primer extension
CSO-5181	GTGCTCGAAGGTTAAGAGG	Oligonucleotide to detect Ψ in Hpr01/Hpr06 by primer extension

CSO-5182	gtttttATCGATGGCAAAAAGATATTTTGGTATGG	Sense oligonucleotide for amplification of Cj0414/Cj0415 promoter for transcriptional fusion
CSO-5183	gtttttGGTACCATTTAAACAAGACTATATTAGTCCTA	Antisense oligonucleotide for amplification of Cj0414/Cj0415 promoter for transcriptional fusion
CSO-5205	TCACCGTCATGGTCTTTGTAGTCACTCTCCATATCTGCTAAACC	Antisense oligonucleotide for amplification of Cj0414 C- terminus. Includes region of complementarity of the FLAG tag
CSO-5206	TCACCGTCATGGTCTTTGTAGTCAGCTAAGCTTTTTCCACTTTTATG	Antisense oligonucleotide for amplification of Cj0415 C-terminus. Includes region of complementarity of the FLAG tag
CSO-5293	TGCATAAAACCTAAGAGCATCA	Deletion of *truD* in *C. jejuni* 81-176
CSO-5431	CTTGCTTTGCCAAATAGCCT	Deletion of *truD* in *C. coli* NCTC12668
CSO-5432	TCCTAGTTAGTCACCCGGGTAATACAAAGGCCTTTCACGCA	Deletion of *truD* in *C. coli* NCTC12668
CSO-5433	ATTGTTTTAGTACCTGGAGGGAATAGCGTTATGATGAGCAAAAAGC	Deletion of *truD* in *C. coli* NCTC12668
CSO-5435	TCTTATCTTTATTGACACTAAATATC	Deletion of *truD* in *C. coli* NCTC12668
CSO-5436	GTAAGGATTTGTTTTTTGAAAATGTG	Deletion of *truD* in *C. coli* NCTC12668
CSO-5622	ATAAGTTTATTTGGATACAATTGTGGTTTCACAACAAAAATTTACACAGAAAG	Sense oligonucleotide for amplification of 5´-UTR of *rpsU* including first 10 codons, overlaps with *metK*
CSO-5623	AGTGAAAAGTTCTTCTCCTTTGCTCTCGTTAGGATGCACCTTGA	Antisense oligonucleotide for amplification of 5´-UTR of *rpsU* including first 10 codons, overlaps with *metK*
HPK1	GTACCCGGGTGACTAACTAGG	Sense oligonucleotide for amplification of kanamycin resistance cassette
HPK2	TATTCCCTCCAGGTACTAAAACA	Antisense oligonucleotide for amplification of kanamycin resistance cassette
pZE-A	GTGCCACCTGACGTCTAAGA	Verification of insert in pJV752.1
pBAD-FW	ATGCCATAGCATTTTTATCC	For vectors with *E. coli* araBAD promoter

7.1.8. Plasmids

Table 7.8: Plasmids

Name	Description/Generation	Origin/marker	Reference
pEF3.2	Plasmid for expressing C-terminus Strep-tagged TruA	p15A/ AmpR	This study
pEF4.19	Plasmid for expressing C-terminus Strep-tagged TruB	p15A/ AmpR	This study
pEF5.1	Plasmid for expressing C-terminus Strep-tagged TruD	p15A/ AmpR	This study
pEF15.1	Plasmid harboring ~1,000 bp region around Cjp03; based on pJV752.1	p15A/ AmpR	This study
pEF16.6	*aac(3)*-IV gentamicin cassette introduced upstream of Cjp03 region in pGD15.1 in reverse orientation to Cjp03	p15A mod/ GmR AmpR	This study
pEF17.2	T→13C mutation in Cjp03 at position 13	p15A mod/ GmR AmpR	This study
pEF18.1	D85N mutation in CDS of Cj1457c	p15A mod/ AmpR KanR	This study
pEF19.1	Plasmid for introduction of *Escherichia coli truD* in *rdxA* of *Campylobacter jejuni* NCTC11168	p15A mod/ AmpR KanR	This study
pEF20.1	Plasmid for introduction of *Helicobacter pylori* (26695, USA) *truD* in *rdxA* of *Campylobacter jejuni* NCTC11168	p15A mod/ AmpR KanR	This study
pEF22.1	Plasmid for introduction of *Helicobacter pylori* (26695, USA) *truD* in *rdxA* of *Helicobacter pylori* 26695 Δ*truD*, based on pSP109-6	p15A/ AmpR/CmR	This study

pEF23.1	Plasmid for introduction of *Campylobacter jejuni* NCTC11168 *truD* in *rdxA* of *Helicobacter pylori* 26695 Δ*truD*	p15A/ AmpR/CmR	This study
pFK20-1	Plasmid for translational reporter fusion of the 5´ UTR of *rpsU* to sfGFP	oriV	Fabian König, Sharma Lab
pGD70-5	Plasmid harboring 1,100 bp region around *flaA* promoter; based on pJV752.1	p15A mod/ AmpR	(Dugar *et al.*, 2016)
pGD76-1	*aac(3)*-IV gentamicin cassette introduced upstream of *flaA* promoter in pGD70-5 in reverse orientation to *flaA*	p15A mod/ GmR AmpR	(Dugar *et al.*, 2016)
pJV752.1	Cloning vector, pZE12-luc with modified p15A origin	p15A mod/ AmpR	This study
pPT33.1	Plasmid for expressing C-terminus Strep-tagged ArsR	p15A/ AmpR	Dr. Hock Siew Tan, Sharma Lab
pSP109-6	Plasmid for introduction of translational fusion of the *tlpB* 5' UTR including the 5th amino acid to *gfpmut3* into the *rdxA* locus	p15A/ AmpR/CmR	(Pernitzsch *et al.*, 2014)
pSSv100-2	pST1 with *metK-gfpmut3* removed and replaced with *hupB-sfGFP* (promoterless) for making transcriptional fusions at *Cla*I site	p15A/ AmpR KanR	Dr. Sarah Svensson, Sharma Lab
pTS1.1	Plasmid for complementation of *truA* in the *rdxA* of *C. jejuni* NCTC11168	p15A/ AmpR KanR	Dr. Hock Siew Tan/Dr. Gaurav Dugar, Sharma Lab
pTS2.6	Plasmid for complementation of *truB* in the *rdxA* of *C. jejuni* NCTC11168	p15A/ AmpR KanR	Dr. Hock Siew Tan/Dr. Gaurav Dugar, Sharma Lab
pTS3.6	Plasmid for complementation of *truD* in the *rdxA* of *C. jejuni* NCTC11168	p15A/ AmpR KanR	Dr. Hock Siew Tan/Dr. Gaurav Dugar, Sharma Lab

7.1.9. Bacterial strains

Table 7.9: Bacterial strains

Name	Description	Strain number	Resistance
Campylobacter jejuni			
wildtype	Kindly provided by Arnoud van Vliet, Institute of Food Research, Norwich, UK	CSS-0032	-
Δ*truA*	*truA*::*aac(3)-IV* Deletion of *truA* (Cj0827)	CSS-2497	Gm^R
Δ*truB*	*truB*::*aac(3)-IV* Deletion of *truB* (Cj1102)	CSS-1108	Gm^R
Δ*truD*	*truD*::*aac(3)-IV* Deletion of *truB* (Cj1102)	CSS-2506	Gm^R
Δ*truB*	*truB*:: *aphA-3* Deletion of *truB* (Cj1102)	CSS-3045	Kan^R
Δ*truD*	*truD*:: *aph(7'')* Deletion of *truD* (Cj1457c)	CSS-3373	Hyg^R
Δ*truAB*	*truA*::*aac(3)-IV, truB*:: *aphA-3* Deletion of *truA* (Cj0827) and *truB* (Cj1102)	CSS-3046	Gm^R Kan^R
Δ*truBD*	*truB*:: *aphA-3, truD*:: *aph(7'')* Deletion of *truB* (Cj1102), deletion of *truD* (Cj1457)	CSS-3376	Kan^R Hyg^R
Δ*truAD*	*truA*::*aac(3)-IV, truD*:: *aph(7'')* Deletion of *truA* (Cj0827), deletion of *truD* (Cj1457)	CSS-3378	Gm^R Hyg^R
Δ*truABD*	*truA*::*aac(3)-IV, truB*:: *aphA-3, truD*:: *aph(7'')* Deletion of *truA* (Cj0827), deletion of *truB* (Cj0827) deletion of *truD* (Cj1457)	CSS-3380	Gm^R Kan^R Hyg^R
C*truD*	*truD*::*aac(3)-IV, rdxA::truD-3xFLAG* Complementation of *truD-3xFLAG* in the *rdxA* locus	CSS-5202	Gm^R Kan^R
C*truA*	*truA*::*aac(3)-IV, rdxA::truA-3xFLAG*	CSS-2868	Gm^R Kan^R

	Complementation of *truA-3xFLAG* in the *rdxA* locus		
C*truB*	*truB*::*aac(3)-IV, rdxA::truB-3xFLAG* Complementation of *truB-3xFLAG* in the *rdxA* locus	CSS-2869	Gm^R Kan^R
C*truD*	*truD*::*aph(7″), rdxA::truD-3xFLAG* Complementation of *truD-3xFLAG* in the *rdxA* locus	CSS-5554	Hyg^R Kan^R
D85N	*truD*::*aph(7″), rdxA::D85N-3xFLAG* Complementation of *D85N-3xFLAG* in the *rdxA* locus	CSS-5549	Hyg^R Kan^R
tRNA-Glu T→T	Cjp03 + $Genta^R$ in its native locus	CSS-6526	Gm^R
tRNA-Glu T→C	Cjp03 + $Genta^R$ in its native locus with the point mutation T→C	CSS-6528	Gm^R
TruA-3xFLAG	*truA*-3xFLAG*::aphA-3* C-terminal 3xFLAG tag at native locus (Cj0827) in NCTC11168 background	CSS-2310	Kan^R
TruB-3xFLAG	*truB*-3xFLAG*::aphA-3* C-terminal 3xFLAG tag at native locus (Cj1102) in NCTC11168 background	CSS-0944	Kan^R
TruD-3xFLAG	*truD*-3xFLAG*::aphA-3* C-terminal 3xFLAG tag at native locus (Cj1457) in NCTC11168 background	CSS-2311	Kan^R
EcTruD	*truD*:: *aph(7″), rdxA::EctruD-3xFLAG* Complementation of Ec*truD-3xFLAG* in the *rdxA* locus	CSS-6530	Hyg^R Kan^R
HpTruD	*truD*:: *aph(7″), rdxA::HptruD-3xFLAG* Complementation of Hp*truD-3xFLAG* in the *rdxA* locus	CSS-6532	Hyg^R Kan^R
ΔCj0414	Cj0414:: *aac(3)-IV* Deletion of Cj0414	CSO-6560	Gm^R
Δ0415	Cj0415:: *aac(3)-IV* Deletion of Cj0415	CSO-6558	Gm^R
ΔΔCj0414_5	Cj0414_5::*aac(3)-IV* Deletion of Cj0414_5 operon	CSS-6681	Gm^R
ΔΔCj0414_5 + Δ*truD*	Cj0414_5::*aac(3)-IV* Deletion of Cj0414_5 operon and truD (Cj1457)	CSS-6683	Hyg^R Gm^R
PCj0414::*hupB-sfGFP*	*rdxA*::PCj0414_5-5'UTR-*hupB-sfGFP* Transcriptional fusion of Cj0414_5 primary promoter with the 5'UTR -*hupB* fused to sfGFP	CSS-6773	Kan^R
PCj0414::*hupB-sfGFP* + Δ*truD*	rdxA::PCj0414_5-5'UTR hupB-sfGFP, *truD*:: *aph(7″)* Deletion of *truD* in PCj0414::hupB-sfGFP	CSS-6845	Hyg^R Kan^R
PCj0414::*hupB-sfGFP* + Δ*Cj0883c*	rdxA::PCj0414_5-5'UTRhupB-sfGFP, *truD*::*aph(7″)* Deletion of Cj0883c in PCj0414::hupB-sfGFP	CSS-7351	Hyg^R Kan^R
PCj0414::*hupB-sfGFP* + Δ*csrA*	rdxA::PCj0414_5-5'UTRhupB-sfGFP, *truD*::*aph(7″)* Deletion of *csrA* in PCj0414::hupB-sfGFP	CSS-7355	Cm^R Kan^R
PCj1358::*hupB-sfGFP* + Δ*truD*	rdxA::1358 -5'UTRhupB-sfGFP, *truD*::*aph(7″)* Deletion of *truD* in PCj1358::hupB-sfGFP	CSS-6847	Hyg^R Kan^R
Cj0414-3xFLAG	Cj0414-3xFLAG*::aphA-3* C-terminal 3xFLAG tag at native locus (Cj0414) in NCTC11168 background	CSS-7343	Kan^R
Cj0415-3xFLAG	Cj0415-3xFLAG*::aphA-3* C-terminal 3xFLAG tag at native locus (Cj0415) in NCTC11168 background	CSS-7345	Kan^R
Δ*truD*	*truD*::*aph(7″)* Deletion of *truD* in *C. jejuni* 81-176	CSS-7353	Hyg^R
Δ*truD*	*truD*::*aph(7″)* Deletion of *truD* in *C. coli* NCTC12668	CSS-7363	Kan^R
Cj*truD*$_{NCTC11168}$	*truD*::*aph(7″), rdxA::truD*$_{NCTC11168}$*-3xFLAG* Complementation of *truD* $_{NCTC11168}$*-3xFLAG* in the *rdxA* locus of *C. jejuni* 81-176	CSS-7365	Hyg^R Kan^R
CjD85N$_{NCTC11168}$	*truD*::*aph(7″), rdxA::D85N* $_{NCTC11168}$*-3xFLAG*	CSS-7367	Hyg^R Kan^R

	Complementation of *D85N$_{NCTC11168}$-3xFLAG* in the *rdxA* locus of *C. jejuni* 81-176		
Helicobacter pylori			
wildtype	Kindly provided by Dr. Scott Merrell	CSS-0065	-
Δ*truD*	*truD::aphA-3* Deletion of *truD* (HP0926)	CSS-5485	Kan^R
Δ*truA*	*truA::aphA-3* Deletion of *truD* (HP0361)	CSS-5488	Kan^R
HpTruD	*truD*:: *aphA-3, rdxA::HpTruD-3xFLAG* Complementation of *HpTruD -3xFLAG* in the *rdxA* locus of *H. pylori*	CSS-6540	Cm^R Kan^R
CjTruD	*truD*:: *aphA-3, rdxA::CjTruD -3xFLAG* Complementation of *CjTruD -3xFLAG* in the *rdxA* locus of *H. pylori*	CSS-6219	Cm^R Kan^R

7.1.10. Media, buffer, and supplements

7.1.10.1. Media and stocks

Brucella Broth (BB):

28 g of BB powder
1 l H_2O

after autoclaving, supplement with

10 µg/ml vancomycin

Mueller Hinton-agar plates

21 g of Mueller Hinton powder
15 g Difco agar
1 l H_2O

after autoclaving, supplement with

10 µg/ml vancomycin

Brain Heart Infusion Broth (BHI):

37 g of Bacto Brain Heart infusion powder
1 l H_2O

after autoclaving, supplement with

10 µg/ml vancomycin
10 % (v/v) of heat-inactivated FBS
1 µg/ml Nystatin
5 µg/ml Trimethoprim

GC-agar plates	36 g of GC agar base
	1 l H_2O
after autoclaving, supplement with	
	10 µg/ml vancomycin
	10 % of heat inactivated DHS
	1 µg/ml Nystatin
	5 µg/ml Trimethoprim
	1 % of Vitamin-Mix
Lennox Broth (LB)	10 g peptone
	5 g yeast extract
	5 g NaCl
	1 l H_2O
LB agar plates	10 g Trypton
	5 g Yeast Extract
	5 g NaCl
	1.5 % Difco-agar
	1 l H_2O
SOB medium	20 g Tryptone
	5 g yeast extract
	0.5 g NaCl
	800 ml of H_2O
	Add 10 ml of 250 mM potassium chloride
	Adjust to pH 7.0 (using NaOH)
	Fill up to 1 l of H_2O
SOC medium	1 l SOB medium
	Add 5 ml magnesium chloride
	Add 20 ml 1 M glucose
Superbroth medium	35 g tryptone
	35 g yeast extract

5 g NaCl
1 l of H_2O

Vitamin Mix

Solution 1:
200 g D(+)-Glucose
20 g L-Glutamin
52 g L-Cystein-hydrochloride monohydrate
0.2 g Cocarboxylase
0.04 g Iron (III)-nitrate nonahydrate
0.006 g Thiamine hydrochloride
0.026 g 4-Aminobenzoic acid
0.5 g Nicotinamide-adenine dinucleotide free acid
0.02 g Vitamin B12
1 l H_2O

Solution 2:
2.2 g L-Cystine
2 g Adenine
0.06 g Guanine-Cl
0.3 g L-Arginin-monohydrochloride
1 g Uracil
600 ml H_2O
Add 30 ml of 32% HCl

Mix Solution 1 and Solution 2 together

Fill up to 2 l with H_2O, aliquot in 50 ml and store protected from light at -20°C.

7.1.10.2. Media supplements

Table 7.10: Antibiotics and media supplements.

C. jejuni

Antibiotic	Solvent	Stock	Working concentration
Chloramphenicol	100 % ethanol	20 mg/ ml	20 µg/ ml
Gentamicin	H_2O	10 mg/ ml	10 µg/ ml
Hygromycin B		250 mg/ ml	250 µg/ ml
Kanamycin	H_2O	50 mg/ ml	50 µg/ ml
Vancomycin	H_2O	10 mg/ ml	10 µg/ ml

H. pylori

Antibiotic	Solvent	Stock	Working concentration
Kanamycin	H_2O	20 mg/ ml	20 µg/ ml
Chloramphenicol	100 % ethanol	8 mg/ ml	8 µg/ ml
Vancomycin	H_2O	10 mg/ ml	10 µg/ ml

Supplement	Working concentration
FBS	heat-inactivated, 10 % (v/v)
DHS	heat-inactivated, 10 % (v/v)

E. coli

Antibiotic	Solvent	Stock	Working concentration
Ampicillin	H_2O	100 mg/ ml	100 µg/ ml
Chloramphenicol	100 % ethanol	20 mg/ ml	20 µg/ ml
Kanamycin	H_2O	20 mg/ ml	20 µg/ ml

7.1.10.3. Buffers and solutions

SDS running buffer (10x stock)	30.275 g Tris base
	144 g Glycin
	10 g SDS
	fill up to 1 l with H_2O

TAE (50x stock)	242 g Tris base 57.1 ml acetic acid 100 ml 0.5 M EDTA pH 8.0 fill up to 1 l with H_2O
TBE (10x stock)	108 g Tris base 55 g boric acid 40 ml 0.5 M EDTA pH 8.0 fill up to 1 l with H_2O
SSC (20x stock)	175.3 g sodium chloride 88.2 g sodium citrate dissolve in 800 ml of H_2O and adjust to pH 7.0 with HCl fill up to 1 l with H_2O
EDTA 0.5M, pH 8.0	186.1 g diNaEDTA* $2H_2O$ dissolve in 800 ml of H_2O and adjust to pH 8.0 with NaOH fill up to 1 l with H_2O
Transfer Buffer (10x stock)	30g Tris base 144 g Glycin fill up to 1 l with H_2O
1x Transfer Buffer	100 ml of 10x Transfer Buffer 200 ml Methanol (20 % final) 700 ml H_2O
TBS (10x stock)	24.11 g Tris Base 87.66 g NaCl dissolve in 1 l of H_2O and adjust to pH 7.4 with HCl

10x DNA loading buffer	1.66 ml Tris-HCl 1M (pH 7.5) 12 ml 0.5 M EDTA (pH 8.0) 0.05 g Bromophenol blue 0.05 g Xylene cyanol 60 ml Glycerol fill up to 100 ml with H_2O
2x Gel loading buffer (RNA, GLII)	1.66 ml Tris-HCl 1M pH 7.5 12 ml 0.5 M EDTA pH 8.0 0.05 g Bromophenol-Blue 0.05 g Xylene cyanol 60 ml Glycerol fill up to 100 ml with H_2O
5x Protein loading buffer	156.5 ml 1M Tris-HCl 1M pH 6.8 50 g SDS 0.25 g Bromophenol-Blue 250 ml Glycerol 38.53 g DTT fill up to 500 ml with H_2O
Stains all stock solution	0.03 g in 30 ml of formamide
Stains all solution	30 ml of stains all stock solution 90 ml of formamide fill up to 200 ml with H_2O
10% APS	15 g ammonium persulfate 150 ml of H_2O
Lower Buffer	60.57 g Tris base dissolve in 400 ml of H_2O and adjust pH to 8.8 with HCl

Upper Buffer	60.57 g Tris base dissolve in 400 ml of H_2O and adjust pH to 6.8 with HCl
Stop Mix	95% (v/v) EtOH (absolute) 5% (v/v) Roti Aqua phenol
30:1 Mix	30 part of 100% EtOH (absolute) 1 part of 3M sodium acetate (pH 5.2)
Agarose gel solution	X% (w/v) pure agarose in 1 x TAE or 1 xTBE
Western blot solution A	20 ml 1M Tris-HCl pH 8.6 50 mg Luminol sodium salt fill up to 200 ml with H_2O
Western blot solution B	50 mg *p*-coumaric acid dissolve in 50 ml of DMSO
Western blot developing solution (for one membrane)	2.0 ml of solution A 200.0 µl of solution B 3.0 µl 3% H_2O_2

PAA gel for separation gel (10 ml) for western blot

% Acrylamid/Bis	10%	12%	15%
1 M Lower Buffer pH 8.8	3.75 ml	3.75 ml	3.75 ml
40 % PAA solution (37.5:1 acrylamide/bisacrylamide)	2.5 ml	3.0 ml	3.75 ml
H_2O	3.75 ml	3.25 ml	2.5 ml
10% (w/v) SDS	100.0 µl	100.0 µl	100.0 µl
10% (w/v) APS	75.0 µl	75.0 µl	75.0 µl
Temed	7.5 µl	7.5 µl	7.5 µl

PAA gel for stacking gel (10 ml) for western blot:

% Acrylamid/Bis	4%
1 M Upper Buffer pH 6.8	1.25 ml
40 % PAA solution (37.5:1 acrylamide/bisacrylamide)	1.0 ml
H_2O	7.5 ml
10 % (w/v) SDS	100.0 µl
10 % (w/v) APS	150.0 µl
Temed	15.0 µl

PAA gel stock solution (7 M Urea, 500 ml) for northern blot, sequencing gel, and cDNA library gel:

% Acrylamid/Bis	6%	10%	15%
40 % PAA solution (19:1 acrylamide/ bisacrylamide)	75 ml	125 ml	187.5 ml
urea	210 g	210 g	210 g
10 x TBE buffer	50 ml	50 ml	50 ml

Northern blot gels (6 % Acrylamid/Bis, 60 ml): 60 ml stock solution
600 µl of 10 % (w/v) APS
60 µl of TEMED

Sequencing gels (10 % Acrylamid/Bis, 50 ml): 50 ml stock solution
500 µl of 10 % (w/v) APS
50 µl of TEMED

cDNA library gels (15 % Acrylamid/Bis, 50 ml): 10 ml stock solution
100 µl of 10 % (w/v) APS
10 µl of TEMED

7.1.10.4. Sterilization

Media and most of the buffers were sterilized by autoclaving at 120 °C and 1 bar before using. Where necessary, some buffers and solutions were sterilized by filtration and glassware was washed and sterilized by heating to 180 °C for at least three hours.

7.2 Microbiological Methods

7.2.1. Growth conditions and phenotypic characterization

7.2.1.1 *Campylobacter jejuni*

***Campylobacter* standard growth conditions.** *C. jejuni* strains were routinely grown on Müller-Hinton (MH) agar plates supplemented with 10 µg/ml vancomycin in microaerobic conditions (10 % CO_2, 5 % O_2, 85 % N_2) for 1-2 passages. Where appropriate, the plates were supplemented with marker-selective antibiotics [20 µg/ml gentamicin (Gm), 250 µg/ml hygromycin B (Hyg), or 50 µg/ml kanamycin (Kan)]. Bacteria were inoculated overnight in 10-15 ml of Brucella Broth (BB) supplemented with 10 µg/ml vancomycin in T25 cell culture flasks to a final OD_{600nm} of 0.005 or 0.01 and grown under agitation at 140-150 rpm at 37 °C (10 % CO_2, 5 % O_2, 85 % N_2). For overday cultures, the bacteria were inoculated from overnight liquid cultures into 50 ml of BB + vancomycin to a final OD_{600nm} of 0.03-0.05 and grown under agitation at 140-150 rpm at 37°C (10 % CO_2, 5 % O_2, 85 % N_2).

Growth curve analysis. Bacteria were inoculated overnight in 15 ml of Brucella Broth (BB) supplemented with 10 µg/ml vancomycin in T25 cell culture flasks to a final OD_{600} of 0.01 and grown under agitation at 140-150 rpm at 37°C (10 % CO_2, 5 % O_2, 85 % N_2). For overday culture, the bacteria were inoculated from the overnight culture in 50 ml of BB + vancomycin to a final OD_{600nm} of 0.03 and grown under agitation at 140-150 rpm at 37°C (10 % CO_2, 5 % O_2, 85 % N_2). The OD_{600nm} at different time points were measured every two hours (from 0 to 10-12 hours and 24-26 hours after inoculation).

Motility assay. *C. jejuni* strains were grown on MH agar plates overnight and inoculated in 10 ml of BB supplemented with 10 µg/ml vancomycin in T25 cell culture flasks to a final OD_{600} of 0.005. When the strains reached an OD_{600nm} of 0.5 the bacteria were harvested by centrifugation at 6,500 x *g* for 5 minutes and resuspended to an OD_{600nm} of 0.5 in fresh broth. 1.0 µl of bacteria were inoculated in a soft-agar plate (BB supplemented with 10 µg/µl of vancomycin + 0.4 % of agar + 5 % of FBS). The plates were incubated for at least 12 hours in microaerobic conditions (10 % CO_2, 5 % O_2, 85 % N_2). Three measurements of the same motility halo diameters were determined for each inoculation and averaged to provide the mean of the swimming distance for

each strain on the plate. All strains were inoculated together and the standard deviation on the plates was calculated based on three biological replicates.

Biofilm formation assay. *C. jejuni* strains were grown on MH agar plates overnight and inoculated in 10 ml of BB supplemented with 10 µg/ml vancomycin in T25 cell culture flasks to a final OD_{600} of 0.005. The next day, the bacteria were diluted in 2 ml of BB to a final OD_{600nm} of 0.002 into a glass tube. The tubes were incubated in microaerobic conditions (10 % CO_2, 5 % O_2, 85 % N_2) without shaking for 3 days. After the incubation time, 500 µl of 1 % crystal violet dissolved in 100 % ethanol were added to the culture and left to incubate for 10 minutes at room temperature. The tubes were rinsed with water 3 to 5 times and 3 ml of de-staining solution (40 % ethanol and 10 % acetic acid) was added and vortexed until the crystal violet was completely dissolved. Biofilm formation was determined by measuring the $A570_{nm}$ of the resulting solution. The standard deviation was measured based on biological triplicate.

Disk diffusion assay. Bacteria were inoculated overnight in 15 ml of Brucella Broth (BB) supplemented with 10 µg/ml vancomycin in T25 cell culture flasks to a final OD_{600nm} of 0.01 and grown under agitation at 140-150 rpm at 37°C (10 % CO_2, 5 % O_2, 85 % N_2). When the bacteria reached an OD_{600nm} of 0.5, 100 µl of the culture was spread using a cotton swab on a new plate supplemented with 10 µg/µl of vancomycin. For each plate, a disk soaked with 10 µl of 30 % H_2O_2 was added in the center of the plate. The plates were incubated for at least 12 hours in microaerobic conditions (10 % CO_2, 5 % O_2, 85 % N_2). Three measurements of each inhibition zone were made, which were averaged to give the diameter of the inhibition zone of each strain on a plate.

7.2.1.2 *Helicobacter pylori*

Helicobacter* standard growth conditions. H. pylori* strains were grown on GC agar plates supplemented with 10 % (v/v) donor horse serum (DHS), 1 % (vol/vol) vitamin mix, 10 µg/ml vancomycin, 5 µg/ml trimethoprim, and 1 µg/ml nystatin. Where appropriate, the plates were supplemented with marker-selective antibiotics [20 µg/ml kanamycin (Kan), 16 µg/ml chloramphenicol (Cm)]. From plate, the bacteria were inoculated overnight in 10 ml of Brain Heart Infusion medium (BHI) supplemented with 10 % (vol/vol) fetal bovine serum (FBS) and 10 µg/ml vancomycin, 5 µg/ml trimethoprim, and 1 µg/ml nystatin to a final OD_{600nm} of 0.02 and grown with shaking at 140-150 rpm (10 % CO_2, 5 % O_2, 85 % N_2) at 37°C. For overday culture, the bacteria were inoculated from overnight cultures into 50 ml of BHI to a final OD_{600nm} of 0.05 and grown under agitation at 140-150 rpm at 37°C (10 % CO_2, 5 % O_2, 85 % N_2).

Growth curve analysis. *H. pylori* strains were grown on GC agar plates supplemented with 10% (v/v) donor horse serum (DHS), 1% (vol/vol) vitamin mix, 10 µg/ml vancomycin, 5 µg/ml trimethoprim, and 1 µg/ml nystatin. From plate, the bacteria were inoculated overnight in 10 ml of Brain Heart Infusion medium (BHI) supplemented with 10% (vol/vol) fetal bovine serum (FBS) and 10 µg/ml vancomycin, 5 µg/ml trimethoprim, and 1 µg/ml nystatin to a final OD_{600nm} of 0.02 and grown with shaking at 140-150 rpm (10 % CO_2, 5 % O_2, 85 % N_2) at 37°C. For growth curve analysis, the strains were inoculated at OD_{600nm} of 0.02-0.025 in T75 flasks and let them grow over 36-38 hours. The OD_{600nm} was measured every 2 hours, starting immediately and 12 hours after inoculation.

7.2.1.3 *Escherichia coli*

***E. coli* standard growth conditions**. *E. coli* strains were grown aerobically at 37°C in Luria-Bertani (LB) broth or on LB agar plates supplemented with appropriate antibiotics [100 µg/ml ampicillin (Amp), 20 µg/ml gentamicin (Gm), or 20 µg/ml kanamycin (Kan)].

7.2.2. Genetic manipulation

7.2.2.1 *Campylobacter jejuni*

Construction of *C. jejuni* deletion mutant strains by homologous recombination with overlap PCR products. For the generation of *C. jejuni truA*, *truB*, and *truD* deletion strains, a construct containing the gentamicin, kanamycin (Skouloubris *et al.*, 1998), or hygromycin B (Cameron & Gaynor, 2014) resistance cassette flanked by ~500 nt up- and downstream of *truA, truB*, or *truD* open reading frame was generated by overlap-PCR (Polymerase Chain Reaction). As an example, deletion of *truA* is described in detail. PCR products of up- and downstream regions of *truA* were generated with the oligonucleotides CSO-2213/2214 and CSO-2215/2216, respectively, and gentamicin resistance cassette was generated with the oligonucleotides HPK1/HPK2. The three PCR products were mixed together in a ratio of 50:90:50 ng and used as templates for overlap PCR using the oligonucleotides CSO-2214/2216. The resulting purified PCR product was used for electroporation into *C. jejuni* NCTC11168 wildtype (CSS-0032). Deletions of *truB* and *truD* were generated analogously. This resulted in the following strains: Δ*truA* (CSS-2497), Δ*truB*, (CSS-3045), and Δ*truD* (CSS-3373).

Construction of *C. jejuni* complementation strains. For the construction of *truA*, *truB,* and *truD* complementation strains in *C. jejuni* NCTC11168, the plasmids pTS1.4, pTS2.6, and pTS3.6 were generated. The *truA*, *truB*, and *truD* genes that carry a 3´ end 3xFLAG sequence, were amplified from genomic DNA of *C. jejuni* strains that express the genes in their native locus with a 3xFLAG using oligonucleotides CSO-2627/1677 for *truA-3xFLAG*, CSO-2628/1677 for *truB-*

3xFLAG and CSO-2629/1677 for *truD-3xFLAG*. In parallel, the plasmid backbone (pST1.1) was amplified using the oligonucleotides CSO-0760/0493. The amplicon contains the *rdxA* upstream and downstream regions, together with the kanamycin resistance cassette and the P*metK* promoter. The oligonucleotides used to amplify the backbone and the *truA-3xFLAG*, *truB-3xFLAG*, and *truD-3xFLAG* regions contain the restriction sites *Nsi*I and *Pst*I. After digestion with the respective restriction enzymes, backbone and inserts were ligated resulting in the plasmids pTS1.4, pTS2.6, and pTS3.6. The inserts flanked by the *rdxA* regions were then amplified using oligonucleotides CSO-2276 and CSO-2277. Afterwards, the PCR products were electroporated into *C. jejuni* NCTC11168 Δ*truA* (CSS-2497), Δ*truB*, (CSS-1108), and Δ*truD* (CSS-3373), respectively. Correct integration of the constructs was subsequently verified by colony PCR using CSO-0349/0759 and by sequencing with CSO-0349, CSO-0759, CSO-3270. This resulted in the complementation strains C*truA* (CSS-2497), C*truB*, (CSS-3045), and C*truD* (CSS-5554).

Construction of the catalytically inactive CjTruD (D85N). Deletion of *truD* (Δ*truD*::Hyg^R) was complemented with a catalytically inactive *truD* (D85N) integrated in the *rdxA* locus. The expression of D85N mutant of *truD* is driven by the P*metK* promoter and fused to a 3xFLAG at its 3´end. Specifically, the point mutation in the *truD* (D85N) was generated by inverse PCR from pTS3.6 with oligonucleotides CSO-3839 and CSO-3840 and transformed into *E. coli*. The resulting plasmid was then amplified using oligonucleotides CSO-2276 and CSO-2277. The PCR product was electroporated into *C. jejuni* NCTC11168 Δ*truD* (CSS-3373). The colony PCR was performed using oligonucleotides CSO-0349 and CSO-0759. The presence of the point mutation was confirmed by sequencing using the oligonucleotides CSO-0349, CSO-0759, CSO-3270. This resulted in the D85N (CSS-5549) strain.

Introduction of chromosomal point mutation in the tRNA-Glu (Cjp03). To introduce the tRNA-Glu T→C point mutation in the tRNA-Glu at position 13 at the native locus, 888-bp region around the tRNA-Glu was amplified using the oligonucleotides CSO-3959/3960 thereby introducing *Xho*I and *Xba*I restriction sites in the corresponding PCR product. The plasmid pJV752.1 was extracted from the strain CSS-0180 and amplified using the oligonucleotides CSO-0873/874 that introduce *Xho*I and *Xba*I restriction sites. After *Xho*I and *Xba*I digestion, the product was then ligated into the similarly digested plasmid pJV752-1, resulting in plasmid pEF15.1. Plasmid pEF15.1 was checked by colony PCR using oligonucleotides pZE-A/CSO-3960 and sequenced with primer pZE-A. Next, the plasmid pEF15.1 was amplified by inverse PCR using CSO-3961/3962, introducing *BamH*I and *Nde*I restriction sites 40 nt upstream of the tRNA-Glu (Cjp03) native promoter. A gentamicin resistance cassette with its own promoter and terminator was amplified using CSO-0483/0576 and ligated into PCR-amplified pEF15 in the reverse orientation to Cjp03 using *Nde*I/*BamH*I restriction sites, resulting in plasmid pEF16.6. Plasmid pEF16.6 was

checked by colony PCR using primers CSO-0576/3960 and sequencing with CSO-3960. The tRNA-Glu T13C point mutation was then introduced into the tRNA-Glu by inverse PCR on pEF16.6 using complementary oligonucleotides harboring the desired mutation, followed by *Dpn*I digestion and transformation of the resulting purified PCR product into *E. coli* TOP10, resulting in pEF17.2. For introduction of the tRNA-Glu T13C mutation, oligonucleotides CSO-3996/3997 were used. To introduce the tRNA-Glu mutation into *C. jejuni*, a PCR product covering the homologous ends and the gentamicin resistance cassette was amplified from the respective WT tRNA-Glu (pEF16.6) using oligonucleotides CSO-3959/3960 and electroporated into *C. jejuni* NCTC11168 (CSS-0032). To confirm the introduction of point mutation in *C. jejuni*, a colony PCR was performed using CSO-0576/3226 sequencing with CSO-3960. This resulted in the tRNA-Glu T13T (CSS-6526) and tRNA-Glu T13C (CSS-6528) strains.

Cloning of transcriptional and translational reporter fusions. For the generation of a transcriptional reporter fusion, the promoter of Cj0414 and Cj0415, genes was fused to the 5' UTR and the coding sequence of the *hupB* gene fused together with sfGFP. The promoter region was amplified using the oligonucleotides CSO-5182/5183 and the plasmid backbone was amplified using the oligonucleotides CSO-3939/0347 using as template the plasmid pSSv100.2. After *Dpn*I digestion of the plasmid backbone, both the linearized plasmid and the amplified promoter region were digested with *Cla*I/*Kpn*I for 3 hours at 37 °C and ligated, resulting in pEF30.1. The resulting plasmid was then amplified using oligonucleotides CSO-2276 and CSO-2277. The PCR product was electroporated into *C. jejuni* NCTC11168 (CSS-0032). The colony PCR was performed using oligonucleotides CSO-0349 and CSO-0023, and sequencing with CSO-3270 and CSO-0023.

7.2.2.2 *Helicobacter pylori*

Construction of *H. pylori* deletion mutant strains by homologous recombination with overlap PCR products. For the generation of *H. pylori truA* and *truD* deletion strains, a construct containing the kanamycin resistance cassette flanked by ~500 nt up- and downstream of *truA* or *truD* open reading frame was generated by overlap-PCR. As an example, PCR products of up- and downstream regions of *truA* were generated with the primer pairs CSO-3496/3497 and CSO-3498/3499, respectively, and kanamycin resistance cassette was generated with the oligonucleotides HPK1/HPK2. The three PCR products were mixed together in a ratio of 50:90:50 ng and used as templates for overlap PCR using CSO-3491/3494. The resulting purified PCR product was used for natural transformation of *H. pylori* wild-type strain (CSO-0065). This resulted in the following strains: Δ*truA* (CSS-5485) and Δ*truD* (CSS-5488).

Complementation of Δ*truD* mutant in *H. pylori* with CjTruD and HpTruD. For the construction of TruD complementation strain in *H. pylori* 26695, the plasmid pSP109-6 was

amplified with primers CSO-4213/4287 that introduce an *Nsi*I restriction site and 37 nt of the 3xFLAG epitope-tag. CjTruD without the first and the last codon was amplified using the oligonucleotides CSO-2629/4216 that carry the *Nsi*I restriction site and 35 nt of the 3×FLAG epitope-tag. The *truD* gene from *H. pylori* 26695 was amplified using the oligonucleotides CSO-4098/4215. After *Nsi*I digestion of the linearized plasmid and insert (CjTruD or HpTruD), the insert was cloned into pSP109-6 resulting in the plasmid pEF22.1 (CjTruD) and pEF23.1 (HpTruD). The plasmids were checked by colony PCR using primers pZE-*Xba*I and CSO-2629 (CjTruD) or CSO-4098 (HpTruD). The *rdxA* (500 bp upstream)-*catGC*-*truD*-*rdxA* (500bp downstream) region was amplified using the oligonucleotides CSO-0017/0018 and transformed into *H. pylori* Δ*truD* strain (CSS-5483). The insertion of *truD* in the *rdxA* locus was verified by colony PCR using the oligonucleotides CSO-0205/0207 and sequenced using the oligonucleotides CSO-0205 and CSO-207.

7.2.2.3 *Escherichia coli*

Chemically competent *E. coli* cells using magnesium chloride ($MgCl_2$). A single colony of *E. coli* TOP10 was cultivated overnight in 5 ml of LB. 50 ml of Superbroth medium supplemented with 10 mM of $MgCl_2$ were inoculated with 350 µl of the overnight culture and the bacteria were grown until early exponential phase (OD_{600nm} of 0.3-0.4). Afterwards, the bacteria were transferred into pre-cooled centrifuge tube and spun down at 1,100 x *g* for 4 minutes at 4 °C. The supernatant was discarded and the bacterial pellet was resuspended in 15 ml of Tbf I buffer and incubated for 20 minutes on ice. The bacteria were centrifuged for 8 minutes at 785 x *g* at 4 °C and resuspended in 900 µl of Tbf II buffer and 30 µl aliquots were snap frozen in liquid nitrogen. The aliquots of competent cells were stored at -80 °C until use.

Transformation of chemically competent *E. coli* (plasmid construction). 30 µl of chemically competent *E. coli* TOP10 cells were incubated on ice for 30 minutes together with 5-10 µl of ligation reaction (50 ng of plasmid DNA and PCR product). To facilitate the entrance of the ligated plasmid inside the cells, the mixture bacteria-ligation reaction was heat-shocked for 90 seconds at 42 °C, followed by an incubation on ice for 5 minutes. Afterwards, 200 µl of SOC medium was added and the bacteria were recovered for 60 minutes at 37 °C shaking at 200 rpm. The bacteria were plated on LB-agar supplemented with the appropriate antibiotic.

7.3. DNA techniques

7.3.1. Quantification of nucleic acids (DNA and RNA)

The concentration of DNA or RNA samples (undiluted or 1:10 diluted) was measured using the NanoDrop2000.

7.3.2. Polymerase chain reaction (PCR)

To amplify specific fragments of DNA, PCR was performed using *Taq* or Phusion DNA polymerases, following the manufactures´ instructions.

7.3.2. Agarose gel electrophoresis

To separate DNA fragments, nine volumes of the samples were mixed with one volume of 10 x DNA loading dye and run on 1-2 % agarose in 1 x TAE for 30-40 minutes at 120-150 V, depending on the fragment size and on the gel apparatus, respectively.

7.3.3. Restriction digestion and ligation

To digest the template plasmid, PCR fragments amplified from plasmids were incubated with *Dpn*I for 3 hours at 37 °C. Restriction digestion on the insert and the plasmid was performed following the manufacturer´s instructions. Ligation of the digested insert and linearized vector was performed by T4 DNA ligase at 16 °C, overnight.

7.4. RNA techniques

7.4.1. RNA preparation

Bacterial cultures grown to exponential phase were collected to a final OD_{600nm} of 2.0 (*C. jejuni*) or 4.0 (*H. pylori*), mixed with 0.2 volumes of stop mix solution (5 % phenol and 95 % ethanol, vol/vol), snap-frozen in liquid nitrogen, and stored at -80 °C.

Total RNA isolation (hot phenol method). After thawing the frozen samples on ice, the cells were harvested by centrifugation for 10 minutes (*H. pylori*) or 20 minutes (*C. jejuni*) at 4 °C, 4,000 x *g*. Cell pellets were resuspended in 600 µl Tris-EDTA buffer (pH 8.0) containing 0.5 mg/ml lysozyme in and 60 µl of 10 % SDS. The samples were incubated for 2 minutes at 64 °C in a water bath and 66 µl of 1 M NaOAc (pH 5.2) was added. Total RNA was extracted using the hot phenol method as described previously (Sharma *et al.*, 2010; Dugar *et al.*, 2013).

7.4.2. DNase I digestion.

Before northern blot, primer extension and cDNA library analyses, potential genomic DNA was removed from total RNA samples by DNase I digestion. Briefly, 40 µg of total RNA was incubated at 37 °C for 45 minutes with 10 µl of DNase I (1 U/µl, Thermo Scientific), 1 µl of RNase inhibitor (20 U/µl) and 10 µl of DNase I buffer including $MgCl_2$ (Thermo Scientific). 1 µl of DNase I (1 U/µl, Thermo Scientific) was added to each sample for an additional 15 minutes. The digested DNA and enzymes were separated by P:C:I and the DNase I treated RNA was precipitated overnight in 1 volume of 30:1 100% ethanol: 3M NaOAc mix. Complete removal of gDNA was verified by control-

PCR using Taq-polymerase and JVO-0352 x JVO-0353 (for *H. pylori*) or CSO-0200 x CSO-0201 (for *C. jejuni*) on DNase I-treated RNA samples.

7.4.3. Northern blot analysis.

For northern blot analysis, 5 µg of total RNA in 2 x Gel Loading Buffer II [(GL II, 95 % (v/v) formamide, 18 µM EDTA (pH 8.0), and 0.025 % (w/v) SDS, 0.025 % (w/v) xylene cyanol, 0.025 % (w/v) and bromophenol blue)] was loaded for each sample, separated in 6 % denaturing PAA gels containing 7 M urea and transferred to Hybond-XL membranes (GE-Healthcare). After blotting, the RNA was UV-crosslinked to the membrane at 254 nm and hybridized to 10 µl of 5′ end-labeled (γ^{32}P) DNA oligonucleotides in 15 ml of Hybri-Quick buffer (Roth) at 42 °C. Afterwards, the membrane was washed in three steps using SSC buffer (20 min – 5 x SSC, 20 min – 1 x SSC and 20 min 0.5 x SSC). The screens were analyzed using Typhoon FLA 7000 and the intensities of the bands quantified using AIDA software (Raytest, Germany).

7.4.4. Rifampicin assay.

To determine the stability of the tRNA-Glu (Cjp03) in *C. jejuni* NCTC11168 wildtype, Δ*truD,* C*truD,* and D85N strains were grown to an OD_{600nm} of 0.4-0.5 and treated with freshly prepared rifampicin to a final concentration of 500 mg/ml. Samples were collected at different time points after treatment. RNA decay was analyzed by northern blot as described above.

7.4.5. CMC treatment and reversion.

CMC treatment and reversion were performed as described previously (Ofengand *et al.*, 2001). For CMC treatment, 1 M CMC was freshly prepared in BEU buffer (50 mM bicine pH 8.5, 4 mM EDTA, 7 M urea). Briefly, 20 µl of 1 M CMC was added to 20 µl of RNA dissolved in water and 80 µl of BEU buffer. For untreated samples, instead of 20 µl of 1 M CMC, 20 µl of BEU buffer was added. The samples were incubated for 40 minutes at 37 °C and then RNA was precipitated overnight with 180 µl water, 1.5 µl of Glycoblue (Ambion), and 900 µl of 30:1 ethanol NaOAc mix. The following day, the samples were centrifuged for 30 minutes at 13,000 rpm at 4 °C and washed with 200 µl of 70 % ethanol. For CMC reversion, the precipitated RNA was resuspended in 50 µl of 50 mM $NaCO_3$ (pH 10.4) and incubated for 4 hours at 37 °C. The RNA was precipitated overnight by adding 250 µl of water, 1.5 µl of Glycoblue, and 900 µl of 30:1 ethanol NaOAc mix.

7.4.6. Primer extension assay.

For primer extension assay, 500-2,000 ng of CMC treated/untreated RNA concentrated in 5.5 µl of H_2O was incubated with 1.0 µl of 5′ end-labeled (γ^{32}P) DNA oligonucleotide. To anneal the

labeled primers to the RNA, the temperature of the PCR machine was slowly decreased from 80 °C to 42 °C. Afterwards, a master mix containing 2.0 µl of 5× reverse transcriptase (RT) Buffer (Thermo Fisher Scientific), 1.0 µl of 10 mM dNTPs and 2.0 µl Maxima RT (diluted 1:5 in H_2O, Thermo Fisher Scientific) was added to each sample and the RT reaction was performed for 1 hour at 50 °C. The reaction was stopped by adding 10 µl of GLII and cDNA products were boiled for 2 minutes at 95 °C and immediately loaded on a pre-warmed 10 % denaturing PAA gel containing 7 M urea. The gel was transferred to Whatman paper and dried for approx. 40 minutes at 80 °C. The dried gel was exposed overnight and analyzed using a PhosphorImager (FLA-7000 Series, Fuji). For the DNA sequencing ladder, 1.5 pmol labeled oligonucleotide and 100-150 ng of PCR product corresponding to the region of interest were used in a reaction with 4.0 µl of sequencing buffer and 0.5 µl polymerase (Jena Bioscience).

7.4.7. *In-vitro* T7 transcription and *in-vitro* pseudouridylation assay.

DNA template containing the sequence of the tRNA-Glu (Cjp03) with the T7 promoter sequence was generated by PCR with DNA oligonucleotides listed in table 6.7. T7 transcription was carried out using the MEGAscript® T7 kit (Ambion). For the *in-vitro* pseudouridylation assay, 35 ODs of *E. coli* or *H. pylori* cultures were harvested by centrifugation for 20 minutes at 4 °C at 4,000 x *g* in 50 ml falcon tubes. After centrifugation, the bacterial pellet was resuspended in 1 ml of media and transferred in 2 ml tubes, and spun down for 4 minutes at 4 °C at 6,000 x *g*. The supernatant was discarded and the bacterial pellet was snap-frozen in liquid nitrogen and stored at -80 °C. After thawing, the bacterial pellet was resuspended in 700 µl of lysis buffer (20 mM Tris-HCl pH 7.5, 150 mM KCl, 1 mM $MgCl_2$, 1 mM DTT, 1mM PMSF, 0.2 % Triton X100, 20 U/ml DNase I, 200 U/ml RNase inhibitor) and mixed with an equal volume of 0.1 mm glass beads (Carl Roth N029.1). The cells were lysed by vortexing the tubes for 30 seconds and cooled on ice for 15 seconds. The vortexing step was repeated 10 times. The lysate was cleared from all cellular debris by centrifugation for 4 minutes at 16,900 x *g* at 4 °C. For the *in-vitro* assay, 2 µl of 10 µM *in-vitro* transcribed tRNA-Glu was incubated with 100 µl of lysate. The mixture was incubated at 37 °C for 45 minutes in the heating block. RNA was isolated by adding 1 volume of P:C:I and precipitated overnight in ethanol and NaOAc. The RNA was precipitated by centrifugation at 4 °C and at 16,900 x *g* for 30 minutes and washed with 70 % ethanol. The RNA was resuspended in 20 µl of H_2O and subjected to CMC treatment followed by primer extension as described above.

7.4.8. Quantitative real-time PCR (qRT-PCR)

The qRT-PCR experiments were performed in technical triplicates and in two biological replicates on a CFX96™ Real-time system (Biorad) using Power SYBR Green RNA-to-CT™ (1-step kit, Applied Biosystems) according to the manufactures´ instructions. For each reaction, 2.0 µl of RNA

sample (50 ng/reaction) was mixed with 0.1 µl of primers (10 µM), 0.08 µl of RT enzyme mix (125 x) and 5 µl Power SYBR Green RT-Mix (2 x). The total volume of the reaction was 10.0 µl. The reaction conditions were set to: 30 min 48 °C, 10 min 95 °C, and 50 cycles at 95 °C for 15 sec, 59 °C for 1 min, followed by a denaturing step at 95 °C for 15 sec. Melting curve detection were performed by stepwise increase of the temperature from 59 °C to 95 °C (0.5 °C every 15 sec). Fold changes were calculated using the $2^{-\Delta\Delta Ct}$ method described in (Livak & Schmittgen, 2001; Westermann *et al.*, 2016).

7.5. Protein techniques

7.5.1. Western blot analysis

Western blot analyses were performed using protein samples from cells collected from *C. jejuni* and *H. pylori* in exponential phase (*C. jejuni*: OD_{600nm} 0.4-0.6; *H. pylori* 0.7-0.8). Cells corresponding to a final OD_{600nm} of 1.0 were harvested by centrifugation at 16,900 x *g*, 4 °C for 2 minutes and resuspended in 100 µl of 1× protein loading dye (62.5 mM Tris-HCl, pH 6.8, 100 mM DTT, 10 % (v/v) glycerol, 2 % (w/v) SDS, 0.01 % (w/v) bromophenol blue) and heated at 95 °C for 8 minutes and shaking at 1,000 rpm. Whole cell lysates corresponding to an OD_{600nm} of 0.05-0.1 were separated by 12 % (vol/vol) SDS sodiumdodecylsulfate-polyacrylamide (SDS-PAA) gels and transferred to nitrocellulose membrane (GE-Healthcare) by semidry blotting. Membranes were blocked for 1 hour with 10 % (w/v) milk powder in Tris-buffered saline Tween-20 (TBS-T) and incubated with primary antibody at 4 °C shaking overnight. On the next day, the membrane was washed three times (20 minutes each) in TBS-T buffer, incubated for 1 hour with secondary antibody and washed again three times (20 minutes each) in TBS-T buffer. After washing, the blot was developed using enhanced chemiluminescence reagent. Membrane were analyzed using Image Quant LAS 4000.

7.5.2. CjTruD, HpTruD, and EcTruD protein identity

For comparison of CjTruD, HpTruD, and EcTruD, the amino acid sequence of the TruD protein corresponding to each bacterium was taken from https://www.genome.jp/kegg/kegg2.html. The protein identity (%) was calculated using the tool https://web.expasy.org/sim/ with the default parameters: number of alignments to be computed: 20; gap open penalty: 12; gap extension penalty: 4; comparison Matrix: BLOSUM62.

7.5.3. PUS enzymes and tRNA comparisons in different bacterial species

The analyses about the presence or absence of the different PUS enzymes and their putative tRNA substrates were based on the manual search of potential homologs of the *E. coli* K-12 PUS enzymes

in the genomes of *Salmonella* Typhimurium SL1344, *Vibrio cholerae* 0395, *Yersinia pestis* PBM19, *Shigella flexneri* 2457T, *Citrobacter rodentium* ICC168, *Serratia marcescens* SM39, *Haemophilus ducreyi* 35000HP, *Wolinella succinogenes* DSM1740, *Campylobacter jejuni* NCTC11168, *Helicobacter pylori* 26695, *Bacillus subtilis* 168, and *Mycoplasma pneumoniae* M129 strain. The amino acid sequence of the corresponding *E. coli* PUS enzyme was BLAST against the MGENES database of *C. jejuni* (cje) or *H. pylori* (hpy) using the website https://www.genome.jp/tools/blast/. The number of tRNAs in *E. coli* K-12, *Salmonella* Typhimurium SL1344, *Vibrio cholerae* 0395, *Yersinia pestis* PBM19, *Shigella flexneri* 2457T, *Citrobacter rodentium* ICC168, *Serratia marcescens* SM39, *Haemophilus ducreyi* 35000HP, *Wolinella succinogenes* DSM1740, *Campylobacter jejuni* NCTC11168, *Helicobacter pylori* 26695, *Bacillus subtilis* 168, and *Mycoplasma pneumoniae* M129 were identified based on GtRNAdb (http://gtrnadb.ucsc.edu/).

7.6. Glycerol gradient

Glycerol gradient experiments were performed accordingly to (Hör *et al.*, 2020a, 2020b). *C. jejuni* wildtype, TruD-3xFLAG, S1-3xFLAG, and L1-3xFLAG strains were grown to an OD_{600nm} of 0.55/0.60. Bacteria were harvested by fast filtration and washed with 700 µl of lysis buffer (20 mM Tris-HCl pH 7.5, 150 mM KCl, 1 mM $MgCl_2$, and 1 mM DTT), transferred in 2.0 ml Eppendorf and spun down for 5 minutes at 4 °C, 16,200 x *g*. The pellet was resuspended in 500 µl of lysis buffer, followed by addition of 750 µl of 0.1 mm of glass beads. The lysis was performed by vortexing at highest power for 30 s followed by cooling 15 s on ice. The procedure was repeated 10 times. The lysate was then cleared by cellular debris by centrifugation for 10 minutes at 4 °C, 16,200 x *g*. 20 µl of the lysate were collected and mixed together with 20 µl of 5 x protein loading dye for the lysate sample. For each strain, 20 Absorbance (260nm) of lysate was loaded on top of the 10-40 % glycerol gradient. Gradient centrifugation was performed for 17 hours at 4 °C, 100,000 x *g*. For each fraction, 590 µl were collected manually (from fraction 1 to 20). The pellet fraction was resuspended in the last ~300 µl of the gradient. The UV profile of each gradient result from the measurement of 1.5 µl of each fraction. For protein analysis, 90 µl of each gradient were mixed with 30 µl of 5 x protein loading dye.

7.7 TruA and TruD expression and purification

The *truA* and *truD* coding sequence were fused to the ribosome binding site of ArsR and at the C-terminus to the Strep-tag (WSHPQFEK). Additionally, two amino acid spacer (SA) was added between the protein and the tag to increase the accessibility of the tag during purification. The *truA* and *truD* coding sequence (excluding the STOP codon) were amplified from the genomic DNA of *C. jejuni* NCTC11168 using the oligonucleotides CSO-2627/2827 and CSO-2629/2869,

respectively. The plasmid backbone was amplified from the plasmid pPT33.1 using the oligonucleotides CSO-2959/1056. Both linearized plasmid and amplified coding sequence were digested with *Nsi*I and ligated overnight at 16 °C, resulting in plasmid pEF3.2 and pEF5.1. Plasmids pEF3.2 and pEF5.1 were checked by colony PCR using oligonucleotides pBAD-FW/CSO-2867 and pBAD-FW/CSO-2869, respectively and sequenced with oligonucleotides pBAD-FW and CSO-0881. Plasmid pEF3.2 and pEF5.1 were introduced into an *E. coli* TOP10 strain resulting in strains CSS-3042 and CSS-3044. Strains CSS-3042 and 3044 and were grown in 1 l of LB broth to a final OD_{600nm} of 0.4 and induced with 0.001 % of L-arabinose at 20 °C overnight for TruD expression and with 0.02 % of L- arabinose at 18 °C overnight for TruA expression. Cells were harvested by centrifugation at 4,000 x *g* for 20 minutes at 4 °C and stored at -80 °C until use. The pellet was resuspended in 1 ml of Buffer W (IBA GmbH, #2-1003-100) and mechanically lysed using Retsch MM400 ball mill (5 times of vibrational frequency of 15 for 3 minutes). 3 ml of Buffer W was added and split into 2 ml tubes, the insoluble aggregates were centrifuged down for 15 minutes at 16,200 x *g* at 4 °C. The lysate was loaded onto the *Strep*-Tactin column and the rest of the protocol was followed as per the manufacture's instructions. After 5 washing steps (1 ml), TruA-Strep and TruD-Strep proteins were eluted using Buffer E (500 µl) in five successive steps (E1 to E5). The majority of TruA and TruD proteins were concentrated in the E3 fraction. Concentration was quantified using Roti®-Quant, and the protein was stored at -20 °C in 20 µl aliquots.

7.8. Sample preparation for Pseudo-seq, RIP-seq, RNA-seq, CLIP-seq, and Ribo-seq

Pseudo-seq *Campylobacter jejuni*. 5 µg of total RNA (DNase I digested) of *C. jejuni* WT and mutant strains was depleted from ribosomal RNA (23S and 16S rRNA) using Ribo-zero (Bacteria) (Illumina), resulting in ~ 1.0 µg of RNA. The RNA was treated with CMC as described above (CMC treatment and reversion).

Pseudo-seq *Helicobacter pylori*. 10 µg of total RNA (DNase I digested) of *H. pylori* WT and mutant strains was depleted from ribosomal RNA (23S and 16S rRNA) using MICROBExpress (Thermo Fisher), resulting in ~ 3.5-3.8 µg of RNA. The RNA was treated with CMC as described above (CMC treatment and reversion).

RIP-sequencing. CoIP of *C. jejuni* strains with an anti-FLAG antibody/anti-pseudouridine antibody was performed as described in (Dugar *et al.*, 2016). The strains were grown to exponential phase (OD_{600nm} of 0.5/0.6). Cells were harvested by centrifugation at 6,000 x *g* for 15 min at 4 °C and cell pellets were resuspended in 1 ml of Buffer A (20 mM Tris-HCl, pH 8.0, 150 mM KCl, 1 mM $MgCl_2$, 1 mM DTT) and centrifuged at 11,200 x *g* for 5 minutes at 4 °C. The supernatant was discarded and snap-frozen in liquid nitrogen and stored at -80 °C. The bacterial pellet was thawed on ice and resuspended in 700 µl of lysis buffer (20 mM Tris pH 8.0, 1 mM $MgCl_2$, 150 mM

KCl, 1 mM DTT) and an equal volume of glass beads (~800 µl) was added. Cells were then lysed using a Retsch MM400 ball mill (frequency 30 s^{-1}, 10 min) in pre-cooled blocks (4 °C), and centrifuged for 2 min at 15,200 x *g*, 4 °C. The supernatant was transferred to a new tube, and additional 400 µl of Buffer A was added to ensure the complete lysis of all the cells, followed by a second round of lysis at 30 s^{-1} for 5 min. The second supernatant was pooled with the first and the combined supernatant was centrifuged for 30 minutes at 15,200 x *g*. The lysate was transferred to a new tube and 35 µl of anti-FLAG antibody or 20 µl of anti-pseudouridine antibody were incubated for 30 minutes at 4 °C on a rocker. For each sample, 75 µl of prewashed Protein A-Sepharose was added and incubated for additional 30 minutes at 4 °C, followed by a centrifugation at 15,200 x *g* for 1 minute. Afterwards, the beads were washed with 500 µl of Buffer A for a total of 5 times. To separate the RNA and protein fraction, 500 µl of Buffer A was added to the beads followed by phenol-chloroform-isoamyl alcohol extraction. To check the correct steps of the coIP, protein samples equivalent to 1.0 OD_{600nm} of cells were collected during different stages of the coIP and were run on a western blot and 100 µl of 1× protein loading buffer was added to the protein samples and boiled for 8 min. Protein sample corresponding to an OD_{600nm} of 0.1 or 0.15 (culture, lysate, supernatant and wash fraction) and 10 or 5 (for proteins precipitated from beads) were used for western blots analysis.

RNA sequencing. RNA-seq analysis was performed on the transcriptome of *C. jejuni* WT, Δ*truD*, C*truD*, and D85N strains grown in Brucella Broth to mid-exponential phase (OD_{600nm} of ~0.55-0.6 for WT, C*truD*, and D85N strains, and OD_{600nm} of ~0.4 for Δ*truD*). Total RNA was extracted using the hot-phenol method described in (Sharma *et al.*, 2010). To gain insights into low expressed transcripts, 23S and 16S rRNAs were depleted from 5.0 µg of DNase I digested RNA using the Ribo-zero kit (Bacteria).

CLIP-sequencing. Bacteria were grown as described above. When the bacteria reached an OD_{600nm} of 0.5-0.6, 50 ml of culture was transferred to a square culture dish and irradiated with 800 mJ/ cm^2 UV-C light (254 nm crosslinked sample) and transferred to a 50 ml centrifuge tube. The same procedure was performed with 50 ml of not irradiated culture (non-crosslinked sample control). The tubes were centrifuged at 4,000 x *g* for 30 minutes at 4 °C. The supernatant was discarded and the bacterial pellet was snap-frozen in liquid nitrogen and stored at -80 °C until use. The pellet was resuspended in 800 µl of NP-T buffer (50 mM NaH_2PO_4, 300 mM NaCl, 0.05 % Tween, pH 8.0) and added in 1 ml of glass beads for the mechanical lysis. The tubes were placed in an adapter that was located in the grinding mill (Retsch MM400) and the cells were lysed at 30 s^{-1} for 10 minutes. The lysate was cleared by centrifugation for 15 minutes at 16,000 x *g* at 4 °C and the supernatant was transferred to a new 2 ml tube. The volume of the lysate was measured and 1 volume of NP-T buffer with 8 M urea was added to each tube that was followed by incubation

of the tubes for 5 minutes at 65 °C by shaking at 900 rpm. The lysate was (1:10) diluted in NP-T buffer and kept on ice. Meanwhile 20 µl of anti-FLAG® M2 magnetic bead suspension was washed 3 times in 800 µl of NP-T buffer and added in the 15 ml tubes containing the diluted lysate. The mixture of lysate and beads was incubated on a tube roller for 1 hour at 4 °C. After the incubation time, the beads were washed 2 times with High salt buffer (50 mM NaH_2PO_4, 1 M NaCl, 0.05 % Tween, pH 8.0) and 2 times with NP-T buffer. For the digestion of unprotected RNA and DNA, each lysate was incubated with 25 u of Benzonase in 100 µl of NP-T buffer + 1 mM $MgCl_2$. The samples were incubated for 10 minutes at 37 °C by shaking at 900 rpm and washed 2 times with NP-T Buffer and 2 times with CIP buffer (100 mM NaCl, 50 mM Tris-HCl pH 7.4, 10 mM $MgCl_2$). To dephosphorylate the 5´ end of the RNA, the beads were incubated with 10 u of CIP (calf intestinal alkaline phosphatase) in 100 µl of CIP buffer at 37 °C for 30 minutes by shaking at 800 rpm. The beads were washed one time with 500 µl of High-salt buffer and 2 times with 500 µl of PNK A buffer. For the verification of the successful IP, 50 µl of beads in PNK buffer were collected and resuspended in 20 µl of 1 x PL and boiled at 95 °C for 8 minutes and 10 µl of each sample was loaded on a western blot. The dephosphorylated RNA was labeled at its 5´ end in 50 µl PNK solution containing 49 µl of PNK A buffer, 0.5 µl of PNK, and 0.5 µl of γ-^{32}P-ATP. The tubes were placed on the magnetic rack, the supernatant was removed and the beads resuspended in 50 µl of PNK solution for 30 minutes at 37 °C without shaking. 10 µl of 1 mM non-radioactive ATP was added and incubated for 5 minutes at 37 °C and then washed in 1 ml of NP-T buffer. The beads were resuspended in 10 µl of 2 x PL, incubated for 2 minutes at 95 °C and moved into new tubes. The elution was repeated one additional time. The magnetic beads were separated from the elution sample after incubation in a magnetic rack and the supernatant (~20 µl) was loaded on a 12 % SDS-PAA gel that was transferred to a nitrocellulose membrane. After semi-dry blotting, the membrane was exposed to a phosphor screen overnight and the radioactive signal was used to identify the RNA-protein complexes. Thus, the membrane was cut in the crosslinked samples as well as in the non-crosslinked sample and in order to remove the protein of interested, the membrane was incubated 1 hour at 37 °C by shaking at 800 rpm with 200 µl of Proteinase K (PK) solution (50 mM Tris-Hcl pH 7.4, 75 mM NaCl, 6 mM EDTA, 1 % SDS, 10 units of Ribonuclease Inhibitor and 0.4 mg Proteinase K). 100 µl of PK solution + 9 M urea was additionally incubated with the membrane for 1 hour at 37 °C by shaking at 800 rpm. ~250 µl of the PK solution/urea was mixed with 250 µl of Phenol:Chloroform:Isoamyl alcohol in a PLG tube and incubated 5 minutes at 30 °C at 1,000 rpm and the aqueous phase was precipitated overnight with 600 µl of Ethanol (100 %), 20 µl of NaAc (3 M, pH 5.2), 1 µl of GlycoBlue. The RNA was precipitated by centrifugation for 30 minutes at 4 °C and washed twice with 80 % Ethanol. The precipitate was dissolved in 10 µl of H_2O. and used for cDNA library preparation (Next Multiplex Small RNA Library Prep Set for Illumina, #E7300, NEB) according to the manufacturer's instructions.

Ribo-seq. For Ribo-seq experiment, *Campylobacter jejuni* NCTC11168 WT, Δ*truD*, and C*truD* strains was grown on Müller-Hinton agar plates supplemented with 10 μg/ml vancomycin. Routinely, *Campylobacter jejuni* strain was grown in 15 ml or 50 ml of Brucella broth liquid supplemented with 10 μg/ml vancomycin media at 37°C in microaerophilic conditions (10% CO_2, 5% O_2) to an OD_{600nm} of ~0.55-0.6 for WT, and C*truD* strains, and OD_{600nm} of ~0.4 for Δ*truD* corresponding to late exponential phase. Before adding chloramphenicol, a total amount of 2 OD_{600} of bacterial cells was mixed with 0.2 volumes of stop mix (95% ethanol and 5% phenol, v/v) for RNA-seq experiment. To stop translation, 50-60 OD of bacterial cells were combined and treated with 1 mg/ml of chloramphenicol for 3 minutes at 37°C in shaking conditions. After chloramphenicol treatment, 100 ml of ice mixed with 1 mg/ml of chloramphenicol was added in 250 ml of polycarbonate centrifuge bottles with 100 ml of bacteria. The bottles were kept on ice for approximately 10 minutes, shaking continuously and centrifuged for 10 minutes at 5000 rpm (Sorvall) at 4°C. The ice was discarded and the cell pellet was resuspended in 2 ml of ice-media and transferred to a 2ml Eppendorf tube. The cells were centrifuged for 5 minutes at 8000 *g*, the supernatant was discarded and the cell pellet was snap freeze in liquid nitrogen. The pellet was lysed using Retsch (15 Herzt, 5 times, 3 minutes), using 1.0 ml of lysis buffer (100 mM NH_4Cl, 25 mM $MgCl_2$, 20 mM Tris-HCl pH 8.0, 0.1 % 10 % NP-40, 0.4% 40% Triton X-100, 0.1 mg/ml chloramphenicol, 50 U/ml DNase I). 17-20 Abs of lysate was loaded on 10-55% sucrose gradient and centrifuged for 2.5 hours, 350,000 rpm, 4°C (Beckman Coulter, Ultracentrifuge). Fractions corresponding to the Free RNA, 30S, 50S, 70S and polysome peaks were collected manually and the Eppendorf tube immediately snap freeze in liquid nitrogen. For RNA-seq experiment, frozen samples were thaw on ice, centrifuged for 20 minutes at 4000 rpm, at 4°C. The supernatant was discarded and the cell pellets were lysed by resuspension in 600 μl of a solution of 0.5 mg/ml of lysozyme in TE buffer and 10 μl 10% SDS. The samples were incubated for 2 minutes at 65°C to complete the lysis. The total RNA was extracted using the hot phenol method. Total RNA was ribosomal RNA depleted using Ribo-zero (Bacteria). For ribosome footprints, frozen samples were thaw on ice and 10% SDS was added in each sample. RNA was isolated using warm PCI extraction. Approximately 800 ng of rRNA depleted RNA and 20 μg of ribosome footprints were size selected using 26 nt and 34 nt markes in a 15% polyacrylamide, 7 M urea gel. The selected RNA was extracted from the gel using a RNA extraction buffer and precipitated using isopropanol and 1.5 μl of Glycoblue for 3 hours in - 20 °C. After precipitation the RNA was dissolved in 10.0 μl of water.

7.9 cDNA library preparation.

cDNA library preparation for Pseudo-seq. cDNA libraries for Pseudo-seq experiments were generated adapting the protocol described in (McGlincy & Ingolia, 2017). Fragmentation of CMC treated and untreated samples were performed using Ambion Kit (AM8740 kit). After fragmentation, products of ~ 40/50 – 150 nt were size-selected on a 15 % PAA, 7 M urea gel. After gel purification, the RNA was concentrated in 10 µl of H_2O and 3.5 µl of it was dephosphorylated for 1 hour at 37 °C using 0.5 µl of T4 PNK (10 U/µl), 0.5 µl of T4 PNK buffer, and 0.5 µl of Nucleoribonuclease inhibitor (20 U/µl, Molox). 0.5 µl of preadenylated DNA linker (100 µM) was ligated to the 3' end of the RNA using 3.5 µl of 50 w/v PEG-8000, 0.5 µl 10X T4 RNA ligase buffer and 0.5 µl T4 RNA ligase. The ligation was performed at 22 °C for 3 hours. The unligated DNA linker was degraded by 0.25 µl Yeast 5´-deadenylase (20 U/µl, NEB) and 0.5 µl RecJ (10 U/µl, Epicenter) directly to the ligation reaction and incubated 45 min at 30 °C. The ligated RNA was concentrated in 12 µl and converted into single stranded cDNA (sscDNA) products using 4 µl of 5x Protoscript II Buffer, 1 µl of 10 mM dNTPs, 1 µl of 0.1 M DTT, 1 µl of Nucleoribonuclease inhibitor (20 U/µl, Molox) and 1 µl of Protoscript II (200 U/µl) for 30 minutes at 50 °C. The RNA template was hydrolyzed by adding 2.2 µl 1 M NaOH to each reaction and incubating at 70 °C for 20 min. The RT products were gel-purified and size-selected on a 15 % PAA, 7 M urea gel and dissolved in 12 µl of 10 mM Tris pH 8.0. The purified cDNA was circularized using 2 µl of 10X CircLigase II buffer, 4 µl of Betaine, 1 µl of 50 mM $MnCl_2$ and 1 µl CircLigase II (100 U/µl) and incubated for 1 hour at 60°C. The PCR was performed in a total volume of 100 µl using 20 µl of 5X of Phusion HF buffer, 2.0 µl of 10 mM dNTPs, 5.0 µl of 10 µM of RPF primer, 5.0 µl of 10 µM of NEBNext Primer for Illumina Sequencing [Set 1: 1-12 (NEB, #E7335L); Set 2: 13-24 (NEB, #E7500L)], 5.0 µl of circularized cDNA, and 1.0 µl of Phusion polymerase (2 U/µl). Different PCR cycles were performed. The PCR product was size-selected from an 8 % PAA gel and dissolved in 12 µl of H_2O. Samples were sequenced using Illumina NextSeq 500 with ~ 15-60 million reads per library.

cDNA library preparation for RNA-seq and for RIP-seq: cDNA libraries for Illumina sequencing were constructed by Vertis Biotechnologie AG (Germany) as described previously (Westermann *et al.*, 2016). Briefly, an oligonucleotide adapter was ligated to the 3' end of the RNA molecules. Afterwards, first-strand cDNA synthesis was performed using M-MLV reverse transcriptase and the 3’ adapter was used as a primer. The firststrand cDNA was purified and the 5' Illumina TruSeq sequencing adapter was ligated to the 3' end of the antisense cDNA. The resulting cDNA was PCR-amplified to about 10-20 ng/µl using a high-fidelity DNA polymerase The cDNA was purified using the Agencourt AMPure XP kit (Beckman Coulter Genomics) and was

analyzed by capillary electrophoresis. Samples were sequenced using Illumina NextSeq 500 with ~ 15 million reads per library for RNA-seq and ~ 2 million reads per library.

cDNA library preparation for CLIP-seq: cDNA libraries for CLIP-seq experiment were prepared using the Next Multiplex Small RNA Library Prep Set for Illumina (#E7300, NEB) according to the manufacturer's instructions. Samples were sequenced using Illumina NextSeq 500 with ~ 20 million reads per library for RNA-seq and ~ 2 million reads per library.

cDNA library preparation for Ribo-seq: cDNA libraries for Illumina sequencing were constructed by Vertis Biotechnologie AG (Germany). Briefly, oligonucleotide adapters were ligated to the 5' and 3' ends of the small RNA samples. First-strand cDNA synthesis was performed using M-MLV reverse transcriptase and the 3' adapter as primer. The resulting cDNA was amplified with PCR using a high-fidelity DNA polymerase.The cDNA was purified using the Agencourt AMPure XP kit (Beckman Coulter Genomics) and was analyzed by capillary electrophoresis.

7.10 Bioinformatic analyses

Processing of sequence reads. To assure high sequence quality, Illumina reads were quality and adapter trimmed via Cutadapt (Martin, 2011; DOI: https://doi.org/10.14806/ej.17.1.200) version 1.16/1.17/2.5 using a cutoff Phred score of 20 in NextSeq mode and reads without any remaining bases were discarded (command line parameters: --nextseq-trim=20 -m 1 -a CTGTAGGCACCATCAATAGATCGGAAGAGCACACGTCTGAACTCCAGTCAC).

Read alignment. After trimming, the pipeline READemption (Förstner et al., 2014) version 0.4.5 was applied to align all reads longer than 11 nt to the respective reference genome (*Campylobacter jejuni* NCTC 11168: NC_002163.1; *Helicobacter pylori* 26695: NC_000915.1) using segemehl version 0.2.0 (Hoffmann et al., 2009) with an accuracy cut-off of 95%.

RNA-seq experiment. After high-throughput sequencing, cDNA reads were processed and mapped to the reference genome of *C. jejuni* NCTC11168 (NC_ 002163) based on the READemption pipeline (Förstner *et al.*, 2014). Aligned cDNA reads were converted into coverage plots in BAM (Binary Alignment/Map) or wiggle format. The wiggle files can be loaded into the Integrated Genome Browser (IGB) that allows to visually check and compare reads that belong to the individual cDNA libraries. The pairwise expression comparison between two strains was performed based on the DESeq2 approach (Love *et al.*, 2014).

RIP-seq experiment and CLIP-seq experiment. The bioinformatic analysis for RIP-seq was performed as described in (Dugar *et al*., 2014) and the bioinformatic analysis for CLIP-seq was performed as described in (Holmqvist *et al*., 2016).

Ribo-seq experiment. The bioinformatic analysis was performed as described in (Gelhausen et al., 2021). The version of HRIBO used is the 1.4.4.Briefly, HRIBO performs adapter trimming with Cutadapt (Martin, 2011) and then maps the reads to the genome with segemehl. Multimapping/rRNA reads are then removed with samtools (Li *et al.*, 2009) before further processing. FastQC (Andrews *et al.*, 2010) and featurecount (Liao *et al*., 2014). Afterwards, the mapped reads are then used to compute differential expression analysis.

Pseudo-seq experiment.

Coverage generation. READemption was applied to generate two kinds of positional coverage files, total coverage based on full-length alignments (reademption coverage --project_path $READEMPTION_FOLDER) and first base coverage mapping only the 5'-end base of each alignment (reademption coverage -b first_base_only --project_path $READEMPTION_FOLDER_FBO). Afterwards, all raw coverage files were merged in a coverage data table with one row for each genomic position and strand. The first three columns consist of sequence id, position and strand (+/-). Column 4 contains the DNA base of the upstream position (A/T/G/C) followed by columns with total coverage and first base coverage values for each sequencing library.

Statistical analysis of pseudouridinylated sites. The coverage data table was used as input for an R script developed for detection of pseudouridinylation sites based on enrichment of CMC-treated libraries compared to untreated ones. The script requires installation of the Bioconductor packages edgeR (REF) and limma (REF). Column names need to be of the format mutant_treatment_batch_dataType without further underscores to allow extraction of variable values. Here, mutant represents the genetic background (WT or specific tRNA pseudouridine synthase deletion), treatment describes if a library was treated with CMC or not (plus/minus), the batch variable is used for batch correction as our samples were not all processed at the same time, and dataType represents either total (cov) or first base coverage (start). Analysis was conducted for each genetic background separately and consisted of the following steps. First, the data table was filtered to keep only rows with a T in column 4 and a value ≥ 5 for first base coverage in at least 50% of the libraries. Afterwards, the data was imported into edgeR and normalized via the TMM method. The resulting DGElist object was passed to the limma voom function for statistical analysis based on the design formula ~0+conds+batch with conds as the concatenation

treatment_dataType. After fitting of a linear model, the following fold change was applied for the comparison: (plus_start / plus_cov) / (minus_start / minus_cov).

8. APPENDIX

Appendix Figure 1

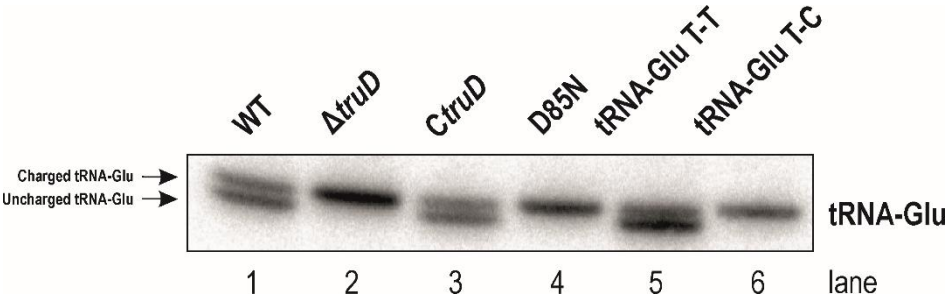

Acidic northern blot of different *C. jejuni* strains. Extraction of RNA samples and acidic northern blot conditions was described in (Janssen *et al.*, 2012).

Appendix Figure 2

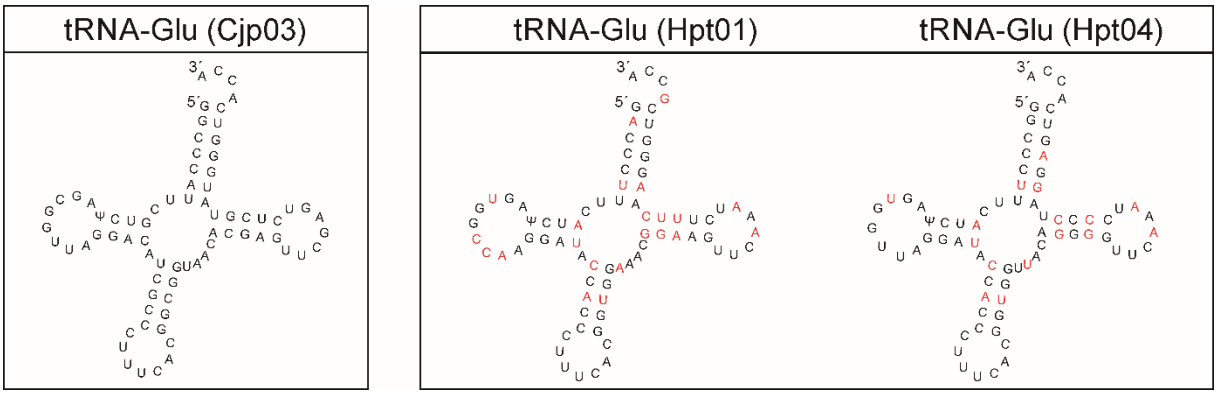

Secondary structure of *C. jejuni* tRNA-Glu (Cjp03) and *H. pylori* tRNA-Glu (Hpt01 & Hpt04). The red nucleotides in red in Hpt01 and Hpt04 are the ones that are different compared to Cjp03.

Appendix Table 1: List of genes encoding for tRNA and rRNA modification factors annotated in *C. jejuni* NCTC11168. The list of genes encoding for tRNA and rRNA modification factors was retrieved from KEGG-database (https://www.genome.jp/kegg/). The genes are listed based on the locus tag.

tRNA modification factors	
Cj0016	7-cyano-7-deazaguanine synthase
Cj0053c	*mnmA*; tRNA-specific 2-thiouridylase MnmA
Cj0123c	tRNA-dihydrouridine synthase
Cj0133	glycoprotease family protein
Cj0159c	6-pyruvoyl-tetrahydropterin synthase
Cj0160c	7-carboxy-7-deazaguanine synthase
Cj0166	*miaA*; tRNA dimethylallyltransferase
Cj0240c	*iscS*; cysteine desulfurase
Cj0272	epoxyqueuosine reductase
Cj0458c	*miaB*; tRNA-2-methylthio-N(6)-dimethylallyladenosine synthase
Cj0500	rhodanese-like domain-containing protein
Cj0577c	*queA*; S-adenosylmethionine-tRNA ribosyltransferase-isomerase
Cj0590	tRNA (cmo5U34)-methyltransferase
Cj0668	*tsaE*; tRNA threonylcarbamoyladenosine biosynthesis protein TsaE
Cj0713	*trmD*; tRNA (guanine-N(1)-)-methyltransferase
Cj0827	*truA*; tRNA pseudouridine synthase A
Cj0831c	*trmA*; tRNA/tmRNA (uracil-C(5))-methyltransferase
Cj0904c	tRNA (cytidine(34)-2'-O)-methyltransferase
Cj0956c	*trmE*; tRNA modification GTPase
Cj0976	tRNA (mo5U34)-methyltransferase
Cj1010	*tgt*; queuine tRNA-ribosyltransferase
Cj1102	*truB*; tRNA pseudouridine synthase B
Cj1188c	*gidA*; tRNA uridine 5-carboxymethylaminomethyl modification protein GidA
Cj1268c	*mnmC*; bifunctional tRNA (mnm(5)s(2)U34)-methyltransferase/FAD-dependent cmnm(5)s(2)U34 oxidoreductase
Cj1278c	*trmB*; tRNA (guanine-N(7)-)-methyltransferase
Cj1344c	tRNA N6-adenosine threonylcarbamoyltransferase
Cj1453c	*tilS*; tRNA(Ile)-lysidine synthase
Cj1457c	*truD*; tRNA pseudouridine synthase D
Cj1504c	*selD*; selenide,water dikinase
Cj1633	tRNA-uridine 2-sulfurtransferase
Cj1724c	7-cyano-7-deazaguanine reductase
rRNA modification factors	
Cj0022c	23S rRNA pseudouridine1911/1915/1917 synthase
Cj0126c	23S rRNA (pseudouridine1915-N3)-methyltransferase
Cj0153c	23S rRNA (guanosine(2251)-2'-O)-methyltransferase RlmB
Cj0154c	16S rRNA (cytidine1402-2'-O)-methyltransferase
Cj0156c	16S rRNA (uracil(1498)-N(3))-methyltransferase
Cj0588	23S rRNA (cytidine1920-2'-O)/16S rRNA (cytidine1409-2'-O)-methyltransferase
Cj0693c	16S rRNA (cytosine1402-N4)-methyltransferase
Cj0708	23S rRNA pseudouridine1911/1915/1917 synthase
Cj0712	*rimM*; ribosome maturation factor RimM
Cj0997	16S rRNA (guanine527-N7)-methyltransferase
Cj1117c	*prmA*; 50S ribosomal protein L11 methyltransferase
Cj1280c	23S rRNA pseudouridine1911/1915/1917 synthase
Cj1454c	ribosomal protein S12 methylthiotransferase

Cj1711c	*ksgA*; rRNA small subunit methyltransferase A
Cj1713	23S rRNA (adenine(2503)-C(2))-methyltransferase RlmN

Appendix Table 2: List of genes encoding tRNA and rRNA modification factors annotated in *H. pylori* 26695. The list of genes encoding for tRNA and rRNA modification factors was retrieved from KEGG-database (https://www.genome.jp/kegg/). The genes are listed based on the locus tag.

tRNA modification factors	
HP_0013	tRNA-uridine 2-sulfurtransferase
HP_0100	epoxyqueuosine reductase
HP_0213	glucose inhibited division protein (gidA)
HP_0220	cysteine desulfurase
HP_0269	tRNA-2-methylthio-N6-dimethylallyladenosine synthase
HP_0281	queuine tRNA-ribosyltransferase
HP_0361	*truA*; tRNA pseudouridine synthase A
HP_0388	tRNA (cmo5U34)-methyltransferase
HP_0419	tRNA (mo5U34)-methyltransferase
HP_0639	7-cyano-7-deazaguanine synthase
HP_0716	tRNA threonylcarbamoyladenosine biosynthesis protein TsaE
HP_0727	tRNA-dihydrouridine synthase B
HP_0728	tRNA(Ile)-lysidine synthase
HP_0747	tRNA (guanine-N7-)-methyltransferase
HP_0926	*truD*; tRNA pseudouridine synthase D
HP_0933	6-pyruvoyltetrahydropterin/6-carboxytetrahydropterin synthase
HP_0934	7-carboxy-7-deazaguanine synthase
HP_1051	tRNA threonylcarbamoyladenosine biosynthesis protein TsaB
HP_1062	S-adenosylmethionine:tRNA ribosyltransferase-isomerase (queA)
HP_1148	*trmD*; tRNA (guanine-N(1)-)-methyltransferase
HP_1413	7-cyano-7-deazaguanine reductase
HP_1415	tRNA delta(2)-isopentenylpyrophosphate transferase (miaA)
HP_1452	tRNA modification GTPase
HP_1584	tRNA N6-adenosine threonylcarbamoyltransferase
rRNA modification factors	
HP_0347	23S rRNA pseudouridine1911/1915/1917 synthase
HP_0374	16S rRNA (uracil1498-N3)-methyltransferase
HP_0552	16S rRNA (cytidine1402-2'-O)-methyltransferase
HP_0553	23S rRNA (guanosine2251-2'-O)-methyltransferase
HP_0707	16S rRNA (cytosine1402-N4)-methyltransferase
HP_0734	ribosomal protein S12 methylthiotransferase
HP_0745	23S rRNA pseudouridine1911/1915/1917 synthase
HP_0949	23S rRNA (pseudouridine1915-N3)-methyltransferase
HP_0956	23S rRNA pseudouridine955/2504/2580 synthase
HP_1063	16S rRNA (guanine527-N7)-methyltransferase
HP_1068	ribosomal protein L11 methyltransferase
HP_1086	23S rRNA (cytidine1920-2'-O)/16S rRNA (cytidine1409-2'-O)-methyltransferase
HP_1149	16S rRNA processing protein RimM
HP_1428	23S rRNA (adenine2503-C2)-methyltransferase
HP_1431	16S rRNA (adenine1518-N6/adenine1519-N6)-dimethyltransferase
HP_1459	23S rRNA pseudouridine2605 synthase

Appendix Table 3. Mapping statistics for Pseudo-seq experiments of *Campylobacter jejuni* WT. The table indicates the total number of sequenced reads (number of input reads), the number of reads that were removed from the analysis because too short, the total number of mapped reads, the number of alignments (i.e. some reads map to different locations with the same score), and the number of uniquely mapped reads. For the number of input reads and the number of uniquely mapped reads, the percentage value are also listed.

Libraries	**CMC +**	**CMC -**
Number of input reads	30,972,699	34,865,544
Number of reads removed as too short	8,284,949	9,457,222
Total number of aligned reads	21,897,164	24,554,889
Total number of uniquely mapped reads	2,007,386	2,370,177
Total number of alignments	61,795,097	69,056,000
% of mapped reads (compared to no. of input reads)	70.7	70.43
% of uniquely aligned reads (in relation to all aligned reads)	9.17	9.65

Appendix Table 4. Mapping statistics for Pseudo-seq experiments of *Helicobacter pylori* WT and PUS mutant strains The table indicates the total number of sequenced reads (number of input reads), the number of reads that were removed from the analysis because too short, the total number of mapped reads, the number of alignments (i.e. some reads map to different locations with the same score), and the number of uniquely mapped reads. For the number of input reads and the number of uniquely mapped reads, the percentage value are also listed.

Libraries	HP_WT_ CMC_-R1	HP_WT_ CMC_-R2	HP_WT_ CMC_+R1	HP_WT_ CMC_+R2	HP_Δ*truA*_ CMC_-R1	HP_ Δ*truA* _ CMC_-R2	HP_ Δ*truA* _ CMC_+R1	HP_ Δ*truA*_ CMC_+R2	HP_ Δ*truD* _ CMC_-R1	HP_ Δ*truD* _ CMC_-R2	HP_ Δ*truD* _ CMC_+R1	HP_ Δ*truD* _ CMC_+R2
Number of input reads	16,427,354	67,063,458	18,048,879	66,418,673	52,281,593	28,671,904	29,856,758	44,945,022	37,481,313	32,676,909	26,651,355	31,454,684
Number of reads removed as too short	9,580	34,760	10,142	44,515	32,059	22,085	14,562	34,123	20,143	22,508	18,154	22,531
Total number of aligned reads	15,594,463	64,270,725	17,160,903	64,096,250	48,715,952	27,971,919	28,301,205	43,163,691	34,914,127	31,136,804	24,823,018	30,215,657
Total number of uniquely mapped reads	3519952	19953327	3758255	19369002	11287326	10166654	6851706	14017731	7357100	7129838	5249214	8256822
Total number of alignments	28,371,854	1,12E+08	31,337,615	1,12E+08	88,169,239	47,160,094	51,299,103	74,790,564	63,861,152	56,620,804	45,452,585	53,623,849
% of mapped reads (compared to no. of input reads)	94.93	95.84	95.08	96.5	93.18	97.56	94.79	96.04	93.15	95.29	93.14	96.06
% of uniquely aligned reads (in relation to all aligned reads)	22.57	31.05	21.9	30.22	23.17	36.35	24.21	32.48	21.07	22.9	21.15	27.33

Appendix Table 5. Mapping statistics for Pseudo-seq experiments of *Campylobacter jejuni* WT and PUS mutant strains The table indicates the total number of sequenced reads (number of input reads), the number of reads that were removed from the analysis because too short, the total number of mapped reads, the number of alignments (i.e. some reads map to different locations with the same score), and the number of uniquely mapped reads. For the number of input reads and the number of uniquely mapped reads, the percentage value are also listed.

Libraries	WT_CMC-_R1	WT_CMC-R2	WT_CMC+R1	WT_CMC+R2	Δ*truABD*_CMC-_R1	Δ*truABD*_CMC-_R2	Δ*truABD*_CMC+_R1	Δ*truABD*_CMC+_R2	Δ*truA*_CMC-_R1	Δ*truA*_CMC-_R2	Δ*truA*_CMC+R1	Δ*truA*_CMC+R2
Number of input reads	16,274,641	15,007,884	15,894,425	18,412,757	15,164,330	14,665,385	17,126,571	15,945,875	15,684,754	13,513,421	14,146,634	17,784,912
Number of reads removed as too short	36,980	28,172	46,648	121,465	36,754	24,321	62,794	19,335	34,626	27,439	157,587	52,573
Total number of aligned reads	15,707,991	14,354,117	15,181,759	16,921,538	14,273,166	13,370,546	16,691,594	15,217,386	15,069,631	12,496,820	13,534,330	16,809,222
Total number of uniquely mapped reads	10,722,188	9,356,093	9,436,878	10,253,119	10,352,594	9,648,789	11,785,414	10,851,679	10,523,092	7,739,418	8,751,741	10,404,903
Total number of alignments	25,179,801	24,005,250	26,297,115	29,872,956	21,369,358	20,011,032	25,068,986	23224,020	23,461,852	21,499,410	22,514,452	29,085,846
% of mapped reads (compared to no. of input reads)	96.52	95.64	95.52	91.9	94.12	91.17	97.46	95.43	96.08	92.48	95.67	94.51
% of uniquely aligned reads (in relation to all aligned reads)	68.26	65.18	62.16	60.59	72.53	72.16	70.61	71.31	69.83	61.93	64.66	61.9

Continue in the next page

Libraries	Δ*truB* _CMC-_R1	Δ*truB*_CMC-_R2	Δ*truB*_CMC+_R1	Δ*truB*_CMC+_R2	Δ*truD* _CMC-_R1	Δ*truD*_CMC-_R2	Δ*truD*_CMC+_R1	Δ*truD*_CMC+_R2
Number of input reads	18,198,860	17,290,352	16,667,313	12,509,943	17,733,001	13,909,278	16,361,692	16,917,250
Number of reads removed as too short	51,278	32,011	86,092	16,727	40,498	55,353	55,229	49,764
Total number of aligned reads	17,334,580	15,918,968	15,609,193	11,564,802	16,591,530	12,603,628	15,541,173	15,610,487
Total number of uniquely mapped reads	12,032,451	10,776,534	10,214,635	7,255,880	11,544,729	8,884,091	9,722,416	9,831,684
Total number of alignments	27,210,946	25,629,908	25,469,230	19,815,659	26,035,276	19,214,655	26,763,686	26,593,794
% of mapped reads (compared to no. of input reads)	95.25	92.07	93.65	92.44	93.56	90.61	94.99	92.28
% of uniquely aligned reads (in relation to all aligned reads)	69.41	67.7	65.44	62.74	69.58	70.49	62.56	62.98

Appendix Table 6. Mapping statistics for RIP-seq experiments of *Campylobacter jejuni* WT and TruD-3xFLAG strains. The table indicates the total number of sequenced reads (number of input reads), the number of reads that were removed from the analysis because too short, the total number of mapped reads, the number of alignments (i.e. some reads map to different locations with the same score), and the number of uniquely mapped reads. For the number of input reads and the number of uniquely mapped reads, the percentage value are also listed.

Libraries	**WT/control**	**TruD-3xFLAG**
Number of input reads	1,333,450	1,661,962
Number of reads removed as too short	16,194	41,610
Total number of aligned reads	1,296,410	1,595,455
Total number of uniquely mapped reads	273,811	530,468
Total number of alignments	3,323,813	3,696,608
% of mapped reads (compared to no. of input reads)	97.22	96
% of uniquely aligned reads (in relation to all aligned reads)	21.12	33.25

Appendix Table 7. 43 different RNAs are enriched in the TruD-3xFLAG CoIP. 5' UTR, CDS, housekeeping RNA, and tRNAs from *C. jejuni* NCTC11168 enriched in the TruD-3xFLAG coIP (RIP-seq) compared to the WT coIP (RIP-seq). 43 RNAs showed GFOLD >1.0 enrichment in the TruD-3xFLAG coIP versus the WT coIP. The modified tRNA-Glu (Cjp03), target of TruD, is marked in red.

Type	Start	End	Strand	Gene	Name	WT coIP	TruD-3xFLAG coIP	GFOLD	log2 FoldChange
5' UTR	1413180	1413219	-	Cj1476c		133	417	1,32375	1,64009
5' UTR	1525411	1525439	+	Cj1597		6	41	1,14405	2,59364
5' UTR	234574	234598	+	Cj0256		30	101	1,07655	1,71214
5' UTR	405091	405332	+	Cj0437		485	1102	1,00678	1,18195
CDS	1200312	1202291	-	Cj1269c	*amiA*	65	808	3,21162	3,61471
CDS	927210	927770	+	Cj0996	*ribA*	24	299	2,94999	3,58417
CDS	1079195	1080041	-	Cj1145c		150	815	2,15027	2,43369
CDS	1546496	1547755	+	Cj1619	*kgtP*	551	2713	2,14608	2,29766
CDS	1302620	1304968	-	Cj1367c		66	376	2,07489	2,49245
CDS	1279918	1280643	-	Cj1347c	*cdsA*	71	397	2,06026	2,46432
CDS	936246	937496	-	Cj1006c		80	388	1,87529	2,26157
CDS	1235522	1236748	-	Cj1306c		56	282	1,85504	2,31061
CDS	82019	83050	+	Cj0069		348	1361	1,7707	1,96428
CDS	1253417	1254092	+	Cj1325		222	855	1,69855	1,93994
CDS	1141634	1143016	-	Cj1213c	*glcD*	124	472	1,5993	1,91965
CDS	1537916	1538416	+	Cj1610	*pgpA*	28	126	1,49349	2,12798
CDS	230279	231589	-	Cj0250c		52	206	1,48454	1,96699
CDS	656901	658331	-	Cj0699c	*glnA*	114	384	1,40276	1,74076
CDS	1422130	1422231	-	Cj1485c		56	194	1,30167	1,77455
CDS	111488	112993	+	Cj0105	*atpA*	355	990	1,27871	1,47749
CDS	1309284	1311755	+	Cj1373		12	62	1,27846	2,2669
CDS	652530	653918	+	Cj0695	*ftsA*	201	570	1,23773	1,49972
CDS	736487	737011	+	Cj0783	*napB*	203	560	1,19692	1,45858
CDS	879636	880841	-	Cj0941c		237	644	1,19382	1,43691
CDS	1143019	1143744	-	Cj1214c		89	268	1,19368	1,57939
CDS	1386264	1386926	-	Cj1447c	*kpsT*	35	120	1,15971	1,7498
CDS	226401	226754	+	Cj0245	*rplT*	63	194	1,15382	1,60744
CDS	1434062	1435549	-	Cj1502c	*putP*	252	655	1,13674	1,37399
CDS	1509407	1509796	-	Cj1579c	*nuoA*	222	567	1,09582	1,3488
CDS	250590	251030	+	Cj0273	*fabZ*	84	236	1,08096	1,48099
CDS	460364	460513	+	Cj0494		2	21	1,07416	2,87048
CDS	1358689	1359294	-	Cj1424c	*gmhA2*	19	69	1,02937	1,80489
CDS	1333149	1334642	-	Cj1399c	*hydA2*	174	432	1,02133	1,30733
CDS	1499289	1501079	-	Cj1568c	*nuoL*	178	441	1,02126	1,3042
CDS	1046471	1047199	-	Cj1114c	*pssA*	70	194	1,02032	1,4577
CDS	811319	812119	+	Cj0865	*dsbB*	9	50	1,01822	2,33282

CDS	933584	934102	-	Cj1003c		44	132	1,01775	1,55743
CDS	1519690	1520985	-	Cj1588c		32	102	1,01202	1,63344
CDS	1502540	1503538	-	Cj1572c	*nuoH*	115	297	1,01036	1,35827
CDS	1487089	1488591	-	Cj1553c	*hsdM*	43	128	1,00831	1,55401
Housekeeping RNA	1293300	1293658	-	Cjs01		23680	50417	1,06462	1,09021
tRNA	**165728**	**165802**	**+**	**Cjp03**	**tRNA-Glu**	**4624**	**12813**	**1,41426**	**1,47012**
tRNA	1549741	1549829	+	Cjp28	tRNA-Leu	162	403	1,01285	1,30893

Appendix Table 8. Mapping statistics for RNA-seq experiments of *Campylobacter jejuni* WT Δ*truD*, C*truD* and D85N. The table indicates the total number of sequenced reads (number of input reads), the number of reads that were removed from the analysis because too short, the total number of mapped reads, the number of alignments (i.e. some reads map to different locations with the same score), and the number of uniquely mapped reads. For the number of input reads and the number of uniquely mapped reads, the percentage value are also listed.

Libraries	C*truD* R1	C*truD* R2	D85N R1	D85N R2	Δ*truD* R1	Δ*truD* R2	WT R1	WT R2
Number of input reads	15,359,508	19,311,039	15,389,411	13,656,222	15,259,083	14,775,908	18,166,008	16,222,357
Number. Of reads – removed as too short	833,304	499,252	432,312	322,302	492,646	357,459	910,169	821,288
Total number of aligned reads	13,522,201	17,451,989	13,926,357	12,368,343	13,015,755	13,419,657	16,106,303	14,167,854
Total number of alignments	23,761,755	28,609,355	23,019,922	20,874,405	20,500,797	20,088,337	27,502,333	23,801,761
% of aligned reads (compared to no. of input reads)	88,04	90,37	90,49	90,57	91,2	90,82	88,66	87,34
% of uniquely aligned reads (in relation to all aligned reads)	61,82	67,72	67,06	65,36	76	74,78	64,29	65,65

Appendix Table 9. 50 different RNAs are upregulated in WT vs Δ*truD*. The table indicates RNAs (5' UTR, CDS, sRNA, and tRNA) with changed levels (log2FC >1.0) and with a p-value <0.05 in the WT vs Δ*truD* strains.

Type	Start	End	Strand	Gene	Name	Δ*truD* R1	Δ*truD* R2	WT R1	WT R2	log2 FoldChange	p-value
5' UTR	688882	689006	+	Cj0735		205	132	1807	2126	3,382971701	2,43E-65
5' UTR	1637679	1637874	-	Cj1727c		344	330	1001	1296	1,60258322	1,19E-17
5' UTR	527407	527435	+	Cj0565		52	48	278	279	2,302686856	2,23E-14
5' UTR	416467	416506	-	Cj0449c		1320	998	3112	4151	1,487975299	2,33E-13
5' UTR	625520	625551	+	Cj0671		443	338	839	1173	1,204712318	1,46E-08
5' UTR	920954	920979	-	Cj0987c		31	35	108	170	1,910784346	3,23E-07
5' UTR	846940	846970	+	Cj0909		361	295	660	859	1,053186607	1,14E-06
5' UTR	166345	166372	+	Cj0169		193	160	376	625	1,347361969	1,15E-06
5' UTR	151577	151607	-	Cj0146c		187	148	330	429	1,017146397	1,32E-05
5' UTR	805981	806007	-	Cj0859c		65	57	156	159	1,192252021	1,88E-05
5' UTR	1470383	1470407	-	Cj1537c		33	36	91	134	1,513330694	3,28E-05
5' UTR	380911	380936	+	Cj0414		17	18	57	71	1,678683784	5,23E-05
5' UTR	1325135	1325165	-	Cj1387c		78	75	144	232	1,14587935	0,000223
5' UTR	66467	66492	-	Cj0045c		81	63	155	217	1,204475466	0,000276
5' UTR	302353	302382	+	Cj0334		281	234	467	736	1,068164435	0,00029
5'-UTR	91071	91100	-	Cj0079c		71	66	152	164	1,034954297	0,000379
5' UTR	1558560	1558601	-	Cj1632c		74	64	136	210	1,165926907	0,000459
5' UTR	1517416	1517436	-	Cj1585c		178	120	278	430	1,094051442	0,000474
5' UTR	314986	315020	-	Cj0343c		86	62	132	218	1,08606908	0,000682
5' UTR	1188384	1188413	+	Cj1258		81	65	151	177	1,006522649	0,000704
5' UTR	448661	448696	+	Cj0481		43	30	74	123	1,276162092	0,001062
5' UTR	766669	766691	+	Cj0817		70	56	119	202	1,192897399	0,00112
5' UTR	1312522	1312554	+	Cj1375		42	23	77	100	1,278680771	0,001739
5'-UTR	1270951	1270994	-	Cj1339c		1222	845	2239	3708	1,373407605	0,003261
5' UTR	325994	326023	+	Cj0358		1224	938	1951	2897	1,008213976	0,007462
5' UTR	1633546	1633591	-	Cj1721c		41	34	64	103	1,005251765	0,009891
5' UTR	118705	118730	+	Cj0113		1051	781	1690	2817	1,145799611	0,012232
5' UTR	1451477	1451496	-	Cj1515c		25	23	50	60	1,089448556	0,015801
5' UTR	892383	892406	-	Cj0952c		114	67	222	399	1,632431041	0,018159
5' UTR	96016	96073	+	Cj0087		1845	1208	2679	4770	1,139237099	0,018738
5' UTR	1519641	1519661	-	Cj1587c		17	14	38	35	1,108947221	0,028191
CDS	689007	689726	+	Cj0735		91	78	966	915	3,303018162	2,91E-89
CDS	**1394285**	**1395403**	**-**	**Cj1457c**	***truD***	**95**	**91**	**393**	**407**	**1,932088399**	**1,83E-34**
CDS	416251	416466	-	Cj0449c		4061	3270	9577	9776	1,231898109	1,13E-29
CDS	805552	805980	-	Cj0859c		415	425	1021	890	1,009251987	8,07E-16
CDS	381667	383388	+	Cj0415		1002	1288	3436	3452	1,409889705	2,64E-15
CDS	65744	66466	-	Cj0045c		727	669	1716	1961	1,228904339	3,14E-14
CDS	380937	381665	+	Cj0414		662	773	1749	1911	1,176115467	1,31E-13

CDS	1558398	1558559	-	Cj1632c		223	197	542	486	1,120289447	5,54E-13
CDS	826268	828199	-	Cj0888c		235	214	533	515	1,04966152	4,67E-11
CDS	920967	921203	-	Cj0988c		27	30	77	130	1,698530804	4,29E-05
CDS	1432607	1433815	+	Cj1500		49	56	112	127	1,013920832	0,000252
CDS	1556025	1556450	+	Cj1628	*exbB2*	4	14	45	42	2,086352348	0,000345
CDS	1229096	1229887	+	Cj1298		33	35	102	91	1,327698335	0,000476
CDS	528182	529648	+	Cj0566		28	14	54	82	1,542354013	0,003709
sRNA	245225	245380	-	CJnc20		3276	2584	9762	12811	1,784913371	8,29E-27
sRNA	1589598	1589666	+	CJas_Cj1667c		17	18	50	89	1,829658952	0,000462
sRNA	1559676	1559722	+	CJnc170		13	18	34	75,5	1,668490396	0,005701
tRNA	943535	943611	+	Cjp21	tRNA-Arg	1096	1272	2640	3704	1,254531197	1,56E-10
tRNA	460270	460346	+	Cjp10	tRNA-Arg	482	536	974	1315	1,001476878	3,84E-07

Appendix Table 10. 16 different RNAs are downregulated in WT vs Δ*truD.* The table indicates RNAs (5' UTR, CDS, sRNA, and tRNA) with changed levels (log2FC <1.0) and with a p-value <0.05 in the WT vs Δ*truD* strains.

Type	**Start**	**End**	**Strand**	**Gene**	**Name**	**Δ*truD* R1**	**Δ*truD* R2**	**WT R1**	**WT R2**	**log2 FoldChange**	**p-value**
5' UTR	665755	665787	+	Cj0709		1244	1091	534	439	-1,43838	1,06E-24
5' UTR	1009461	1009492	-	Cj1074c		1706	1432	894	825	-1,04167	4,03E-19
5' UTR	916408	916464	-	Cj0982c		2517	2252	1250	1388	-1,02312	9,23E-18
5' UTR	1174037	1174264	-	Cj1245c		612	520	323	234	-1,20392	4,39E-12
5' UTR	1562886	1562907	-	Cj1637c		770	584	377	363	-1,04122	2,81E-10
5'-UTR	431001	431049	+	Cj0466		253	248	134	132	-1,08758	8,69E-07
5' UTR	751766	751796	+	Cj0801		97	79	34	49	-1,2392	0,001962
5' UTR	728484	728499	+	Cj0777		80	66	39	43	-1,03673	0,00798
5' UTR	1132203	1132301	+	Cj1202		36	45	21	19	-1,19803	0,019306
CDS	915568	916407	-	Cj0982c	*cjaA*	23612	30363	13731	13332	-1,17616	1,32E-14
CDS	1130028	1132292	+	Cj1201	*metE*	556	547	272	265	-1,21289	1,19E-12
CDS	1129228	1130016	+	Cj1200		126	135	60	55	-1,35398	5,52E-06
CDS	522658	523986	+	Cj0560		152	131	79	73	-1,0793	4,81E-05
CDS	1091201	1091428	-	Cj1158c		22	34	17	11	-1,24102	0,040421
sRNA	1179587	1179772	+	6S RNA		1483578	1201216	758375	746986	-1,00424	1,5E-25
tRNA	872889	872974	+	Cjt01	tRNA-Leu	8013	25788	8500	5687	-1,4612	0,025656

Appendix Table 11. 44 different RNAs are upregulated in C*truD* vs Δ*truD.* The table indicates RNAs (5' UTR, CDS, sRNA, and tRNA) with changed levels (log2FC >1.0) and with a p-value <0.05 in the C*truD* vs Δ*truD* strains.

Type	Start	End	Strand	Gene	Name	C*truD* R1	C*truD* R2	Δ*truD* R1	Δ*truD* R2	log2 FoldChange	p-value
5' UTR	688882	689006	+	Cj0735		1256	2408	205	132	3,19694522	1,95E-58
5' UTR	1637679	1637874	-	Cj1727c		917	1598	344	330	1,66121239	7,31E-19
5' UTR	416467	416506	-	Cj0449c		2388	4968	1320	998	1,40699305	4,27E-12
5' UTR	166345	166372	+	Cj0169		376	768	193	160	1,43928391	1,99E-07
5' UTR	625520	625551	+	Cj0671		708	1222	443	338	1,07243467	4,71E-07
5' UTR	846940	846970	+	Cj0909		574	973	361	295	1,01061419	3,07E-06
5' UTR	1470383	1470407	-	Cj1537c		92	168	34	36	1,64972178	5,6E-06
5' UTR	91071	91100	-	Cj0079c		132	256	71	66	1,25310307	1,51E-05
5' UTR	448661	448696	+	Cj0481		102	168	43	30	1,6618352	1,73E-05
5' UTR	920954	920979	-	Cj0987c		77	164	31	35	1,59862562	2,17E-05
5'-UTR	1188384	1188413	+	Cj1258		134	254	81	65	1,17575868	7,1E-05
5' UTR	380911	380936	+	Cj0414		48	75	17	18	1,57961513	0,000148
5' UTR	302353	302382	+	Cj0334		393	889	281	234	1,04750761	0,000381
5' UTR	766669	766691	+	Cj0817		126	238	70	56	1,28569306	0,000437
5'-UTR	1325135	1325165	-	Cj1387c		135	245	78	75	1,08018576	0,000512
5' UTR	33520	33592	-	Cj0025c		73	147	49	27	1,27390449	0,000853
5' UTR	1312522	1312554	+	Cj1375		64	128	42	23	1,31786208	0,001238
5' UTR	1558560	1558601	-	Cj1632c		109	227	74	64	1,01753225	0,002302
5' UTR	1127323	1127345	-	Cj1197c		235	515	169	128	1,06769323	0,002468
5' UTR	1451477	1451496	-	Cj1515c		38	92	25	23	1,22762606	0,006317
5' UTR	118705	118730	+	Cj0113		1746	3412	1051	781	1,24308788	0,006563
5' UTR	1270951	1270994	-	Cj1339c		1911	3943	1222	845	1,24521413	0,00765
5' UTR	892383	892406	-	Cj0952c		189	440	114	67	1,5280269	0,027062
5' UTR	96016	96073	+	Cj0087		2387	5180	1845	1208	1,04754749	0,030664
5' UTR	1519641	1519661	-	Cj1587c		27	44	17	14	1,01725469	0,044865
CDS	**1394285**	**1395403**	**-**	**Cj1457c**	***truD***	**1906**	**2743**	**95**	**92**	**4,43154728**	**1,4E-189**
CDS	689007	689726	+	Cj0735		835	1178	91	78	3,36525461	1,01E-92
CDS	416251	416466	-	Cj0449c		7493	11933	4061	3270	1,18314159	1,72E-27
CDS	380937	381665	+	Cj0414		1949	2349	662	773	1,39170609	1,7E-18
CDS	381667	383388	+	Cj0415		3522	4169	1002	1288	1,5581814	2,29E-18
CDS	1636407	1637678	-	Cj1727c	*metB*	1115	1716	505	588	1,14832	2,47E-18
CDS	65744	66466	-	Cj0045c		1622	1854	727	669	1,13746066	2,19E-12
CDS	1517567	1517989	+	Cj1586	*cgb*	232	255	102	106	1,04702987	1,93E-05
CDS	1432607	1433815	+	Cj1500		112	142	49	56	1,07283051	0,000104
CDS	920967	921203	-	Cj0988c		54	130	27	30	1,41500363	0,000708
CDS	1556025	1556450	+	Cj1628	*exbB2*	28	49	4	14	1,84957842	0,001617
rRNA	396449	399360	+	Cjr05		20281	61403	12266	16421	1,18834975	0,013056
rRNA	698743	701654	+	Cjr08		20281	61403	12266	16421	1,18834975	0,013056

rRNA	41568	44457	+	Cjr02		20274	61398	12264	16419	1,18830583	0,013072
rRNA	39249	40761	+	Cjr01		2204	17053	1687	2782	1,69122845	0,029284
rRNA	394130	395642	+	Cjr04		2204	17053	1687	2782	1,69122845	0,029284
rRNA	696424	697936	+	Cjr07		2204	17053	1687	2782	1,69122845	0,029284
sRNA	245225	245380	-	CJnc20		8195	15134	3276	2584	1,74956366	8,09E-26
sRNA	1589598	1589666	+	CJas_Cj1667c		65	57	17	18	1,65012952	0,001654

Appendix Table 12. 26 different RNAs are downregulated in C*truD* vs Δ*truD.* The table indicates RNAs (5' UTR, CDS, sRNA, and tRNA) with changed levels (log2FC <1.0) and with a p-value <0.05 in the C*truD* vs Δ*truD* strains.

Type	**Start**	**End**	**Strand**	**Gene**	**Name**	**C*truD* R1**	**C*truD* R2**	**Δ*truD* R1**	**Δ*truD* R2**	**log2 FoldChange**	**p-value**
5' UTR	665755	665787	+	Cj0709		367	563	1244	1091	-1,54954	3,65E-28
5' UTR	1009461	1009492	-	Cj1074c		603	986	1706	1432	-1,20731	7,05E-25
5' UTR	916408	916464	-	Cj0982c		957	1468	2517	2252	-1,19511	1,7E-23
5' UTR	541348	541370	+	Cj0581		490	970	1504	1249	-1,16459	2,86E-15
5' UTR	1562886	1562907	-	Cj1637c		244	421	770	584	-1,25701	4,25E-14
5' UTR	361588	361757	-	Cj0393c		467	846	1325	1092	-1,12018	2,51E-13
5' UTR	1122148	1122179	-	Cj1193c		142	247	415	380	-1,26688	1,13E-11
5' UTR	1174037	1174264	-	Cj1245c		240	340	612	520	-1,17399	1,38E-11
5' UTR	1343912	1344160	-	Cj1411c		385	645	1047	750	-1,02868	1,55E-10
5' UTR	1049761	1049887	-	Cj1116c		447	874	1307	9656	-1,03004	2,64E-10
5' UTR	1387706	1387736	-	Cj1448c		146	260	395	343	-1,09618	4,67E-09
5' UTR	1345030	1345047	-	Cj1412c		191	376	644	460	-1,2061	1,66E-08
5' UTR	431001	431049	+	Cj0466		89	166	253	248	-1,21429	4,94E-08
5' UTR	234574	234598	+	Cj0256		123	202	319	261	-1,06084	1,44E-06
5' UTR	1213826	1213863	-	Cj1280c		81	165	256	182	-1,08236	2,01E-05
5' UTR	656033	656042	+	Cj0698		65	105	160	136	-1,02339	0,000151
5' UTR	751766	751796	+	Cj0801		25	49	97	79	-1,50057	0,000221
5' UTR	728484	728499	+	Cj0777		30	41	80	66	-1,26477	0,001416
5' UTR	1132203	1132301	+	Cj1202		20	26	36	45	-1,02494	0,042871
CDS	1212857	1213825	-	Cj1280c		1770	2721	4155	3640	-1,01479	1,85E-27
CDS	1130028	1132292	+	Cj1201	*metE*	242	298	556	547	-1,22709	6,7E-13
CDS	915568	916407	-	Cj0982c	*cjaA*	13318	16284	23612	30363	-1,06083	3,68E-12
sRNA	1179587	1179772	+	6S_RNA		539296	841828	1483578	1201216	-1,17891	1,4E-34
tRNA	878400	878475	-	Cjp20	tRNA-Lys	2960	3719	5956	5880	-1,01896	1,05E-15
tRNA	872889	872974	+	Cjt01	tRNA-Leu	5225	5581	8013	5788	-1,83691	0,005032
tRNA	533206	533280	-	Cjp13	tRNA-Gln	5871	8272	8597	16732	-1,1	0,009173

Appendix Table 13. 25 different RNAs are upregulated in Δ*truD* vs D85N. The table indicates RNAs (5' UTR, CDS, sRNA, and tRNA) with changed levels (log2FC >1.0) and with a p-value <0.05 in the Δ*truD vs* D85N strains.

Type	Start	End	Strand	Gene	Name	D85N R1	D85N R2	Δ*truD* R1	Δ*truD* R2	log2 FoldChange	p-value
5' UTR	751766	751796	+	Cj0801		28	33,5	97	79	1,568751699	0,000133955
5' UTR	665755	665787	+	Cj0709		508	385,5	1243,5	1091	1,469524231	1,79549E-25
5' UTR	728484	728499	+	Cj0777		27	30	80	66	1,431320892	0,000395412
5' UTR	1562886	1562907	-	Cj1637c		323	301,5	770	584	1,191522521	8,58025E-13
5' UTR	1174037	1174264	-	Cj1245c		289	247	612	520	1,159616808	2,8395E-11
5' UTR	1122148	1122179	-	Cj1193c		205	174,5	415	380	1,155030066	5,85043E-10
5' UTR	1132203	1132301	+	Cj1202		19	20,5	36	45	1,137160126	0,026722065
5' UTR	431001	431049	+	Cj0466		131	116	253	248	1,108653655	6,31427E-07
5' UTR	656033	656042	+	Cj0698		83	66	160	136	1,073083119	8,24972E-05
5' UTR	1343912	1344160	-	Cj1411c		468	447	1047	750	1,047967623	8,04304E-11
5' UTR	193624	193645	-	Cj0197c		55	60	128	98	1,047614939	0,001162682
5' UTR	1009461	1009492	-	Cj1074c		870	760	1706	1432	1,025160248	1,74314E-18
CDS	734971	735711	+	Cj0781		9193	6807	15925	16211	1,096710139	1,78281E-16
CDS	1130028	1132292	+	Cj1201		312	250	556	547	1,060974039	4,57401E-10
CDS	1129228	1130016	+	Cj1200		69	65	126	135	1,03883265	0,000403203
CDS	1132302	1133150	+	Cj1202		92	91	172	183	1,037310063	3,31189E-05
sRNA	1179587	1179772	+	6S_RNA		653074	621514	1483578	1201216	1,150889894	4,9102E-33
sRNA	1575014	1575112	+	CJnc180		475	456	10283	871	1,105842579	4,00245E-13
tRNA	872889	872974	+	Cjt01		4798	2649	8013	25788	2,306544753	0,00042876
tRNA	533206	533280	-	Cjp13		6143	4089	8597	16732	1,416180747	0,000528456
tRNA	878691	878766	-	Cjt04		1889	1567	3492	3414	1,084050294	9,95417E-12
tRNA	878400	878475	-	Cjp20		3231	2715	5956	5880	1,07874402	2,18745E-17
tRNA	1287737	1287826	-	Cjp25		24999	22812	43808	51076	1,074601092	2,03936E-11
tRNA	878480	878556	-	Cjt2		11916	7584	18363	19858	1,068306219	2,31597E-10
tRNA	878095	878171	-	Cjt02		11907	7599	18283	19783	1,061984845	2,74396E-10

Appendix Table 14. 43 different RNAs are downregulated in Δ*truD* vs D85N. The table indicates RNAs (5' UTR, CDS, sRNA, and tRNA) with changed levels (log2FC <1.0) and with a p-value <0.05 in the Δ*truD vs* D85N strains.

Type	Start	End	Strand	Gene	Name	D85N R1	D85N R2	Δ*truD* R1	Δ*truD* R2	log2 FoldChange	p-value
5' UTR	688882	689006	+	Cj0735		1879	2069	205	132	-3,48179	4,16E-69
5' UTR	380911	380936	+	Cj0414		85	85	17	18	-2,20057	7,91E-08

5' UTR	920954	920979	-	Cj0987c		132	167	31	35	-2,10682	1,66E-08
5' UTR	1470383	1470407	-	Cj1537c		118	162	34	36	-1,9305	9,56E-08
5' UTR	1637679	1637874	-	Cj1727c		1074	1257	344	330	-1,71758	4,77E-20
5' UTR	1312522	1312554	+	Cj1375		82	121	42	23	-1,5775	0,000104
5' UTR	448661	448696	+	Cj0481		93	133	43	30	-1,56199	5,72E-05
5' UTR	166345	166372	+	Cj0169		467	613	193	160	-1,54615	2,3E-08
5' UTR	416467	416506	-	Cj0449c		2980	3579	1320	998	-1,43436	1,65E-12
5' UTR	33520	33592	-	Cj0025c		88	115	49	27	-1,3553	0,000389
5' UTR	766669	766691	+	Cj0817		124	203	70	56	-1,31695	0,000319
5' UTR	314986	315020	-	Cj0343c		179	207	86	62	-1,31063	3,97E-05
5' UTR	625520	625551	+	Cj0671		842	1022	443	338	-1,18825	2,36E-08
5' UTR	91071	91100	-	Cj0079c		130	179	71	66	-1,10034	0,000159
5' UTR	1325135	1325165	-	Cj1387c		153	187	78	75	-1,08973	0,000466
5' UTR	1519641	1519661	-	Cj1587c		32	35	17	14	-1,0838	0,032796
5' UTR	118705	118730	+	Cj0113		1494	2489	1051	781	-1,06664	0,019703
5' UTR	66467	66492	-	Cj0045c		136,5	178	81	63	-1,05858	0,001463
5' UTR	1188384	1188413	+	Cj1258		131	184	81	65	-1,05397	0,000395
5' UTR	1451477	1451496	-	Cj1515c		44	56	25	23	-1,04915	0,020682
5' UTR	1229886	1229917	+	Cj1299		261	327	139	135	-1,03047	3,46E-05
CDS	1394285	1395403	-	Cj1457c	*truD*	2145	1877	95	91	-4,35153	1,9E-182
CDS	689007	689726	+	Cj0735		1172	950	91	78	-3,56609	3,5E-104
CDS	381667	383388	+	Cj0415		6446	4314	1002	1288	-2,13328	4,32E-33
CDS	1432607	1433815	+	Cj1500		240	234	49	56	-2,09315	7,42E-15
CDS	380937	381665	+	Cj0414		3446	2651	662	773	-1,99552	1,63E-36
CDS	1556025	1556450	+	Cj1628	*exbB2*	39	37	4	14	-1,98589	0,000701
CDS	920967	921203	-	Cj0988c		107	131	27	30	-1,98244	1,65E-06
CDS	1433819	1434046	+	Cj1501		17	19	7	4	-1,73821	0,044062
CDS	1636407	1637678	-	Cj1727c	*metB*	1872	1510	505	588	-1,54049	5,82E-32
CDS	1517567	1517989	+	Cj1586	*cgb*	285	336	102	106	-1,50159	6,5E-10
CDS	314200	314985	-	Cj0343c		1707	1403	598	679	-1,19716	4,87E-19
CDS	482563	482931	+	Cj0517	*crcB*	105	94	42	40	-1,19024	0,000139
CDS	416251	416466	-	Cj0449c		8760	8694	4061	3270	-1,17684	3,36E-27
CDS	1312555	1313850	+	Cj1375		2293	1919	810	952	-1,16895	2,02E-20
CDS	848410	849309	-	Cj0912c	*cysM*	3967	3185	1469	1617	-1,12384	4,16E-23
CDS	826268	828199	-	Cj0888c		5836917	449	235	214	-1,11614	2,7E-12
CDS	1406696	1407283	-	Cj1472c	*ctsE*	140	132	59	63	-1,08651	8,02E-05
CDS	1635443	1636324	-	Cj1726c	*metA*	1038	741	357	445	-1,05461	2,55E-09
CDS	276125	276874	-	Cj0303c	*modA*	1336	1118	586	533	-1,04957	1,13E-18
CDS	1405147	1406706	-	Cj1471c	*ctsE*	262	240	112	119	-1,03714	2,72E-07

CDS	1558398	1558559	-	Cj1632c		458	446	223	197	-1,03114	4,11E-11
sRNA	245225	245380	-	CJnc20		11325	11861	3276	2584	-1,91223	1,59E-30

Appendix Table 15. 1 RNAs is downregulated in C*truD* vs D85N. The table indicates RNAs (5' UTR, CDS, sRNA, and tRNA) with changed levels (log2FC <1.0) and with a p-value <0.05 in the C*truD vs* D85N strains.

Type	Start	End	Strand	Gene	Name	C*truD* R1	C*truD* R2	D85N R1	D85N R2	log2 FoldChange	p-value
CDS	1432607	1433815	+	Cj1500		112	142	240	234	-1,02032	3,6E-05

Appendix Table 16. 4 RNAs are upregulated in WT vs C*truD.* The table indicates RNAs (5' UTR, CDS, sRNA, and tRNA) with changed levels (log2FC >1.0) and with a p-value <0.05 in the WT vs C*truD* strains.

Type	Start	End	Strand	Gene	Name	C*truD* R1	C*truD* R2	WT R1	WT R2	log2 FoldChange	p-value
5' UTR	527407	527435	+	Cj0565		26	60	278	279	2,772005	2,92E-19
CDS	528182	529648	+	Cj0566		10	23	54	82	2,13602	9,37E-05
CDS	1229096	1229887	+	Cj1298		29	68	102	91	1,07813	0,003532
CDS	532203	533075	+	Cj0571		26	47	50	102	1,132011	0,018206

Appendix Table 17. 4 RNAs are downregulated in WT vs C*truD.*The table indicates RNAs (5' UTR, CDS, sRNA, and tRNA) with changed levels (log2FC <1.0) and with a p-value <0.05 in the WT vs C*truD* strains.

Type	Start	End	Strand	Gene	Name	C*truD* R1	C*truD* R2	WT R1	WT R2	log2FoldChange	p-value
CDS	1394285	1395403	-	Cj1457c	*truD*	1906	2743	393	407	-2,49946	7,59E-98
rRNA	39249	40761	+	Cjr01		2204	17053	2049	2106	-1,98014	0,010714
rRNA	394130	395642	+	Cjr04		2204	17053	2049	2106	-1,98014	0,010714
rRNA	696424	697936	+	Cjr07		2204	17053	2049	2106	-1,98014	0,010714

Appendix Table 18. 9 RNAs are upregulated in WT vs D85N. The table indicates RNAs (5' UTR, CDS, sRNA, and tRNA) with changed levels (log2FC >1.0) and with a p-value <0.05 in the WT vs D85N strains.

Type	Start	End	Strand	Gene	Name	D85N R1	D85N R2	WT R1	WT R2	log2 FoldChange	p-value
5' UTR	527407	527435	+	Cj0565		26	28	278	278,5	3,269787	3,34E-23
tRNA	1590632	1590709	-	Cjp33	tRNA-Pro	1771	1154	4652	3534	1,397789	1,8E-15
tRNA	943535	943611	+	Cjp21	tRNA-Arg	1313	893	2640	3704	1,453339	1,3E-13
tRNA	1590531	1590607	-	Cjp32	tRNA-His	5309	4257,5	10307	10509	1,035474	1,42E-12
tRNA	1215241	1215316	-	Cjp24	tRNA-Phe	883	585	2039	2032	1,391113	3,48E-12
tRNA	1590271	1590355	-	Cjt05	tRNA-Leu	1266	978	2710	2239	1,049714	5,9E-10
tRNA	1215057	1215133	+	Cjp23	tRNA-Met	182	161	437	342	1,089018	1,91E-07
CDS	528182	529648	+	Cj0566		22	23	54	82	1,511112	0,004211
tRNA	826066	826152	+	Cjp16	tRNA-Leu	3455,5	1551	4960	6381	1,121251	0,011199

Appendix Table 19. 3 RNAs are downregulated in WT vs D85N. The table indicates RNAs (5' UTR, CDS, sRNA, and tRNA) with changed levels (log2FC <1.0) and with a p-value <0.05 in the WT vs D85N strains.

Type	Start	End	Strand	Gene	Name	D85N R1	D85N R2	WT R1	WT R2	log2 FoldChange	p-value
CDS	1394285	1395403	-	Cj1457c	*truD*	2145	1877	393	407	-2,41944	1,89E-91
CDS	32134	33519	-	Cj0025c		1471	1136	646	603	-1,14934	1,77E-16
CDS	1432607	1433815	+	Cj1500		240	234	112	127	-1,07922	1,31E-05

Appendix Table 20. Mapping statistics for CLIP-seq experiments of *Campylobacter jejuni* TruD-3xFLAG, C*truD* and D85N. The table indicates the total number of sequenced reads (number of input reads), the number of reads that were removed from the analysis because too short, the total number of mapped reads, the number of alignments (i.e. some reads map to different locations with the same score), and the number of uniquely mapped reads. For the number of input reads and the number of uniquely mapped reads, the percentage value are also listed.

Libraries	CLIP_CtruD	CLIP_CtruD_XL	CLIP_D85N	CLIP_D85N_XL	CLIP_TruD_3XFLAG	CLIP_TruD_3XFLAG_XL
Number of input reads	22,274,345	21,323,045	21,9411,114	22,332,068	17,101,699	19,450,051
Number of reads removed as too short	747,312	1,096,732	963,509	1,083,654	1,638,603	1,321,308
Total number of aligned reads	3,574,331	8,375,402	5,463,433	9,280,293	6,261,595	6,896,981
Total number of uniquely mapped reads	846,624	2,400,279	1,432,493	2,619,045	1,388,721	1,752,793
Total number of alignments	8,977,802	20,245,020	13,439,167	22,520,763	15,918,682	17,086,392
% of mapped reads (compared to no. of input reads)	16.05	39.28	24.9	41.56	36.61	35.46
% of uniquely aligned reads (in relation to all aligned reads)	23.69	28.66	26.22	28.22	22.18	25.41

Appendix Table 21. Mapping statistics for Ribo-seq experiment of *Campylobacter jejuni* WT, Δ*truD*, C*truD*. The table indicates the total number of sequenced reads (number of input reads), the number of reads that were removed from the analysis because too short, the total number of mapped reads, the number of alignments (i.e. some reads map to different locations with the same score), and the number of uniquely mapped reads. For the number of input reads and the number of uniquely mapped reads, the percentage value are also listed.

Libraries	C*truD* R1 RBP	C*truD* R2 RBP	C*truD* R1 RNA-seq	C*truD* R2 RNA-seq	Δ*truD* R1 RBP	Δ*truD* R2 RBP
Number of input reads	26,843,096	69,666,931	20,496,380	61,231,466	27,796,392	65,062,768
Number of reads removed as too short	0	0	0	0	0	0
Total number of aligned reads	26,655,133	68,592,230	20,182,590	59,670,577	27,609,263	64,117,294
Total number of uniquely mapped reads	14,059,192	34,210,418	13,565,271	37,066,968	13,485,910	35,506,357
Total number of alignments	51,545,296	136,541,734	31,725,096	10,0156,502	55,552,467	120,428,033
% of mapped reads (compared to no. of input reads)	99.3	98.46	98.47	97.45	99.33	98.55
% of uniquely aligned reads (in relation to all aligned reads)	52.74	49.88	67.21	62.12	48.85	55.38

Libraries	Δ*truD* R1 RNA-seq	Δ*truD* R2 RNA-seq	WT R1 RBP	WT R2 RBP	WT R1 RNA-seq	WT R2 RNA-seq
Number of input reads	23,283,501	59,650,833	24,677,824	68,133,625	27,638,870	45,173,776
Number of reads removed as too short	0	0	0	0	0	0
Total number of aligned reads	23,055,602	58,630,614	24,510,463	67,391,641	27,277,610	44,006,966
Total number of uniquely mapped reads	15,324,563	37,882,502	11,883,534	30,821,262	18,075,881	28,892,671
Total number of alignments	36,247,288	94,327,269	49,535,947	139,903,362	43,392,472	70,216,516
% of mapped reads (compared to no. of input reads)	99.02	98.29	99.32	98.91	98.69	97.42
% of uniquely aligned reads (in relation to all aligned reads)	66.47	64.61	48.48	45.73	66.27	65.65

Appendix Table 22. 28 genes are differentially translated in C*truD* vs Δ*truD*. The table indicates RNAs (ORFs only) with changed TE (Translational Efficiency) levels (log2FC <0.5/>0.5) and with a p-value <0.05 in the C*truD* vs Δ*truD* strains. Only the annotated ORFs were checked and used for the analysis. The tool "xtail" was used for the calculation of differential expression.

Start	Stop	Strand	Locus_tag	log2FC_TE	p-value
576225	576965	+	Cj0616	1,853891628	8,62189E-08
1492003	1493991	+	Cj1564	1,751132815	2,77522E-06
1409278	1409595	-	Cj1475c	1,618441061	0,000169275
416251	416466	-	Cj0449c	1,216728084	2,11033E-06
339071	339283	+	Cj0370	1,201034889	0,000548564
675560	676192	-	Cj0719c	1,19608107	1,60098E-05
1055060	1055713	-	Cj1122c	1,126637409	0,000261416
421850	422479	-	Cj0457c	1,11850465	0,000783938
16452	16691	-	Cj0011c	1,097090178	5,99543E-05
852181	852378	-	Cj0916c	1,037114068	0,000300801
671169	671498	+	Cj0717	1,016517506	8,44207E-05
484826	485143	+	Cj0519	0,999745164	0,000657864
669832	671172	+	Cj0716	0,932173919	3,48895E-05
107664	108317	+	Cj0099	0,923506162	0,000257566
1620389	1620700	-	Cj1708c	0,916012149	4,81975E-05
158139	158339	-	Cj0155c	0,802898536	0,000468226
457683	458153	+	Cj0492	0,796727851	0,000415469
1128243	1129235	+	Cj1199	-0,900858561	9,45057E-05
315398	316648	+	Cj0345	-0,906086811	0,000168765
480700	481896	+	Cj0515	-0,911549227	0,001003002
524034	524963	-	Cj0561c	-0,918094584	0,000857089
933075	933587	-	Cj1002c	-0,966330606	0,000477257
165938	166105	-	Cj0168c	-0,979246504	1,22098E-05
245504	246013	-	Cj0266c	-1,024087295	7,50056E-05
167050	167295	+	Cj0170	-1,05689604	4,56715E-05
1302620	1304968	-	Cj1367c	-1,068167766	2,46655E-05
767555	767782	+	Cj0818	-1,183452966	0,000232571
609255	609770	+	Cj0648	-1,486648365	2,2962E-05

Appendix Table 23.15 genes are differentially translated in C*truD vs* WT. The table indicates RNAs (ORFs only) with changed TE (Translational Efficiency) levels (log2FC <0.5/>0.5) and with a p-value <0.05 in the C*truD vs* WT strains. Only the annotated ORFs were checked and used for the analysis. The tool "xtail" was used for the calculation of differential expression.

Start	Stop	Strand	Locus_tag	log2FC_TE	p-value
324913	325230	-	Cj0356c	1,459671366	0,000123511
224256	224657	-	Cj0241c	1,450455793	0,000173692
617113	618219	-	Cj0660c	1,442395903	0,000484318
788015	788212	-	Cj0839c	1,31750145	2,79242E-05
1402445	1403209	+	Cj1467	1,287385519	0,000795835
404585	404995	+	Cj0436	1,008628019	0,000430928
23392	23559	-	Cj0018c	0,995955506	0,000637267
79257	79736	-	Cj0066c	-0,995136812	0,000182769
1468409	1470382	-	Cj1537c	-1,195308436	6,94477E-05
1565113	1565664	+	Cj1640	-1,31827317	0,000185408
1263676	1265454	+	Cj1335	-1,343966285	5,15785E-05
933075	933587	-	Cj1002c	-1,53412923	3,87033E-05
689656	691584	+	Cj0736	-2,010715274	0,000804531
1322526	1323950	+	Cj1385	-2,380220985	3,69825E-09
1322041	1322355	-	Cj1384c	-2,858502034	5,24604E-07

Appendix Table 24.22 genes are differentially translated in Δ*truD* vs WT. The table indicates RNAs (ORFs only) with changed TE (Translational Efficiency) levels (log2FC <0.5/>0.5) and with a p-value <0.05 in the Δ*truD* vs WT strains. Only the annotated ORFs were checked and used for the analysis. The tool "xtail" was used for the calculation of differential expression.

Start	Stop	Strand	Locus_tag	log2FC_TE	p-value
129078	129800	-	Cj0128c	1,460982901	2,51246E-07
23392	23559	-	Cj0018c	1,305337633	7,99576E-06
609255	609770	+	Cj0648	1,22286179	0,00014067
167050	167295	+	Cj0170	1,194366454	1,38937E-05
245504	246013	-	Cj0266c	1,09422887	4,70384E-05
677498	678313	-	Cj0722c	1,059843691	2,17894E-05
165938	166105	-	Cj0168c	1,051966455	5,94195E-06
668191	668895	+	Cj0713	0,895989832	0,000417787
116657	117436	+	Cj0111	0,894210528	0,000187752
457683	458153	+	Cj0492	-0,856826131	0,000274404
26411	27289	-	Cj0021c	-0,910422835	9,04681E-05
19251	19775	-	Cj0014c	-0,953188077	0,000107722
1244256	1245392	-	Cj1316c	-0,961032969	5,91922E-05
1280652	1280990	-	Cj1348c	-0,964919018	9,21565E-05
16452	16691	-	Cj0011c	-1,211016706	5,88599E-05
810963	811322	+	Cj0864	-1,238955395	7,70016E-07
846971	847390	+	Cj0909	-1,272224317	1,81813E-07
576225	576965	+	Cj0616	-1,335645008	0,000139393
1580836	1582926	+	Cj1658	-1,411027608	3,60948E-06
1263676	1265454	+	Cj1335	-1,490926051	1,38798E-06
1322526	1323950	+	Cj1385	-1,920735973	2,05811E-06
339071	339283	+	Cj0370	-2,194414191	4,6863E-10

9. REFERENCES

Adams, R.L.P., Knowler, J.T. & Leader, D.P. (1992) The biochemistry of the nucleic acids. *Springer Netherlands,* Dordrecht.

Ahn, K.-S., Ha, U., Jia, J., Wu, D. & Jin, S. (2004) The *truA* gene of *Pseudomonas aeruginosa* is required for the expression of type III secretory genes. *Microbiology*, 150, 539–547.

Akanuma, G., Nanamiya, H., Natori, Y., Yano, K., Suzuki, S., Omata, S., et al. (2012) Inactivation of ribosomal protein genes in *Bacillus subtilis* reveals importance of each ribosomal protein for cell proliferation and cell differentiation. *Journal of Bacteriology*, 194, 6282–6291.

Albanna, A., Sim, M., Hoskisson, P.A., Gillespie, C., Rao, C.V. & Aldridge, P.D. (2018) Driving the expression of the *Salmonella enterica* sv Typhimurium flagellum using flhDC from Escherichia coli results in key regulatory and cellular differences. *Scientific Reports*, 8, 16705.

Alexandrov, A., Chernyakov, I., Gu, W., Hiley, S.L., Hughes, T.R., Grayhack, E.J., et al. (2006) Rapid tRNA decay can result from lack of nonessential modifications. *Molecular Cell*, 21, 87–96.

Alseth, I., Dalhus, B. & Bjørås, M. (2014) Inosine in DNA and RNA. *Current Opinion in Genetics & Development*, 26, 116–123.

Alzheimer, M., Svensson, S.L., König, F., Schweinlin, M., Metzger, M., Walles, H., et al. (2020) A three-dimensional intestinal tissue model reveals factors and small regulatory RNAs important for colonization with *Campylobacter jejuni*. *PLoS Pathogens*, 16, e1008304.

Andersen, N.M. & Douthwaite, S. (2006) YebU is a m5C methyltransferase specific for 16 S rRNA nucleotide 1407. *Journal of Molecular Biology*, 359, 777–786.

Apirion, D. (1973) Degradation of RNA in *Escherichia coli*. *Molecular and General Genetics* MGG.

Aravind, L. & Koonin, E.V. (2001) THUMP--a predicted RNA-binding domain shared by 4-thiouridine, pseudouridine synthases and RNA methylases. *Trends in Biochemical Sciences*, 26, 215–217.

Arena, F., Ciliberto, G., Ciampi, S. & Cortese, R. (1978) Purification of pseudouridylate synthetase I from *Salmonella* typhimurium. *Nucleic Acids Research*, 5, 4523–4536.

Auffinger, P. & Westhof, E. (1997) Rules governing the orientation of the 2'-hydroxyl group in RNA. *Journal of Molecular Biology*, 274, 54–63.

Auffinger, P. & Westhof, E. (1998) Hydration of RNA base pairs. *Journal of Biomolecular Structure* and ….

Auxilien, S., Crain, P.F., Trewyn, R.W. & Grosjean, H. (1996) Mechanism, specificity and general properties of the yeast enzyme catalysing the formation of inosine 34 in the anticodon of transfer RNA. *Journal of Molecular Biology*, 262, 437–458.

Ayadi, L., Galvanin, A., Pichot, F., Marchand, V. & Motorin, Y. (2018) RNA ribose methylation (2'-O-methylation): Occurrence, biosynthesis and biological functions. *Biochimica et biophysica acta. Gene regulatory mechanisms*, 1862, 253–269.

Azevedo, C. & Saiardi, A. (2016) Why always lysine? The ongoing tale of one of the most modified amino acids. *Advances in biological regulation*, 60, 144–150.

Bakin, A., Lane, B.G. & Ofengand, J. (1994) Clustering of pseudouridine residues around the peptidyltransferase center of yeast cytoplasmic and mitochondrial ribosomes. *Biochemistry*, 33, 13475–13483.

Bakin, A.V. & Ofengand, J. (1998) Mapping of pseudouridine residues in RNA to nucleotide resolution. *Methods in Molecular Biology*, 77, 297–309.

Balakin, A.G., Smith, L. & Fournier, M.J. (1996) The RNA world of the nucleolus: two major families of small RNAs defined by different box elements with related functions. *Cell*, 86, 823–834.

Bar-Yaacov, D., Mordret, E., Towers, R., Biniashvili, T., Soyris, C., Schwartz, S., et al. (2017) RNA editing in bacteria recodes multiple proteins and regulates an evolutionarily conserved toxin-antitoxin system. *Genome Research*, 27, 1696–1703.

Basu, P. & Altuvia, S. (2021) RelA binding of mRNAs modulates translation or sRNA-mRNA basepairing depending on the position of the GGAG site. *Molecular Microbiology*.

Becker, H.F., Motorin, Y., Planta, R.J. & Grosjean, H. (1997c) The yeast gene YNL292w encodes a pseudouridine synthase (Pus4) catalyzing the formation of psi55 in both mitochondrial and cytoplasmic tRNAs. *Nucleic Acids Research,* 25, 4493–4499.

Behm-Ansmant, I., Urban, A., Ma, X., Yu, Y.-T., Motorin, Y. & Branlant, C. (2003) The Saccharomyces cerevisiae U2 snRNA:pseudouridine-synthase Pus7p is a novel multisite-multisubstrate RNA:Psi-synthase also acting on tRNAs. *RNA* (New York), 9, 1371–1382.

Boccaletto, P., Machnicka, M.A., Purta, E., Piatkowski, P., Baginski, B., Wirecki, T.K., et al. (2018) MODOMICS: a database of RNA modification pathways. 2017 update. *Nucleic Acids Research*, 46, D303–D307.

Boccaletto, P., Stefaniak, F., Ray, A., Cappannini, A., Mukherjee, S., Purta, E., et al. (2022) MODOMICS: a database of RNA modification pathways. 2021 update. *Nucleic Acids Research*, 50, D231–D235.

Bohnsack, K.E., Höbartner, C. & Bohnsack, M.T. (2019) Eukaryotic 5-methylcytosine (m^5C) RNA Methyltransferases: Mechanisms, Cellular Functions, and Links to Disease. *Genes*, 10.

Bremer, H., Konrad, M.W., Gaines, K. & Stent, G.S. (1965) Direction of chain growth in enzymic RNA synthesis. *Journal of molecular biology*.

Brenner, S., Jacob, F. & Meselson, M. (1961) An Unstable Intermediate Carrying Information from Genes to Ribosomes for Protein Synthesis. *Nature*, 190, 576–581.

Burnham, P.M. & Hendrixson, D.R. (2018) *Campylobacter jejuni*: collective components promoting a successful enteric lifestyle. *Nature Reviews. Microbiology*, 16, 551–565.

Bykhovskaya, Y., Casas, K., Mengesha, E., Inbal, A. & Fischel-Ghodsian, N. (2004) Missense mutation in pseudouridine synthase 1 (PUS1) causes mitochondrial myopathy and sideroblastic anemia (MLASA). *American Journal of Human Genetics*, 74, 1303–1308.

Cabello-Villegas, J. & Nikonowicz, E.P. (2005) Solution structure of psi32-modified anticodon stem-loop of Escherichia coli tRNAPhe. *Nucleic Acids Research*, 33, 6961–6971.

Cahová, H., Winz, M.-L., Höfer, K., Nübel, G. & Jäschke, A. (2015) NAD captureSeq indicates NAD as a bacterial cap for a subset of regulatory RNAs. *Nature*, 519, 374–377.

Cameron, A., Frirdich, E., Huynh, S., Parker, C.T. & Gaynor, E.C. (2012) Hyperosmotic stress response of *Campylobacter jejuni*. *Journal of Bacteriology*, 194, 6116–6130.

Cameron, A. & Gaynor, E.C. (2014) Hygromycin B and apramycin antibiotic resistance cassettes for use in *Campylobacter jejuni*. *Plos One*, 9, e95084.

Campo, M. Del, Kaya, Y. & Ofengand, J. (2001) Identification and site of action of the remaining four putative pseudouridine synthases in *Escherichia coli*. *RNA* (New York), 7, 1603–1615.

Carlile, T.M., Rojas-Duran, M.F. & Gilbert, W.V. (2015) Pseudo-Seq: Genome-Wide Detection of Pseudouridine Modifications in RNA. *Methods in Enzymology*, 560, 219–245.

Carlile, T.M., Rojas-Duran, M.F., Zinshteyn, B., Shin, H., Bartoli, K.M. & Gilbert, W.V. (2014) Pseudouridine profiling reveals regulated mRNA pseudouridylation in yeast and human cells. *Nature*, 515, 143–146.

Charette, M. & Gray, M.W. (2000) Pseudouridine in RNA: what, where, how, and why. *IUBMB Life*, 49, 341–351.

Cohn, W.E. (1959) 5-Ribosyl uracil, a carbon-carbon ribofuranosyl nucleoside in ribonucleic acids. *Biochimica et biophysica acta*, 32, 569–571.

Cohn, W.E. & Volkin, E. (1951) Nucleoside-5′-phosphates from ribonucleic acid. *Nature*.

Cortese, R., Kammen, H.O., Spengler, S.J. & Ames, B.N. (1974) Biosynthesis of pseudouridine in transfer ribonucleic acid. *The Journal of Biological Chemistry*, 249, 1103–1108.

Costard, S., Espejo, L., Groenendaal, H. & Zagmutt, F.J. (2017) Outbreak-Related Disease Burden Associated with Consumption of Unpasteurized Cow's Milk and Cheese, United States, 2009-2014. *Emerging Infectious Diseases*, 23, 957–964.

Crick, F.H. (1966) Codon--anticodon pairing: the wobble hypothesis. *Journal of Molecular Biology*, 19, 548–555.

Cui, Q., Yin, K., Zhang, X., Ye, P., Chen, X., Chao, J., et al. (2021) Targeting PUS7 suppresses tRNA pseudouridylation and glioblastoma tumorigenesis. Nature Cancer.

Davis, F.F. & Allen, F.W. (1957) Ribonucleic acids from yeast which contain a fifth nucleotide. *Journal of Biological Chemistry*.

de Crécy-Lagard, V., Ross, R.L., Jaroch, M., Marchand, V., Eisenhart, C., Brégeon, D., et al. (2020) Survey and Validation of tRNA Modifications and Their Corresponding Genes in Bacillus subtilis sp Subtilis Strain 168. *Biomolecules*, 10.

Decatur, W.A. & Schnare, M.N. (2008) Different mechanisms for pseudouridine formation in yeast 5S and 5.8S rRNAs. *Molecular and Cellular Biology*, 28, 3089–3100.

Delvillani, F., Papiani, G., Dehò, G. & Briani, F. (2011) S1 ribosomal protein and the interplay between translation and mRNA decay. *Nucleic Acids Research*, 39, 7702–7715.

Deng, X., Chen, K., Luo, G.-Z., Weng, X., Ji, Q., Zhou, T., et al. (2015) Widespread occurrence of N6-methyladenosine in bacterial mRNA. *Nucleic Acids Research*, 43, 6557–6567.

Denmon, A.P., Wang, J. & Nikonowicz, E.P. (2011) Conformation effects of base modification on the anticodon stem-loop of Bacillus subtilis tRNA(Tyr). *Journal of Molecular Biology*, 412, 285–303.

Deogharia, M., Mukhopadhyay, S., Joardar, A. & Gupta, R. (2019) The human ortholog of archaeal Pus10 produces pseudouridine 54 in select tRNAs where its recognition sequence contains a modified residue. *RNA* (New York), 25, 336–351.

Desrosiers, R., Friderici, K. & Rottman, F. (1974) Identification of methylated nucleosides in messenger RNA from Novikoff hepatoma cells. *Proceedings of the National Academy of Sciences of the United States of America*, 71, 3971–3975.

Dimitrova, D.G., Teysset, L. & Carré, C. (2019) RNA 2'-O-Methylation (Nm) Modification in Human Diseases. *Genes*, 10.

Dominissini, D., Moshitch-Moshkovitz, S., Schwartz, S., Salmon-Divon, M., Ungar, L., Osenberg, S., et al. (2012) Topology of the human and mouse m6A RNA methylomes revealed by m6A-seq. *Nature*, 485, 201–206.

Drazic, A., Myklebust, L.M., Ree, R. & Arnesen, T. (2016) The world of protein acetylation. *Biochimica et Biophysica Acta*, 1864, 1372–1401.

Dugar, G., Herbig, A., Förstner, K.U., Heidrich, N., Reinhardt, R., Nieselt, K., et al. (2013) High-resolution transcriptome maps reveal strain-specific regulatory features of multiple *Campylobacter jejuni* isolates. *PLoS Genetics*, 9, e1003495.

Dugar, G., Leenay, R.T., Eisenbart, S.K., Bischler, T., Aul, B.U., Beisel, C.L., et al. (2018) CRISPR RNA-Dependent Binding and Cleavage of Endogenous RNAs by the *Campylobacter jejuni* Cas9. *Molecular Cell*, 69, 893–905.e7.

Dugar, G., Svensson, S.L., Bischler, T., Wäldchen, S., Reinhardt, R., Sauer, M., et al. (2016) The CsrA-FliW network controls polar localization of the dual-function flagellin mRNA in Campylobacter jejuni. *Nature Communications*, 7, 11667.

Duqué, B., Rezé, S., Rossero, A., Membré, J.-M., Guillou, S. & Haddad, N. (2021) Quantification of *Campylobacter jejuni* gene expression after successive stresses mimicking poultry slaughtering steps. *Food microbiology*, 98, 103795.

Durairaj, A. & Limbach, P.A. (2008) Mass spectrometry of the fifth nucleoside: a review of the identification of pseudouridine in nucleic acids. *Analytica Chimica Acta*, 623, 117–125.

Duval, M., Korepanov, A., Fuchsbauer, O., Fechter, P., Haller, A., Fabbretti, A., et al. (2013) Escherichia coli ribosomal protein S1 unfolds structured mRNAs onto the ribosome for active translation initiation. *PLoS Biology*, 11, e1001731.

Edelheit, S., Schwartz, S., Mumbach, M.R., Wurtzel, O. & Sorek, R. (2013) Transcriptome-wide mapping of 5-methylcytidine RNA modifications in bacteria, archaea, and yeast reveals m5C within archaeal mRNAs. *PLoS Genetics*, 9, e1003602.

Eisenbart, S.K., Alzheimer, M., Pernitzsch, S.R., Dietrich, S., Stahl, S. & Sharma, C.M. (2020) A Repeat-Associated Small RNA Controls the Major Virulence Factors of *Helicobacter pylori*. *Molecular Cell*, 80, 210–226.e7.

Emmerechts, G., Herdewijn, P. & Rozenski, J. (2005) Pseudouridine detection improvement by derivatization with methyl vinyl sulfone and capillary HPLC-mass spectrometry. *Journal of Chromatography. B, Analytical Technologies in the Biomedical and Life Sciences*, 825, 233–238.

Erickson, H.P. (2009) Size and shape of protein molecules at the nanometer level determined by sedimentation, gel filtration, and electron microscopy. *Biological procedures online*, 11, 32–51.

Eyler, D.E., Franco, M.K., Batool, Z., Wu, M.Z., Dubuke, M.L., Dobosz-Bartoszek, M., et al. (2019) Pseudouridinylation of mRNA coding sequences alters translation. *Proceedings of the National Academy of Sciences of the United States of America*, 116, 23068–23074.

Feederle, R. & Schepers, A. (2017) Antibodies specific for nucleic acid modifications. *RNA Biology*, 14, 1089–1098.

Feng, J., Meyer, C.A., Wang, Q., Liu, J.S., Shirley Liu, X. & Zhang, Y. (2012) GFOLD: a generalized fold change for ranking differentially expressed genes from RNA-seq data. *Bioinformatics*, 28, 2782–2788.

Floch, P., Mégraud, F. & Lehours, P. (2017) *Helicobacter pylori* Strains and Gastric MALT Lymphoma. *Toxins*, 9.

Förstner, K.U., Vogel, J. & Sharma, C.M. (2014) READemption-a tool for the computational analysis of deep-sequencing-based transcriptome data. *Bioinformatics*, 30, 3421–3423.

Foster, P.G., Nunes, C.R., Greene, P., Moustakas, D. & Stroud, R.M. (2003) The first structure of an RNA m5C methyltransferase, Fmu, provides insight into catalytic mechanism and specific binding of RNA substrate. *Structure*, 11, 1609–1620.

Frindert, J., Zhang, Y., Nübel, G., Kahloon, M., Kolmar, L., Hotz-Wagenblatt, A., et al. (2018) Identification, Biosynthesis, and Decapping of NAD-Capped RNAs in B. subtilis. *Cell reports*, 24, 1890–1901.e8.

Frommer, M., McDonald, L.E., Millar, D.S., Collis, C.M., Watt, F., Grigg, G.W., et al. (1992) A genomic sequencing protocol that yields a positive display of 5-methylcytosine residues in individual DNA strands. *Proceedings of the National Academy of Sciences of the United States of America*, 89, 1827–1831.

Fukuda, R. & Nagasawa-Fujimori, H. (1983) Mechanism of the rifampicin induction of RNA polymerase beta and beta' subunit synthesis in Escherichia coli. *The Journal of Biological Chemistry*, 258, 2720–2728.

Galvanin, A., Vogt, L.-M., Grober, A., Freund, I., Ayadi, L., Bourguignon-Igel, V., et al. (2020) Bacterial tRNA 2'-O-methylation is dynamically regulated under stress conditions and modulates innate immune response. *Nucleic Acids Research*, 48, 12833–12844.

Ganot, P., Bortolin, M.L. & Kiss, T. (1997) Site-specific pseudouridine formation in preribosomal RNA is guided by small nucleolar RNAs. *Cell*, 89, 799–809.

Garalde, D.R., Snell, E.A., Jachimowicz, D., Sipos, B., Lloyd, J.H., Bruce, M., et al. (2018) Highly parallel direct RNA sequencing on an array of nanopores. *Nature Methods*, 15, 201–206.

Gelhausen, R., Svensson, S.L., Froschauer, K., Heyl, F., Hadjeras, L., Sharma, C.M., et al. (2021) HRIBO: high-throughput analysis of bacterial ribosome profiling data. *Bioinformatics*, 37, 2061–2063.

Goldman, S.R., Sharp, J.S., Vvedenskaya, I.O., Livny, J., Dove, S.L. & Nickels, B.E. (2011) NanoRNAs prime transcription initiation in vivo. *Molecular Cell*, 42, 817–825.

Golovina, A.Y., Dzama, M.M., Osterman, I.A., Sergiev, P.V., Serebryakova, M.V., Bogdanov, A.A., et al. (2012) The last rRNA methyltransferase of E. coli revealed: the yhiR gene encodes adenine-N6 methyltransferase specific for modification of A2030 of 23S ribosomal RNA. *RNA* (New York), 18, 1725–1734.

Gottesman, S. & Storz, G. (2011) Bacterial small RNA regulators: versatile roles and rapidly evolving variations. *Cold Spring Harbor Perspectives in Biology,* 3.

Gros, F., Hiatt, H., Gilbert, W., Kurland, C.G., Risebrough, R.W. & Watson, J.D. (1961) Unstable ribonucleic acid revealed by pulse labelling of *Escherichia coli. Nature*, 190, 581–585.

Grosjean, H., Keith, G. & Droogmans, L. (2004) Detection and quantification of modified nucleotides in RNA using thin-layer chromatography. *Methods in Molecular Biology*, 265, 357–391.

Guerry, P., Alm, R.A., Power, M.E., Logan, S.M. & Trust, T.J. (1991) Role of two flagellin genes in *Campylobacter* motility. *Journal of Bacteriology*, 173, 4757–4764.

Gutgsell, N., Englund, N., Niu, L., Kaya, Y., Lane, B.G. & Ofengand, J. (2000) Deletion of the Escherichia coli pseudouridine synthase gene truB blocks formation of pseudouridine 55 in tRNA in vivo, does not affect exponential growth, but confers a strong selective disadvantage in competition with wild-type cells. *RNA* (New York), 6, 1870–1881.

Gutgsell, N.S., Campo, M. Del, Raychaudhuri, S. & Ofengand, J. (2001) A second function for pseudouridine synthases: A point mutant of RluD unable to form pseudouridines 1911, 1915, and 1917 in Escherichia coli 23S ribosomal RNA restores normal growth to an RluD-minus strain. *RNA* (New York), 7, 990–998.

Guzzi, N., Cieśla, M., Ngoc, P.C.T., Lang, S., Arora, S., Dimitriou, M., et al. (2018) Pseudouridylation of tRNA-Derived Fragments Steers Translational Control in Stem Cells. *Cell*, 173, 1204–1216.e26.

Hamma, T. & Ferré-D'Amaré, A.R. (2006) Pseudouridine synthases. *Chemistry & Biology*, 13, 1125–1135.

Han, S.T., Kim, A.C., Garcia, K., Schimmenti, L.A., Macnamara, E., Network, U.D., et al. (2022) PUS7 deficiency in human patients causes profound neurodevelopmental phenotype by dysregulating protein translation. *Molecular Genetics and Metabolism*.

He, C. (2010) Grand challenge commentary: RNA epigenetics? *Nature Chemical Biology*, 6, 863–865.

Heinicke, F., Zhong, X., Zucknick, M., Breidenbach, J., Sundaram, A.Y.M., T Flåm, S., et al. (2020) Systematic assessment of commercially available low-input miRNA library preparation kits. *RNA Biology*, 17, 75–86.

Heiss, N.S., Knight, S.W., Vulliamy, T.J., Klauck, S.M., Wiemann, S., Mason, P.J., et al. (1998) X-linked dyskeratosis congenita is caused by mutations in a highly conserved gene with putative nucleolar functions. *Nature Genetics*, 19, 32–38.

Helm, M. (2006) Post-transcriptional nucleotide modification and alternative folding of RNA. *Nucleic Acids Research*, 34, 721–733.

Helm, M., Lyko, F. & Motorin, Y. (2019) Limited antibody specificity compromises epitranscriptomic analyses. *Nature Communications*, 10, 5669.

Hoagland, M.B., Stephenson, M.L., Scott, J.F., Hecht, L.I. & Zamecnik, P.C. (1958) A soluble ribonucleic acid intermediate in protein synthesis. *The Journal of Biological Chemistry*, 231, 241–257.

Hoang, C. & Ferré-D'Amaré, A.R. (2001) Cocrystal structure of a tRNA Psi55 pseudouridine synthase: nucleotide flipping by an RNA-modifying enzyme. *Cell*, 107, 929–939.

Höfer, K. & Jäschke, A. (2018a) Epitranscriptomics: RNA modifications in bacteria and archaea. *Microbiology spectrum*, 6.

Höfer, K. & Jäschke, A. (2018b) Epitranscriptomics: RNA modifications in bacteria and archaea. In Regulating with RNA in Bacteria and Archaea (ed. Storz, G. & Papenfort, K.). *ASM Press*, Washington, DC, USA, pp. 399–420.

Holmes, C.W., Penn, C.W. & Lund, P.A. (2010) The *hrcA* and *hspR* regulons of *Campylobacter jejuni*. *Microbiology*, 156, 158–166.

Holmqvist, E., Li, L., Bischler, T., Barquist, L. & Vogel, J. (2018) Global Maps of ProQ Binding In Vivo Reveal Target Recognition via RNA Structure and Stability Control at mRNA 3' Ends. *Molecular Cell*, 70, 971–982.e6.

Holmqvist, E. & Vogel, J. (2018) RNA-binding proteins in bacteria. *Nature Reviews. Microbiology*, 16, 601–615.

Holmqvist, E., Wright, P.R., Li, L., Bischler, T., Barquist, L., Reinhardt, R., et al. (2016) Global RNA recognition patterns of post-transcriptional regulators Hfq and CsrA revealed by UV crosslinking in vivo. *The EMBO Journal*, 35, 991–1011.

Hör, J., Garriss, G., Giorgio, S. Di, Hack, L.-M., Vanselow, J.T., Förstner, K.U., et al. (2020a) Grad-seq in a Gram-positive bacterium reveals exonucleolytic sRNA activation in competence control. *The EMBO Journal*, 39, e103852.

Hör, J., Giorgio, S. Di, Gerovac, M., Venturini, E., Förstner, K.U. & Vogel, J. (2020b) Grad-seq shines light on unrecognized RNA and protein complexes in the model bacterium *Escherichia coli*. *Nucleic Acids Research*, 48, 9301–9319.

Hori, H. (2017) Transfer RNA methyltransferases with a SpoU-TrmD (SPOUT) fold and their modified nucleosides in tRNA. *Biomolecules*, 7.

Horowitz, S., Horowitz, A., Nilsen, T.W., Munns, T.W. & Rottman, F.M. (1984) Mapping of N6-methyladenosine residues in bovine prolactin mRNA. *Proceedings of the National Academy of Sciences of the United States of America*, 81, 5667–5671.

Huang, C., Wu, G. & Yu, Y.-T. (2012) Inducing nonsense suppression by targeted pseudouridylation. *Nature Protocols*, 7, 789–800.

Hur, S. & Stroud, R.M. (2007) How U38, 39, and 40 of many tRNAs become the targets for pseudouridylation by TruA. *Molecular Cell*, 26, 189–203.

Ingolia, N.T., Brar, G.A., Rouskin, S., McGeachy, A.M. & Weissman, J.S. (2012) The ribosome profiling strategy for monitoring translation in vivo by deep sequencing of ribosome-protected mRNA fragments. *Nature Protocols*, 7, 1534–1550.

Ishida, K., Kunibayashi, T., Tomikawa, C., Ochi, A., Kanai, T., Hirata, A., et al. (2011) Pseudouridine at position 55 in tRNA controls the contents of other modified nucleotides for low-temperature adaptation in the extreme-thermophilic eubacterium Thermus thermophilus. *Nucleic Acids Research*, 39, 2304–2318.

Itoh, K., Mizugaki, M. & Ishida, N. (1989) Detection of elevated amounts of urinary pseudouridine in cancer patients by use of a monoclonal antibody. *Clinica Chimica Acta*, 181, 305–315.

Janssen, B.D., Diner, E.J. & Hayes, C.S. (2012) Analysis of aminoacyl- and peptidyl-tRNAs by gel electrophoresis. *Methods in Molecular Biology*, 905, 291–309.

Jayalath, K., Frisbie, S., To, M. & Abeysirigunawardena, S. (2020) Pseudouridine Synthase RsuA Captures an Assembly Intermediate that Is Stabilized by Ribosomal Protein S17. *Biomolecules*, 10.

Jenjaroenpun, P., Wongsurawat, T., Wadley, T.D., Wassenaar, T.M., Liu, J., Dai, Q., et al. (2021) Decoding the epitranscriptional landscape from native RNA sequences. *Nucleic Acids Research*, 49, e7.

Jeter, V.L. & Escalante-Semerena, J.C. (2021) Sirtuin-dependent reversible lysine acetylation controls the activity of acetyl-Coenzyme A synthetase in *Campylobacter jejuni*. *Journal of Bacteriology*, JB0033321.

Jia, G., Fu, Y., Zhao, X., Dai, Q., Zheng, G., Yang, Y., et al. (2011) N6-methyladenosine in nuclear RNA is a major substrate of the obesity-associated FTO. *Nature Chemical Biology*, 7, 885–887.

Johnson, L. & Söll, D. (1970) In vitro biosynthesis of pseudouridine at the polynucleotide level by an enzyme extract from Escherichia coli. *Proceedings of the National Academy of Sciences of the United States of America*, 67, 943–950.

Jorgensen, S.E., Buch, L.B. & Nierlich, D.P. (1969) Nucleoside triphosphate termini from RNA synthesized in vivo by *Escherichia coli. Science*.

Kambampati, R. & Lauhon, C.T. (2003) MnmA and IscS are required for in vitro 2-thiouridine biosynthesis in *Escherichia coli. Biochemistry*, 42, 1109–1117.

Kanehisa, M. (2019) Toward understanding the origin and evolution of cellular organisms. Protein *Science*, 28, 1947–1951.

Kanehisa, M., Furumichi, M., Sato, Y., Ishiguro-Watanabe, M. & Tanabe, M. (2021) KEGG: integrating viruses and cellular organisms. *Nucleic Acids Research*, 49, D545–D551.

Kanehisa, M. & Goto, S. (2000) KEGG: Kyoto encyclopedia of genes and genomes. *Nucleic Acids Research*, 28, 27–30.

Karijolich, J. & Yu, Y.T. (2008) Insight into the protein components of the box H/ACA RNP. *Current proteomics.*

Karijolich, J. & Yu, Y.-T. (2011) Converting nonsense codons into sense codons by targeted pseudouridylation. *Nature*, 474, 395–398.

Karikó, K., Buckstein, M., Ni, H. & Weissman, D. (2005) Suppression of RNA recognition by Toll-like receptors: the impact of nucleoside modification and the evolutionary origin of RNA. Immunity, 23, 165–175.

Kaya, Y., Campo, M. Del, Ofengand, J. & Malhotra, A. (2004) Crystal structure of TruD, a novel pseudouridine synthase with a new protein fold. *The Journal of Biological Chemistry*, 279, 18107–18110.

Kaya, Y. & Ofengand, J. (2003a) A novel unanticipated type of pseudouridine synthase with homologs in bacteria, archaea, and eukarya. *RNA* (New York), 9, 711–721.

Keffer-Wilkes, L.C., Veerareddygari, G.R. & Kothe, U. (2016) RNA modification enzyme TruB is a tRNA chaperone. *Proceedings of the National Academy of Sciences of the United States of America*, 113, 14306–14311.

Keller, P., Freund, I., Marchand, V., Bec, G., Huang, R., Motorin, Y., et al. (2018) Double methylation of tRNA-U54 to 2'-O-methylthymidine (Tm) synergistically decreases immune response by Toll-like receptor 7. *Nucleic Acids Research*, 46, 9764–9775.

Kellner, S., Burhenne, J. & Helm, M. (2010) Detection of RNA modifications. *RNA Biology*, 7, 237–247.

Kierzek, E., Malgowska, M., Lisowiec, J., Turner, D.H., Gdaniec, Z. & Kierzek, R. (2014) The contribution of pseudouridine to stabilities and structure of RNAs. *Nucleic Acids Research*, 42, 3492–3501.

Kim, J.-C., Oh, E., Kim, J. & Jeon, B. (2015) Regulation of oxidative stress resistance in *Campylobacter jejuni*, a microaerophilic foodborne pathogen. *Frontiers in microbiology*, 6, 751.

Kinghorn, S.M., O'Byrne, C.P., Booth, I.R. & Stansfield, I. (2002) Physiological analysis of the role of truB in Escherichia coli: a role for tRNA modification in extreme temperature resistance. *Microbiology*, 148, 3511–3520.

Kinoshita-Daitoku, R., Kiga, K., Miyakoshi, M., Otsubo, R., Ogura, Y., Sanada, T., et al. (2021) A bacterial small RNA regulates the adaptation of *Helicobacter pylori* to the host environment. *Nature Communications*, 12, 2085.

Kiss, T. (2001) Small nucleolar RNA-guided post-transcriptional modification of cellular RNAs. The EMBO Journal, 20, 3617–3622.

Kiss, T. (2002) Small nucleolar RNAs: an abundant group of noncoding RNAs with diverse cellular functions. *Cell*, 109, 145–148.

Konrad, M., Toivonen, J.E. & Cook, J. (1976) The 5' ends of bacterial RNA. II. The triphosphate-terminated ends of primary gene transcripts. *Biochimica et Biophysica Acta*, 425, 63–75.

Korbel, J.O., Jensen, L.J., von Mering, C. & Bork, P. (2004) Analysis of genomic context: prediction of functional associations from conserved bidirectionally transcribed gene pairs. *Nature Biotechnology*, 22, 911–917.

Kreuder, A.J., Ruddell, B., Mou, K. & Hassall, A. (2020) Small noncoding RNA CjNC110 influences motility, autoagglutination, AI-2 localization, hydrogen peroxide sensitivity, and chicken colonization in *Campylobacter* …. Infection and ….

Kurimoto, R., Chiba, T., Ito, Y., Matsushima, T., Yano, Y., Miyata, K., et al. (2020) The tRNA pseudouridine synthase TruB1 regulates the maturation of let-7 miRNA. *The EMBO Journal*, e104708.

Laguerre, S., González, I., Nouaille, S., Moisan, A., Villa-Vialaneix, N., Gaspin, C., et al. (2018) Large-Scale Measurement of mRNA Degradation in *Escherichia coli*: To Delay or Not to Delay. *Methods in Enzymology*, 612, 47–66.

Lara-Tejero, M. & Galán, J.E. (2000) A bacterial toxin that controls cell cycle progression as a deoxyribonuclease I-like protein. *Science*, 290, 354–357.

Le, M.T., van Veldhuizen, M., Porcelli, I., Bongaerts, R.J., Gaskin, D.J.H., Pearson, B.M., et al. (2015) Conservation of σ28-Dependent Non-Coding RNA Paralogs and Predicted σ54-Dependent Targets in Thermophilic *Campylobacter* Species. *Plos One*, 10, e0141627.

Lee, K., Sung, M.-K., Kim, J., Kim, K., Byun, J., Paik, H., et al. (2014) Proteome-wide remodeling of protein location and function by stress. *Proceedings of the National Academy of Sciences of the United States of America*, 111, E3157–66.

Lee, R.C., Feinbaum, R.L. & Ambros, V. (1993) The *C. elegans* heterochronic gene lin-4 encodes small RNAs with antisense complementarity to lin-14. *Cell*, 75, 843–854.

Lei, Z. & Yi, C. (2017) A Radiolabeling-Free, qPCR-Based Method for Locus-Specific Pseudouridine Detection. *Angewandte Chemie*, 56, 14878–14882.

Levi, O. & Arava, Y.S. (2021) RNA modifications as a common denominator between tRNA and mRNA. *Current Genetics*.

Li, X., Xiong, X. & Yi, C. (2016) Epitranscriptome sequencing technologies: decoding RNA modifications. *Nature Methods*, 14, 23–31.

Li, X., Zhu, P., Ma, S., Song, J., Bai, J., Sun, F., et al. (2015) Chemical pulldown reveals dynamic pseudouridylation of the mammalian transcriptome. *Nature Chemical Biology*, 11, 592–597.

Linder, B., Grozhik, A.V., Olarerin-George, A.O., Meydan, C., Mason, C.E. & Jaffrey, S.R. (2015) Single-nucleotide-resolution mapping of m6A and m6Am throughout the transcriptome. *Nature* Methods, 12, 767–772.

Liu, H., Begik, O., Lucas, M.C., Ramirez, J.M., Mason, C.E., Wiener, D., et al. (2019) Accurate detection of m6A RNA modifications in native RNA sequences. *Nature Communications*, 10, 4079.

Liu, N., Dai, Q., Zheng, G., He, C., Parisien, M. & Pan, T. (2015) N(6)-methyladenosine-dependent RNA structural switches regulate RNA-protein interactions. *Nature*, 518, 560–564.

Livak, K.J. & Schmittgen, T.D. (2001) Analysis of relative gene expression data using real-time quantitative PCR and the 2− ΔΔCT method. *Methods*.

Lorenz, C., Lünse, C.E. & Mörl, M. (2017) tRNA Modifications: Impact on Structure and Thermal Adaptation. *Biomolecules*, 7.

Love, M.I., Huber, W. & Anders, S. (2014) Moderated estimation of fold change and' ' dispersion for RNA-seq data with DESeq2. Genome Biology, 15, 550.

Lovejoy, A.F., Riordan, D.P. & Brown, P.O. (2014) Transcriptome-wide mapping of pseudouridines: pseudouridine synthases modify specific mRNAs in *S. cerevisiae. Plos One*, 9, e110799.

Luciano, D.J., Vasilyev, N., Richards, J., Serganov, A. & Belasco, J.G. (2017) A Novel RNA Phosphorylation State Enables 5' End-Dependent Degradation in *Escherichia coli. Molecular Cell*, 67, 44–54.e6.

Ma, X., Zhao, X. & Yu, Y.-T. (2003) Pseudouridylation (Psi) of U2 snRNA in S. cerevisiae is catalyzed by an RNA-independent mechanism. *The EMBO Journal*, 22, 1889–1897.

Marbaniang, C.N. & Vogel, J. (2016) Emerging roles of RNA modifications in bacteria. Current *Opinion in Microbiology*, 30, 50–57.

Marchand, V., Pichot, F., Neybecker, P., Ayadi, L., Bourguignon-Igel, V., Wacheul, L., et al. (2020) HydraPsiSeq: a method for systematic and quantitative mapping of pseudouridines in RNA. *Nucleic Acids Research*, 48, e110.

Masuda, M., Nishihira, T., Itoh, K., Mizugaki, M., Ishida, N. & Mori, S. (1993) An immunohistochemical analysis for cancer of the esophagus using monoclonal antibodies specific for modified nucleosides. Cancer, 72, 3571–3578.

McCown, P.J., Ruszkowska, A., Kunkler, C.N., Breger, K., Hulewicz, J.P., Wang, M.C., et al. (2020) Naturally occurring modified ribonucleosides. Wiley interdisciplinary reviews. *RNA*, 11, e1595.

McGlincy, N.J. & Ingolia, N.T. (2017) Transcriptome-wide measurement of translation by ribosome profiling. *Methods*, 126, 112–129.

McKenney, K.M., Rubio, M.A.T. & Alfonzo, J.D. (2017) The Evolution of Substrate Specificity by tRNA Modification Enzymes. *The Enzymes*, 41, 51–88.

Mengel-Jørgensen, J. & Kirpekar, F. (2002) Detection of pseudouridine and other modifications in tRNA by cyanoethylation and MALDI mass spectrometry. *Nucleic Acids Research*, 30, e135.

Meyer, K.D., Saletore, Y., Zumbo, P., Elemento, O., Mason, C.E. & Jaffrey, S.R. (2012) Comprehensive analysis of mRNA methylation reveals enrichment in 3' UTRs and near stop codons. *Cell*, 149, 1635–1646.

Mishima, E. & Abe, T. (2019) Immuno-northern blotting: detection of modified RNA using gel separation and antibodies to modified nucleosides. *Epitranscriptomics.*

Mishima, E., Jinno, D., Akiyama, Y., Itoh, K., Nankumo, S., Shima, H., et al. (2015) Immuno-Northern Blotting: Detection of RNA Modifications by Using Antibodies against Modified Nucleosides. Plos One, 10, e0143756.

Moazed, D. & Noller, H.F. (1989) Intermediate states in the movement of transfer RNA in the ribosome. *Nature*, 342, 142–148.

Motorin, Y. & Marchand, V. (2018) Detection and Analysis of RNA Ribose 2'-O-Methylations: Challenges and Solutions. *Genes*, 9.

Nakamoto, M.A., Lovejoy, A.F., Cygan, A.M. & Boothroyd, J.C. (2017) mRNA pseudouridylation affects RNA metabolism in the parasite *Toxoplasma gondii. RNA* (New York), 23, 1834–1849.

Neal-McKinney, J.M. & Konkel, M.E. (2012) The *Campylobacter jejuni* CiaC virulence protein is secreted from the flagellum and delivered to the cytosol of host cells. *Frontiers in cellular and infection microbiology*, 2, 31.

Ni, J., Tien, A.L. & Fournier, M.J. (1997) Small nucleolar RNAs direct site-specific synthesis of pseudouridine in ribosomal RNA. *Cell,* 89, 565–573.

Nickels, B.E. (2012) A new way to start: nanoRNA-mediated priming of transcription initiation. Transcription.

Nie, W., Wang, S., He, R., Xu, Q., Wang, P., Wu, Y., et al. (2020) A-to-I RNA editing in bacteria increases pathogenicity and tolerance to oxidative stress. *PLoS Pathogens*, 16, e1008740.

Nobles, K.N., Yarian, C.S., Liu, G., Guenther, R.H. & Agris, P.F. (2002) Highly conserved modified nucleosides influence Mg2+-dependent tRNA folding. *Nucleic Acids Research*, 30, 4751–4760.

Nurse, K., Wrzesinski, J., Bakin, A., Lane, B.G. & Ofengand, J. (1995) Purification, cloning, and properties of the tRNA psi 55 synthase from *Escherichia coli. RNA* (New York), 1, 102–112.

O'Brien, J., Hayder, H., Zayed, Y. & Peng, C. (2018) Overview of microrna biogenesis, mechanisms of actions, and circulation. *Frontiers in endocrinology*, 9, 402.

Ofengand, J. (2002) Ribosomal RNA pseudouridines and pseudouridine synthases. *FEBS Letters*, 514, 17–25.

Ofengand, J., Campo, M. Del & Kaya, Y. (2001) Mapping pseudouridines in RNA molecules. *Methods*, 25, 365–373.

Pajaniappan, M., Hall, J.E., Cawthraw, S.A., Newell, D.G., Gaynor, E.C., Fields, J.A., et al. (2008) A temperature-regulated *Campylobacter jejuni* gluconate dehydrogenase is involved in respiration-dependent energy conservation and chicken colonization. *Molecular Microbiology*, 68, 474–491.

Palade, G.E. (1955) A small particulate component of the cytoplasm. *The Journal of biophysical and biochemical cytology*, 1, 59–68.

Palmer, D.T., Blum, P.H. & Artz, S.W. (1983) Effects of the *hisT* mutation of *Salmonella* typhimurium on translation elongation rate. *Journal of Bacteriology*, 153, 357–363.

Pan, H., Agarwalla, S., Moustakas, D.T., Finer-Moore, J. & Stroud, R.M. (2003) Structure of tRNA pseudouridine synthase TruB and its RNA complex: RNA recognition through a combination of rigid docking and induced fit. *Proceedings of the National Academy of Sciences of the United States of America*, 100, 12648–12653.

Pan, T. (2018) Modifications and functional genomics of human transfer RNA. *Cell Research*, 28, 395–404.

Parkhill, J., Wren, B.W., Mungall, K., Ketley, J.M., Churcher, C., Basham, D., et al. (2000) The genome sequence of the food-borne pathogen *Campylobacter jejuni* reveals hypervariable sequences. *Nature*, 403, 665–668.

Peattie, D.A. (1979) Direct chemical method for sequencing RNA. *Proceedings of the National Academy of Sciences of the United States of America*, 76, 1760–1764.

Pernitzsch, S.R., Alzheimer, M., Bremer, B.U., Robbe-Saule, M., Reuse, H. De & Sharma, C.M. (2021) Small RNA mediated gradual control of lipopolysaccharide biosynthesis affects antibiotic resistance in *Helicobacter pylori*. *Nature Communications*, 12, 4433.

Pernitzsch, S.R. & Sharma, C.M. (2012) Transcriptome complexity and riboregulation in the human pathogen *Helicobacter pylori*. *Frontiers in cellular and infection microbiology*, 2, 14.

Pernitzsch, S.R., Tirier, S.M., Beier, D. & Sharma, C.M. (2014) A variable homopolymeric G-repeat defines small RNA-mediated posttranscriptional regulation of a chemotaxis receptor in *Helicobacter pylori. Proceedings of the National Academy of Sciences of the United States of America*, 111, E501–10.

Persson, B.C., Jäger, G. & Gustafsson, C. (1997) The spoU gene of Escherichia coli, the fourth gene of the spoT operon, is essential for tRNA (Gm18) 2'-O-methyltransferase activity. *Nucleic Acids Research*, 25, 4093–4097.

Pickerill, E.S., Kurtz, R.P., Tharp, A., Guerrero Sanz, P., Begum, M. & Bernstein, D.A. (2019) Pseudouridine synthase 7 impacts Candida albicans rRNA processing and morphological plasticity. *Yeast*, 36, 669–677.

Pomerantz, S.C. & McCloskey, J.A. (1990) Analysis of RNA hydrolyzates by liquid chromatography-mass spectrometry. *Methods in Enzymology*, 193, 796–824.

Porcelli, I., Reuter, M., Pearson, B.M., Wilhelm, T. & van Vliet, A.H.M. (2013) Parallel evolution of genome structure and transcriptional landscape in the Epsilonproteobacteria. *BMC Genomics*, 14, 616.

Purchal, M.K., Eyler, D.E., Tardu, M., Franco, M.K., Korn, M.M., Khan, T., et al. (2022) Pseudouridine synthase 7 is an opportunistic enzyme that binds and modifies substrates with diverse sequences and structures. P*roceedings of the National Academy of Sciences of the United States of America*, 119.

Radomska, K.A., Ordoñez, S.R., Wösten, M.M.S.M., Wagenaar, J.A. & van Putten, J.P.M. (2016) Feedback control of *Campylobacter jejuni* flagellin levels through reciprocal binding of FliW to flagellin and the global regulator CsrA. *Molecular Microbiology*, 102, 207–220.

Rafels-Ybern, À., Torres, A.G., Grau-Bove, X., Ruiz-Trillo, I. & Ribas de Pouplana, L. (2018) Codon adaptation to tRNAs with Inosine modification at position 34 is widespread among Eukaryotes and present in two Bacterial phyla. *RNA Biology*, 15, 500–507.

Rajan, K.S., Doniger, T., Cohen-Chalamish, S., Chen, D., Semo, O., Aryal, S., et al. (2019) Pseudouridines on *Trypanosoma brucei* spliceosomal small nuclear RNAs and their implication for RNA and protein interactions. *Nucleic Acids Research*.

Raychaudhuri, S., Conrad, J., Hall, B.G. & Ofengand, J. (1998) A pseudouridine synthase required for the formation of two universally conserved pseudouridines in ribosomal RNA is essential for normal growth of *Escherichia coli. RNA* (New York), 4, 1407–1417.

Raychaudhuri, S., Niu, L., Conrad, J., Lane, B.G. & Ofengand, J. (1999) Functional effect of deletion and mutation of the Escherichia coli ribosomal RNA and tRNA pseudouridine synthase RluA. *The Journal of Biological Chemistry*, 274, 18880–18886.

Reinhart, B.J., Slack, F.J., Basson, M., Pasquinelli, A.E., Bettinger, J.C., Rougvie, A.E., et al. (2000) The 21-nucleotide let-7 RNA regulates developmental timing in *Caenorhabditis elegans*. *Nature*, 403, 901–906.

Richards, J. & Belasco, J.G. (2016) Distinct Requirements for 5'-Monophosphate-assisted RNA Cleavage by Escherichia coli RNase E and RNase G. *The Journal of Biological Chemistry*, 291, 5038–5048.

Richards, J., Sundermeier, T., Svetlanov, A. & Karzai, A.W. (2008) Quality control of bacterial mRNA decoding and decay. *Biochimica et Biophysica Acta*, 1779, 574–582.

Rintala-Dempsey, A.C. & Kothe, U. (2017) Eukaryotic stand-alone pseudouridine synthases - RNA modifying enzymes and emerging regulators of gene expression? *RNA Biology*, 14, 1185–1196.

Sáenz-Lahoya, S., Bitarte, N., García, B., Burgui, S., Vergara-Irigaray, M., Valle, J., et al. (2019) Noncontiguous operon is a genetic organization for coordinating bacterial gene expression. *Proceedings of the National Academy of Sciences of the United States of America*, 116, 1733–1738.

Safra, M., Nir, R., Farouq, D., Vainberg Slutskin, I. & Schwartz, S. (2017) TRUB1 is the predominant pseudouridine synthase acting on mammalian mRNA via a predictable and conserved code. *Genome Research*, 27, 393–406.

Sahlin, K., Sipos, B., James, P.L. & Medvedev, P. (2021) Error correction enables use of Oxford Nanopore technology for reference-free transcriptome analysis. *Nature Communications*, 12, 2.

Sakakibara, Y. & Chow, C.S. (2017) Pseudouridine modifications influence binding of aminoglycosides to helix 69 of bacterial ribosomes. *Organic & Biomolecular Chemistry*, 15, 8535–8543.

Salama, N.R., Hartung, M.L. & Müller, A. (2013) Life in the human stomach: persistence strategies of the bacterial pathogen *Helicobacter pylori*. *Nature Reviews. Microbiology*, 11, 385–399.

Salaün, L., Linz, B., Suerbaum, S. & Saunders, N.J. (2004) The diversity within an expanded and redefined repertoire of phase-variable genes in *Helicobacter pylori*. *Microbiology*, 150, 817–830.

Samuelsson, T. & Olsson, M. (1990) Transfer RNA pseudouridine synthases in Saccharomyces cerevisiae. *The Journal of Biological Chemistry*, 265, 8782–8787.

Satapathy, S.S., Dutta, M. & Ray, S.K. (2010) Variable correlation of genome GC% with transfer RNA number as well as with transfer RNA diversity among bacterial groups: α-Proteobacteria and …. *Microbiological research*.

Saunders, N.J., Peden, J.F., Hood, D.W. & Moxon, E.R. (1998) Simple sequence repeats in the *Helicobacter pylori* genome. *Molecular Microbiology*, 27, 1091–1098.

Schaefer, M., Pollex, T., Hanna, K. & Lyko, F. (2009) RNA cytosine methylation analysis by bisulfite sequencing. *Nucleic Acids Research*, 37, e12.

Schauerte, M., Pozhydaieva, N. & Höfer, K. (2021) Shaping the Bacterial Epitranscriptome-5'-Terminal and Internal RNA Modifications. *Advanced Biology*, e2100834.

Schmidt, A., Kochanowski, K., Vedelaar, S., Ahrné, E., Volkmer, B., Callipo, L., et al. (2016) The quantitative and condition-dependent Escherichia coli proteome. *Nature Biotechnology*, 34, 104–110.

Schultz, S.K.-L. & Kothe, U. (2020) tRNA elbow modifications affect the tRNA pseudouridine synthase TruB and the methyltransferase TrmA. *RNA* (New York), 26, 1131–1142.

Schwartz, S., Bernstein, D.A., Mumbach, M.R., Jovanovic, M., Herbst, R.H., León-Ricardo, B.X., et al. (2014) Transcriptome-wide mapping reveals widespread dynamic-regulated pseudouridylation of ncRNA and mRNA. *Cell*, 159, 148–162.

Schwartz, S. & Motorin, Y. (2017) Next-generation sequencing technologies for detection of modified nucleotides in RNAs. *RNA Biology*, 14, 1124–1137.

Sergiev, P.V., Serebryakova, M.V., Bogdanov, A.A. & Dontsova, O.A. (2008) The ybiN gene of Escherichia coli encodes adenine-N6 methyltransferase specific for modification of A1618 of 23 S ribosomal RNA, a methylated residue located close to the ribosomal exit tunnel. *Journal of Molecular Biology*, 375, 291–300.

Sharma, C.M., Hoffmann, S., Darfeuille, F., Reignier, J., Findeiss, S., Sittka, A., et al. (2010) The primary transcriptome of the major human pathogen *Helicobacter pylori*. *Nature*, 464, 250–255.

Shatkin, A.J. (1976) Capping of eucaryotic mRNAs. *Cell*, 9, 645–653.

Skouloubris, S., Thiberge, J.M., Labigne, A. & Reuse, H. De. (1998) The *Helicobacter pylori* UreI protein is not involved in urease activity but is essential for bacterial survival in vivo. *Infection and Immunity*, 66, 4517–4521.

Smirnov, A., Förstner, K.U., Holmqvist, E., Otto, A., Günster, R., Becher, D., et al. (2016) Grad-seq guides the discovery of ProQ as a major small RNA-binding protein. *Proceedings of the National Academy of Sciences of the United States of America*, 113, 11591–11596.

Song, J., Zhuang, Y., Zhu, C., Meng, H., Lu, B., Xie, B., et al. (2020) Differential roles of human PUS10 in miRNA processing and tRNA pseudouridylation. *Nature Chemical Biology*, 16, 160–169.

Soppa, J. (2010) Protein acetylation in archaea, bacteria, and eukaryotes. *Archaea*, 2010.

Sørensen, M.A., Fricke, J. & Pedersen, S. (1998) Ribosomal protein S1 is required for translation of most, if not all, natural mRNAs in *Escherichia coli* in vivo. *Journal of Molecular Biology*, 280, 561–569.

Spenkuch, F., Motorin, Y. & Helm, M. (2014) Pseudouridine: still mysterious, but never a fake (uridine)! *RNA Biology*, 11, 1540–1554.

Sprinzl, M., Hartmann, T., Meissner, F., Moll, J. & Vorderwülbecke, T. (1987) Compilation of tRNA sequences and sequences of tRNA genes. *Nucleic Acids Research*, 15 Suppl, r53–188.

Stahl, M. & Stintzi, A. (2011) Identification of essential genes in C. jejuni genome highlights hyper-variable plasticity regions. *Functional & Integrative Genomics*, 11, 241–257.

Storz, G., Vogel, J. & Wassarman, K.M. (2011) Regulation by small RNAs in bacteria: expanding frontiers. *Molecular Cell*, 43, 880–891.

Sun, L., Xu, Y., Bai, S., Bai, X., Zhu, H., Dong, H., et al. (2019) Transcriptome-wide analysis of pseudouridylation of mRNA and non-coding RNAs in Arabidopsis. *Journal of Experimental Botany*, 70, 5089–5600.

Suzuki, T., Ikeuchi, Y., Noma, A., Suzuki, T. & Sakaguchi, Y. (2007) Mass spectrometric identification and characterization of rna-modifying enzymes. In RNA Modification, *Methods in Enzymology*. Elsevier, pp. 211–229.

Svensson, S.L., Pryjma, M. & Gaynor, E.C. (2014) Flagella-mediated adhesion and extracellular DNA release contribute to biofilm formation and stress tolerance of *Campylobacter jejuni*. *Plos One*, 9, e106063.

Svensson, S.L. & Sharma, C.M. (2021) RNase III-mediated processing of a trans-acting bacterial sRNA and its cis-encoded antagonist. *eLife*, 10.

Svensson, S.L. & Sharma, C.M. (2022) Small RNAs that target G-rich sequences are generated by diverse biogenesis pathways in Epsilonproteobacteria. *Molecular Microbiology*, 117, 215–233.

Sze, C.W., Morado, D.R., Liu, J., Charon, N.W., Xu, H. & Li, C. (2011) Carbon storage regulator A (CsrA(Bb)) is a repressor of Borrelia burgdorferi flagellin protein FlaB. *Molecular Microbiology*, 82, 851–864.

Szymanski, C.M., King, M., Haardt, M. & Armstrong, G.D. (1995) *Campylobacter jejuni* motility and invasion of Caco-2 cells. *Infection and Immunity*, 63, 4295–4300.

Tagel, M., Ilves, H., Leppik, M., Jürgenstein, K., Remme, J. & Kivisaar, M. (2020) Pseudouridines of tRNA Anticodon Stem-Loop Have Unexpected Role in Mutagenesis in Pseudomonas sp. *Microorganisms*, 9.

Tanzer, A., Hofacker, I.L. & Lorenz, R. (2018) RNA modifications in structure prediction - Status quo and future challenges. *Methods*, 156, 32–39.

Tatusov, R.L., Fedorova, N.D., Jackson, J.D., Jacobs, A.R., Kiryutin, B., Koonin, E.V., et al. (2003) The COG database: an updated version includes eukaryotes. *BMC Bioinformatics*, 4, 41.

The biochemistry of the nucleic acids. (1972) . *Elsevier*.

Torres, A.G., Piñeyro, D., Filonava, L., Stracker, T.H., Batlle, E. & Ribas de Pouplana, L. (2014) A-to-I editing on tRNAs: biochemical, biological and evolutionary implications. *FEBS Letters*, 588, 4279–4286.

Tram, G., Day, C.J. & Korolik, V. (2020) Bridging the gap: A role for *Campylobacter jejuni* biofilms. *Microorganisms*, 8.

Tscherne, J.S., Nurse, K., Popienick, P., Michel, H., Sochacki, M. & Ofengand, J. (1999) Purification, cloning, and characterization of the 16S RNA m5C967 methyltransferase from *Escherichia coli*. *Biochemistry*, 38, 1884–1892.

Vaidyanathan, P.P., AlSadhan, I., Merriman, D.K., Al-Hashimi, H.M. & Herschlag, D. (2017) Pseudouridine and N6-methyladenosine modifications weaken PUF protein/RNA interactions. *RNA* (New York), 23, 611–618.

van der Feltz, C., DeHaven, A.C. & Hoskins, A.A. (2018) Stress-induced Pseudouridylation Alters the Structural Equilibrium of Yeast U2 snRNA Stem II. *Journal of Molecular Biology*, 430, 524–536.

Vasilyev, N., Gao, A. & Serganov, A. (2019) Noncanonical features and modifications on the 5'-end of bacterial sRNAs and mRNAs. Wiley interdisciplinary reviews. *RNA,* 10, e1509.

Wakasugi, K. & Schimmel, P. (1999) Two distinct cytokines released from a human aminoacyl-tRNA synthetase. *Science*, 284, 147–151.

Wanichthanarak, K., Nookaew, I. & Petranovic, D. (2014) yStreX: yeast stress expression database. *Database: the Journal of Biological Databases and Curation*, 2014.

Wassenaar, T.M. & Blaser, M.J. (1999) Pathophysiology of *Campylobacter jejuni* infections of humans. *Microbes and Infection*, 1, 1023–1033.

Watanabe, Y. & Gray, M.W. (2000) Evolutionary appearance of genes encoding proteins associated with box H/ACA snoRNAs: cbf5p in Euglena gracilis, an early diverging eukaryote, and candidate Gar1p and Nop10p homologs in archaebacteria. *Nucleic Acids Research*, 28, 2342–2352.

Weerakoon, D.R. & Olson, J.W. (2008) The *Campylobacter jejuni* NADH:ubiquinone oxidoreductase (complex I) utilizes flavodoxin rather than NADH. *Journal of Bacteriology*, 190, 915–925.

Weichmann, F., Hett, R., Schepers, A., Ito-Kureha, T., Flatley, A., Slama, K., et al. (2020) Validation strategies for antibodies targeting modified ribonucleotides. *RNA* (New York), 26, 1489–1506.

Westermann, A.J., Förstner, K.U., Amman, F., Barquist, L., Chao, Y., Schulte, L.N., et al. (2016) Dual RNA-seq unveils noncoding RNA functions in host-pathogen interactions. *Nature*, 529, 496–501.

Wolf, J., Gerber, A.P. & Keller, W. (2002) tadA, an essential tRNA-specific adenosine deaminase from *Escherichia coli*. *The EMBO Journal*, 21, 3841–3851.

Wösten, M.M.S.M., Wagenaar, J.A. & van Putten, J.P.M. (2004) The FlgS/FlgR two-component signal transduction system regulates the fla regulon in *Campylobacter jejuni*. *The Journal of Biological Chemistry*, 279, 16214–16222.

Xu, L. & Seki, M. (2020) Recent advances in the detection of base modifications using the Nanopore sequencer. *Journal of Human Genetics*, 65, 25–33.

Yamaki, Y., Nobe, Y., Koike, M., Yamauchi, Y., Hirota, K., Takahashi, N., et al. (2020) Direct determination of pseudouridine in RNA by mass spectrometry coupled with stable isotope labeling. *Analytical Chemistry*.

Yu, C.T. & Allen, F.W. (1959) Studies on an isomer of uridine isolated from ribonucleic acids. *Biochimica et Biophysica Acta*, 32, 393–406.

Yue, Y., Liu, J. & He, C. (2015) RNA N6-methyladenosine methylation in post-transcriptional gene expression regulation. *Genes & Development*, 29, 1343–1355.

Zaringhalam, M. & Papavasiliou, F.N. (2016) Pseudouridylation meets next-generation sequencing. *Methods*, 107, 63–72.

Zhang, W., Eckwahl, M.J., Zhou, K.I. & Pan, T. (2019) Sensitive and quantitative probing of pseudouridine modification in mRNA and long noncoding RNA. *RNA* (New York), 25, 1218–1225.

Zhao, X., Patton, J.R., Davis, S.L., Florence, B., Ames, S.J. & Spanjaard, R.A. (2004) Regulation of nuclear receptor activity by a pseudouridine synthase through posttranscriptional modification of steroid receptor RNA activator. *Molecular Cell*, 15, 549–558.

Zoysa, M.D. De & Yu, Y.-T. (2017) Posttranscriptional RNA Pseudouridylation. *The Enzymes*, 41, 151–167.

10. List of Figures

11. List of Tables

12. Curriculum Vitae

Elisabetta Fiore

13. List of pubblications

Manuscript related to this PhD thesis, which are in preparation and/or submitted:

Fiore E, Dugar G, Bischler T, Barquist L, Sharma CM (2022). RNA substrates of tRNA PUS enzymes and functionality beyond pseudouridylation in Epsilonproteobacteria.
(Research article)

Manuscript that are not related to this PhD thesis, which are in preparation and/or submitted:

Eisenbart SK, Hadjeras L, Alzheimer A, Narayan M, König F, **Fiore E**, Sharma S, Bischler T, Julia Bosselmann J, Kucklick M, Svensson SL, Seidler J, Barquist L, Engelmann S, Sharma CM. RNA interactome capture reveals bacterial RNA-binding protein landscapes.
(Research article)

Froschauer K, Svensson SL**,** Gelhausen R, **Fiore E**, Kible P, Claude A, Eggenhofer F, Kucklick M, Engelmann S, Backofen R, Sharma S (2022) Complementary Ribo-seq approaches refine the translatome and provide a small protein census in a bacterial pathogen.
(Research article)

Previous studies that were published prior to the beginning of and/or are unrelated to this PhD thesis:

Pepe S, Pinatel E, **Fiore E**, Puccio S, Peano C, Brignoli T, Vannini A, Danielli A, Scarlato V, Roncarati D (2018). The *Helicobacter pylori* Heat-Shock Repressor HspR: Definition of Its Direct Regulon and Characterization of the Cooperative DNA-Binding Mechanism on Its Own Promoter. *Front Microbiol*, 14;9:1887.

Roncarati D, Pinatel E, **Fiore E**, Peano C, Loibman S, Scarlato V (2019). *Helicobacter pylori* Stress-Response: Definition of the HrcA Regulon. *Microorganisms*, 7(10): 436.

14. Acknoledgments

First, I would like to thank Professor Cynthia Sharma for giving me the opportunity to work in her group and for teaching me to think critically about my work. I also thank her for the moral support over the last months and for encouraging me to believe in myself. Moreover, I would like to thank her for encouraging me to visit and present my work in national and international conferences.

I would also like to thank Professor Dagmar Beier and Professor Utz Fischer for being part of my committee and for their help and feedback in the annual meetings. I would also like to thank Professor Thomas Dandekar for chairing the doctoral committee and the defense of this thesis.

Then I would like to thank the Sharma group. First, I am grateful to the former lab members who helped me in the first period of my PhD to establish methods and techniques necessary for my work. Thank you because it is mainly because of you that I became curious about my project and you helped me to think critically. Thanks Gaurav, Patrick, Sandy, Mona, Sarah, and Sara. A special thanks go to Mona who supported me throughout the PhD journey and especially in the last period of my life and my thesis. Thank you for sharing food, tears, and joy over the past few months.

Another special thanks go to some members of the group who accompanied me during this long time. You are my German family and I thank you for sharing joy, pain, and wonderful experiences and adventures with me. Wherever I am, I will always keep all these wonderful memories in my heart. Thanks Anjie, Beli, Fabian, Philipp, and Kathrin.

Thanks to the rest of the group that supported me mentally and scientifically. Thanks Sahil, Lydia Shalini, Annamaria, and Manasa. Thanks, Christine, for your technical support in the lab.

Thanks to my small Italian family here in Würzburg that helped me throughout the PhD and the pandemic. Thanks Elisa, Silvia, Gianluca, and Gianluca.

I am very grateful to all the people that read this thesis. Thanks Mona, Fabian, Sahil, and Shalini. Thanks, Kathrin, for the last-minute check.

I thank the Graduate School of Life Sciences (GSLS) of the University of Wurzburg for giving me the possibility to become part of their interdisciplinary PhD program. Especially thanks to Irina and Heike for their support over the last months.

Thanks to Hilde for her technical support, but also for all the laughs in different balconies.

My last and biggest thanks go to my family who have always supported me and always pushed me to do the thing that make me happy. Thank you for making me believe in myself again and for supporting me in my life choices. Without you, I would never have made it.